



PHD

**Surface acidity and colour reactions on clay minerals and oxides.**

Barber, R. P.

*Award date:*  
1981

*Awarding institution:*  
University of Bath

[Link to publication](#)

## Alternative formats

If you require this document in an alternative format, please contact:  
[openaccess@bath.ac.uk](mailto:openaccess@bath.ac.uk)

### General rights

Copyright and moral rights for the publications made accessible in the public portal are retained by the authors and/or other copyright owners and it is a condition of accessing publications that users recognise and abide by the legal requirements associated with these rights.

- Users may download and print one copy of any publication from the public portal for the purpose of private study or research.
- You may not further distribute the material or use it for any profit-making activity or commercial gain
- You may freely distribute the URL identifying the publication in the public portal ?

### Take down policy

If you believe that this document breaches copyright please contact us providing details, and we will remove access to the work immediately and investigate your claim.

UNIVERSITY OF BATH  
LIBRARY  
19 OCT 1981



SURFACE ACIDITY AND COLOUR REACTIONS

ON CLAY MINERALS AND OXIDES

Submitted by R.P. Barber  
for the degree of Ph.D.  
at the University of Bath

1981

COPYRIGHT

Attention is drawn to the fact that copyright of this thesis rests with the author. This copy of the thesis has been supplied on condition that anyone who consults it is understood to recognise that its copyright rests with its author and that no quotation from the thesis and no information derived from it may be published without the prior written consent of the author.

This thesis may be made available for consultation within the University Library and may be photocopied or lent to other Libraries for the purposes of consultation.

R. P. Barber.



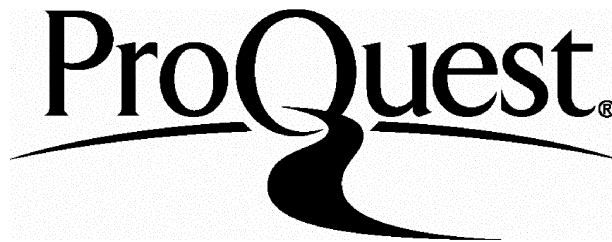
ProQuest Number: U320215

All rights reserved

INFORMATION TO ALL USERS

The quality of this reproduction is dependent upon the quality of the copy submitted.

In the unlikely event that the author did not send a complete manuscript and there are missing pages, these will be noted. Also, if material had to be removed, a note will indicate the deletion.



ProQuest U320215

Published by ProQuest LLC(2015). Copyright of the Dissertation is held by the Author.

All rights reserved.

This work is protected against unauthorized copying under Title 17, United States Code.  
Microform Edition © ProQuest LLC.

ProQuest LLC  
789 East Eisenhower Parkway  
P.O. Box 1346  
Ann Arbor, MI 48106-1346

### Acknowledgements

The author wishes to thank Dr. A.W. Flegmann for his guidance and encouragement throughout the course of this work. The author is also very grateful to English Clays Lovering Pochin Co., Ltd., in particular Dr. W.B. Jepson, for their cooperation and generous support. The author wishes to thank Mrs. J. Watts for her speed and proficiency in typing this thesis.

Acknowledgement is made to the Science Research Council and to English Clay Lovering Pochin and Co., Ltd., for the CASE award of a research studentship.

### SUMMARY

A reliable method was devised for the determination of surface acidity of clay minerals and oxides, by the adsorption of *m*-nitroaniline from aqueous solution, which accounted for the energy of adsorption of the protonated and unprotonated forms. The Hammett acidity function ( $H_0$ ) of a sample of  $H^+$ -Kaolinite was 2.21, at bulk pH 3.0

The reaction of crystal violet (CV) and crystal violet lactone (CVL) were studied in solution and on clay minerals. CV and CVL decompose in methanolic and ethanolic solution if exposed to light, to yield demethylated derivatives. The products of CVL differ from CV and this suggests, the colourless lactone is more photolabile than CV. A colourless solution of CVL will undergo lactone cleavage on clay minerals and oxides to form a violet zwitterion. This zwitterion can be displaced from the surface by water vapour. Minerals with a high surface acidity resist the displacement of the zwitterion to a greater extent than do those with a low surface acidity, the counterion being an important factor in determining the acid strength of the surface. CVL undergoes demethylation on silica and Silton to yield the same products as in solution. Silton is a brand name of an acid-treated dioctahedral montmorillonite.

The reactions of methylene blue (MB) and benzoyl leuco methylene blue (BLMB) were studied on clay minerals and in solution. The first order rate constant for the production of methylene blue from BLMB at 39 and 50°C were  $1.54 \times 10^{-6}$  and  $3.47 \times 10^{-6} \text{ sec}^{-1}$ ,

respectively.

If sodium cobalti-nitrite or ceric ammonium nitrate were added to an acidic solution of BLMB, the rate of MB production was greatly enhanced. The overall reaction was 2nd order in the case of  $\text{Na}_3\text{Co}(\text{NO}_2)_6$  and 3rd order in the case of  $(\text{NH}_4)_2\text{Ce}(\text{NO}_3)_6$ . The rate constants for the reactions were  $8.95 \text{ l M}^{-1} \text{ sec}^{-1}$  and  $6.25 \times 10^8 \text{ l}^2 \text{ M}^{-2} \text{ sec}^{-1}$ . This suggested that two electrons were transferred from BLMB to  $\text{Na}_3\text{Co}(\text{NO}_2)_6$  simultaneously, and singly to  $(\text{NH}_4)_2\text{Ce}(\text{NO}_3)_6$ . MB and BLMB demethylated on silica gel and Silton, to yield Azure A, B, C, sym-dimethylthionine, and thionine. Production of MB from BLMB requires light and operates via a photon induced free radical mechanism. The presence of  $\text{Co}^{3+}$  or  $\text{Ce}^{4+}$ , electron acceptors, on silica or Silton accelerates the reaction rate and does not require light.

CONTENTS

	<u>Page</u>
CHAPTER 1	
Introduction	1
1.1	
General Introduction	1
1.2	
The structure of clay minerals	3
1.3	
Colour and the absorption of light	12
1.4	
Reactions of clay minerals	24
1.5	
Methods of studying reactions on solid surfaces.	26
CHAPTER 2	
Surface Acidity of Kaolinite	29
2.1	
Introduction	29
2.1.2	
An accurate method to determine the surface acidity by adsorption from solution, of a sample of Kaolinite	33
2.1.3.	
The Langmuir Equation : Theory	36
2.2.	
Experimental	40
2.3	
Results and Discussion	44
2.3.1	
Crystal violet in acidic solution	44
2.3.2	
An adsorption isotherm of Crystal Violet on H <sup>+</sup> -Kaolinite	48
2.3.3	
To determine the amount of water tolerable to produce a sharp reflectance spectrum of Crystal Violet on Kaolinite.	50

	Page
2.3.4. An estimation of the surface acidity of a sample of H <sup>+</sup> -Kaolonite	52
2.3.5. Isomers of Nitroaniline	55
2.3.6. Adsorption Isotherms of p and m-Nitroaniline as an indicator	59
2.3.7. A method to determine the surface acidity of H <sup>+</sup> - Kaolinite using m-Nitroaniline as an indicator	63
2.4 Conclusions	68
CHAPTER 3 Reactions of Crystal Violet and Crystal Violet Lactone on Clay Minerals and Oxides	69
3.1 Introduction	69
3.1.2. The behaviour of crystal violet in aqueous acid solution	72
3.1.3. The behaviour of crystal violet lactone on clay minerals and oxides	75
3.1.4 Possible modes of fading	78
3.1.5. The uses of Crystal Violet and Crystal Violet Lactone	82
3.2 Experimental	83
3.3 Results and Discussion	90
3.3.1 Purity of Crystal Violet and Crystal Violet Lactone	90
3.3.2 Radial Thin Layer Chromatography of some triarylmethane dyes	95
3.3.3 Radial Thin Layer Chromatography of Crystal Violet Lactone	109

	Page
3.3.4 Thin Layer Chromatography of Crystal Violet lactone irradiated on silica gel.	111
3.3.5 Diffuse Reflectance Studies of Crystal Violet and Crystal Violet Lactone absorbed upon silica gel	118
3.3.6 The effect of humidity and light upon Crystal Violet lactone adsorbed upon Silton.	142
3.3.7 The effect of humidity and light upon Crystal Violet lactone adsorbed on Wyoming bentonite	156
3.3.8 Reflectance of Crystal Violet and Crystal Violet lactone adsorbed on Kaolinite	167
3.4. Conclusions	182
CHAPTER 4 Reactions of methylene blue and benzoyl leucomethylene blue on clay minerals and oxides	184
4.1 Introduction	184
4.1.2 Photochemistry of methylene blue	188
4.1.3 Reactions of Thiazine dyes	192
4.1.4 Reactions of Benzoyl leucomethylene blue	194
4.1.5 Uses of thiazine dyes and their derivatives	196
4.2 Experimental	198
4.3 Results and Discussion	204
4.3.1 Methylene blue in aqueous solution	204

	Page
4.3.2 Hydrolysis and autooxidation of benzoyl leuco methylene blue	209
4.3.3 Hydrolysis of benzoyl leuco methylene blue in the presence of $\text{Co}^{3+}$	212
4.3.4 The effect of the hydrogen-ion concentration upon the spectral characteristics of methylene blue.	214
4.3.5 The hydrolysis of benzoyl leuco methylene blue in the presence of $\text{Ce}^{4+}$	220
4.3.6 Radial Thin Layer Chromatography of MB and related thiazine dyes.	224
4.3.7 A diffuse reflectance study of MB adsorbed on silica gel.	230
4.3.8 A diffuse reflectance study of BLMB adsorbed on silica gel	239
4.3.9 The isolation and identification of the reaction products of MB and BLMB on silica gel	246
4.3.10 The rate of demethylation of MB on silica gel	249
4.3.11 The rate of demethylation of BLMB on silica gel	251
4.3.12 The reaction of BLMB on silica gel in the presence of $\text{Co}^{3+}$ and $\text{Ce}^{4+}$	252
4.3.13 A diffuse reflectance study of MB adsorbed on Silton	255
4.3.14 A diffuse reflectance study of BLMB adsorbed on Silton	260
4.3.15 The reactions of BLMB on Silton in the presence of $\text{Co}^{3+}$ and $\text{Ce}^{4+}$	263
4. Conclusions	265
References	267



CHAPTER 1

INTRODUCTION

## INTRODUCTION

1.1 General Introduction

The determination of surface acidity, on clay minerals and oxides, using Hammett indicators is well known, Walling, C., (1950); Benesi, H.A., (1956); Benesi, H.A., (1957). Recently certain aspects of surface acidity determination, using Hammett indicators, have been questioned, Laura, R.D., (1976). The course of this research was envisaged to clarify these discrepancies, and to produce a more accurate method to determine surface acidity, using adsorption of an indicator on clay minerals and oxides. A method was developed, as described in the text, which was more accurate than any previously used, and overcame the objections raised by Laura, R.D., (1976).

The formation of colour, and subsequent fading of crystal violet lactone, and benzoyl leuco methylene blue on clay minerals and oxides are of general and commercial interest. The research was designed to:

- (i) determine the extent of the formation of the, violet coloured, zwitterion 2-carboxy-crystal violet from crystal violet lactone, on different clay minerals and oxides.
- (ii) to deduce the mechanism for the fading of 2-carboxy-crystal violet upon different clay minerals and oxides.
- (iii) to determine the extent of methylene blue produced from benzoyl leuco methylene on several clay minerals and oxides.

- (iv) to identify the mechanism of methylene blue formation, in sulphuric acid in the presence of sodium cobaltinitrite, or ceric ammonium nitrate, from benzoyl leuco methylene blue.
- (v) to determine the rate of demethylation of methylene blue on silica gel.

## 1.2 The Structure of Clay Minerals

In the early 1920's X-ray crystallography was first applied to the problem of analysing clay minerals. It was shown that clay minerals, in the main, were essentially crystalline. A classical X-ray diffraction study was performed by Pauling, L., (1930)a and Pauling, L., (1930)b; in which he concluded that the micas, talc, pyrophyllite, chlorite and kaolinite had layer structures composed of sheets of cristobalite ( $\text{SiO}_2$ ) and either gibbsite ( $\text{Al}_2(\text{OH})_6$ ) or brucite, ( $\text{Mg}_3(\text{OH})_6$ ). Thus a scheme of classification was established. By 1940 the structure of all the major layer silicates related to clay minerals had been established, Grim, R.E., (1968); Marshall, C.E., (1949), MacKenzie, R.C., and Mitchell, B.D., (1966).

Layer silicates are condensations of sheets of linked  $\text{Si}(\text{O},\text{OH})_4$  tetrahedra with  $\text{M}_{2-3}(\text{OH})_6$  octahedra, where M is either a di or trivalent cation. When the sheets are in 1:1 proportions the general formula for the halfunit cell is  $\text{Si}_2^{\text{iv}} \cdot \text{M}_{2-3}^{\text{vi}} \cdot \text{O}_5(\text{OH})_4$ , and they are known as dimorphic minerals. The best known example of this type is kaolinite. When the sheets are condensed in the proportions 2:1 the minerals are known as trimorphic. The octahedral sheet is sandwiched between two layers of inward pointing tetrahedra and has a general formula  $\text{Si}_4^{\text{iv}} \cdot \text{M}_{2-3}^{\text{vi}} \cdot \text{O}_{10}(\text{OH})_2$ .

Defects in the regular array occur when  $\text{Si}^{4+}$  and/or  $\text{M}^{2+/3+}$  are substituted by cations of similar size but lower valency. This is known as isomorphous replacement.

If all the octahedral sites are filled with cations the

mineral is known as trioctahedral. Whereas if only two out of three octahedral positions are filled then the mineral is known as dioctahedral.

Isomorphous replacement results in a deficiency of positive charge, hence the lattice has a net negative charge. Neutrality is maintained by sorption of cations, from solution, these cations may be exchangeable. The extent of isomorphous replacement will determine the properties of the mineral, e.g. swelling in water.

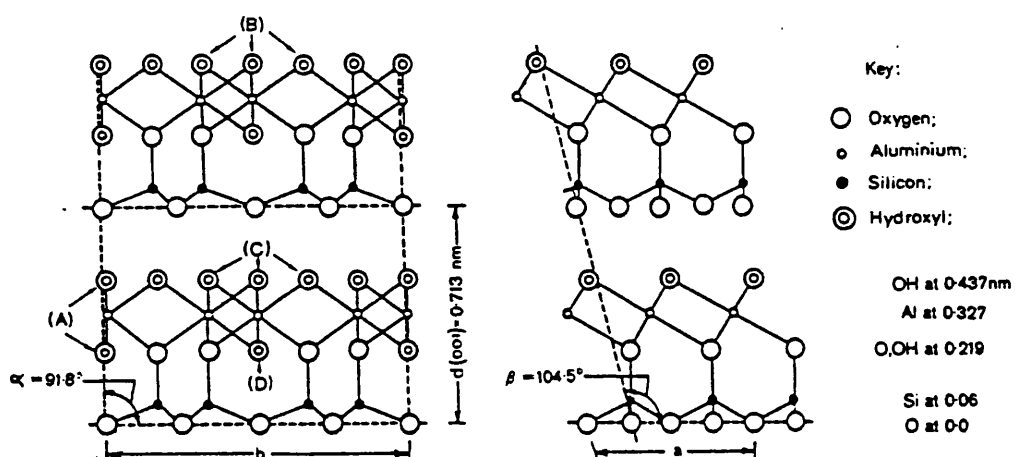
### 1.2.1 The 1:1 Type Minerals

Only the dioctahedral clay mineral, kaolinite, will be discussed here. Other 1:1 type minerals include the dioctahedral minerals halloysite, and the trioctahedral minerals, serpentines; (antigorite, and chrysotile).

#### Kaolinite

The layer structure of kaolinite is shown in Figure (1-1).

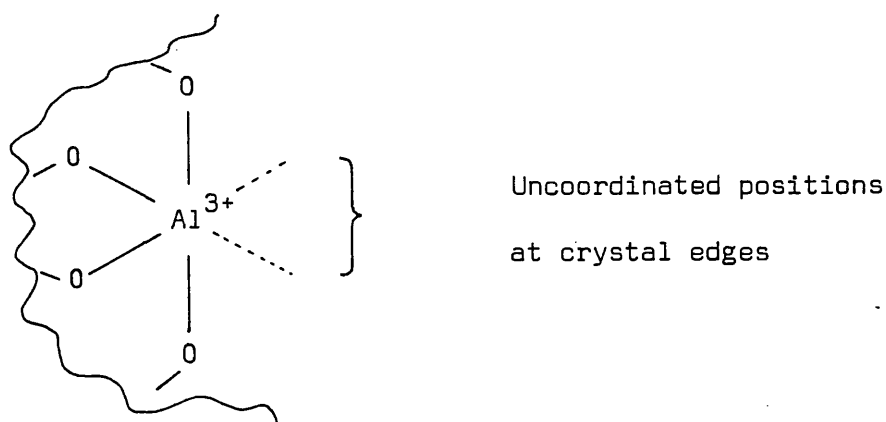
Figure (1-1) Kaolinite layer viewed along the a axis (left) and along the b axis (right). Height of atoms above the basal oxygen plane are given in nanometres (nm) from Brindley, G.W.(1961).



The basal (d(001)) spacing of kaolinite is  $\approx 0.72\text{nm}$ . From Figure (1-1) it will be seen that kaolinite is electrically neutral. But in reality kaolinite carries a small net negative charge, due to isomorphous replacement; Quirk, J.P., (1960). This is a permanent negative charge and is not pH dependent; Schofield, R.K., (1949).

Due to the positioning of -O and OH groups from adjacent layers, H bonds are formed. The H bonds cause layers to 'stack' together, hence the crystal is three dimensional and has faces and edges. The edges of kaolinite form a substantial part of the total surface area, 10-20%. The H-bonding is sufficiently strong to prevent some organic molecules being adsorbed into the interlayers. It has been proposed that the faces exhibit Bronsted acidity, Hofmann, U., et al., (1961), and the edges exhibit Lewis acidity. This is because the edges have  $\text{Al}^{3+}$  which is not fully coordinated; Figure (1-2).

Figure (1-2)  $\text{Al}^{3+}$  at Kaolinite Crystal Edges



Thus the crystal edge is a site for the sorption of cations and anions, from solution. The sorption is a function of pH, anions being adsorbed at high pH and cations at low pH. The crystal edge is also a site for electron transfer reactions, Solomon, D.H., (1968); and Theng, B.K.G., (1971).



### 1.2.2. The 2:1 Type Minerals

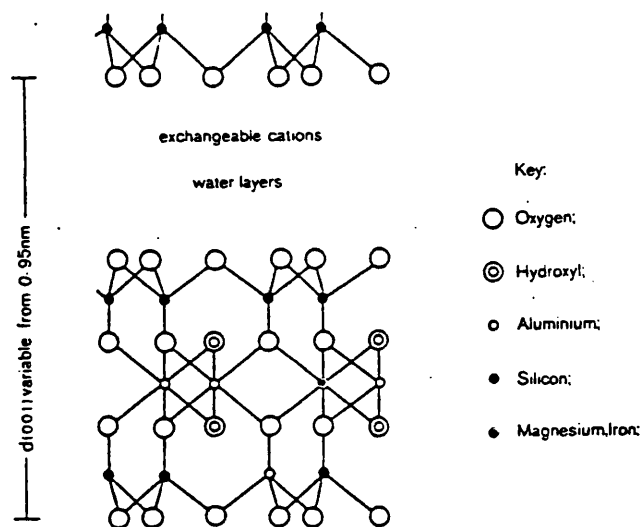
Of all the 2:1 type minerals, dioctahedral montmorillonite is the most widely used as an adsorbent. This is because montmorillonite has a very high surface area,  $\sim 760\text{m}^2\text{g}^{-1}$ , and a large cation exchange capacity; ( $\sim 1.0\text{ mol Kg}^{-1}$ , monovalent cations). Dioctahedral montmorillonites will readily form interlayer complexes with organic molecules, MacEwan, D.M.C., (1961); Weiss, A., (1963); Greenland D.J., (1965). This can clearly be demonstrated by X-ray diffraction, since the basal spacing changes when organic molecules are adsorbed into the interlayer.

Other 2:1 type minerals include pyrophyllite-talc; vermiculite, mica and brittle mica. Only montmorillonite will be discussed in detail.

## 1.2.2 Montmorillonite

The structure of montmorillonite was first discovered by Hofmann, U., et al., (1933). This basic structure was slightly modified by Marshall, C.E., (1935); Maegdefrau, E., and Hofmann, U., (1937); Hendricks, S.B., (1942) and this structure is the one generally regarded as correct, Figure (1-3).

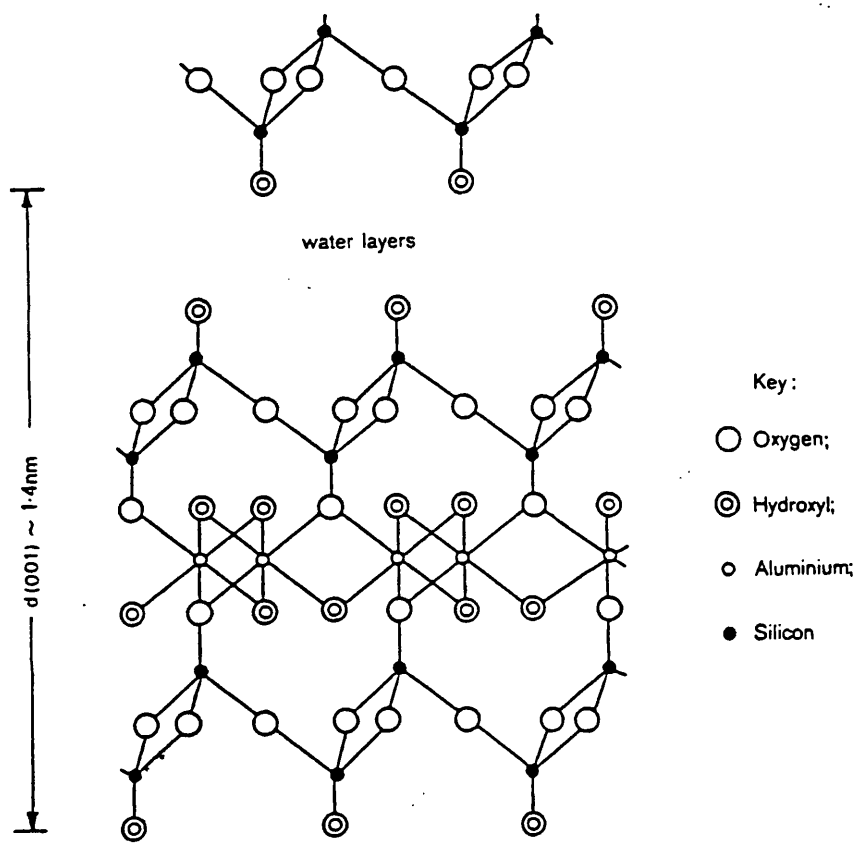
Figure (1-3) The Hofmann-Endell-Wilm-Marshall-Maegdefrau-Hendricks structure of a montmorillonite layer viewed along the a axis. Basal spacing is given in nm units.



The cation in the octahedral layer is almost exclusively  $\text{Al}^{3+}$  in montmorillonite. The permanent net negative charge upon the lattice causes adsorption of exchangeable cations upon the surface and the interlayer. The amount of water adsorbed depends upon the nature of the exchangeable cations adsorbed on the surface and the interlayers. The basal ( $d(001)$ ) spacing of montmorillonite will therefore vary from 0.95nm for the fully collapsed state, to 1.9nm for a divalent cation such as  $\text{Mg}^{2+}$ , Norrish, K. (1954). The nature of the exchangeable cation also affects the number of uncharged polar organic molecules adsorbed, because they are adsorbed by displacement of water molecules.

An alternative structure for montmorillonite has been proposed by Edelman, C.H., and Favejee, J.C.L., (1940), in which every alternate  $\text{SiO}_4$  tetrahedron is inverted. The apical oxygens of the tetrahedra, which are sticking out of the plane, are replaced by hydroxyl groups, Figure (1-4).

Figure (1-4) The montmorillonite layer structure viewed along the a axis according to Edelman and Favejee. Basal spacing in nm units.



In this type of structure no isomorphous replacement is necessary to produce an observable cation exchange capacity. This would be achieved by the dissociation of the apical hydroxyl groups. It has been postulated, by Grim, R.E., and Kulbicki, G., (1961), that both types of structure exist. The Hofmann-Endell-Wilm-Marshall-Maegdefrau-Hendricks structure being the Wyoming type montmorillonite, Figure (1-3), and the Edelman-Farejee structure the Cheto-type montmorillonite, Figure (1-4).

### 1.3 Colour and the Absorption of Light

#### 1.3.1. The Perception of Colour

Colour is a response by the human eye and brain to light of a particular wavelength. The visible region of the spectrum extends from 400 to 800nm. This represents a very small fraction of the total electro-magnetic spectrum.

Light can be regarded as either a wave, or as discrete particles (photons). The wave model, produced by Maxwell over a century ago suggested light was an electro magnetic wave with mutually perpendicular electric and magnetic vectors, these varied in a wavelike manner with respect to both time and distance. The wavefront of such a wave travelled at  $3 \times 10^8 \text{ m.s}^{-1}$ , in vacuo. The particulate theory, established by Plank and Einstein in 1905, regarded light as discrete photons, which travelled with the same velocity as the wave front in the Maxwell model. Both models have been used with equal validity.

The velocity of light (c) is a product of its frequency ( $\nu$ ) and its wavelength ( $\lambda$ ), if represented by a waveform.

$$c = \nu \cdot \lambda$$

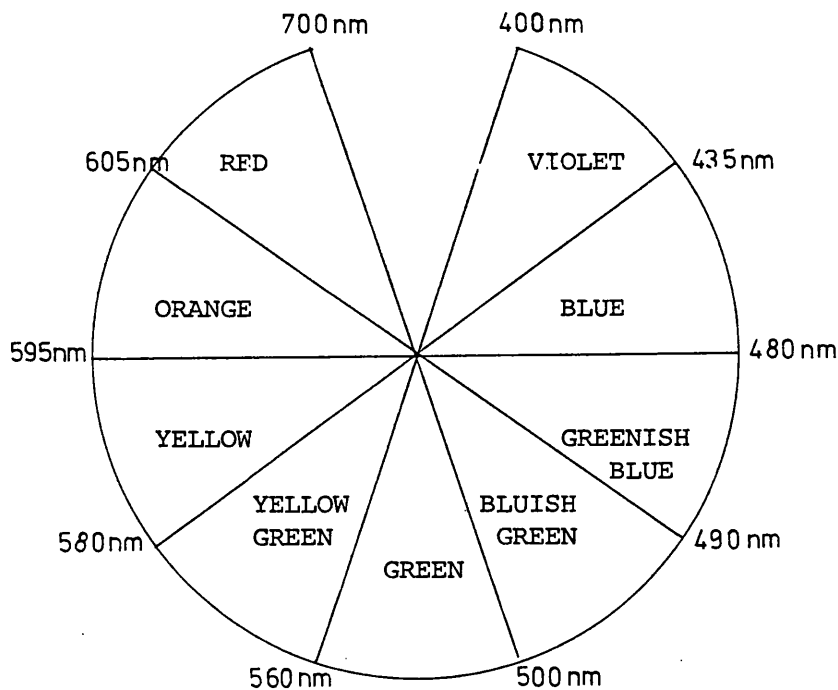
The well known Plank equation relates the frequency of the radiation with the energy (E) of a photon; where (h) is Plank's constant =  $(6.625 \times 10^{-34} \text{ J.S.})$ .

$$E = h \cdot \nu$$

If the wavelenths of light, between 400 and 800nm, are mixed, the sensation of white light is produced in the eye. White light can be split into its component parts by passage through a prism or diffraction grating. The dominant hues are in the order; red; orange; yellow; green; blue; and violet. The red end of the visible spectrum is at 800nm, and the blue end at 400nm.

The visible spectrum can be divided, for most purposes, into nine regions corresponding to colours which are easily recognisable. A colour circle can be drawn which shows some interesting features, Figure (1-5).

Figure (1-5) Colour Circle according to Griffiths, J., (1976)



The scale around the circumference has no physical significance. If all the colours of the circle are mixed white light is produced. But also if any two opposite sectors are mixed, such as blue and yellow light, white light is produced, at least as far as the eye is concerned. Such colours are called complementary colours. Purple is a non-spectral colour, but can be made by the addition of red and violet light. If these are mixed with green light, white light is produced. This is called additive mixing of colours. Additive mixing is not often observed in the normal environment, but subtractive mixing is much more widely observed. Subtractive mixing is when white light, which consists of a mixture of all the wavelengths, is passed through a filter which removes a narrow band of wavelengths. The colour observed would be the complementary colour to the one removed. If the absorbance maximum of a substance is at 650nm the observed colour will be bluish green. The colour of a substance which absorbs between 400 and 700nm can be deduced from Figure (1-5).

### 1.3.2 The Absorption of Light

The absorption of light by an organic molecule corresponds to a disturbance of the electron cloud of the molecule. Quantum theory predicts that a molecule can only exist in a limited number of discrete energy states. Equation (1-1) relates the possible energies of these states,  $E_n$ , to the wave function  $\psi_n$ .

$$\mathcal{H} \psi_n = E_n \cdot \psi_n \quad (1-1)$$

In the equation,  $\mathcal{H}$  is called the Hamiltonian operator, and is not simply a constant but 'operates' upon  $\psi_n$ . The vibrational and rotational energies of the molecule are ignored when dealing with the absorption of light (Frank-Condon principle). Due to Heisenberg's uncertainty principle only the probability of finding an electron at a particular position can be determined. Thus the probability state function is

$$\psi_n^2 \cdot d\tau \quad (1-2)$$

or more strictly  $\psi_n \cdot \psi_n^* \cdot d\tau$  where  $\psi_n^*$  is the complex conjugate of  $\psi_n$ . Thus the value of the product integrated over all space will be unity

$$\int_{-\infty}^{+\infty} \psi_n^2 \cdot d\tau = 1 \quad (1-3)$$

When a photon of light is absorbed by a molecule, it is promoted to an excited state. The energy of the light corresponds to the level of promotion.

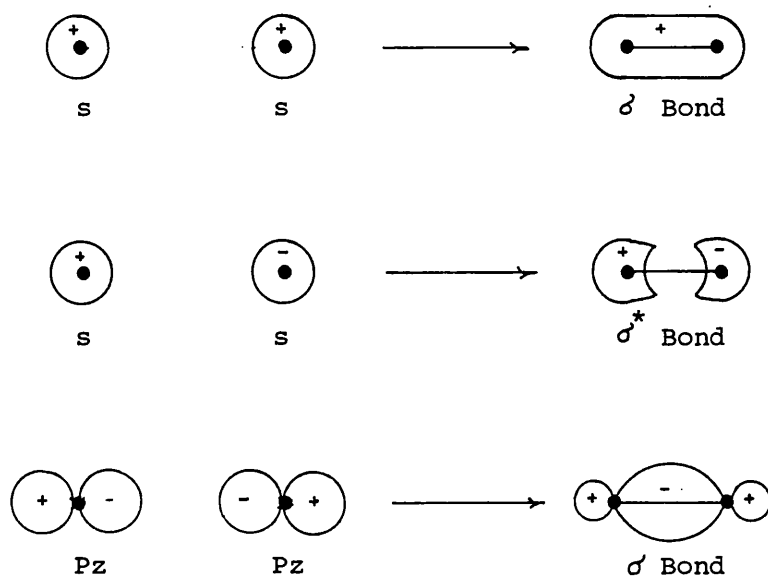


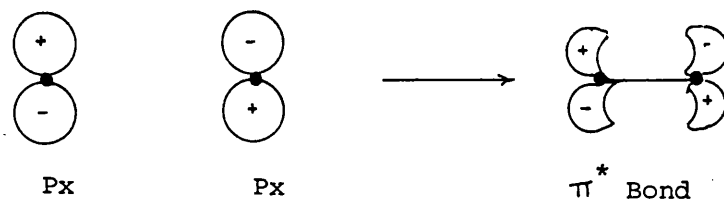
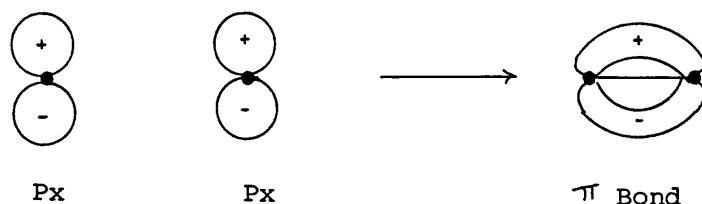
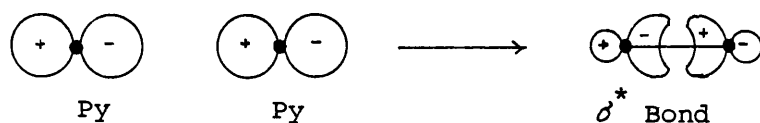
$$E \text{ excited state} - E \text{ ground state} = h\nu \quad (1-4)$$

Although equation (1-1) appears simple it is not as yet possible to calculate the exact solution for complex molecules, only approximations can be made. Generally coloured molecules are large and require further simplification to be handled mathematically.

A simple but very useful approximation relies upon the assumption that a molecular orbital can be expressed as the linear combination of atomic orbitals, the (LCAO) method. Molecules are assumed to be formed from the overlap of atomic orbitals. Since atomic orbitals are wavefunctions they have phase. In-phase overlap (++) or (--) leads to reinforcement whereas out of phase overlaps leads to cancellation. Several types of orbital and their overlapping are shown in Figure (1-6)

Figure (1-6) The Linear Combination of Atomic Orbitals.





The pictures above do not represent actual physical processes.

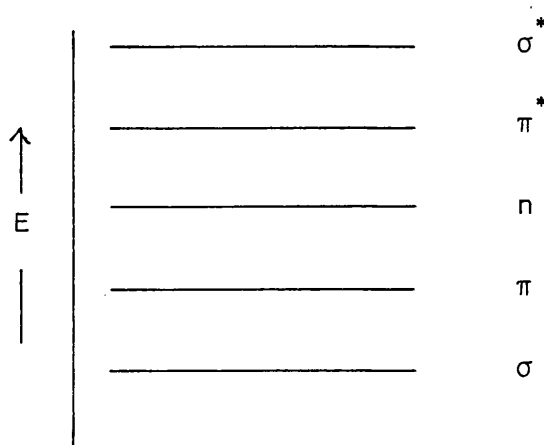
The end on overlap of two s or two p-orbitals results in a strong  $\sigma$  bond, if in phase, and a strong antibonding orbital if out of phase. Hence molecules with many sigma bonds are stable due to the high energy of the bond. P-orbitals can also overlap in a sideways manner. This is less effective than a sigma bond and is called a  $\pi$  bond. If orbitals are of higher energy than  $\sigma$  orbitals. The  $\pi$  bond differs in shape from a  $\sigma$  bond, in that its wavefunction (and thus the electron probability), has a maximum above and below the internuclear axis. Thus the  $\pi$  bond occupies a larger space than the  $\sigma$  bond, and the nuclei have less hold on the  $\pi$  electrons. The  $\pi$  bond will therefore be weaker than the  $\sigma$  bond, and the electrons will be more easily displaced. Since electronic excitation involves the displacement of

an electron from one molecular orbital to another, it would be expected that it would require less energy to displace a  $\pi$  electron than a  $\sigma$  electron from its orbital. Hence the lowest energy transitions usually involve the  $\pi$  electrons. Out of phase overlap of P orbitals results in an antibonding orbital, designated  $\pi^*$ . Just as a  $\pi$  bond has lower energy than a  $\sigma$  bond, so the  $\pi^*$  bond is less antibonding than  $\sigma^*$ . Thus the following order of orbital energies generally holds,  $\sigma < \pi < \pi^* < \sigma^*$ .

The energy gap is so large between the  $\sigma$  and  $\pi$  orbitals, that the orbitals can be treated separately. Transitions can occur from the lone pair electrons, (n), non-bonding orbital, of a heteroatom into one of the vacant (usually lowest)  $\pi^*$  orbitals of the molecule.

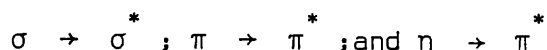
Non bonding molecular orbitals are essentially delocalised  $\pi$  orbitals, and non bonding atomic orbitals are essentially localised upon the heteroatom. Figure (1-7) shows the differences in energy of molecular orbitals.

Figure (1-7) The Energy Levels of Molecular Orbitals.



Light is absorbed when energy is transferred from the photon to a molecule. Absorption of the light causes an electronic excitation, and this causes the promotion of an electron from a lower orbital to one of higher energy. The major transitions

occurring in simple organic molecules are:-



as can be seen from Figure (1-7) the  $\sigma \rightarrow \sigma^*$  is the largest transition, and the  $n \rightarrow \pi^*$  transition is the smallest. It has already been said that  $\sigma$  and  $\pi$  orbitals can be treated separately. These transitions, occurring in small organic molecules, absorb light at the following frequencies

$\sigma \rightarrow \sigma^*$	vacuum ultraviolet (150nm)
$\pi \rightarrow \pi^*$	ultra-violet (200nm) (unconjugated)
$n \rightarrow \pi^*$	ultra-violet (200 - 400nm)

It can be seen from Plank's equation that the larger the energy of the transition the shorter the wavelength will be:

$$E = h\nu = \frac{hc}{\lambda}$$

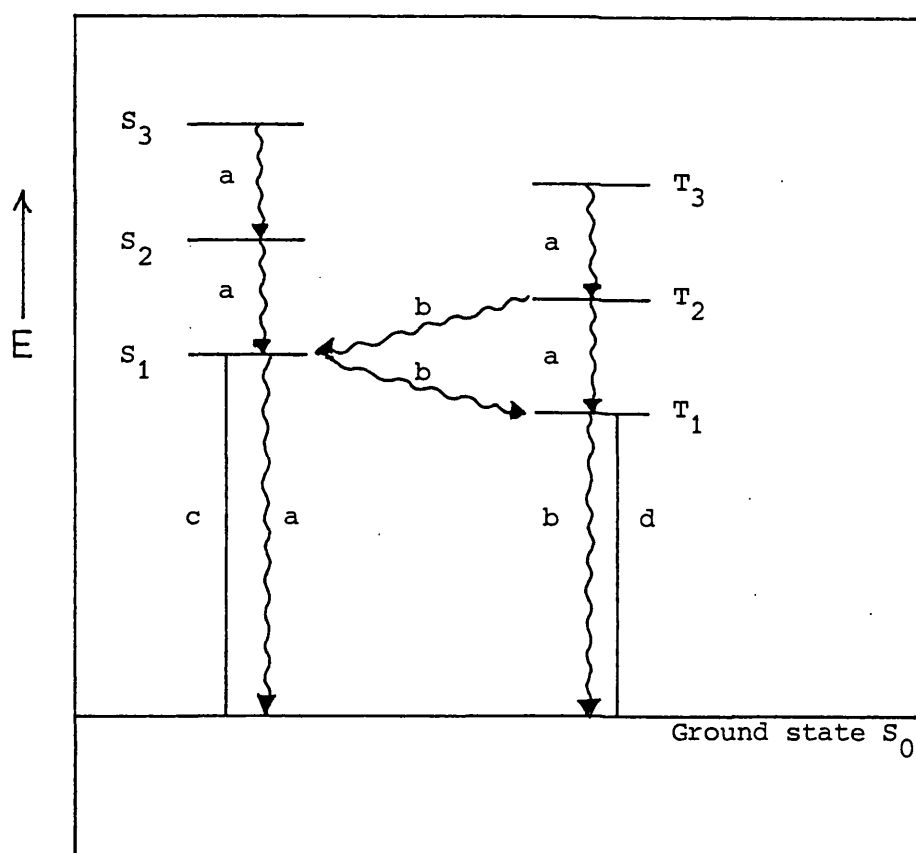
Where,  $h$  is Plank's constant,  $c$  is the velocity of light and  $\lambda$  is the wavelength.

Molecular orbital treatment of organic molecules and the absorption of light is reviewed in some depth in Griffiths, J., (1976).

Once a molecule has absorbed light it must rapidly dissipate the energy in order to prevent destruction of the molecule.

Collisions with solvent molecules is accompanied by rapid transfer of vibrational energy from the excited molecule, to the solvent, liberating heat, until it reaches the lowest vibrational level of the lowest excited singlet state ( $S_1$ ) Figure (1-8).

Figure (1-8) Energy Dissipation from Electronically Excited States



- a internal conversion.
- b intersystem crossing.
- c fluorescence.
- d phosphorescence

This process is termed internal conversion. Loss of excitation energy between singlet and triplet states is quantum mechanically forbidden, but can occur under the correct conditions. This is termed intersystem crossing. This is a relatively slow process, ( $1 - 10^{-2}$  secs), indicating its forbidden nature. Energy may also be lost from the lowest singlet excited state to the ground state by fluorescence. Phosphorescence occurs from the lowest triplet state ( $T_1$ ) to the ground state. This has a relatively long life-time.

Coloured molecules are usually large and complex, and in most cases it is difficult to predict, simple, fundamental processes to account for the absorption band, with the exception of the  $\eta \rightarrow \pi^*$  transition. These transitions retain their characteristics even in large molecules. Coloured organic molecules can be divided into four classes of chromogen.

- (a)  $\eta \rightarrow \pi^*$  chromogens.
- (b) donor-acceptor chromogens
- (c) acyclic and cyclic polyene chromogens
- (d) cyanine type chromogens.

(a)  $\eta \rightarrow \pi^*$  chromogens

These transition correspond to the promotion of an electron from a lone pair, non-bonding orbital of the heteroatom into one of the vacant, usually the lowest  $\pi^*$  orbitals.

$\eta \rightarrow \pi^*$  transitions can be classified into two types, symmetry forbidden transitions, in which the lone pair electrons occupy an essentially pure P orbital, and symmetry allowed transitions,

in which the lone pair orbital has some s characters.

It is possible to characterise  $n \rightarrow \pi^*$  transitions by the following criteria:

- (i) low intensity absorption bands, with an extinction coefficient usually less than 500.
- (ii)  $n \rightarrow \pi^*$  bands will always shift to shorter wavelengths when the solvent polarity is increased.
- (iii)  $n \rightarrow \pi^*$  bands disappear in strongly acidic media.
- (iv) the suspected  $n \rightarrow \pi^*$  band will be absent from the spectrum of the isoconjugate hydrocarbon.

(b) Donor-acceptor Chromogens

The donor-acceptor chromogen contains an electron donor group (i.e. an atom possessing lone pair electrons) directly linked to a conjugated  $\pi$  orbital system. The lone pair electrons must be aligned with the adjacent P orbitals of the  $\pi$  system, thus they are partially delocalized. The visible absorption band corresponds to the migration of the lone pair electrons from the heteroatom toward the rest of the system.

(c) Acyclic and Cyclic Polyene Chromogens

A polyene chromogen can be regarded as a collection of  $sp^2$  (or  $sp^1$ ) hybridised atoms in which complete overlap of the P

orbitals occurs. This gives a conjugated  $\pi$  electron system with as many electrons as there are atoms. A classical picture of this is a molecule with an alternating sequence of single and double bonds forming either open chains, or ring systems, or both. Polyene chromogens can exhibit  $\pi \rightarrow \pi^*$ ; and  $\eta \rightarrow \pi^*$  transitions.

(d) Cyanine - Type Chromogens

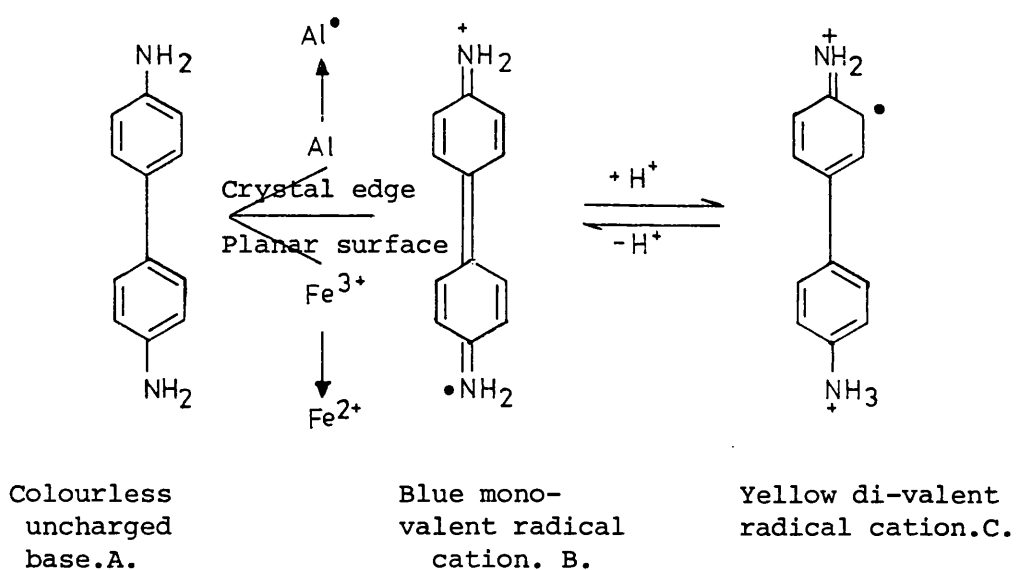
Odd alternant hydrocarbons possess a non-bonding molecular orbital midway between the bonding and antibonding  $\pi^*$  orbitals. The anion of such a system will contain two paired electrons in the NBMO, because this is much closer to the  $\pi^*$  orbital, the first absorption band will lie at unusually long wavelengths.



1.4 Reactions Upon Clay Minerals

When certain aromatic amines are adsorbed upon clay minerals they are converted to their coloured derivatives, Hauser, E.A., and Leggett, M.B., (1940); Meunier, P., (1942). Reactions occur with both 1:1 and 2:1 type minerals. It has been shown by Weil-Malherbe, H., and Weiss, J. (1948) that both Bronsted acidity and redox reactions occur with certain aromatic amines. Treatment with ammonia results in loss of Bronsted acidity and treatment with stannous chloride, a Lewis base, results in loss of Lewis acidity.

In colour reactions of aromatic amines with clay minerals both Lewis and Bronsted acidity affect the adsorption of the amines, both at the crystal surface and edges. Solomon, D.H., et al., (1968)a, and Solomon, D.H., et al., (1968)b, have proposed a model based on charge transfer between clay and adsorbed organic molecule. The reaction of benzidine upon layer silicates is perhaps one of the best known clay-organic reactions.



Several workers have agreed that the mechanism for the formation of the blue monovalent radical cation involves electron transfer from the diamine to the mineral, Hauser, E.A., and Leggett M.B., (1940); Hendricks, S.B., and Alexander, L.T., (1940). The blue colour is thought to arise from conjugation of the NBO of the nitrogen and the  $\pi$  electrons of the benzene ring. If the pH of the system falls below 2 the radical cation B can accept a further proton on the lone pair of the nitrogen atom, giving a yellow colour.

Benzidine has been used as an indicator of clay mineral types. Treatment of kaolinite edges with sodium hexametaphosphate showed an appreciable decrease in the colour intensity formed, Michaels, A.S., (1958). This indicated to Solomon, D.H. et al., (1968)b, that in some minerals, such as kaolinite, the crystal edges have oxidizing (electron-accepting) sites while others such as montmorillonite have sites mainly on the planar surfaces. It was suggested that the Lewis acids at the crystal edge were aluminium atoms which were incompletely coordinated. Solomon, D.H., et al., (1968)b also proved conclusively that octahedrally coordinated ferric ions affect the colour formed with benzidine.

## 1.5 Methods of Studying Reactions upon Solid Surfaces

The study of reactions upon solid surfaces can be divided into two types, direct and indirect methods. Direct methods involve spectroscopic measurements such as N.M.R., I.R., u/v, visible and E.S.R. The direct method has the advantage of studying the reaction in situ. But has the disadvantage that the spectrum formed is often complicated by the surface and it is often difficult to identify several products of a reaction. The indirect method involves removal of the substance to be studied from the surface and then examining the material in solution. This has the advantage of being able to separate several components and quantify accurately small quantities. The disadvantage of this method is that the material may not be the same if desorbed from the clay mineral. Also it may not be possible to remove the products from the clay mineral. Very little needs to be mentioned about the indirect methods since this is explained in some detail in Chapter 3.

A convenient method to study the fates of coloured organic molecules upon clay minerals is visible spectroscopy. In particular, diffuse reflectance spectroscopy in the range 200-800nm.

The most general theory of diffuse reflectance was developed by Kubelka, P., and Munk, F. (1931); Kubelka, P., (1948). For infinitely thick layers, (for practical purposes, with fine powders, this is already achieved at a layer depth of a few millimeters), the Kubelka-Munk equation reads:-

$$F(R_{\infty}) \equiv \frac{(1 - R_{\infty})^2}{2R_{\infty}} = \frac{k}{s}$$

Where  $R_{\infty} = \Phi_{\text{sample}} / \Phi_{\text{standard}}$ , is the relative diffuse reflectance of such a layer, referred to a non-absorbing standard, e.g. MgO or NaCl,  $K$  is the molar absorption coefficient of the sample, defined by Lambert's law.

$\Phi = \Phi_0 \exp(-k.d)$ , and  $s$  is the scattering coefficient, which will provisionally be assumed to be independent of wavelength.

According to the Kubelka-Munk equation, a plot of  $F(R_{\infty})$  as a function of the extinction coefficient  $K$ , should yield a straight line.  $K$  can be determined from transmission experiments. This theory has been confirmed for weakly absorbing materials, Kortum, G., and Schottler, H., (1953).

Diffuse reflectance is particularly useful when the sample to be studied is diluted with an adsorbent. Since all uncertainties about regular reflection, or differing grain size are virtually eliminated. The dilution should be  $10^{-3}$  to  $10^{-5}$  adsorbate: white standard, so that if the surface area of the standard is high there is not complete coverage of the surface. This stops adsorbate - adsorbate interactions and the spectrum of the adsorbed single molecule is observed. This spectrum can be similar or very different from the solution spectrum, depending upon the adsorbent - adsorbate interactions.

If the forces holding the adsorbed molecule are only Van-der Waals forces, the difference between the transmittance and reflectance spectrum are: the reflectance spectrum is broadened; the bands are displaced toward longer wavelengths; the vibrational structure, if present at all, is strongly suppressed. Diffuse

reflectance can also be used when the interactions between adsorbent and adsorbate are strong (chemiadsorption). Generally the changes in the spectrum of adsorbate are large compared to the free molecule Kortum, G., and Vogel, J. (1960); Kortum, G., (1962). Similarly photochemical reactions can easily be followed quantitatively and evaluated kinetically using diffuse reflectance spectroscopy, Kortum, G., et al., (1962).

## CHAPTER 2

### SURFACE ACIDITY OF KAOLINITE .

## Surface Acidity of Kaolinite

### 2.1 Introduction

It has been shown in Chapter 1 that kaolinite is a three dimensional crystal and has flat faces, (d (001)), and edges, page 6 . The faces have strong Bronsted acid sites upon them, which are pH independent and are caused by isomorphous replacement. The edges have a pH dependent charge, and exhibit Lewis acidity, Solomon, D.H. (1968). Isomorphous substitution causes the lattice to have a net negative charge. This is neutralised by cations from solution.

The surface acidity of certain kaolinites and montmorillonites have been estimated by examining the colour changes of pH indicators when absorbed upon clay minerals, in non polar solvents, Walling, C., (1950); Benesi, H.A., (1956); Benesi, H.A., (1957). The basis of determining the acid strength of the surface, is the colour change of a Hammett indicator, Hammett, L.P., and Deyrup, A.J. (1932). The acid strength is expressed as the Hammett acidity function ( $H_0$ ).  $H_0$  gives a quantitative estimate of the ability of the surface to convert an adsorbed base to its conjugate acid. It is related to the pKa of the indicator by:-

$$H_0 = pK_a + \log \frac{B}{A} \quad (2-1)$$

Where B and A are the concentrations of basic and acidic forms, of the indicator respectively.  $H_0$  can be considered as an extension of the pH scale into media where the activity of

the hydrogen ion is very different to its stoichiometric concentration. The method relies upon a series of indicators being chosen such that they change colour in different concentrations of sulphuric acid. The  $H_0$  of the surface is then said to lie between the indicator, in the series, that is not protonated and the previous indicator, that is protonated, in the series. Hammett indicators have been used extensively for determining the surface acidity of clay minerals. But the reliability of certain measurements, Henmi, T., and Wada, K., (1974), have been doubted by others, Laura, R.D., (1976). Laura, R.D., (1976) states that three fundamental conditions must be fulfilled in order to produce meaningful results for the measurement of surface acidity, using Hammett indicators:-

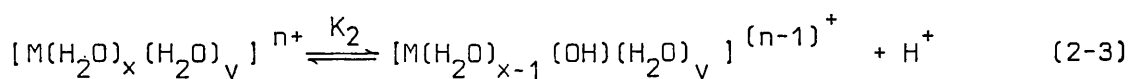
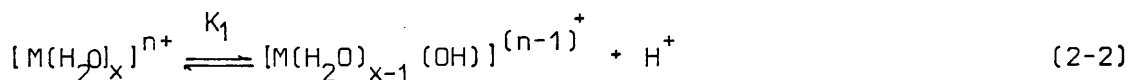
- (i) Clay mineral surfaces must act as proton donors;
- (ii) The proton transfer on clay surfaces must strictly only be a function of relative acidities/basicities of clay surfaces and the indicator base, and;
- (iii) The phenomenon of colour change must only be due to protonation.

Laura, R.D., (1976) also states that in the measurement of the surface acidity of montmorillonite by Henmi, T., and Wada, K., (1974) none of these conditions are fulfilled, and that the surface of montmorillonite is basic. This statement is correct but misleading. The lattice is negatively charged and so must be basic, but in any real system the negative lattice maintains neutrality by adsorbing cations from solution. The adsorbed cations then polarise water molecules which give the clay its acidic properties, Henmi, T., and Wada, K., (1976). The argument by Laura is purely semantic. Laura, R.D., (1976) cites various references which



produce anomalous results using Hammett indicators. In such cases, certain indicators are not protonated when their pKa suggests they should and vice versa.

An enhancement of surface acidity was observed when a Kaolinite sample was dried, Solomon, D.H., and Murray, H.H., (1972). Mortland, M.M., (1970) attributed this effect to an increase in the polarization of the fewer water molecules remaining in the exchangeable cation hydration shell. At high relative humidity the polarization effect exerted by the cation upon the water is spread over many more water molecules. The equilibria below, according to Mortland, M.M., and Raman, K.V., (1968) show the situations of low and high relative humidity.



Where  $K_1$  and  $K_2$  are the equilibrium constants for the reactions; M is the exchangeable cation of valency n; x and y are the number of water molecules in the inner and outer coordination spheres of the cation respectively. Equilibrium (2-2) represents the dry system where  $K_1 > K_2$ . These equilibria represent typical Bronsted acidity.

In the colour reactions of clay minerals with aromatic amines both Lewis and Bronsted acidity are involved.

This work was designed to clarify some of the arguments raised by Laura, R.D. (1976). It seemed likely that any anomalous

results were caused by differences in the energy of adsorption of the protonated and the un-protonated forms upon the clay mineral. If the protonated form is adsorbed far more readily than the un-protonated form, protonation of that indicator is more likely than in solution. Where the reverse is true, an unprotonated indicator will not be protonated when its pKa dictates it should. If several indicators are used to measure the acid strength of a particular clay mineral many different values could be obtained. It is the value of the dissociation constant in the solid phase ( $K^S$ ) which is required, not the pKa in solution, where:-



$$K^S = \frac{[D^S][H^+]}{[D^S H^+]} \quad (2-5)$$

Where  $D^S$  is the concentration of the unprotonated dye in the solid phase.

$K^S$  is the true surface equilibrium constant for the indicator. If  $K^S$  is greatly different from the dissociation constant in solution there will be large discrepancies in the  $H_0$  measured. To obtain reliable results, the value of  $K^S$  must be determined for each indicator, on the particular surface to be measured.

2.1.2. A Method to Determine the Surface Acidity, by adsorption from solution, of kaolinite

It was postulated that in order to obtain a reliable value for the Hammett acidity function ( $H_0$ ), the dissociation constant of the adsorbed base, on the surface, must be obtained.

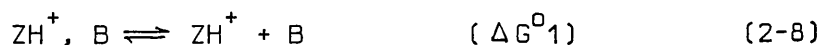


$$K^S = \frac{[B^S][H^+]}{[B^S H^+]} \quad (2-7)$$

The superscripts refer to the surface phase.

A value for  $K^S$  cannot be directly found since this requires a value for the Hammett acidity function. But if the energy of adsorption for the unprotonated and protonated indicator are known, the value of  $K^S$  can be obtained:-

1. Refers: to the desorption of the free base from the surface,



2. to the adsorption (or strictly ion exchange) of the protonated base,



3. to the surface protonation itself,



4. to the acid dissociation of the dye in solution



$$\text{In general } \Delta G^{\circ 1} + \Delta G^{\circ 2} = \Delta G^{\circ 3} + \Delta G^{\circ 4} \quad (2-12)$$

$$\text{and if } \Delta G_n^{\circ} = RT \ln K_n \quad (2-13)$$

$$\text{then } K_1 \cdot K_2 = K_3 \cdot K_4 \quad (2-14)$$

$$\text{and therefore } K_3 = \frac{K_1 \cdot K_2}{K_4} \quad (2-15)$$

or if the equilibrium constant, for the adsorption of the free base is written  $K'_1$  then,

$$K'_1 = \frac{1}{K_1} \quad (2-16)$$

$$\text{and } K_3 = \frac{K_2}{K'_1 \cdot K_4} \quad (2-17)$$

If the equilibrium constant, ( $K_3$ ), for the surface protonation, is written in terms of a dissociation constant, ( $K^S$ ), then:

$$K^S = \frac{1}{K_3} \quad , \quad \text{and} \quad (2-18)$$

$$\text{Therefore } K^S = \frac{K'_1 \cdot K_4}{K_2} \quad (2-19)$$

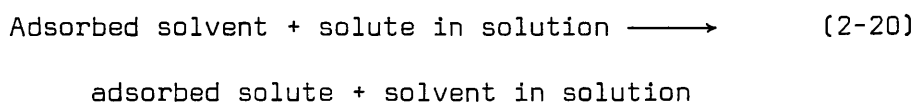
If the pH of the bulk solution is chosen such that only one species is present, and that species is adsorbed without further protonation, the value of  $K_1$  and  $K_2$  can be determined from an adsorption isotherm. Adsorption of dyes from solution often produces an isotherm the shape of which has been deduced by Langmuir, on certain assumptions, originally for the adsorption of gases onto solids. The assumptions are often reasonable approximations for dye adsorption from solution. The approximations are:-

1. The adsorption should be reversible; a purely physical process.
2. The adsorbate should not affect the adsorption of further adsorbate molecules, i.e. the energy of adsorption of each molecule is identical.
3. The solute and solvent must occupy the same area, when adsorbed on the surface.
4. The surface should be ideal.
5. The solution should be dilute.

2.1.3. The Langmuir Equation : Theory. (Hiemenz, P.C., 1977)

The Langmuir isotherm is an isotherm that is both easy to understand theoretically and is widely applicable to experimental data.

Considering dilute solutions only:-



The equilibrium constant for this reaction is:-

$$K' = \frac{a_2^s \cdot a_1^b}{a_1^s \cdot a_2^b} \quad (2-21)$$

Where 1 refers to the solvent, 2 refers to the solute; a is the activity of the species and superscripts s and b signify surface and bulk values respectively.

Next assume that the two dimensional surface is ideal, this allows us to replace activity at the surface with the mole fraction at the surface  $x^s$ :

$$K' = \frac{x_2^s \cdot a_1^b}{x_1^s \cdot a_2^b} \quad (2-22)$$

Since the surface only contains two components:

$$x_1^s + x_2^s = 1 \quad (2-23)$$

Therefore

$$K' = \frac{x_2^s \cdot a_1^b}{(1-x_2^s)a_2^b} \quad (2-24)$$

Rearrange to:-

$$x_2^s = \frac{K' a_2^b / a_1^b}{\left[ K' a_2^b / a_1^b \right] + 1} \quad (2-25)$$

In dilute solution the activity of the solvent is essentially constant, so that ratio  $K' / a_1^b$  may be defined as a new constant  $K$ .

$$x_2^s = \frac{K \cdot a_2^b}{K a_2^b + 1} \quad (2-26)$$

This is one form of the Langmuir adsorption isotherm.

If the solvent and solute occupy equal areas on the surface,  $x_1^s \cdot A$ , equals the fraction of the surface occupied by the solvent,  $\theta$ . Since  $\theta_1 + \theta_2 = 1$ , the ratio  $\theta_2 / \theta_1$ , rearranges the same as the ratio  $x_2^s / x_1^s$ , to give:

$$\theta_2 = \frac{K a_2^b}{K a_2^b + 1} \quad (2-27)$$

The subscript and superscript are now redundant since the equation is solely in terms of the solute.

At infinite dilution  $a \rightarrow 0$  and equation (2-27) becomes:

$$\theta = Ka \quad (2-28)$$

If  $Ka \gg 1$  equation (2.27) becomes

$$\theta = 1 \quad (2-29)$$

Equation (2.28) shows that  $\theta$  increases linearly with an initial slope of  $K$ . This slope will be greater the further to the right the equilibrium represented by equation (2.20) lies. Equation (2.29) indicates the saturation of the surface occurs at high concentrations of solute.

Experimentally the number of moles of solute adsorbed per unit weight of adsorbent,  $n_2^s/w$ , are measured and not the fraction of sites filled by solute.

The fraction covered is related to these quantities as follows:-

$$\theta = \frac{n_2^s \cdot N_A \sigma^0}{A} = \frac{n_2^s N_A \sigma^0}{W \text{ Asp}}$$

$A$  = Total surface area  
 $\text{Asp}$  = Specific surface area of adsorbent  
 $N_A$  = Avogadro's Number.  
 $\sigma^0$  = area occupied per adsorbed molecule.

Heimenz, P., (1977) also describes an equation for systems where the Langmuir assumptions are not strictly adhered to,



yet the experimental data resembles the Langmuir equation Fig (2-3)

The Langmuir equation is then written as:-

$$m \cdot \frac{n_2^S}{W} = \frac{(m/b)c}{(m/b)c + 1} \quad (2.30)$$

Where the constants m and b have no physical significance.

Equation (2-30) can be rearranged to produce a straight line plot,

(2.31).

$$\frac{c}{n_2^S/w} = mc + b \quad (2.31)$$

Therefore a plot of  $c/n_2^S/w$  versus c should yield a straight line.

If the experimental system matches the model, the values of m and b can be assigned a physical significance:-

$$m = \frac{N_A \sigma^0}{A_{sp}} \quad (2-32)$$

and  $\frac{m}{b} = K \quad (2-33)$

## 2.2 Experimental

### 2.2.1. Materials

#### (i) Kaolinite

The kaolinite used was an American Petroleum Institute Project 49 standard clay mineral obtained from Ward's Natural Science Establishment, Inc. Rochester, New York. To ensure standard conditions for all samples, the material was firstly ground in a glass pestle and mortar for 10 mins; a 1 gram sample of this material was then ground in an agate mortar for 30 mins.

#### (ii) Crystal Violet

The crystal violet used was a sample obtained from Hopkin and Williams. The unpurified compound was assayed for purity by a melting point determination  $184^{\circ}\text{C}$  (decomposed), and thin layer chromatography. The results of the thin layer chromatography, (TLC) can be seen on page 101 Chapter 3, this shows a large number of impurities but that the major band, crystal violet, accounted for 95% of the total absorbance of the compound.

#### (iii) Ortho, Meta and Para Nitroaniline

The samples of ortho, meta and para-nitroaniline used in the study were commercial samples supplied by Hopkin and Williams.

These compounds were used without further purification.

(iv) All the water used in the study was high purity double distilled water, specific conductance  $10^{-6} \text{ ohm}^{-1} \text{ cm}^{-1}$ . All other chemicals used were of Analar grade unless otherwise stated.

## 2.2.2. Methods

### (i) Preparation of a Homoionic Kaolinite

The preparation of a homoionic kaolinite is described on page 87 Chapter 3.

### (ii) Adsorption Isotherm

One gram of a homoionic kaolinite was slurried at 10wt % solids in a dye solution of known initial concentration. The solution above the solids was adjusted to a final fixed pH. The slurry was then vigorously shaken for 16hrs at 20<sup>o</sup>C by a mechanical shaker. All glass-ware had been soaked in a saturated solution of the dye and then thoroughly washed until no dye was present in the washings. This prevented any dye being lost due to adsorption onto the glass surface. The control was a tube treated in the same way but with only the solvent present, hence if any residual dye was removed over the 16hrs it would be included in the control.

The slurry was then centrifuged at 5,000 rpm for 20 mins. The supernatant was decanted and recentrifuged under the same conditions, to remove any residual clay particles. The supernatant was then photometrically assayed for the concentration of dye remaining in solution. It was therefore possible to determine the amount of dye adsorbed, by difference, upon the clay. The equilibrium concentration was then plotted versus amount adsorbed.

(iii) Visible Spectroscopy

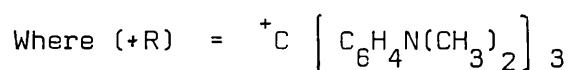
All visible spectra were obtained from a Pye Unicam SP1800 series 2 spectrophotometer with an AR25 linear recorder. Diffuse reflectance spectra were obtained on the same instrument, but with a Pye Unicam SP890 diffuse reflectance unit in the position of the normal mirror arrangement.

## 2.3 Results and Discussion

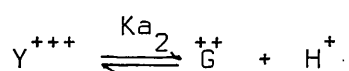
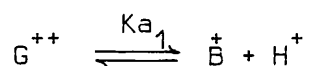
### 2.3.1 Crystal Violet in Aqueous Acidic Solution

When crystal violet is in aqueous acidic solution, it can exist as one of three coloured species; violet, green or yellow. The hydrogen ion concentration and the pKa's of the protonations determines the distribution of the ionic species. This behaviour has been thoroughly studied by Cigen, R., (1958). The three coloured species are the mono, di and tricaticonic species of crystal violet. Cigen designated the three species in the following way:-

Violet	(B)	= +R	monocationic
Green	(G)	= +RH <sup>+</sup>	di-cationic
Yellow	(Y)	= +RH <sub>2</sub> <sup>++</sup>	tri-cationic



A diagram summarizing the protonation and hydration equilibria of crystal violet can be seen on page 72 Chapter 3. The visible spectra of the three species can be seen on page 92 Chapter 3. The violet and yellow forms represent the spectra of the pure mono and tri cationic form respectively. The spectra of the pure green species cannot be experimentally determined because the pKa's for the conversion of the green to blue, and green to yellow species are not sufficiently separated. Hence the green species cannot exist alone in solution



The dissociation constants as determined by Cigen for the above reactions are:-

$$K_{a_1} = \frac{[B^+][H^+]}{[G^{++}]} = 4.07 \times 10^{-3} \text{ M}; (\text{p}K_{a_1} = 2.39)$$

$$K_{a_2} = \frac{[G^{++}][H^+]}{[Y^{+++}]} = 1.22 \times 10^{-1} \text{ M}; (\text{p}K_{a_2} = 0.91)$$

The  $\lambda$  max values for the blue and yellow species, determined experimentally, are 592nm and 435nm respectively. The  $\lambda$  max for the green species has been determined by calculation (Cigen, R., (1958)) and is 635nm.

It can be calculated from the dissociation constants, that at pH 1.65, the green species accounts for  $\sim 74\%$  of the total dye concentration, while the yellow and blue species account for 13% each. In Figure (2-1), it will be seen that the peak heights for the blue, and green species are similar at pH 1.65. This is because the 592nm peak height is greater than it should be, due to overlap of the 625nm peak. If the  $\log_{10}$  of the ratio of absorbances (635nm/592nm), are plotted versus pH, a straight line is produced, Figure (2-2). Although Figure (2-2) is an empirical observation it enables the pH of a solution to be determined, by finding the  $\log_{10}$  (absorbance 635nm/absorbance 592nm).;  $\log_{10} (A_{635\text{nm}}/A_{592\text{nm}})$ .

$$\text{pH} = \text{p}K_a - \log \frac{(A_{625})}{(A_{592})}$$

FIGURE (2-1), The absorbance of the three species of Crystal Violet in acidic solution.

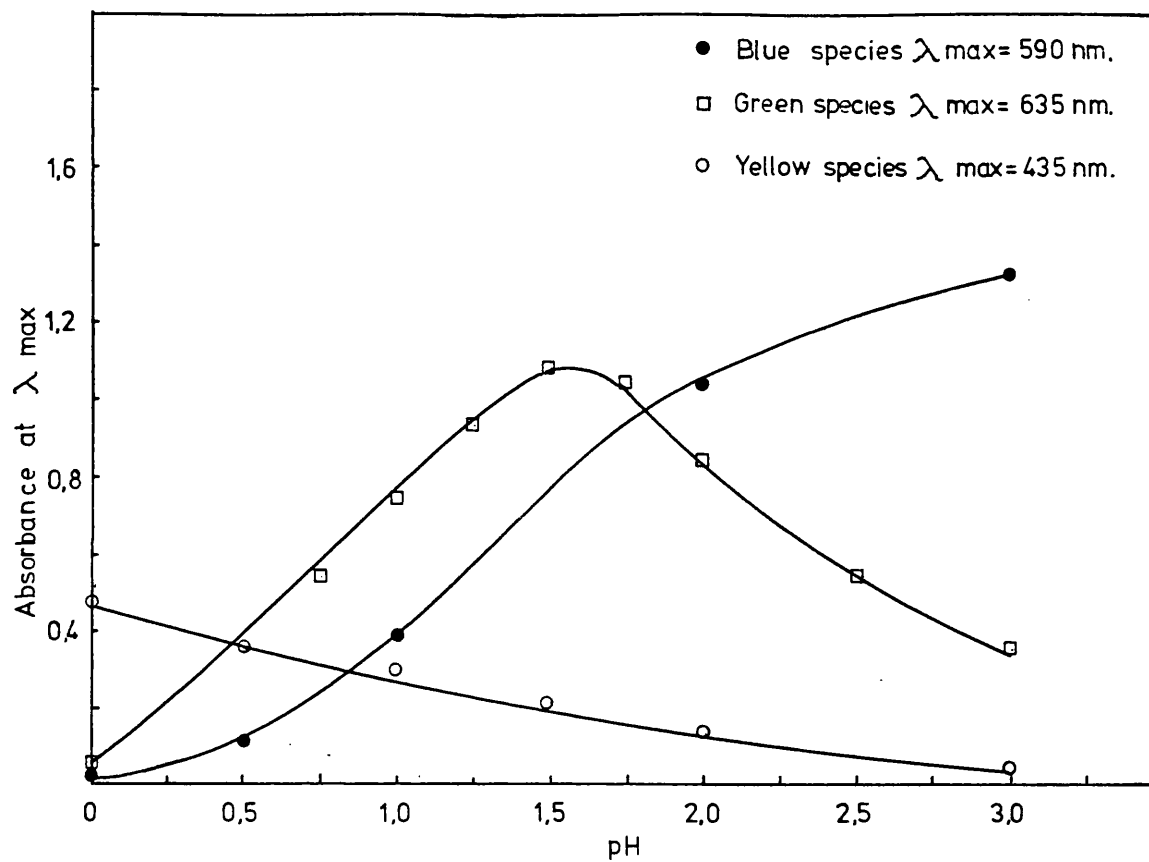
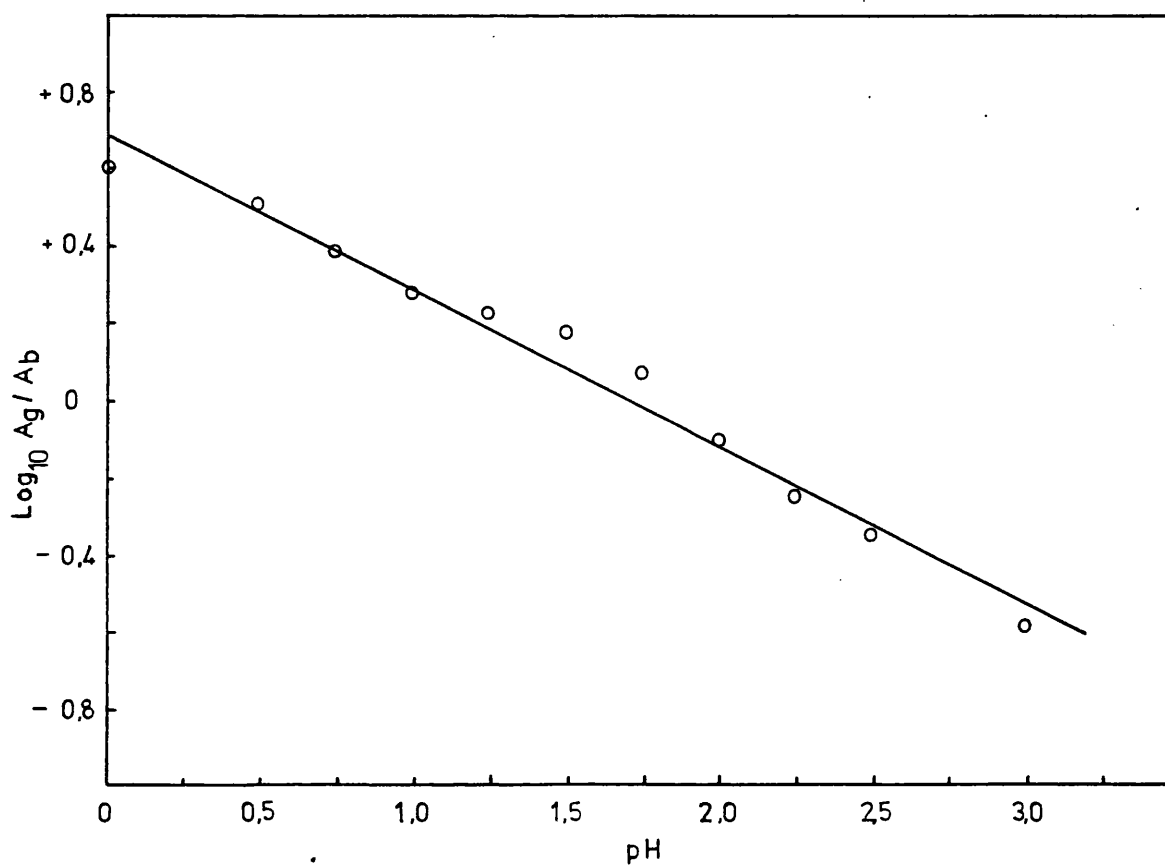
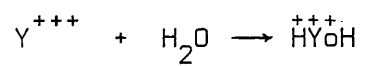
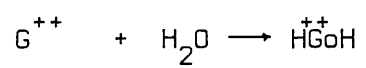
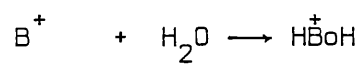


FIGURE (2-2). Ratio of absorbance at 635 nm to absorbance at 590 nm of crystal violet as a function of pH.





All absorbance values were extrapolated to zero time  
due to the formation of the colourless hydrated species shown below:-



Colourless

### 3.2.2. An Adsorption Isotherm of Crystal Violet upon H<sup>+</sup>-Kaolinite

The adsorption isotherm of crystal violet upon H<sup>+</sup>-kaolinite is shown in Figure (2-3). It can be seen that at pH 3.0, measured in the aqueous phase at equilibrium with sedimented solids, that the isotherm was of the Langmuir type. This shows that even at high coverage, 25  $\mu$ moles CV/g kaolinite, 99% of the crystal violet was adsorbed upon the kaolinite surface.

FIGURE (2—3) . Adsorption Isotherm of Crystal violet on  $H^+$ -Kaolinite  
at 20°C and pH 3,0

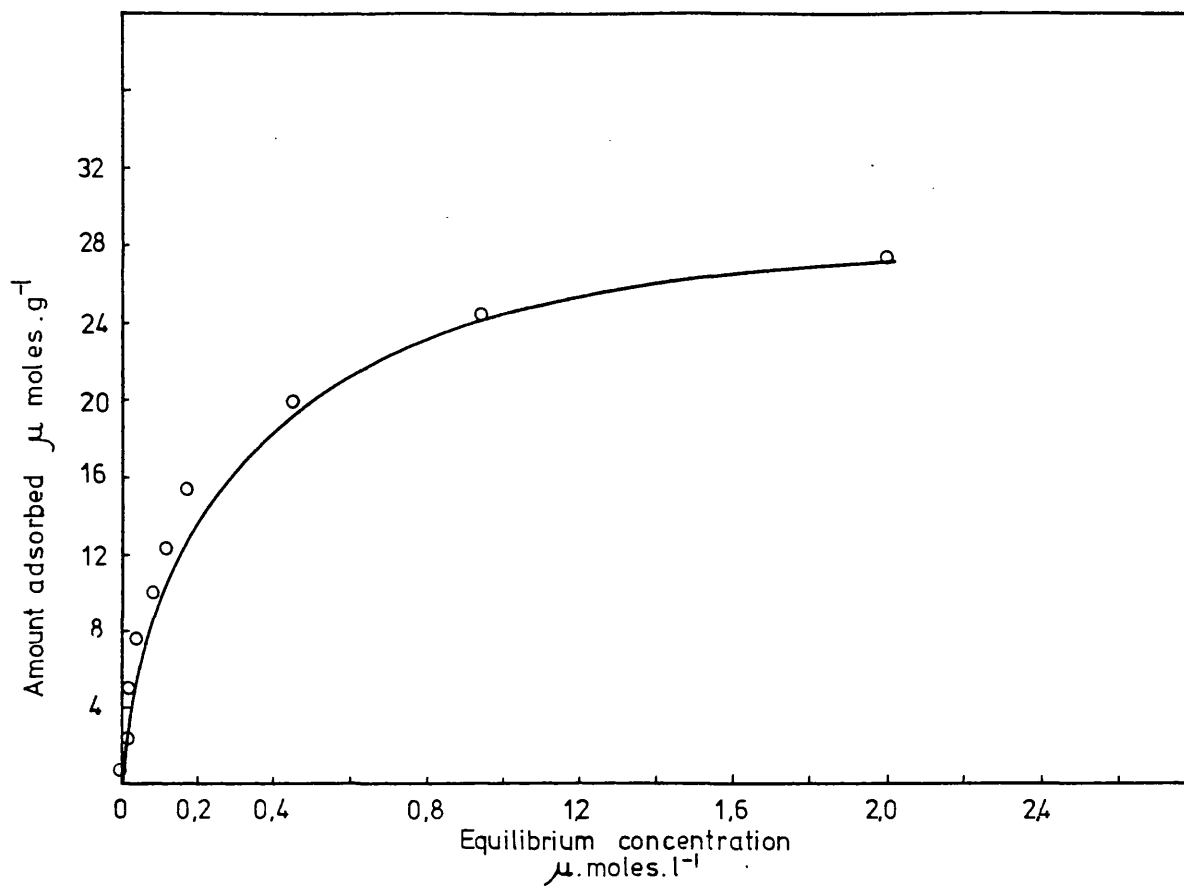
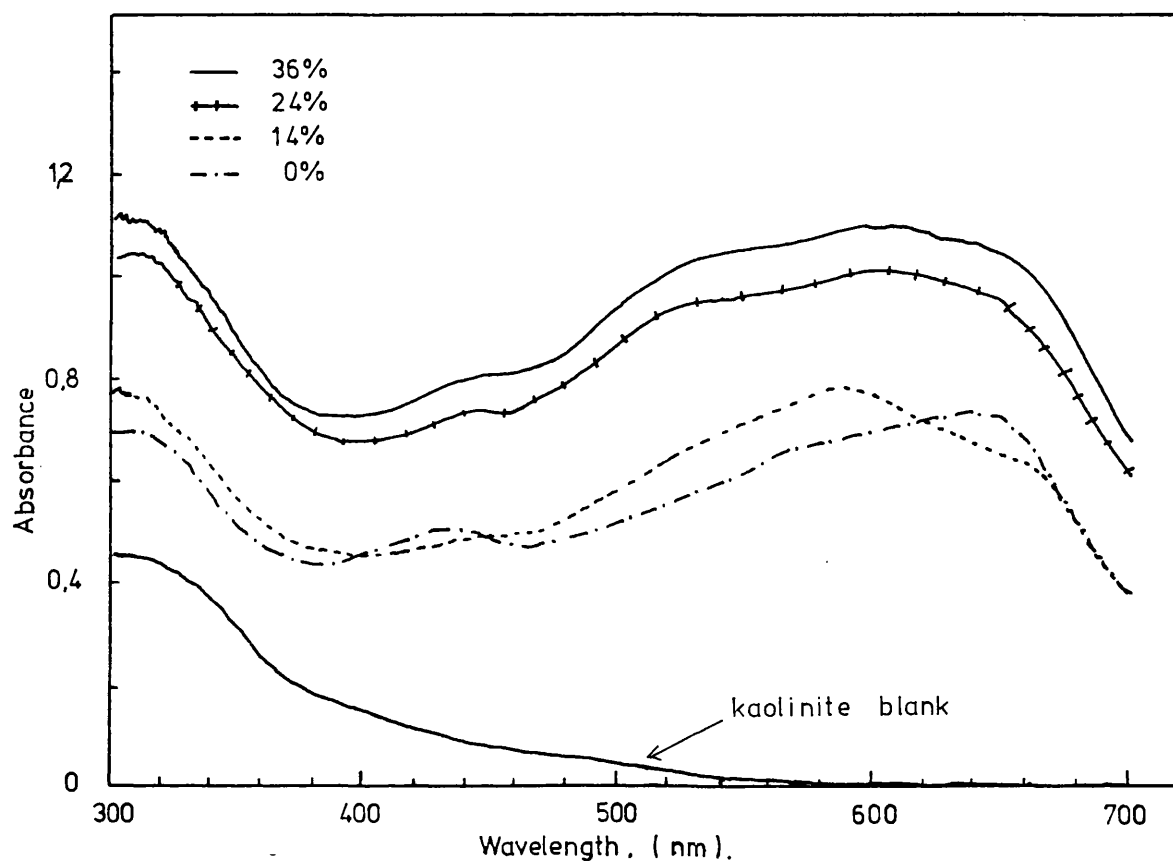


FIGURE.(2—4) Diffuse reflectance spectra of crystal violet at four  
moisture levels.



2.3.3 To Determine the Amount of Water Tolerable to Produce  
a Sharp Reflectance Spectrum of Crystal Violet on Kaolinite

The amount of water remaining in a sample of kaolinite has drastic effects upon the spectrum of the adsorbed CV, Figure (2-4). The spectrum is broadened and shows no detail rendering it unusable for measurements. A reduction in water content can be achieved either by heating the sample or applying pressure and squeezing the water out. Either method is appropriate for water, but since the solution to be removed was  $10^{-3}$  molar HCl, the application of heat was ruled out as this would change the acid concentration. Therefore the moisture was removed by mechanical pressure in a hydraulic press. Figure (2-5) shows a typical graph of initial water content against water remaining after pressure has been applied. This curve represents an application of 1500 psi for 10 mins, and it can be seen that the curve plateaus at 30% moisture. Higher pressure reduces the plateau to below 30%. An acceptable spectrum of CV adsorbed upon kaolinite was obtained at 12% moisture. The spectrum did not differ significantly from a dry sample, Figure (2.6). To reduce the moisture content to this level a pressure of 7500 psi was applied for 10 mins. At this moisture level it was estimated that there would be at least a molecular layer of  $10^{-3}$  M HCl covering the kaolinite surface

FIGURE.(2—5). The effect of pressure on drying Kaolinite.

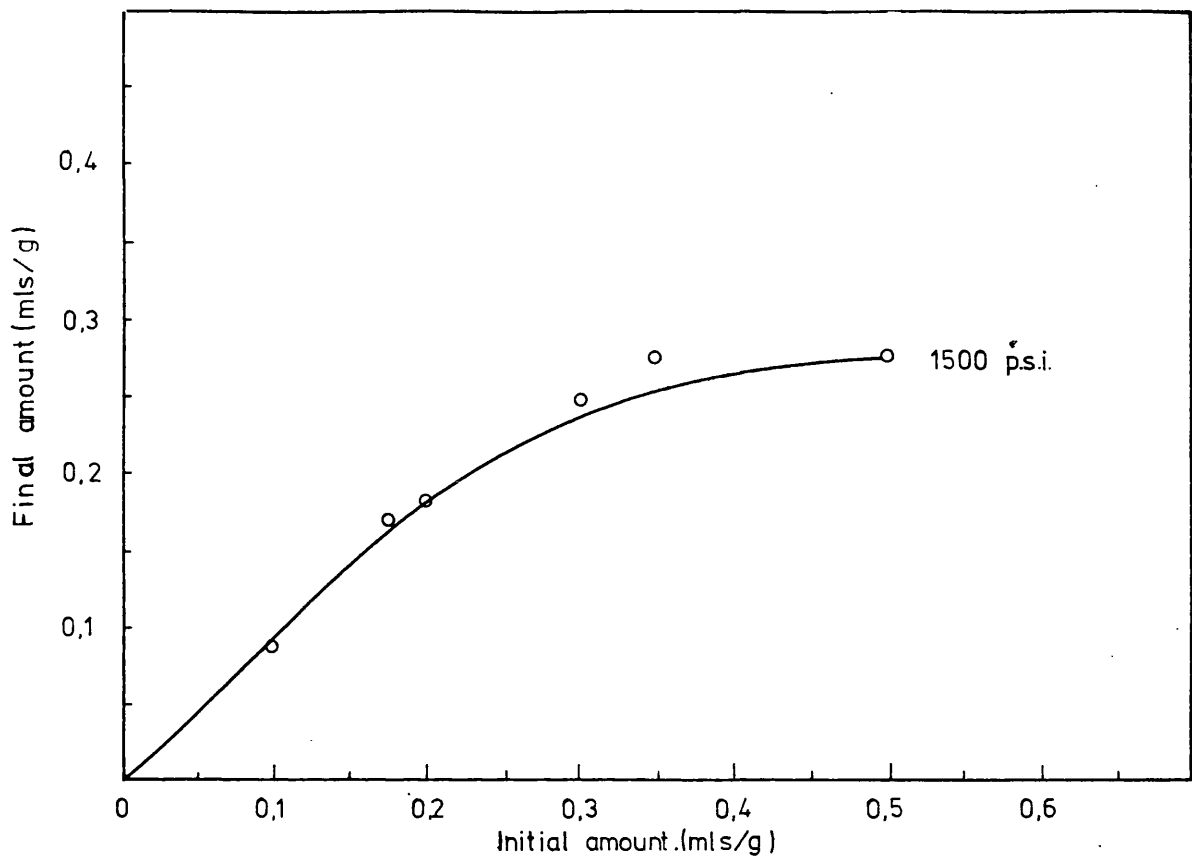
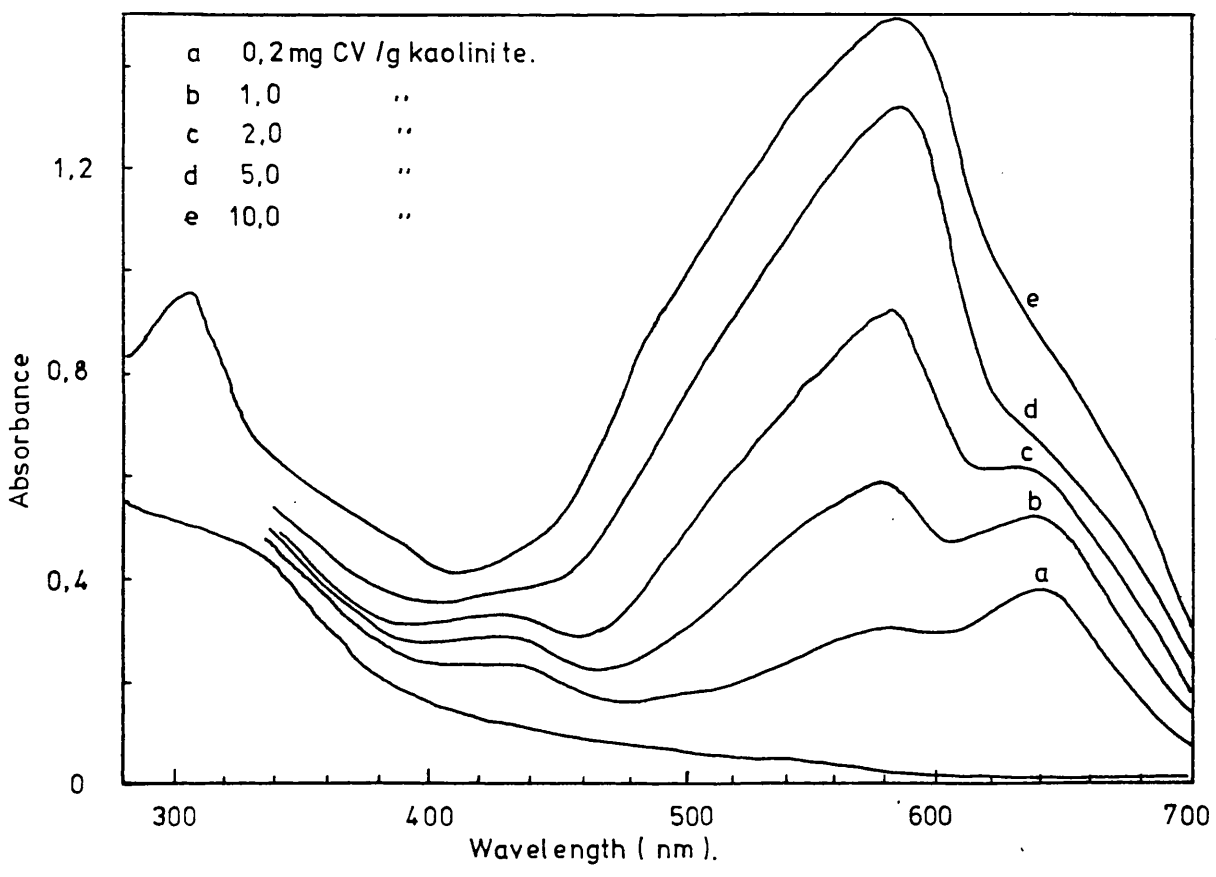


FIGURE.(2—6). Diffuse reflectance spectra of Crystal violet on kaolinite.



2.3.4 An Estimation of the Surface Acidity of a Sample of  
H<sup>+</sup>-Kaolinite

The ratio of the (G<sup>++</sup>/B<sup>+</sup>), on a sample of H<sup>+</sup>-kaolinite at a bulk pH of 3.0, was measured for several different coverages of crystal violet. Table (2-1) shows the peak height at the wavelength maximum for the three species, (B<sup>+</sup>), (G<sup>+</sup>) and (Y<sup>++</sup>) at 12% moisture content.

TABLE (2-1) The Absorbance of the Green and Blue Species of CV on  
H<sup>+</sup>- Kaolinite

Concentration of CV mg/g Kaolinite	Absorbance (590nm)	Absorbance (670nm)	Absorbance (430nm)
5.0	0.97	0.63	0.26
4.0	0.97	0.70	0.30
2.0	0.87	0.68	0.28
1.0	0.71	0.50	0.18
0.2	0.43	0.27	0.13

In table (2-2) the ratios of Abs 670nm/Abs 590nm are shown. These values represent the  $\lambda$  max upon the H<sup>+</sup>-kaolinite surface, of the green and violet species respectively.

TABLE (2-2) The Ratio of Green/Blue Species of CV on H<sup>+</sup>-Kaolinite

CV coverage mg/g Kaolinite	A670/A590
5.0	0.65
4.0	0.72
2.0	0.78
1.0	0.70
0.2	0.63

Mean ratio A670/A590 = 0.70 ± 0.18 (99% confidence).

$$\log_{10} (A670/A590) = -0.15$$

If it is assumed that the dissociation constant for the reaction below, on the surface is the same as in acidic solution, the ratio  $\frac{A670}{A590}$  can accurately predict the pH of the surface.



Therefore if:-

$$\text{Log}_{10} (A670_{nm}/A590_{nm}) = -0.15$$

From Figure (2-2) a value of the surface pH can be directly determined. A value of pH = 2.10 was obtained. That is approximately 1.0 pH unit below that of bulk solution.

This method provides a simple but relatively accurate method, compared to the methods used by Walling, C., (1950) and Benesi, H.A., (1956). This method has the ability to measure small differences

in the  $H_0$  of the surface, whereas methods employed by Walling, C., (1950) and Benesi, H.A., (1956) can only specify that the  $H_0$  lies between two adjacent indicators in a series.

The nearer the pKa of the dye on the surface is to the pKa in bulk solution, the more accurate the results will be.

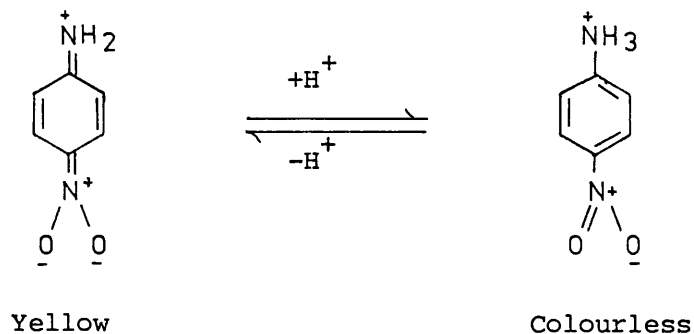
Crystal violet is unsuitable to determine more accurate results, because the dissociation constants of the coloured species lie too closely together, and the formation of colourless hydrated species requires extrapolating the results back to zero time.



### 2.3.5. Isomers of Nitroaniline

The isomers of Nitroaniline exhibit indicator properties . They are indicators because, when protonated, they change colour, from yellow to colourless, Figure (2-7 to 2-9).

The protonation of p-nitroaniline.



To evaluate the pKa for the reaction in bulk solution, the absorbance of the yellow uncharged species is plotted as a function of bulk pH, Figure (2-10)

$$K_a = \frac{[x.NO_2 \text{ aniline}][H^+]}{[x.NO_2 \text{ aniline}.H^+]}$$

At the point of inflection of the curve, i.e. when  $[x.NO_2 \text{ aniline}] = [x.NO_2 \text{ aniline}.H^+]$ , the pH will equal the pKa for the reaction. Figure (2-10) shows the curves for the three isomers of nitroaniline.

FIGURE (2—7). The spectra of o-Nitroaniline as a function of pH.

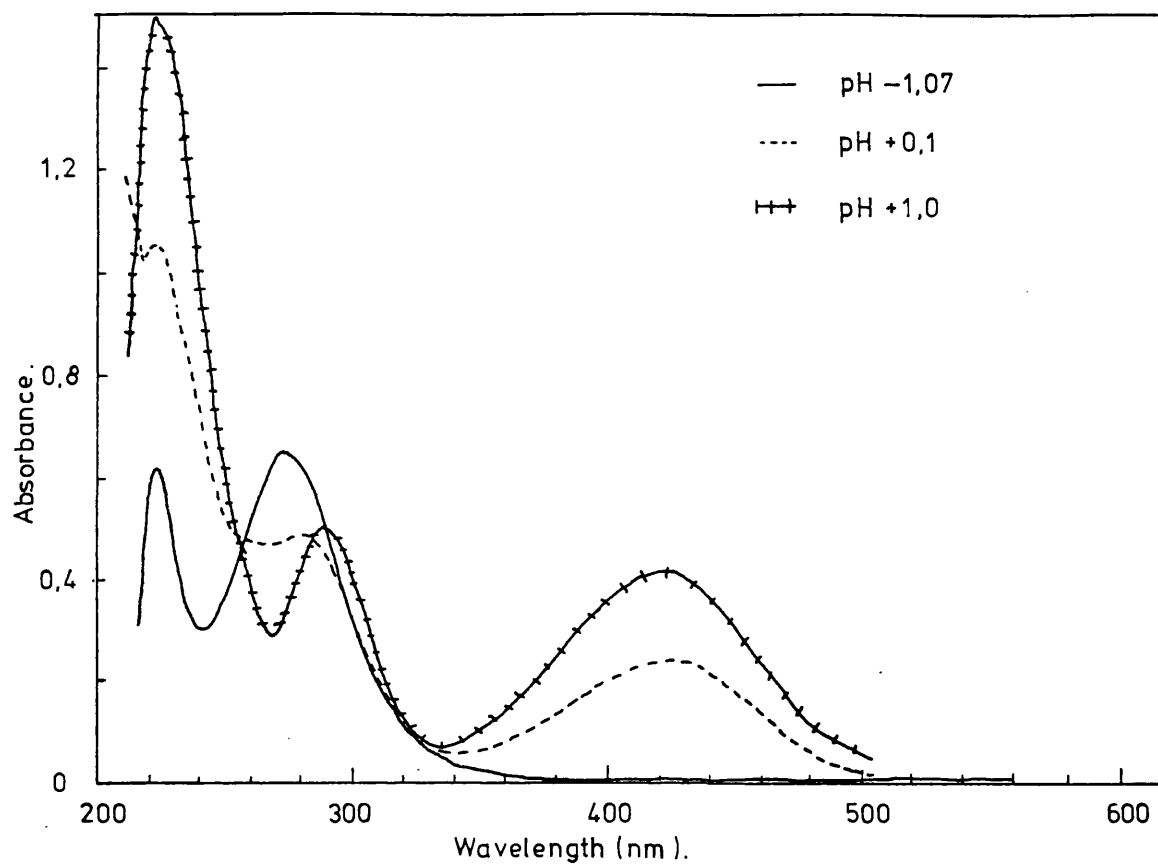


FIGURE (2—8). The spectra of m-Nitroaniline as a function of pH.

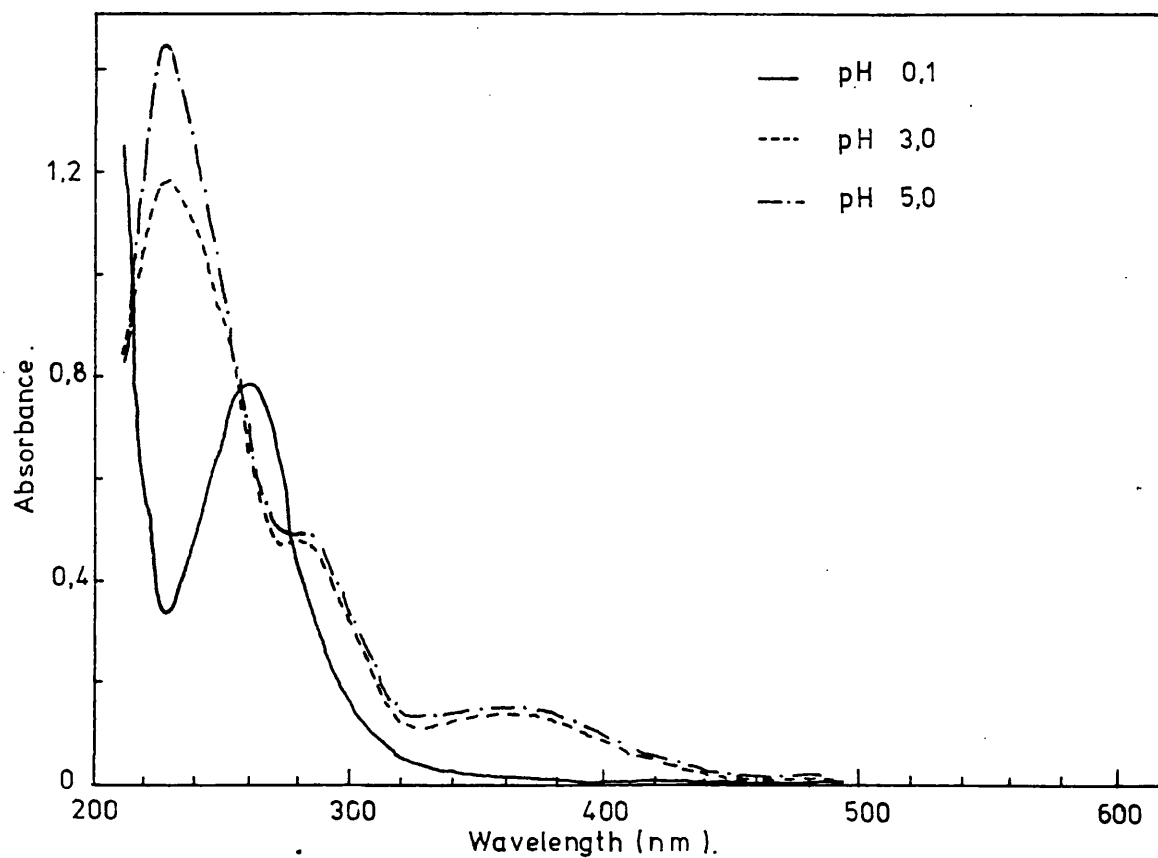


FIGURE (2—9). The spectra of p-Nitroaniline as a function of pH.

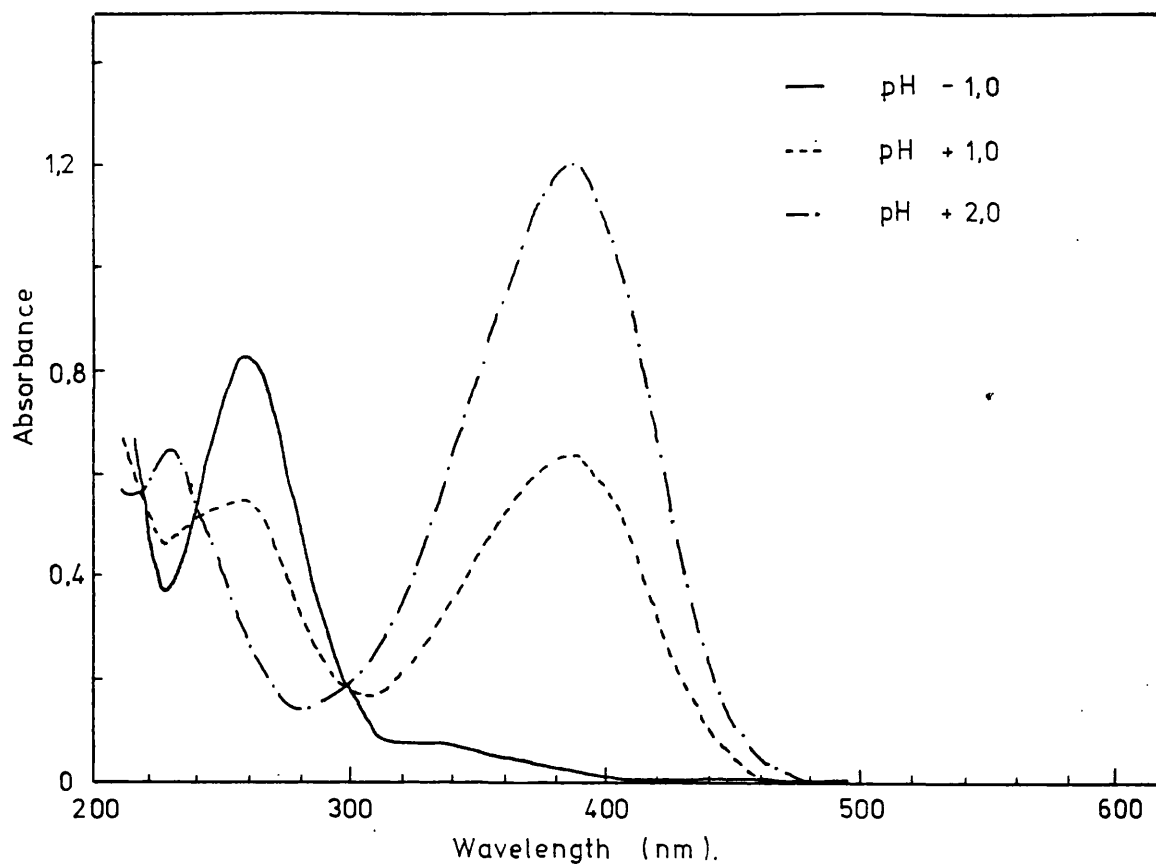
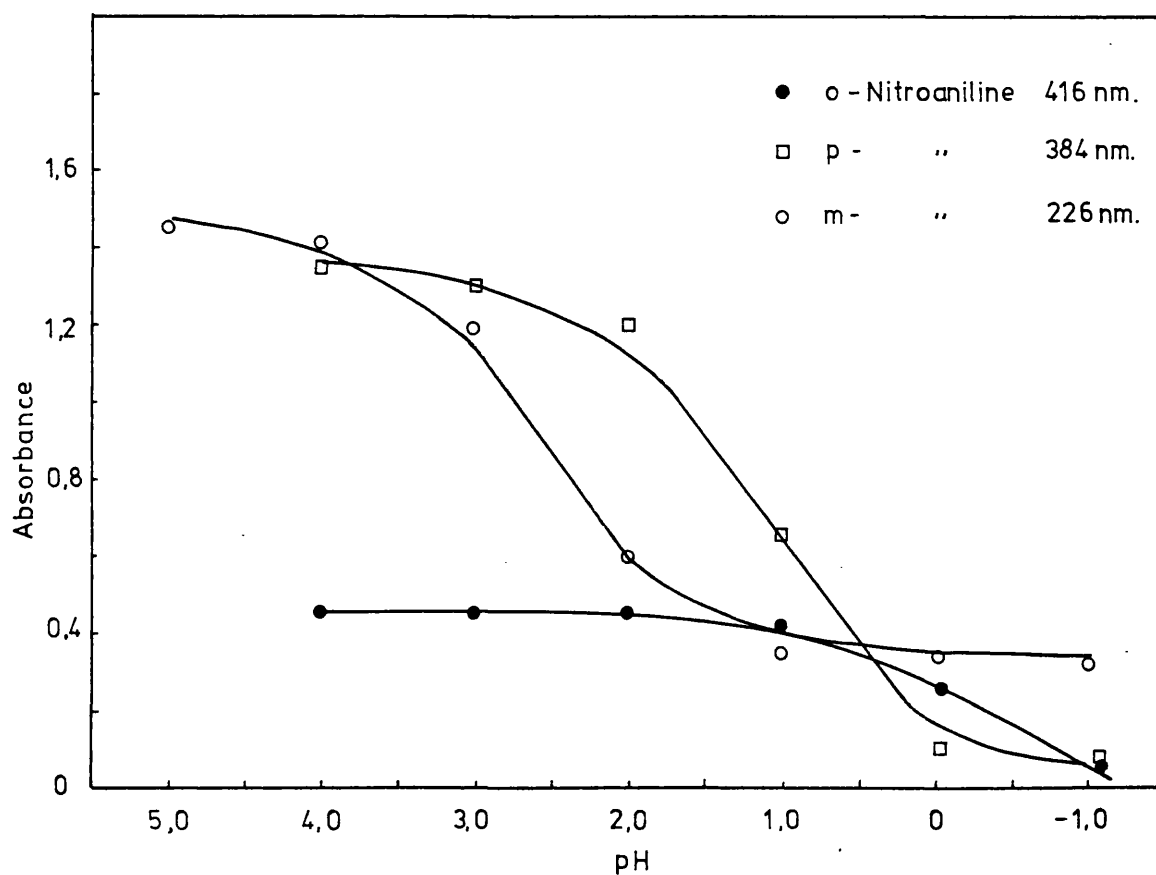


FIGURE (2—10). The absorbance at the  $\lambda_{\max}$  of o, m, and p-Nitroaniline as a function of pH.



Isomers of Nitro Aniline	pKa value obtained from Fig. (2-10)
ortho	-0.26
meta	+2.5
para	+1.0

The molar extinction coefficients for the three isomers were evaluated in H<sub>2</sub>O, pH 5.0 and 0.1, at their respective values of  $\lambda$  max.

Isomers of Nitro Aniline	pH 5.0	$\lambda$ max(nm)	pH 0.1	$\lambda$ max (nm)
ortho-Nitroaniline	4500	416	-	
meta-Nitroaniline	13200	384	8000	260
para-Nitroaniline	1560	358	8200	260

Ortho-nitroaniline was not used as an indicator, for the determination of surface acidity, because of its low pKa value, i.e. in order to produce ~90% of the protonated form, a hydrogen ion concentration of 11 molar would be needed. At this concentration the acid would have damaging effects upon clay minerals.

2.3.6. Adsorption Isotherms of para and meta-Nitroaniline  
upon H<sup>+</sup>-Kaolinite

Adsorption isotherms of para and meta-nitroaniline at a bulk pH of 5.0 and 0.1 are shown in Figures (2-11 and 2-12). It can be seen from Figures (2-11 and 2-12) that the isotherms at pH 0.1 are the Langmuir type, or L2 according to Giles, C.H., et al., (1960). The isotherm of m-nitroaniline at pH 5.0 resembles an L4 isotherm, again using the Giles notation. The adsorption of p-nitroaniline at pH 5.0 was at such a low level the results were difficult to evaluate, and so p-nitroaniline was not used for surface acidity determinations. Since both the m-nitroaniline isotherms resembled the Langmuir shape, the Langmuir equation was applied. The shape of the m-nitroaniline curve at pH 5.0 was assumed to be two consecutive Langmuir curves.

A value of K was obtained by plotting the linear form of the Langmuir equation, equation (2-14).

$$\frac{c}{n_2^s/W} = mc + b \quad (2-14)$$

A plot of  $c/n_2^s/W$  versus  $c$  yields a straight line, and K can be estimated from  $m/b$ , where  $m$  is the slope and  $b$  is the intercept. The data were plotted in this form in Figure (2-13 and 2-14). From Figures (2-13 and 2-14) the value of  $K_1'$  and  $K_2$  were estimated. For m-nitroaniline,  $K_1' = 196$ , and  $K_2 = 259$ ; where  $K_1'$  and  $K_2$  are the equilibrium constants for the adsorption of the free base of m-nitroaniline upon H<sup>+</sup>-kaolinite, and the ion exchange of the protonated base of m-nitroaniline, respectively.

FIGURE (2—11). Adsorption isotherm of m-Nitroaniline upon  $H^+$ -Kaolinite, at  $20^\circ C$ .

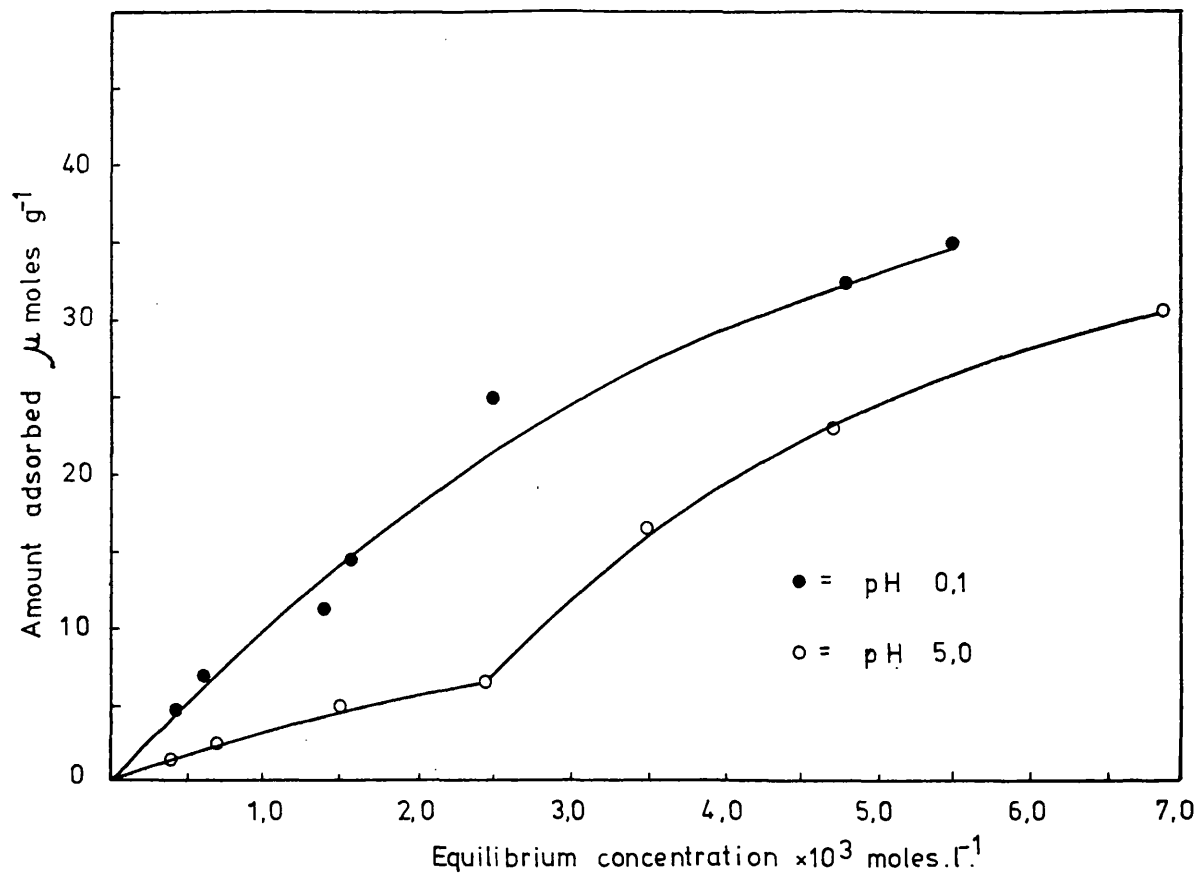


FIGURE (2—12). Adsorption isotherm of p-Nitroaniline on  $H^+$ -Kaolinite, at  $20^\circ C$ .

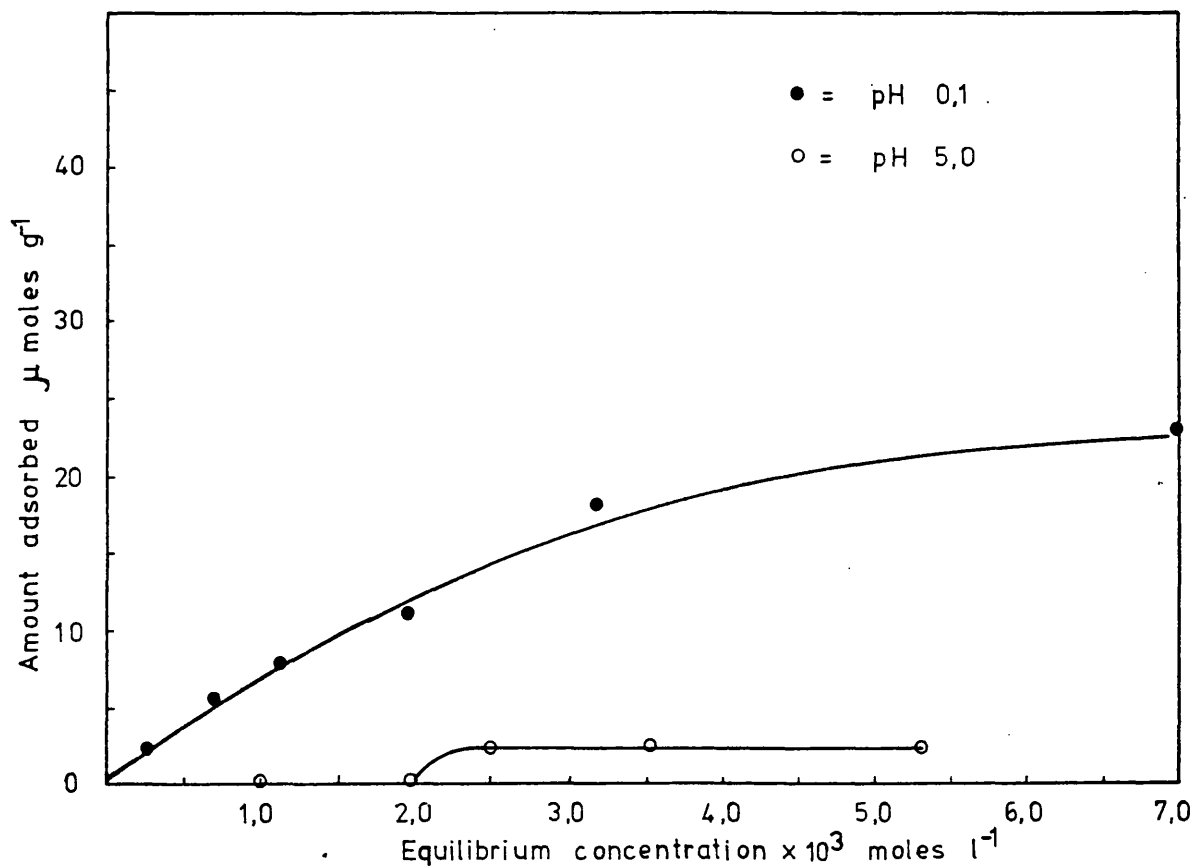


FIGURE (2-13) . Linear plot of the adsorption of m and p-Nitroaniline on H<sup>+</sup>Kaolinite at 20°C , pH 0,1.

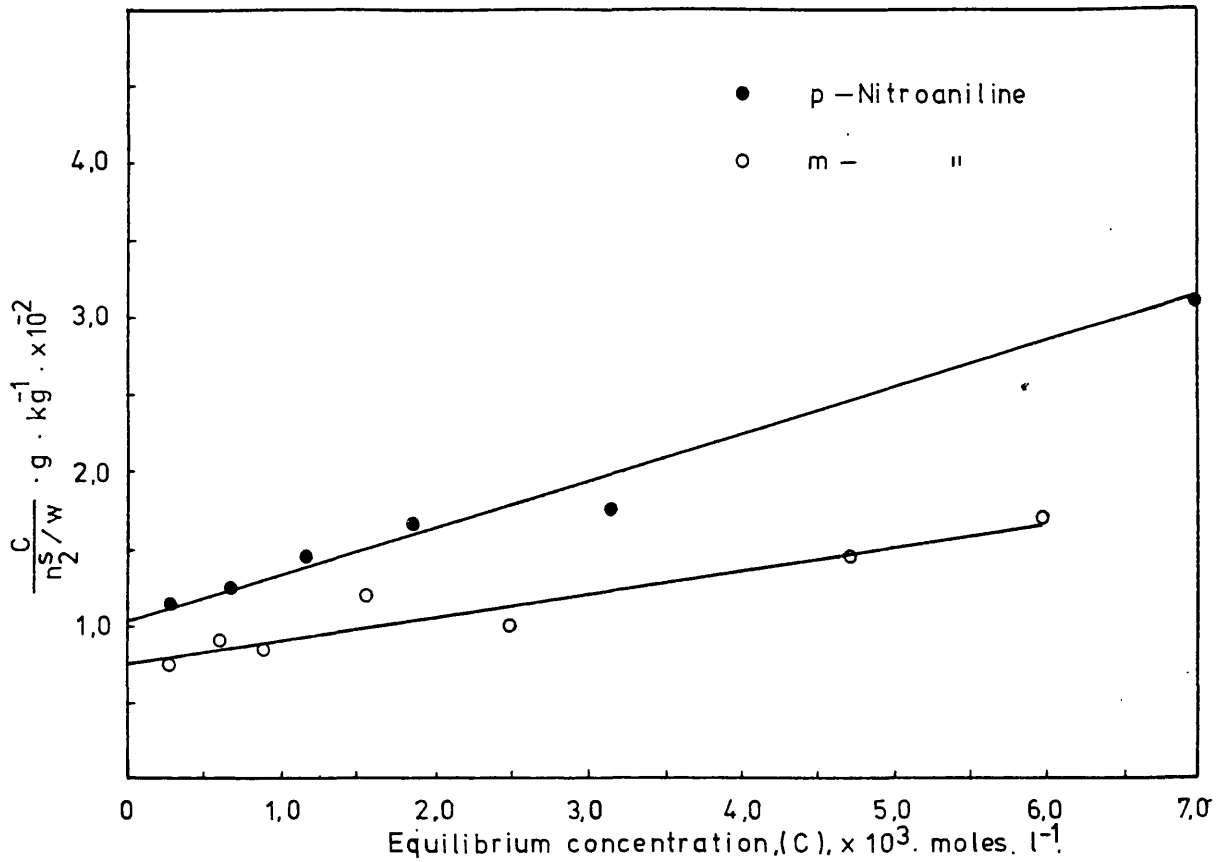
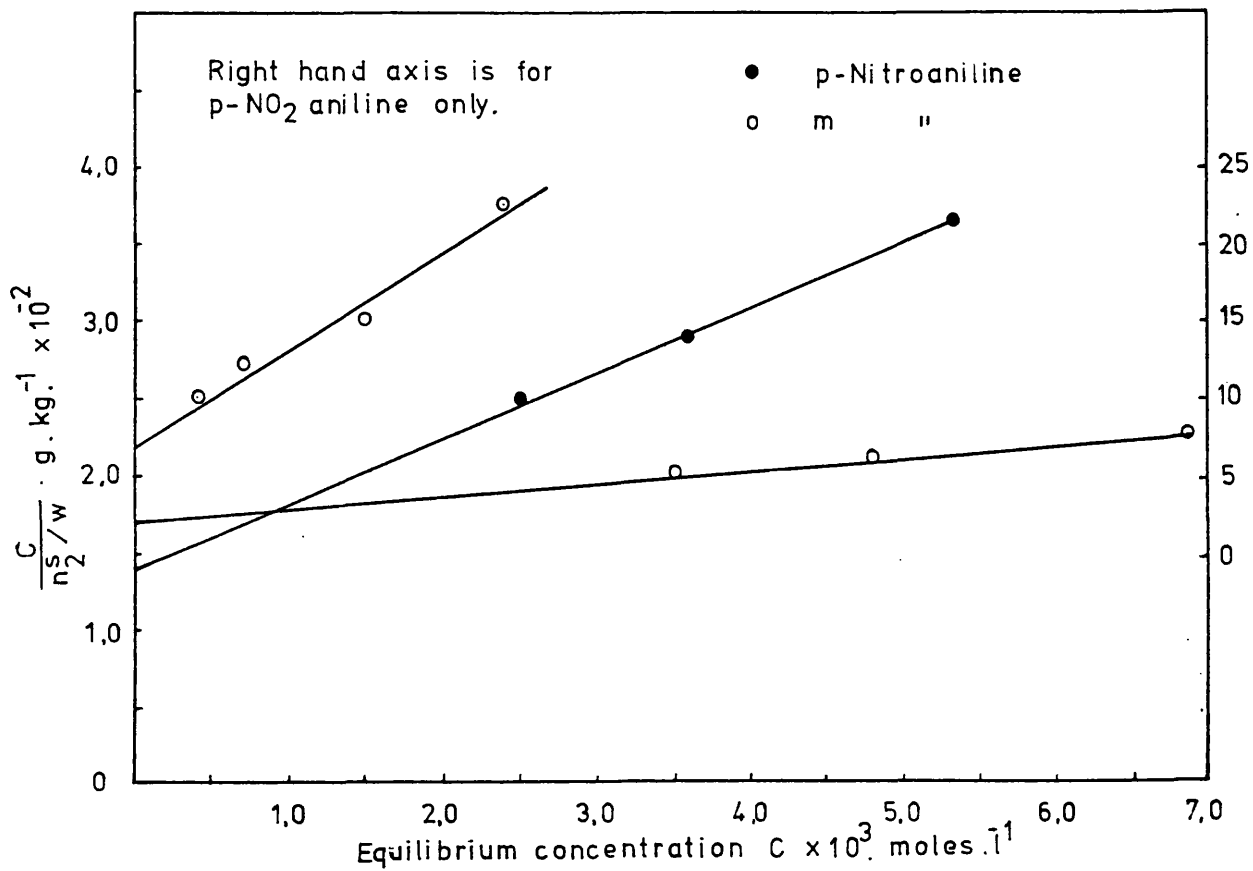


FIGURE (2-14) Linear plot of the adsorption of m and p-Nitroaniline on H<sup>+</sup>-Kaolinite at 20°C , pH 5,0



Equation (2-19) shows:-

$$K^S = \frac{K'_1 \cdot K_4}{K_2} \quad (2-19)$$

Where  $K_4$  is the acid dissociation constant of the dye in solution and  $K^S$  is the surface dissociation constant for the indicator.

$$\text{Then } K^S = \frac{196 \times 3.16 \times 10^{-3}}{259} = 2.39 \times 10^{-3}$$

$$\underline{\underline{pK^S = 2.62}}$$

The  $pK^S$  for the protonation of m-nitroaniline on a  $H^+$ -kaolinite surface has been determined, and a value of 2.62 obtained, c.f. a value of 2.50 was obtained in bulk solution.



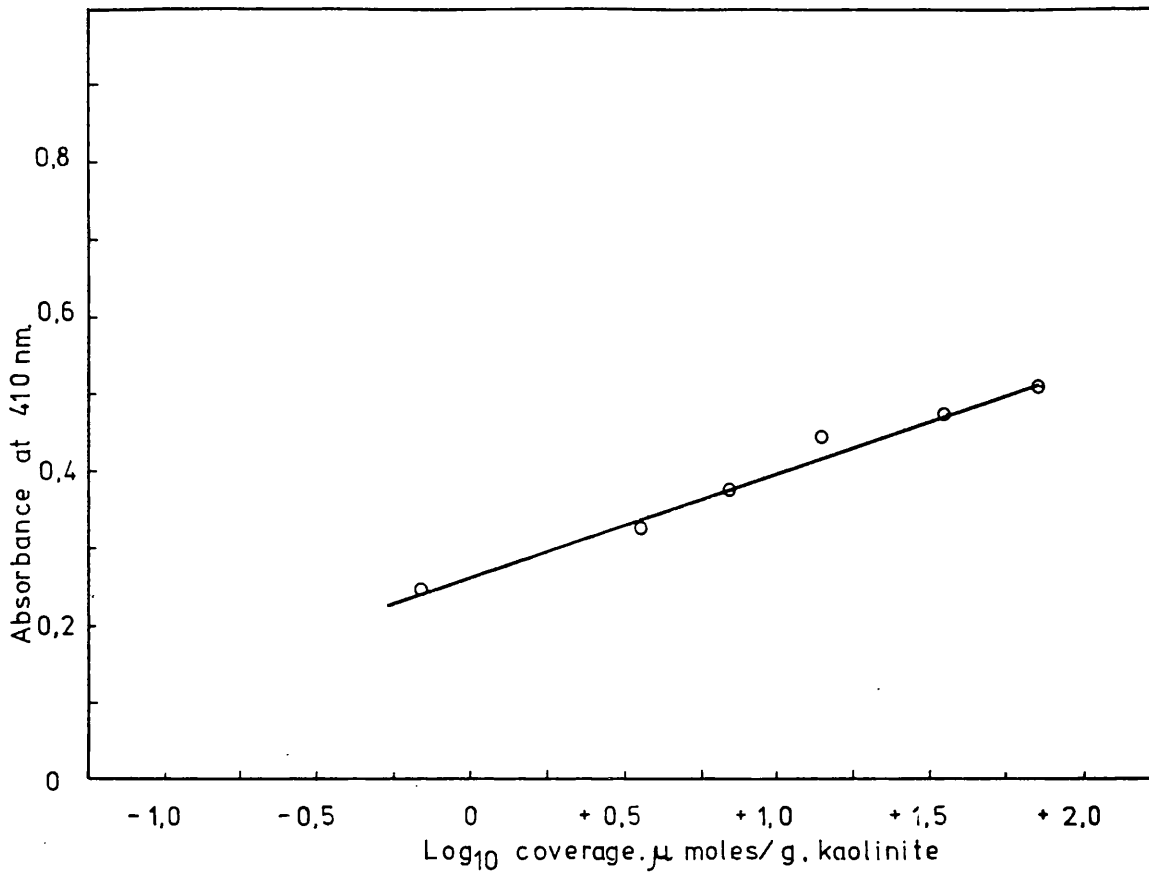
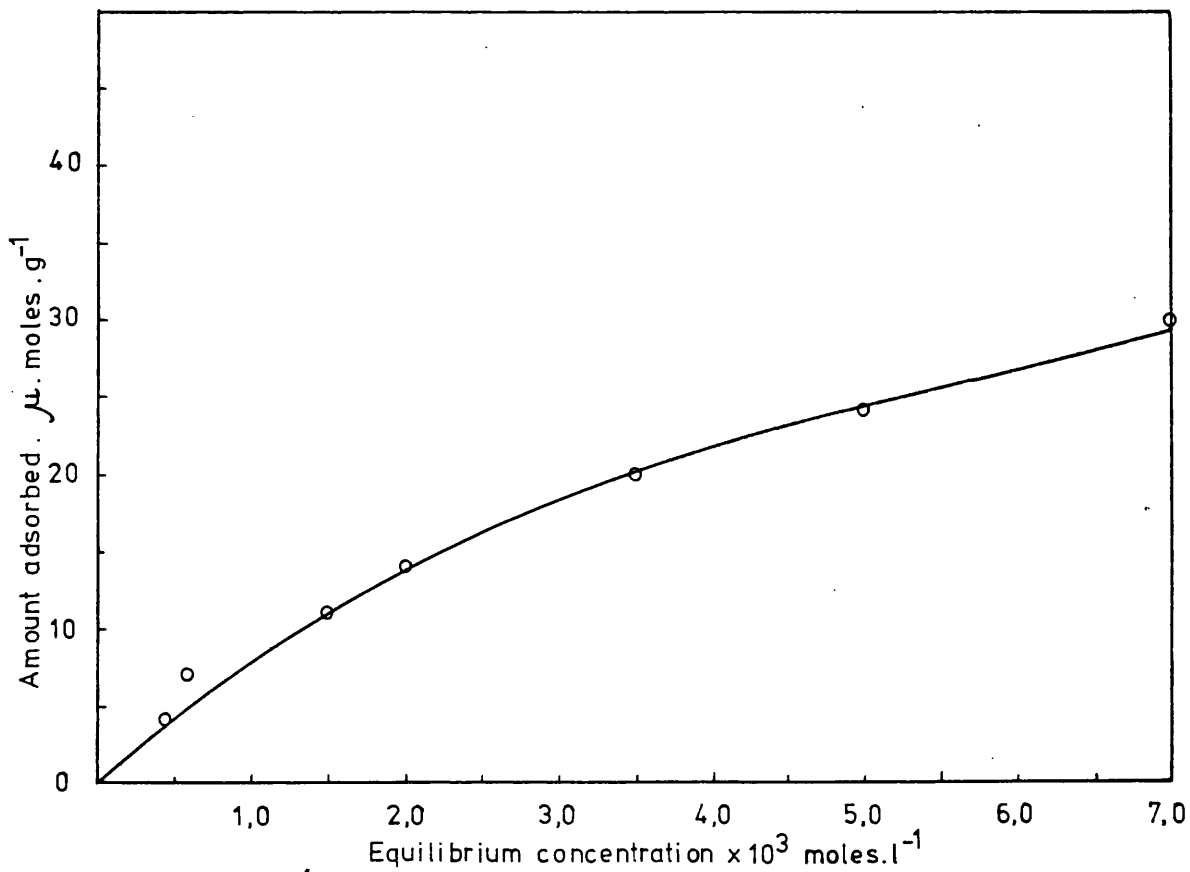
2.3.7. A Method to Determine the Surface Acidity of  $H^+$ -Kaolinite using m-Nitroaniline as an Indicator.

(i) Diffuse Reflectance of m-Nitroaniline on  $H^+$ -Kaolinite

In order to estimate the Hammett acidity function ( $H_0$ ) of the surface, a value of the ratio of (Protonated Base)/(Free Base) is required. Since the free base of m-nitroaniline is yellow and the protonated form colourless a measurement of the yellow concentration will determine the ratio, if the total concentration is known. A calibration curve of absorbance at 410nm versus amount of m-nitroaniline added at pH 5.0 bulk solution is shown in Figure (2-15).

(ii) Adsorption of m-Nitroaniline upon Kaolinite at pH 3.0

The  $H_0$  of the surface was measured at bulk pH 3.0. This was close to the  $pK^s$  of the dye, and so the ratio of (Protonated Base)/(Free Base) was near to 1.0. More accurate results could be obtained in this region, as a large proportion of the m-nitroaniline was in the coloured, free base form. More than 90% of the applied dye must be adsorbed upon the surface to obtain reliable measurements. Otherwise non-adsorbed dye in solution would alter the ratio of protonated to free base observed by diffuse reflectance. Figure (2-16) shows an adsorption isotherm of m-nitroaniline at pH 3.0. The equilibrium concentration was determined by raising the pH to 5.0, after separation, by centrifugation from the clay mineral. At this solution pH all the non-adsorbed dye was in the yellow form. As can be seen from Figure (2.16) at an initial concentration of  $0.5 \times 10^{-3}$  Molar, 87% of the dye was adsorbed upon the clay mineral.

FIGURE (2—15). The absorbance of m-Nitroaniline on  $H^+$ kaolinite.FIGURE (2—16). The adsorption isotherm of m-Nitroaniline on  $H^+$ kaolinite at 20°C; pH 3.0.

(iii) Diffuse Reflectance of m-Nitroaniline on H<sup>+</sup>-Kaolinite  
at bulk pH 3.0

The diffuse reflectance spectrum of m-nitroaniline upon H<sup>+</sup>-kaolinite is shown in Figure (2.17). From Figure (2-17) the peak height was determined, at 410nm, as being 0.27 absorbance units. From the calibration curve, Figure (2-15), a value of 1.4  $\mu$  moles/g Kaolinite was obtained, for the free base. The total initial amount of m-nitroaniline applied was  $5 \times 10^{-6}$  moles. Therefore if it is assumed that all material was adsorbed the amount of the protonated base would be:-

$$(5 \times 10^{-6}) - (1.4 \times 10^{-6}) = 3.6 \times 10^{-6} \text{ moles, g}^{-1}$$

The ratio of protonated to free base would then be:-

$$\frac{\text{Protonated}}{\text{Free base}} = \frac{3.6 \times 10^{-6}}{1.4 \times 10^{-6}} = \underline{\underline{2.57}}$$

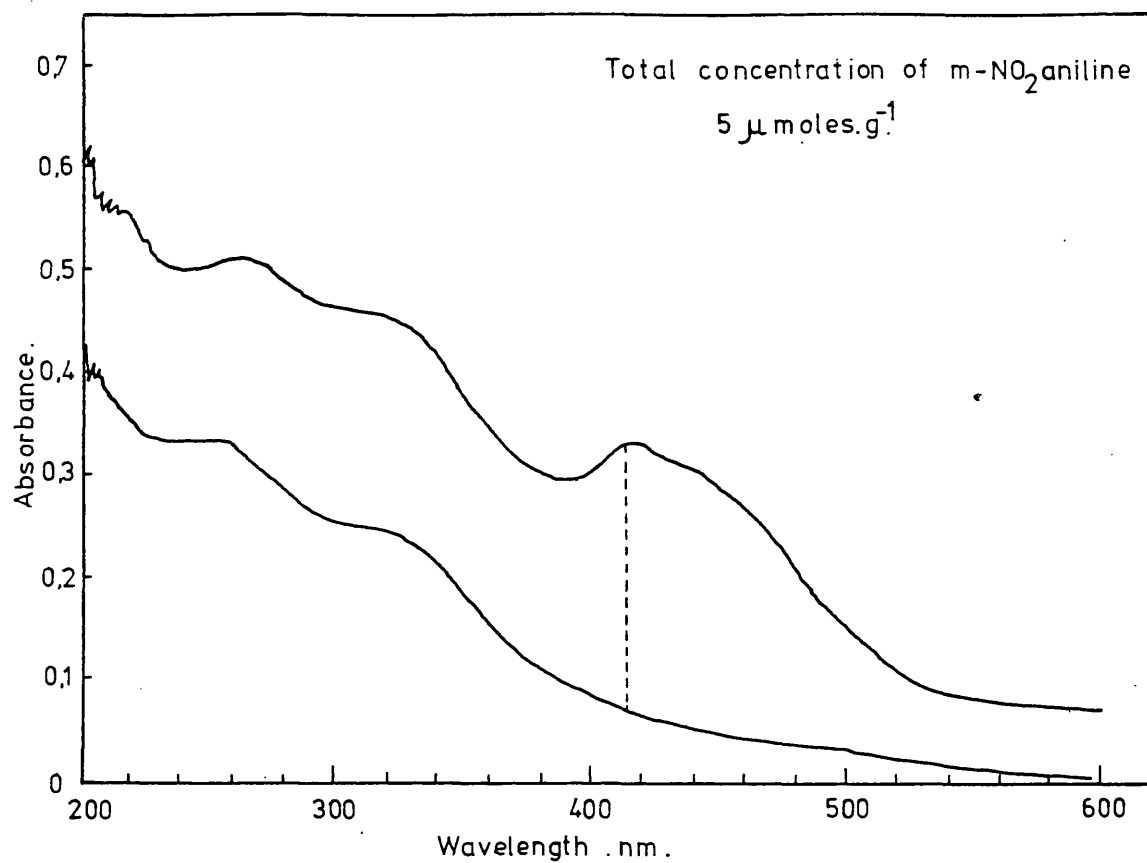
If this value is then applied, using the value of  $pK^s$ , an accurate value for the Hammett acidity function can be found.

$$H_0 = pK^s - \log \frac{\text{Protonated base}}{\text{Free base}}$$

$$\underline{\underline{H_0 = 2.62 - \log(2.57) = 2.21}}$$

This method is more accurate than the method using crystal violet as the indicator of surface acidity, because it takes into account the surface dissociation constant of the indicator

FIGURE (2—17). Diffuse reflectance spectrum of m-Nitroaniline  
on  $H^+$ -Kaolinite at pH 3.0



rather than relying upon a value from bulk solution. The value of  $H_0$  determined from crystal violet as indicator was 2.1, and a value of  $H_0 = 2.21$  from m-nitroaniline as indicator. If the value of the bulk acid dissociation constant were used for m-nitroaniline:

$$H_0 = pK^b - \log \frac{\text{Protonated base}}{\text{Free base}}$$

$$\text{Then: } \underline{\underline{H_0 = 2.5 - \log (2.57) = 2.09}}$$

This value is the same as the value obtained by crystal violet, within experimental error. Clearly any measurement of surface acidity must take into account the dissociation constant for the indicator upon the surface and not assume that the value will be the same as in bulk solution.

The amount of indicator added should be a minimum value to permit the measurements to be made, because large amounts of indicator will not be completely adsorbed, ie. when the surface is covered by a monomolecular layer no more will be adsorbed if the Langmuir assumptions are to be applied. Also large amounts of indicator will change the value of the surface acidity by consuming protons, and hence lower the surface acidity.

## 2.4 Conclusions

The results have shown that crystal violet can be adsorbed upon a clay mineral, and by diffuse reflectance a value for the Hammett surface acidity function ( $H_0$ ), can be obtained. The value of  $H_0$  obtained upon  $H^+$ -kaolinite, at bulk pH 3.0, was 2.1.

Using m-nitroaniline as an indicator of surface acidity, the value for the Hammett acidity function of m-nitroaniline adsorbed upon  $H^+$ -kaolinite was 2.21, at bulk pH 3.0.

The discrepancy between the two values can be attributed to the ability to determine the surface dissociation constant for m-nitroaniline, and not for crystal violet. The dissociation constant for m-nitroaniline in bulk solution was +2.5, and on the surface was +2.62. It was not possible to determine the surface dissociation constant for crystal violet due to its complicated ionization, and hydration.

To obtain reliable results for the Hammett acidity function, upon a clay mineral, the surface dissociation constant for the chosen indicator, upon the chosen adsorbent, must be calculated. In this way results obtained for the  $H_0$  of a surface which appear incorrect could be rationalized by calculation of the surface dissociation constant.

## CHAPTER 3

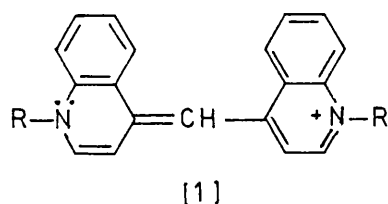
REACTIONS OF CRYSTAL VIOLET AND CRYSTAL VIOLET  
LACTONE ON CLAY MINERALS AND OXIDES

Reactions of Crystal Violet and Crystal Violet Lactone on Clay Minerals and Oxides.

3.1 Introduction

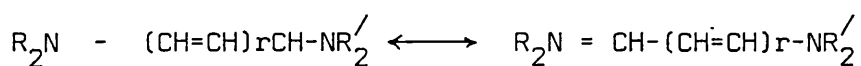
Crystal violet is an important dye which is used extensively for scientific and commercial purposes; from staining tissues to dyeing textiles. The literature is abundant with references relating to crystal violet, Barker, C.C. et al., (1959); Barker, C.C. et al., (1960); Cigen, R. (1958) ;Cigen, R. (1960); Goldacre, R.S., (1949); Lewis G.N., et al., (1942); Nemcova. I. et al., (1969); Sequoia, E. (1971); Turgeon, J.C., and La Mer, V.K., (1952). Numerous accounts of crystal violet lactone also occur, mostly in the patent literature.

Crystal violet is a triarylmethane dye. The first dyes of this type were discovered by Grenville William (1856), and were called cyanines. Originally the name referred to the dyes Williams had discovered, having the general formula (1)



Considerable research into these and related dyes was carried out, due to their ability to sensitize silver halide crystals in photographic plates, to wavelength of light to which they normally would be inactive. This has now become more general and refers to any system resembling (2)





(2a)

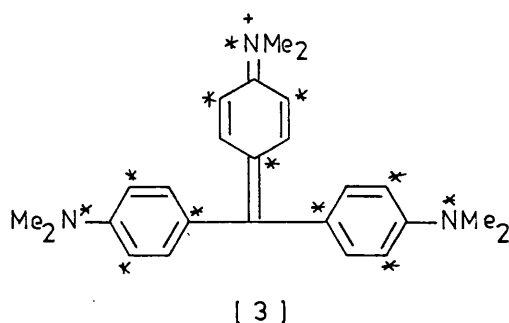
(2b)

Griffiths, J., (1976) defines a cyanine type chromogen as any conjugated system that is isoconjugate with an odd alternant hydrocarbon, and that can be represented by at least two equivalent or near equivalent resonance forms.

As far as the Huckel molecular orbital (HMO) theory, is concerned, unsaturated hydrocarbons can be divided into two distinct types. The alternant hydrocarbon (AH), contain open chains with an odd or even number of atoms, and/or rings containing an even number of atoms. Non-alternant hydrocarbons (NAH) contain at least one ring possessing an odd number of carbon atoms. A systematic definition of the types, involves indexing the molecule. The full structure is drawn out, and any one of the carbon atoms is "starred". A continuous path is then traced through the molecule, starring each alternate atom in the same way. If it is found that no two adjacent atoms are both starred or unstarred, the molecule is an alternant. If it is not possible to avoid having two adjacent starred or unstarred positions the molecule is a non-alternant. The starring sequence is always arranged so that the number of atoms starred are the greater.

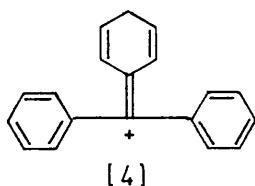
Alternant molecules containing an odd number of carbon atoms, must have an odd number of molecular orbitals. If one "pairs" the orbitals, then obviously there will be one molecular orbital remaining. This orbital lies at the "centre of gravity" of the energy levels of the other orbitals, i.e. at the non-bonding energy level.

If aromatic ring systems are made part of the conjugated chain of a cyanine, the characteristic properties of the chromogen are not altered. Thus the system will still be isoconjugate with an odd alternant hydrocarbon anion, and will absorb at long wavelengths by virtue of the presence of a non-bonding molecular orbital (NBMO). The di and triarylmethane dyes are examples of this type. Crystal violet is an odd alternant system, but it is found on "starring" the molecule that the number of starred positions exceeds the number of unstarred positions by two (3).



This means that crystal violet has two NBMO's which are necessarily degenerate, and in the simple model the 590nm band is due to the two degenerate transitions involving promotion of an electron from one of these orbitals to the lowest anti-bonding orbital, Griffiths, J., (1976).

Structurally the parent triphenyl methyl cation (4) is not planar, but each phenyl group is rotated approximately 30 degrees out of the plane, so that the shape is similar to a propeller, Gomes de Mesquita, A.H., et al., (1965).

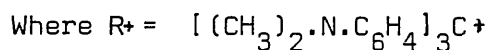
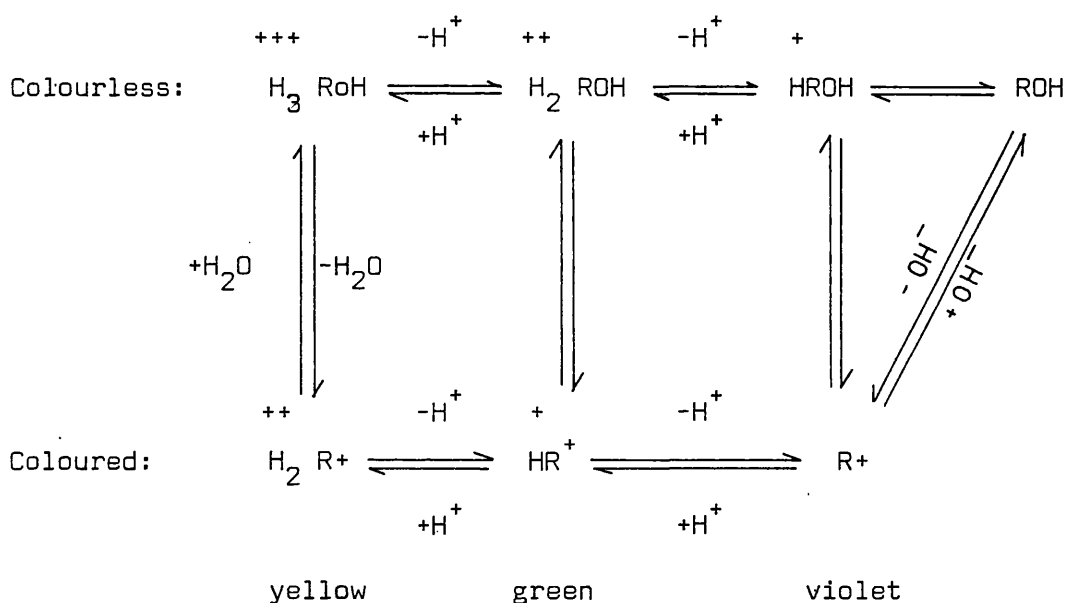


Almost certainly crystal violet will adopt a similar conformation.

### 3.1.2 The Behaviour of Crystal Violet in Aqueous Acidic Solution

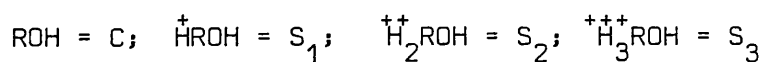
When crystal violet (CV) is in aqueous acidic solution it can exist in three different coloured forms, yellow, green and violet. A very complete study of the behaviour of CV in aqueous acidic solution has been published by Cigen, R., (1958). The diagram below summarises the behaviour of CV in aqueous acidic solution, Figure (3-1)

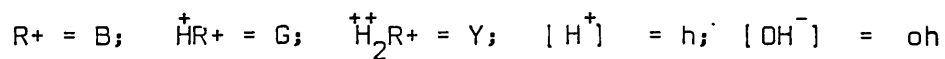
Figure (3-1) Protolytic Equilibria of Crystal Violet



The dissociation, hydration and kinetic constants were evaluated for all the species in the diagram by Cigen, R., (1958).

If the molecular species involved, in the proton transfer, and hydration equilibria, are designated as follows:-





Then the acid-base dissociation equilibrium constants are:-

$$K_1 = \frac{h[G]}{Y}; \quad K_2 = \frac{h[B]}{[G]}; \quad K'_1 = \frac{h[S_2]}{[S_3]};$$

$$K'_2 = \frac{h[S_1]}{[S_2]}; \quad K'_3 = \frac{h[C]}{[S_1]}$$

and hydration equilibrium constants are:-

$$K_4 = \frac{[S_3]^\infty}{[Y]^\infty}; \quad K_5 = \frac{[S_2]^\infty}{[G]^\infty}; \quad K_6 = \frac{[S_1]^\infty}{[B]^\infty}$$

The values for the equilibrium constants as determined by Cigen, R., (1958) are:

---

$K_1 = 0.122$	$K_2 = 0.00406$		Molar
$K'_1 = 486 \times 10^{-5}$	$K'_2 = 1.78 \times 10^{-5}$	$K'_3 = 2.46 \times 10^{-6}$	Molar
$K_4 = 79$	$K_5 = 0.0319$	$K_6 = 1.46 \times 10^{-4}$	

---

The spectra of the three coloured species are shown in Figure (3-2)

It can be seen from Figure (3-1) that all the hydrated species are colourless. The hydration constants are in the order  $K_4 > K_5 > K_6$ . The rate of hydration and hence loss of colour being greatest for the trication and least for the mono-cation.

FIGURE (3-2) Spectrum of Crystal Violet Lactone in ethanolic solution

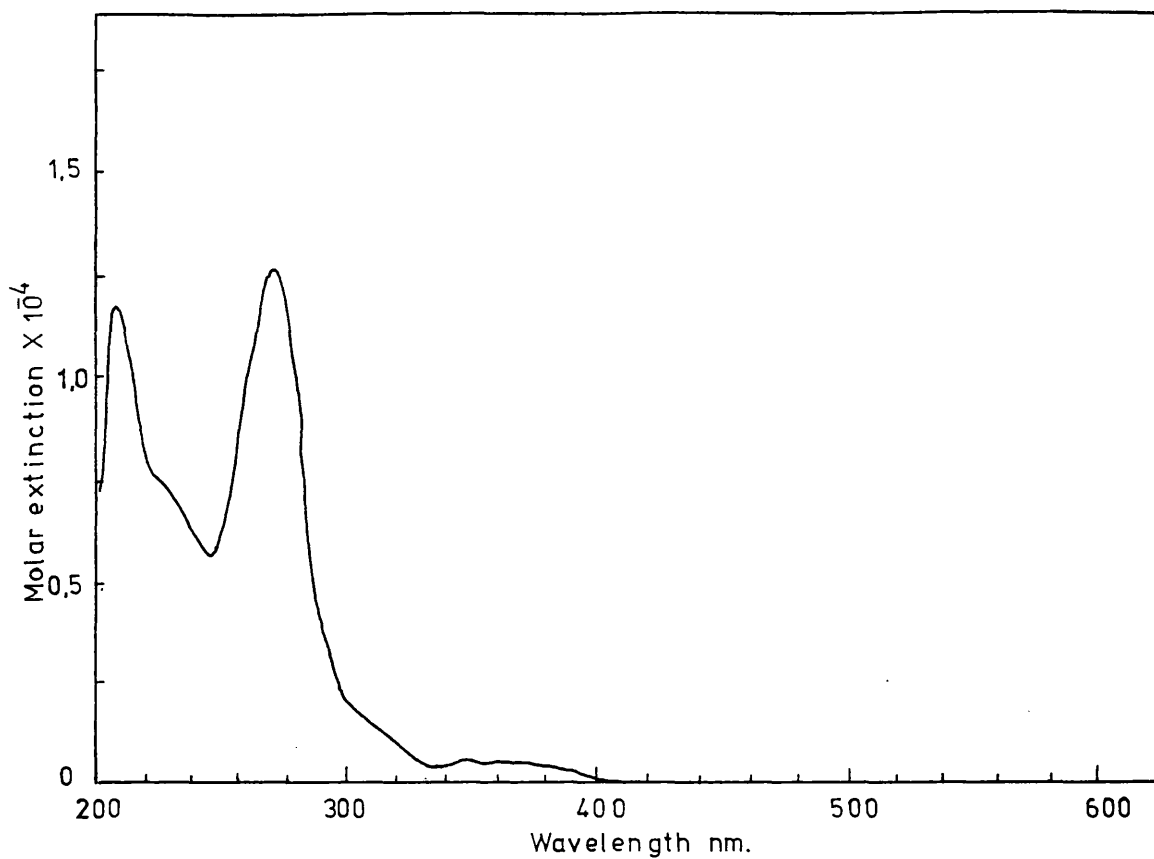
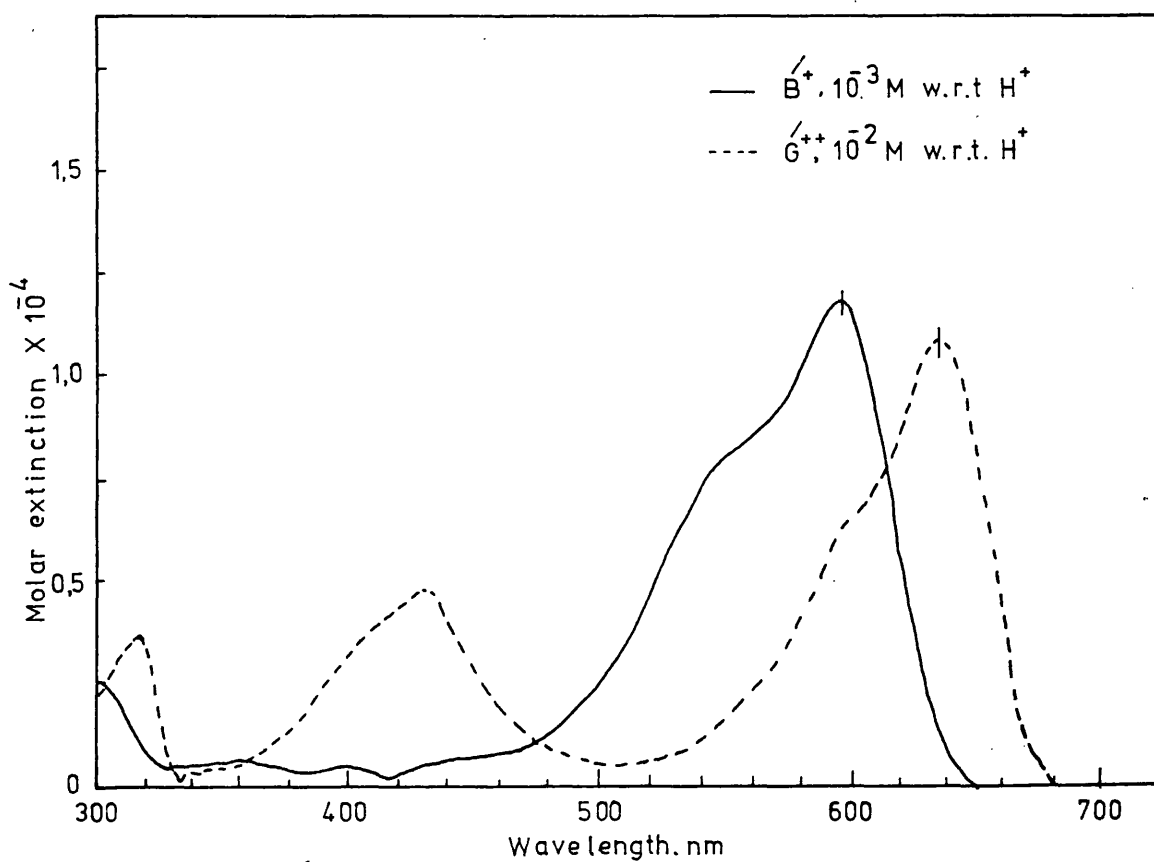


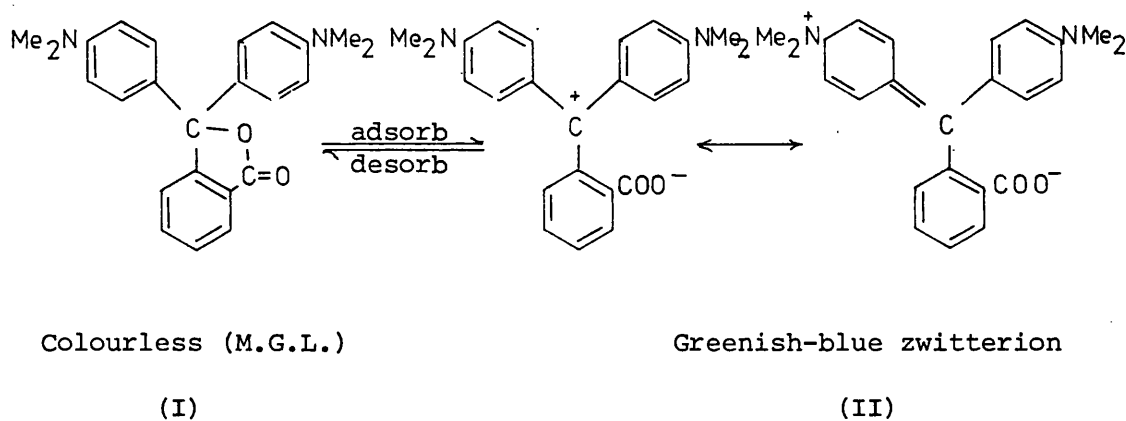
FIGURE (3-3) Spectra of the Blue and Green Species of Crystal Violet Lactone in acidified ethanol



### 3.1.3 The Behaviour of Crystal Violet Lactone on Clay Minerals and Oxides

Crystal violet lactone is colourless in ethanolic solution, see Figure (3-2). When a colourless solution of CVL is applied to a clay mineral or oxide, and the solvent allowed to evaporate, a violet colour is formed.

It has been shown by Kortum, G., and Vogel, J. (1960) that the colourless lactone of malachite green-o-carboxylic acid (MGL) when adsorbed onto dried NaCl is greenish-blue. The reflectance spectrum on dried NaCl corresponds to the spectrum of malachite green in methanolic solution. Hence the lactone ring has undergone reversible cleavage on the surface and a resonance stabilised Zwitterion is formed:



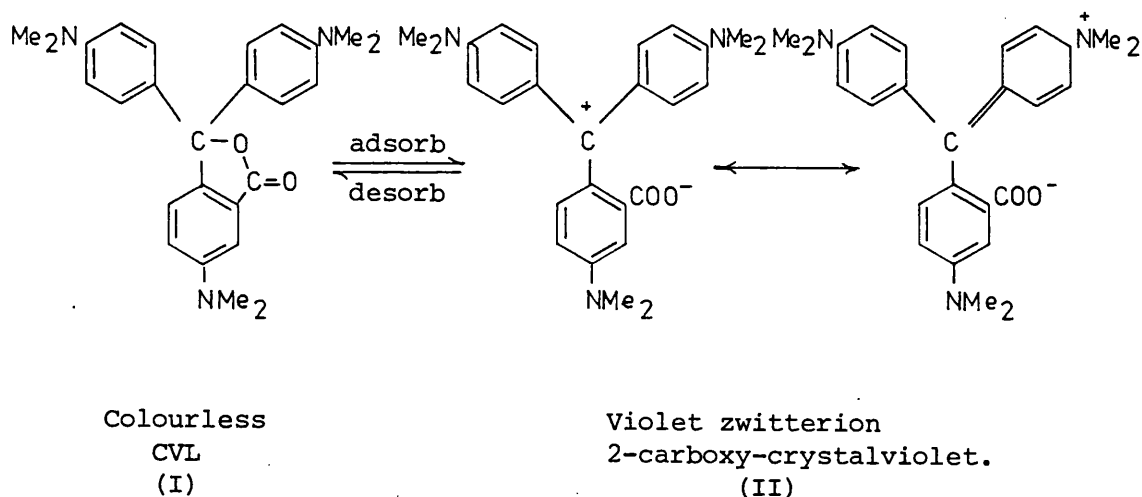
The IR spectrum of the adsorbed lactone shows that this explanation is correct, because the  $\text{-COO}^-$  band can be observed as well as the ring frequencies, Kortum, G. and Delf, H. (1964). Since the lactone cannot be converted to the Zwitterion by heating in solution, or melting, the ring cleavage must have a high activation

energy. This energy barrier is lowered during adsorption, by the polarising effect of the ionic lattice, so that a partial cleavage occurs even at room temperature. A plot of  $F(R'_{\infty})$  for the maxima of the bands at  $16,500 \text{ cm}^{-1}$  and/or  $24,000 \text{ cm}^{-1}$ , which corresponds to the cleaved lactone, against the mole ratio  $x$  gives a Langmuir isotherm. This implies that when the first monolayer is saturated no further cleavage takes place.

The degree of ring cleavage, as measured by the band intensities, decreases from LiCl through to CsCl for a given surface coverage on these adsorbents. The positions of the zwitterion bands are virtually unchanged. On the contrary, exchange of the anions ( $\text{F}^-$ ,  $\text{Cl}^-$ ,  $\text{Br}^-$ ,  $\text{I}^-$ ) has no effect on the intensity of either band. Thus the bonding is mainly coulombic, between the lattice cations and the carboxylate groups, because the positive charge of the zwitterion is distributed by resonance over the greater part of the molecule. Therefore the smaller the lattice cation, the greater the polarizing effect on the lactone ring and the more the equilibrium  $\text{I} \rightarrow \text{II}$  is shifted to the right. A similar effect is observed on alkaline earth oxides. The stronger polarizing effect of the double charge is shown by the greater degree of ring cleavage for a given surface coverage, compared with the alkali metal ions.

The ring opening is reversible, after desorption, the colourless lactone is reformed. This also occurs in the presence of water (moist air). The zwitterion is displaced by  $\text{H}_2\text{O}$  but this also depends upon the size of the lattice cation. Displacement is slow from LiCl, i.e. after 13 hours the crystals are still blue on exposure to moist air. The larger the cation the smaller the polarizing effect and hence the greater the necessity to pre-dry the solid in order to affect the ring cleavage.

Therefore a similar situation will occur when CVL is adsorbed upon clay minerals and oxides. The intense blue colour formed, is 2 carboxy-crystal violet, analogous to the zwitterion (II) of malachite green lactone.



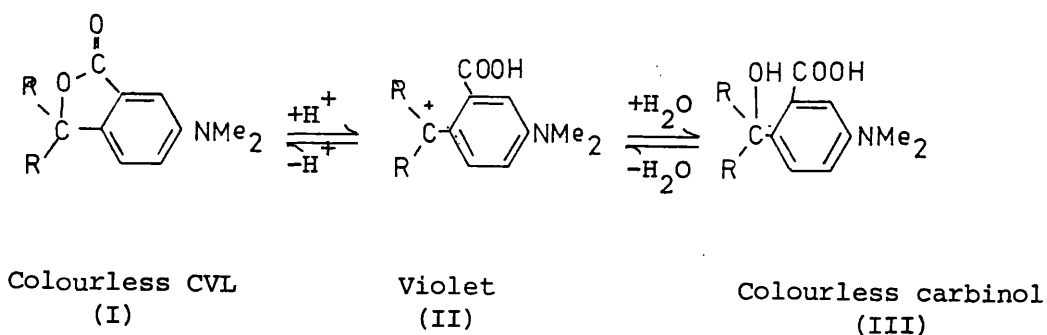
The expected effect of having an electron withdrawing substituent such as  $\text{COO}^-$  in an ortho position to the central carbon atom of crystal violet, would be to stabilize the carbo-cation, and cause a bathochromic shift of the first visible absorption band. This is observed, 2-carboxy. CV  $\lambda_{\text{max}}^{\text{ETOH/HCl}} = 602\text{nm}$  cf, CV  $\lambda_{\text{max}}^{\text{ETOH/HCl}} = 590\text{nm}$ . Also the extinction coefficient of 2 carboxy-CV should be smaller than CV due to the steric hinderance of the  $\text{COO}^-$  in the ortho position. This causes the ring to be twisted further out of the plane, and hence reduce  $\pi$  orbital overlap Barker C.C. et al., (1959).



3.1.4. Possible Modes of Fading; Crystal Violet and Crystal Violet Lactone.

(i) Reversible Fading Reactions.

Since 2 CO<sub>2</sub>. CV is structurally very similar to CV<sup>+</sup> the zwitterion derivative should undergo the same proton transfer and/or acid-base equilibria as the parent dye. Hence it should be capable of protonation to the di and tricaticonic species. Similarly all forms would be susceptible to hydration. From this study it has been shown that when CVL is dissolved in absolute ethanol it is colourless, but if the solution is made 10<sup>-3</sup> M with respect to H<sup>+</sup> using concentrated HCl only, a blue colour is produced. Increasing the concentration of H<sup>+</sup> to 10<sup>-2</sup> M causes the colour to change to green Figure (3-3), λ<sub>max</sub> 640nm. Further addition of acid causes the colour to be discharged. The absolute ethanol used was dried, but if the coloured solutions were left open to the atmosphere they rapidly decolourized (30 mins). This shows that the coloured species formed were susceptible to either ring reformation or hydration, in a moist atmosphere.



Where R = Ph.NMe<sub>2</sub>

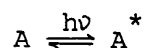
The loss of colour can be ascribed to either, the formation of (I), or (III), or both. The formation of the colourless compounds is reversible under the correct conditions. The formation of compounds (I) and (III) can account for reversible fading in solution and on mineral surfaces.

(ii) Irreversible Fading

Irreversible fading is caused by exposure of CyL, adsorbed on to clay minerals or oxides, to light. Photochemical changes can be broadly divided into two types:-

(a) Reversible Changes (Phototropy)

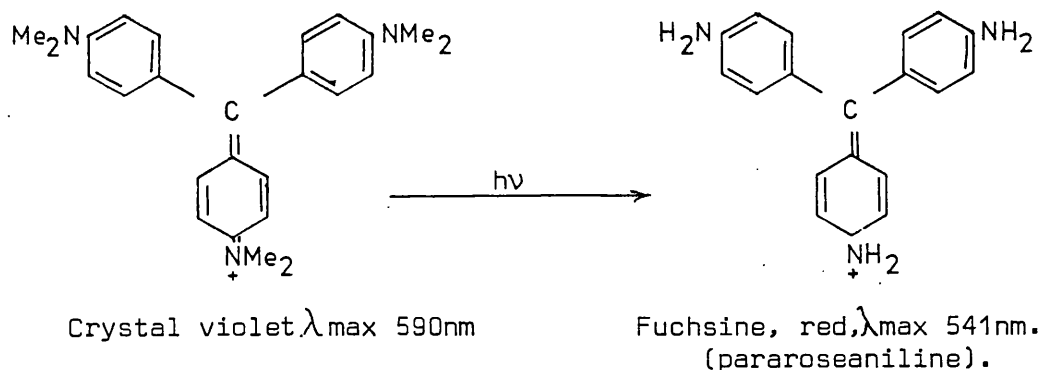
A strict definition of phototropy is given by Luck, W., and Sand, H., (1964), which states that phototropy is a reversible process that is produced by light absorption and leads to a quantum-mechanically stable, but thermodynamically unstable state. The phrase quantum mechanically stable is used to exclude fluorescence, phosphorescence and optical transitions.



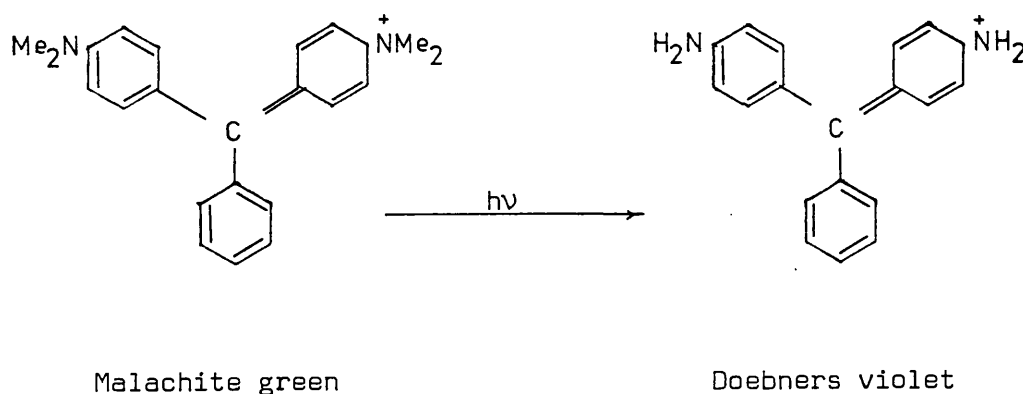
The term thermodynamically unstable state distinguishes phototropy from ordinary photochemical reactions, Egerton G.S., and Morgan A.G., (1970). Phototropy is generally restricted to azo compounds which are yellow or orange, because they exist in two geometrically isomeric forms. These have different spectra, and phototropy causes conversion from one form into the other.

(b) Irreversible Changes (Fading)

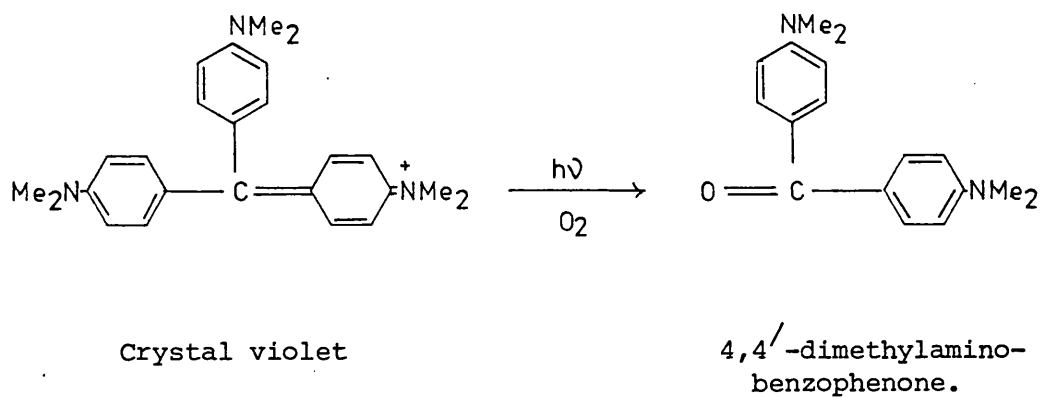
In general indirect methods, such as isolation and identification of photochemical breakdown products, are used to study reaction mechanisms. This represents the end result of extensive chemical changes and can only indirectly provide evidence for the fading process. A limited amount of work has been done on the fading products of triarylmethane dyes in solution. It was shown by Henriquez, P.C., (1933) that an aqueous solution of crystal violet irradiated with a mercury arc lamp for a few days turned red. Since the red compound possessed a free amino group, and had dyeing properties, it was concluded that the fading product was Fuchsine (pararoseaniline).



Malachite green undergoes similar change and turns violet.



If crystal violet was exposed to light for longer periods the solution turned colourless. The fading products were isolated by Iwamoto, K., (1935). 4, 4' dimethylamino-benzophenone was found to be a major product.



### 3.1.5. The Uses of Crystal Violet and Crystal Violet Lactone

Crystal violet is used as a biological stain and as a textile dye. CV is not used extensively for textile dyeing because although CV produces a brilliant shade it is not light fast, as are many di and triarylmethane dyes.

Crystal violet lactone is widely used as a dye in the carbonless copying process. CVL is encapsulated in gelatin or a synthetic polymer. The encapsulated dye is then applied to the underside of a sheet of paper. The upper surface of the sheet below has a clay mineral coating. Writing ruptures the capsules and releases the dye. The CVL released immediately reacts to form a violet colour. The colour fades within a few weeks when exposed to light, see page 197 Chapter 4.

## 3.2 Experimental

### 3.2.1. Materials

#### (i) Clay Minerals and Oxides

The silica gel used was Merck Silica gel G (nach Stahl), a standard chromatographic silica. The material had a surface area of  $500 \text{ m}^2/\text{g}$  as specified by the manufacturer.

The Siltan was a sample provided by English Clays Lovering, Pochin and Co., Ltd., St. Austell, Cornwall. Siltan is a brand name; the material is produced by the Mizusawa Company in Japan. It is an acid treated di-octahedral montmorillonite, Sugara, Y., et al., (1970), with a specific surface area, measured by the BET  $\text{N}_2$  adsorption method, Braunauer, S. Emmett, E. and Teller, E. (1938), of at least  $180 \text{ m}^2/\text{g}$ . The clay particle diameters are at least 75% by weight 10 microns or less and not more than 45% by weight of the particles have diameter of 1 micron or less. We have measured by X-ray diffraction (XRD) the basal spacing of siltan, it was found to be  $(d(001)) \sim 1.44 \text{ nm}$ . The Siltan was dried for XRD in vacuo at  $20^\circ\text{C}$  over  $\text{P}_2\text{O}_5$  for 16hrs. The XRD was measured using the 'Powder Method', Azaroff, L.V. and Buerger, M.J. (1958). The X-ray wavelength  $\text{CoK} = 1.7902 \text{ \AA}$ , and the camera was 57.415mm radius

The Upton Wyoming bentonite #25 and the kaolinite used were both American Petroleum Institute Project 49, standard clay minerals, obtained from Ward's Natural Science Establishment, Inc. Rochester, New York.

(ii) All the water used was prepared by double distillation in an all pyrex still and stored for short periods in pyrex bottles. The water had a specific conductance of  $10^{-6}$  ohm<sup>-1</sup> cm<sup>-1</sup>. All chemicals used were of Analar grade unless otherwise stated. Crystal violet was a Hopkin and Williams technical stain which was shown to be ~90% pure by T.L.C.

The crystal violet lactone, (6 (dimethylamino)-3,3 bis dimethylaminophenyl isobenzofuranone) used was kindly provided by English Clays Loverings, Pochin and Co., Ltd., St. Austell, Cornwall. The CVL had a melting point of 169<sup>o</sup>C cf. Moriga, H. and Oda, R. (1964) 168-169<sup>o</sup>C.

### 3.2.2 Methods

#### (i) Analytical Thin Layer Chromatography

The adsorbents used were either Silica gel G or Silica Gel GF254, both were supplied by Merck. The adsorbent was mixed with the solvent (usually water) 1:2 w/v and vigorously stirred in a blender for 30 secs. The slurry was then evacuated with stirring for a further 1 min, to remove any air bubbles. The slurry was then spread on five 20 x 20cm glass plates, using a Shandon plate spreader. The layer was 0.3mm thick when wet and 0.25mm when dry. The layer was allowed to dry in the air, then heated to 105°C for 30 mins to activate the layer. All TLC was performed on a radial TLC apparatus (supplied by Schleicher and Schüll . Inc. Selecta Sol Chromatography Chamber U.S.A.). The TLC apparatus was wrapped in aluminium foil to exclude light when in use.

Developed chromatograms were then examined in day-light and under a dual wavelength u/v light (Shandon). (254/280nm) samples were applied using disposable micropipettes (Microcaps, Drummond Scientific Co., Broomhall, Pennsylvania U.S.A.) or by a Hamilton liquid microliter syringe (Distributed by Pierce Box 117 Rockford, Illinois, 61105).

Two to twenty microliters of 0.5% w/v methanolic or ethanolic solutions of the dyes were applied to the plate, each dye on one spot (3mm max diameter) on a concentric circle approximately 1cm radius from the centre of the plate.

Crystal violet is a basic dye. Basic dyes are water



soluble as the chloride or perchlorate salts. Many TLC solvent systems have been devised in order to separate basic dyes, Stahl, E. (1969), 618-619. In the course of this work many solvent systems have been tried but the most satisfactory was one devised by Marshall, P.N. and Lewis, S.M. (1974)a, (Butan -1-ol, 12 vols : 1% w/v aqueous  $\text{NH}_4\text{Cl}$ , 5 vols : 2% v/v aqueous formic acid ( 90% pure) 2 vols). After vigorous shaking, the two phases were allowed to separate and the aqueous phase was discarded. Development was at ambient temperature (  $20^\circ\text{C}$ ) and usually took 4-6hrs. The chromatogram was dried in a draught of cold air.

If after examination, a particular band was of interest, it was scraped off and sucked into a tube which contained ethanol washed cotton wool. 3mls of absolute ethanol was then run through the tube to elute the compound.

(ii) Fading of Crystal Violet Lactone on Silica Gel G.

30 grams of silica gel G was washed in a Soxhlet apparatus for 16hrs using absolute ethanol as solvent. This ensured removal of organic u/v absorbing materials. The silica was allowed to dry and then slurried (1:2) w/v with ethanol/water (1:1) v/v. 100mgs of CVL had been previously dissolved in the ethanol. The plates were spread as described above. The plates were white when wet, but turned bright violet on drying. The dry plates were placed in an incubator at  $40^\circ \pm 0.5^\circ\text{C}$ , with constant irradiation from a 100 watt fluorescent light, 22cms from the plates  $13.0 \text{ watts/m}^2$ , for 60 days.

After 60 days the plates were removed and washed with the developing solvent for 16 hrs in a Shandon plate washer. This concentrated the mobile components into a narrow band at the end of the plate. This narrow band was scraped off the plate and placed in a soxhlet apparatus. The silica was firstly extracted with acetone for 8hrs. Each solvent was then evaporated in a Buchi rotary film evaporator. The extracts were then separated by TLC. The remaining silica which contained material which was not mobile in the developing solvent was removed from the plate and extracted using DMF in a soxhlet apparatus.

(iii) Transmission Spectroscopy

All ultra violet and visible transmission spectroscopy was performed on a Pye Unicam SP1800 series 2 with an AR25 linear recorder. A matched pair of quartz cells were used, 1 cm path length.

(iv) pH measurements

Measurement of pH to  $\pm 0.05$  pH units were made with a combination electrode, Phillips/Pye Unicam PW9418 pH meter. The pH values quoted refer to the aqueous phase in equilibrium with the sedimented solids.

(v) Preparation of Homionic Clay Minerals and Oxides

Kaolinite

The kaolinite was ground in an agate mortar for several minutes prior to preparing the homoionic clay. Homoionic  $\text{Al}^{3+}$  and  $\text{Ca}^{2+}$ -kaolinite were prepared by suspending 10g of kaolinite

in a 5% w/v suspension of 1 Molar,  $\text{AlCl}_3$  or  $\text{CaCl}_2$ , at pH 3.0. The kaolinite was equilibrated four times, each time with a fresh solution. The kaolinite and solution being separated by centrifugation (5,000 rpm, Griffin and George bench centrifuge) for 10 minutes. The kaolinite was washed with water, then with 90% ethanol:water v/v to ensure no exchange between  $\text{H}^+$  and  $\text{Al}^{3+}$ , or  $\text{Ca}^{2+}$  took place. After washing, the concentration of the ion in solution was  $< 1 \times 10^{-4} \text{M}$ . The kaolinite was finally centrifuged and dried at  $110^\circ\text{C}$ .

The  $\text{H}^+$  and  $\text{NH}_4^+$  kaolinite were prepared in a similar manner, except that the HCl used, was  $10^{-2} \text{M}$ , and the  $\text{NH}_4\text{Cl}$  was 1 Molar. After final equilibration and centrifugation the clay was evacuated to remove any excess  $\text{HCl}(\text{g})$  or  $\text{NH}_3(\text{g})$ . Finally they were washed as described above. All samples of homoionic clay were stored under vacuo over  $\text{P}_2\text{O}_5$ .

The same procedures were followed in the preparation of the other homoionic clay minerals and oxides.

(vi) Diffuse Reflectance of Crystal Violet and Crystal Violet Lactone on Clay Minerals and Oxides

The clay minerals, and oxides used, together with the treatment to produce homoionic clay minerals have been described above.

Diffuse reflectance spectra were measured on a Pye Unicam SP1800, the normal mirror arrangement being removed and replaced by the diffuse reflectance attachment (Pye Unicam SP890 Dif. Refl. Unit). The samples were placed in a metal sample holder supplied by Pye Unicam. These were metal planchets approximately 30mm in diameter with a central depression 25mm in diameter and 2mm

deep. Each disk held 0.4 to 0.8g of material; the weight depended upon which clay mineral was used. When in position a quartz window was placed over the depression in the sample holder to retain the dry powder. All spectra were recorded against a clay mineral or oxide standard.

The clay minerals were ground in an agate mortar for 30 mins. To a weighed amount of clay, a known amount of dye was added, in ethanolic solution, in the concentration range 0.1 to 2.0 mg/ml. This gave a final dye/clay ratio of 0.1 to 10 mg dye/g clay. Each suspension was made to a constant volume, to facilitate mixing. The dye/clay suspensions were thoroughly mixed; at these concentrations the dye was rapidly adsorbed, 10-20 mins, and then the solvent was evaporated. Approximately 99% of the dye stuff was adsorbed on to the clay minerals, as shown by an adsorption isotherm page 48 Chapter 2. The dye/clay complex was then reground in an agate mortar to ensure homogeneity. The sample was then packed into the metal disks, and pressed firmly in with a metal die.

The samples were stored in vacuo at  $40^{\circ} \pm 0.5^{\circ}\text{C}$  in three controlled humidities, 100, 62.5 and 0% relative humidity. The 100% RH atmosphere was produced by distilled water, 62.5RH by 100mls of aqueous KOH (285.7 g/l) and 0% RH, by storing over  $\text{P}_2\text{O}_5$ . The samples were constantly illuminated from four fluorescent strip lights which produced  $13.0 \text{ watts/m}^2$  at the level of the samples. Control samples were stored in the dark.

### 3.3 Results and Discussion

#### 3.3.1. Purity of Crystal Violet and Crystal Violet Lactone

Several criteria were used to establish the degree of purity of the dyes used.

##### (i) Melting Point

Compound	Measured mp <sup>o</sup> C	Literature value <sup>o</sup> C
CRYSTAL VIOLET-HCl	184 (decomp)	NOT AVAILABLE
CRYSTAL VIOLET LACTONE	169	168 - 169*

\* Moriga, H., and Oda, R. (1964).

##### (ii) Thin Layer Chromatography

When commercial crystal violet was subjected to TLC, twelve components could be resolved, Table (3-1). 2 to 10  $\mu$ ls of 0.5% w/v methanolic solution was applied in order to obtain accurate R<sub>f</sub> values for the major and minor components. Although twelve components could be separated, band number 7 accounted for ~90% of the extinction of the dye.

Only one band could be resolved when CVL was subjected to TLC using the normal developing solvent, Table (3-2). But this was near the solvent front. Therefore a second solvent system was used

(methanol:water 60/40 v/v). This also showed only one component  
Rf = 0.55.

(iii) Ultra Violet and Visible Spectroscopy

The spectrum of crystal violet in ethanolic solution is shown in Figure (3-4),  $\lambda_{\max} = 590\text{nm}$ ,  $\Sigma m\epsilon^+ = 100,000$ . These figures agree with the best literature estimates. Cigen R. (1959). The u/v spectrum of CVL is shown in Figure (3-2),  $\lambda_{\max}^{\text{ETOH}} = 272\text{nm}$   
 $\Sigma m = 50,000$ .

(iv) Nuclear Magnetic Resonance Spectroscopy

The N.M.R. spectra of CV and CVL are shown in Figures (3-5) and 3-6). All proton peaks have been assigned, and agree with structural formulae.

FIGURE (3—4). The Spectra of the Three coloured species of Crystal Violet in acidic solution

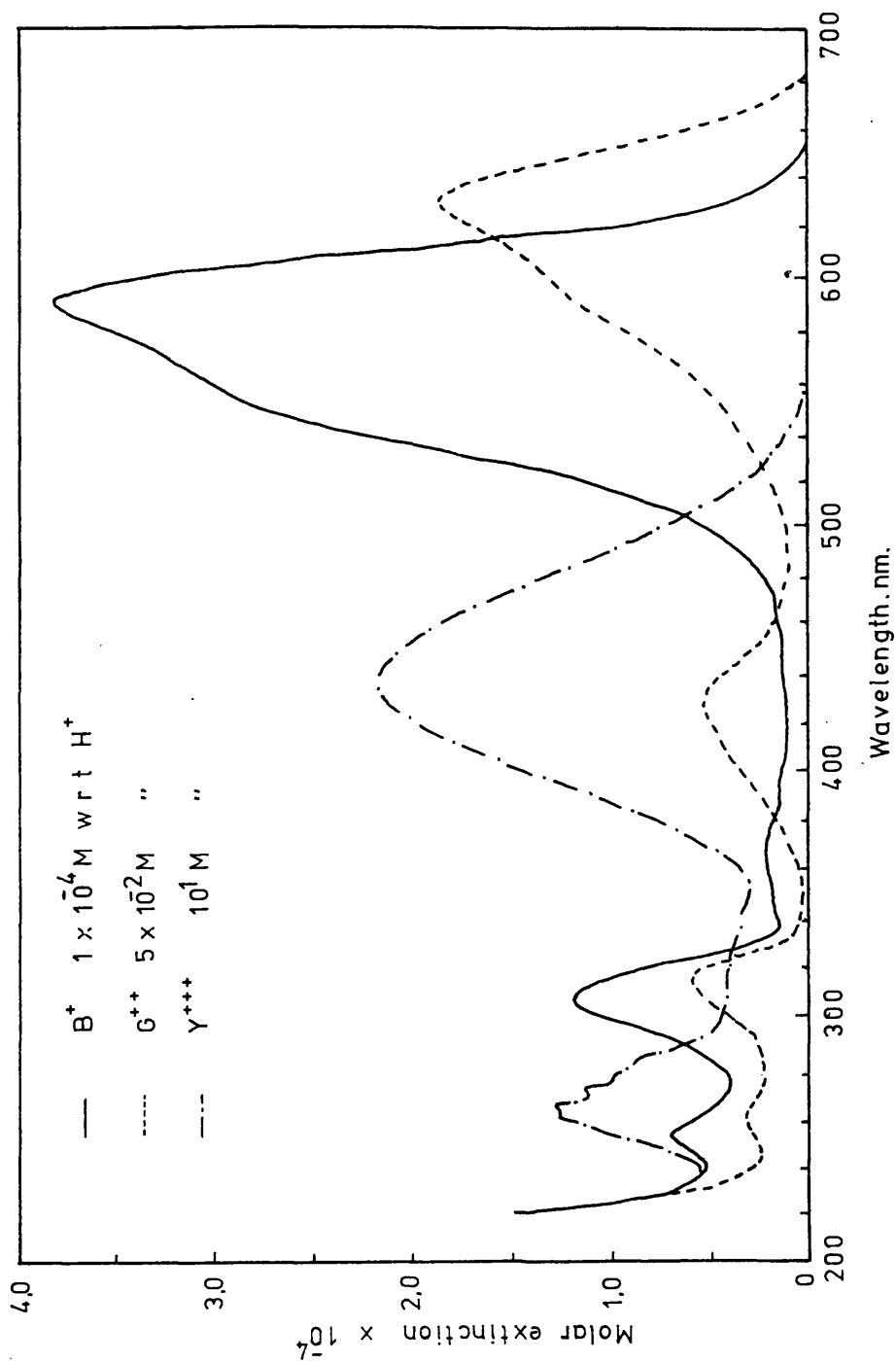


FIGURE. (3—5) Proton N.M.R. of Crystal Violet

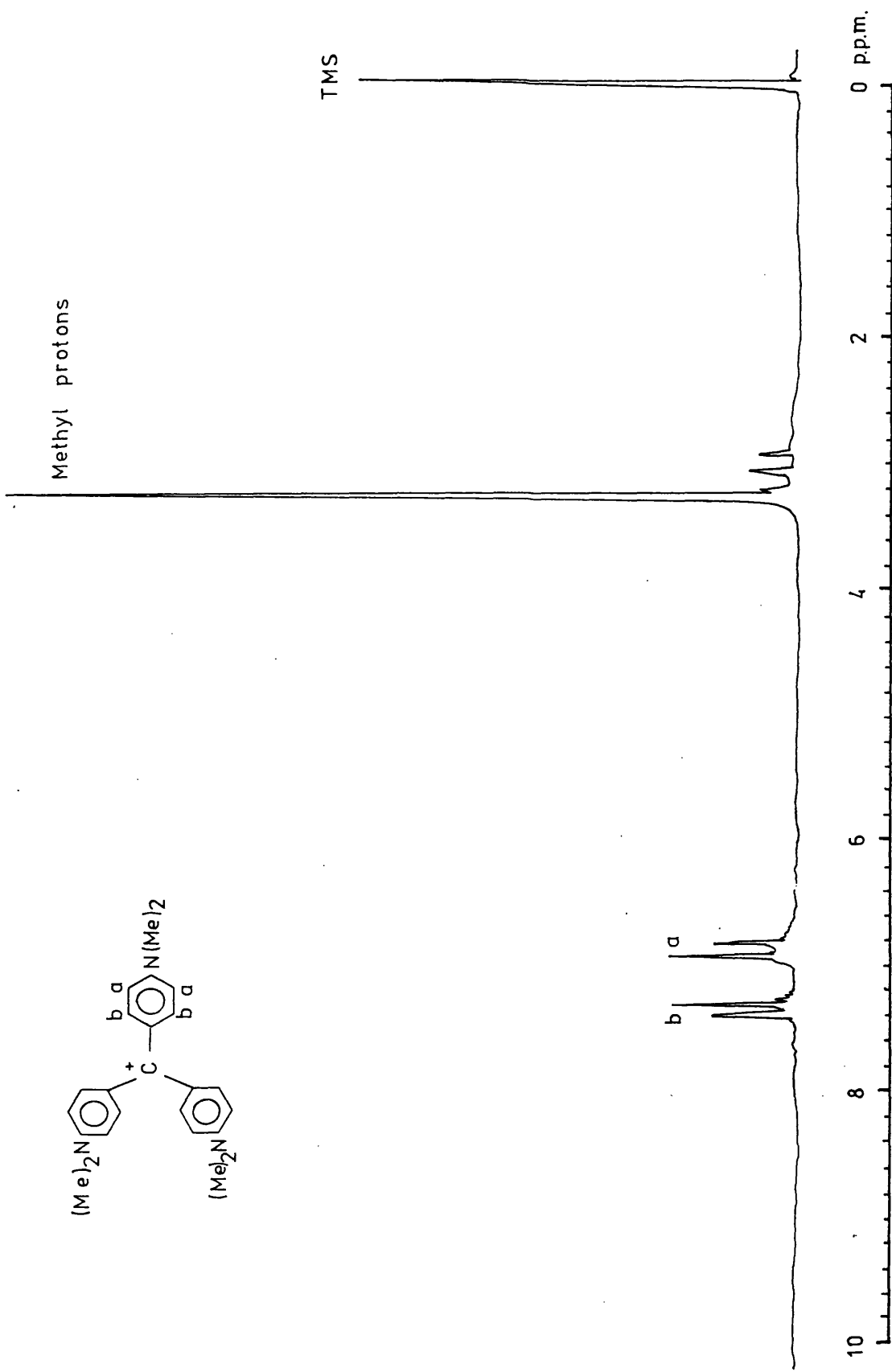
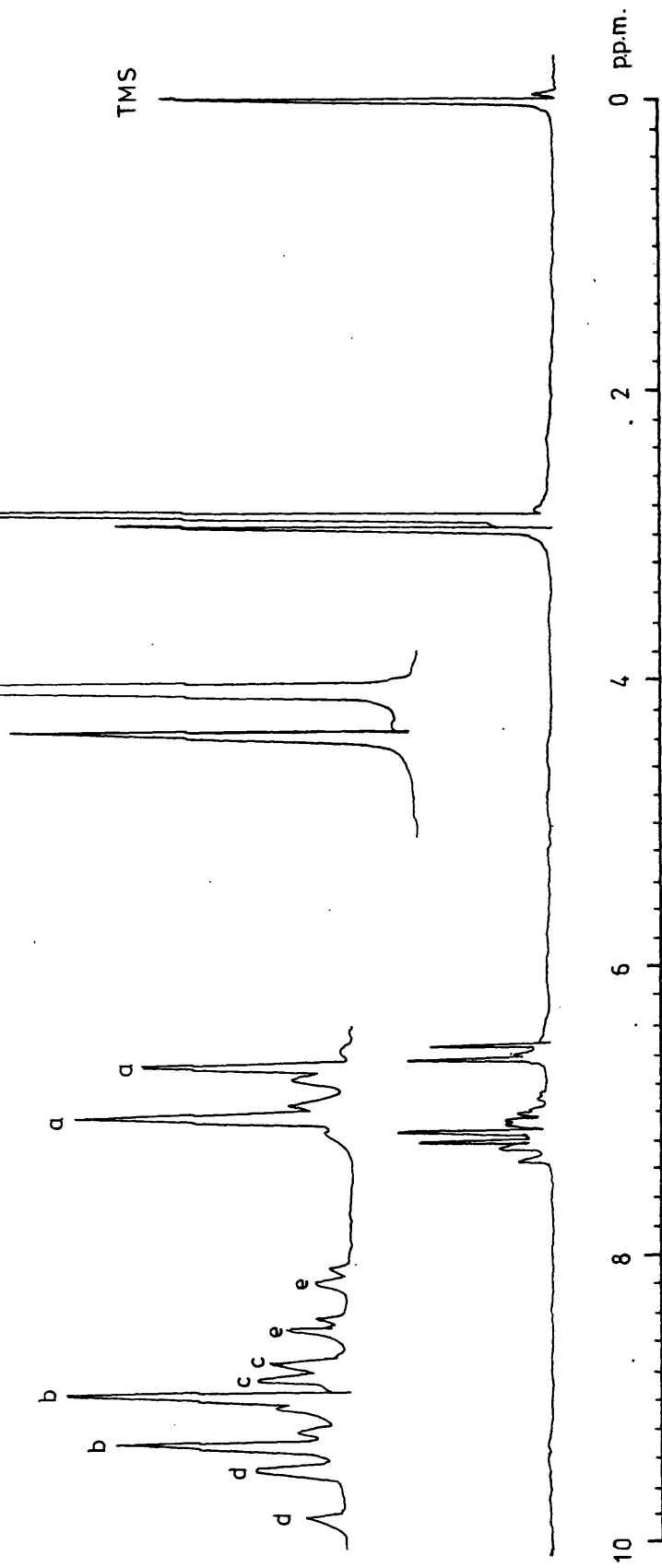
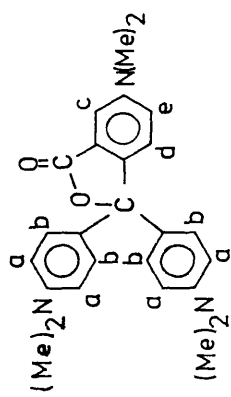




FIGURE (3—6) Proton N.M.R. of Crystal Violet Lactone



### 3.3.2. Radial Thin Layer Chromatography of Some Triarylmethane Dyes

Plates 1 and 2 show a typical radial chromatogram with unknown and standard components.

The Rf values for the standards used are shown in Tables (3-1 to 3-6). The  $\lambda$  max shown in the tables refer to the  $\lambda$  max of the component when desorbed from the silica by absolute ethanol.

A commercial sample of pararoseaniline, pararoseaniline-HCl (Eastman Technical Stain) was separated using RTLC. A second commercial sample of pararoseaniline, Fuchsine BDH stain, (fuchsine is a synonym for pararoseaniline), was separated. The separations, Table (3-3) and (3-4), show completely different components. From structural considerations pararoseaniline should have a greater Rf than CV in the same system, pararoseaniline is smaller and less polar than crystal violet. The separation of the BDH sample resolved eight components, none with an Rf greater than that of CV. The major components only having an Rf of 0.12 and 0.05, c.f. CV = 0.52. The Eastman sample showed only two components, with Rf values of 0.74 and 0.68. Desorption of band No. 1 showed it to have a  $\lambda$  max of 554nm. Therefore this band is pararoseaniline. The composition of the BDH stain is unknown.

Plates 3 and 4 show a typical chromatogram examined under two wavelengths of u/v light, c.f. Plates 1 and 2

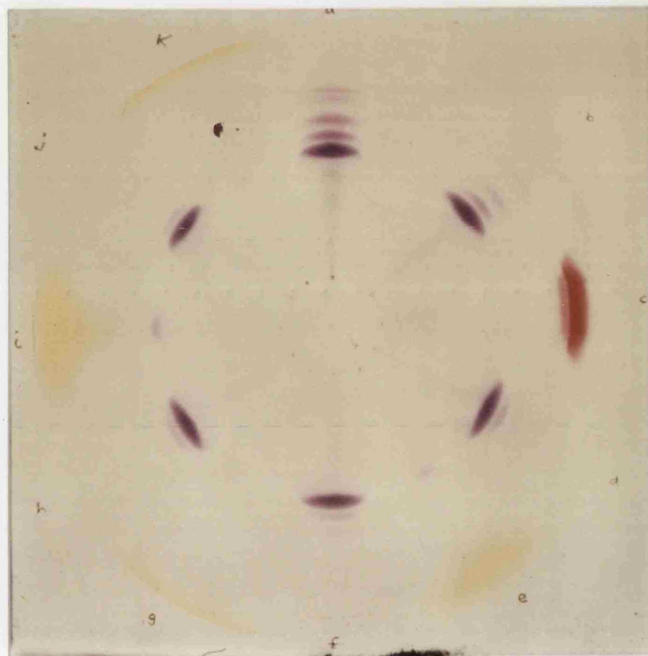
If a solution of CV in methanol exposed to light it will change colour. When the components of the solution are separated by TLC, several changes are seen. Table (3-7); no new bands appear

PLATE 1. Radial Thin Layer Chromatography of Crystal Violet,  
Crystal Violet Lactone and their derivatives.



- a Fraction D see Table (3 -14) for Rf values  
e Fraction C see Table (3 -13) "  
g Pararoseaniline Table (3 - 4) "  
i CVL in methanolic solution see Table (3 - 7) for Rf values.  
k Fraction E see Table (3 -15) for Rf values.  
b,d, etc. CV standard. see Table (3 -1) for Rf values.

PLATE 2. Radial Thin Layer Chromatography of Crystal Violet ,  
Crystal Violet Lactone and Their Derivatives.



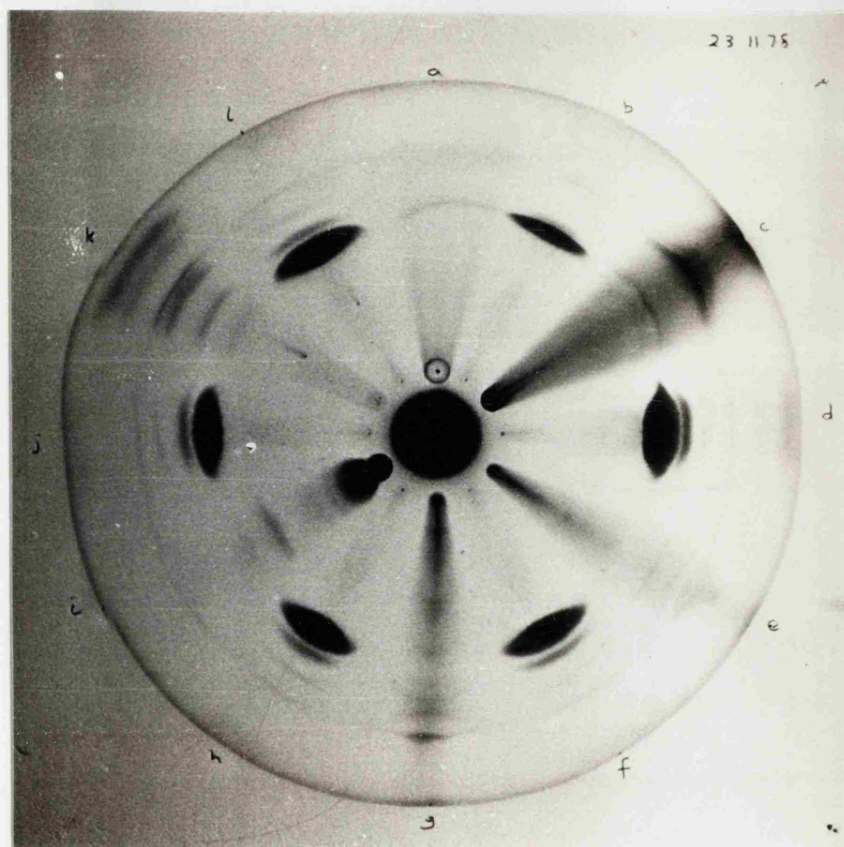
c .Pararoseaniline. Eastman Tech. Stain. see Table (3 -4) for Rf values.

i and e 4,4' bis dimethylamino benzophenone see Table (3-6)  
for Rf values.

k and g 4 di methylamino benzophenone see Table (3 -5) for Rf values.

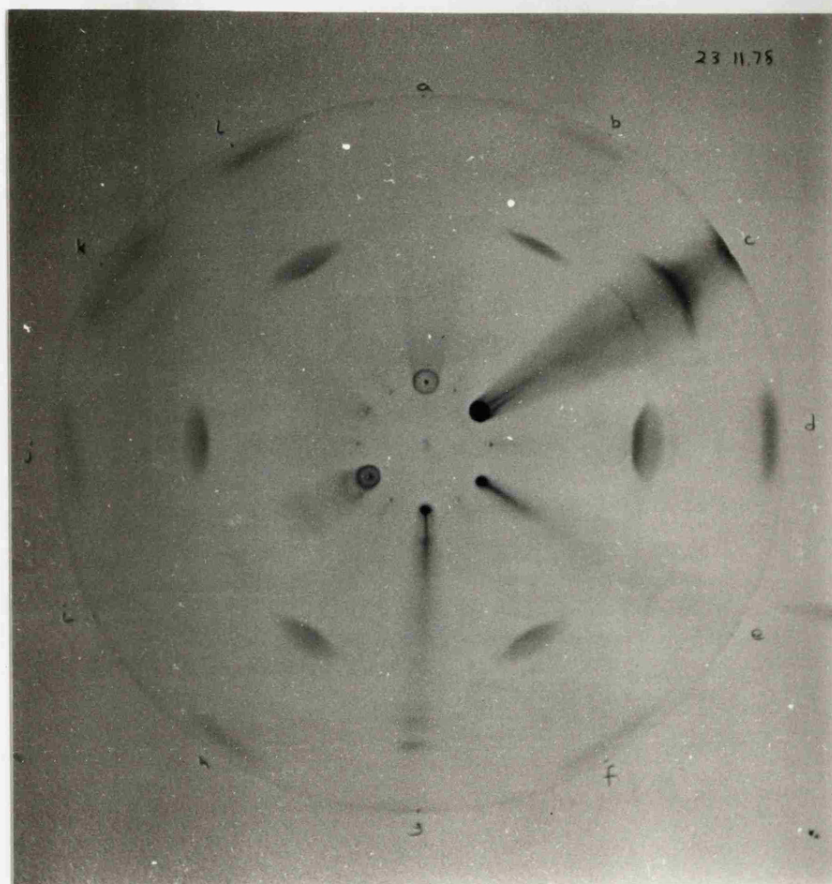
a ,b, d,f,h,and j CV standard. see Table (3 -1) , for Rf values.

PLATE 3    Radial Thin Layer Chromatography of Crystal Violet,  
Crystal Violet Lactone and Their Derivatives



- a    Fraction E;    see Table (3-15) for Rf values  
c    "    B;    "    (3-12)    "  
e    "    C;    "    (3-13)    "  
g    "    D;    "    (3-14)    "  
i    Fuchsin (BDH);    "    (3-3)    "  
k    CVL in methanolic solution; see Table (3-7) for Rf values.  
b,d, etc. Crystal Violet standard, see Table (3-1) for Rf values

PLATE 4 Radial Thin Layer Chromatography of Crystal Violet,  
Crystal Violet Lactone and Their Derivatives



- a Fraction E; see Table (3-15) for Rf values  
 c " B; " (3-12) "  
 e " C; " (3-13) "  
 g " D; " (3-14) "  
 i Fuchsin (BDH); " (3-3) "  
 k CVL in methanolic solution; see Table (3-7) for Rf values.  
 b,d, etc. Crystal Violet standard, see Table (3-1) for Rf values

but the amount of bands 3,4,5 and 6, Table (3-1) increase.

Component 3 has the same Rf and  $\lambda$  max as the standard pararoseaniline.

Since the bands 4,5 and 6 have Rf values which lie between pararoseaniline and CV, and they appear in larger quantities after irradiation, it was concluded that they were probably triarylmethane dyes with fewer methyl groups than CV and more than pararoseaniline.

It is possible to form eight intermediates dyes between CV and pararoseaniline, see Table (3-8).

Table (3-1) Radial Thin Layer Chromatography of Crystal Violet

ADSORBENT : Silica gel GF254  
 SOLVENT : BUTAN-1-OL/NH<sub>4</sub>Cl 2% aq/HCOOH 1% aq (12:5:2)  
 RUNNING TIME : 6 hours

NO.	Colour	Size of band large, medium small (L.M.S.)	* Mean Rf	+ λ Max (nm) Experimental value	Comments
1	Yellow	S	0.93		
2	Blue	M	0.84		
3	Red	M	0.77	542	Pararoseaniline
4	Blue	S	0.74	548	
5	Blue	M	0.67	558	
6	Violet	L	0.61	564	
7	Violet	VL	0.52	594	Cv major component.
8	Blue	S	0.45		
9	Blue	S	0.38		
10	Red	S	0.34		
11	Blue	S	0.26		
12	Blue	S	0.17		

\* The mean Rf is the mean of at least 6 separate samples.

The standard deviation for 6 samples = 0.01 Rf.

+ λMax of coloured material desorbed from silica by ethanol.



Table (3-2) Radial Thin Layer Chromatography of Crystal Violet  
Lactone

ADSORBENT : As Table (3-1)  
SOLVENT : "  
RUNNING TIME : "

NO	Colour	Size	* Mean Rf	+ $\lambda$ max	Comments
1	Violet	L	0.95	272nm	CVL

Table (3-3) Radial Thin Layer Chromatography of Fuchsin (BDH stain)

ADSORBENT : As Table (3-1)  
SOLVENT : "  
RUNNING TIME : "

NO	Colour	Size	* Mean Rf	Experimental $\lambda$ max (nm)	Comments
1	yellow	S	.52		
2	blue/pink	M	.40		
3	blue	S	.36		
4	blue	S	.27		
5	green/ yellow	S	.24		
6	pink/ purple	M	.19		
7	purple	L	.12		
8	purple	L	.05		

Table (3-4) Radial Thin Layer Chromatography of Pararoseaniline-HCl (Eastman Tech. Stain, Mwt = 323.83)

ADSORBENT : As Table (3-1)

SOLVENT :

RUNNING TIME :

No.	Colour	Size	* Mean Rf	+ Experimental $\lambda$ max (nm)	Comments
1	Red	L	0.74	542	Pararoseaniline
2	Red	M	0.68	557	

Table (3-5) Radial Thin Layer Chromatography of 4, Dimethylaminobenzophenone

ADSORBENT : As Table (3-1)

SOLVENT :

RUNNING TIME :

NO	Colour	Size	* Mean Rf	+ Experimental $\lambda$ max (nm)	Comments
1	Yellow	L	0.93	330	

Table (3-6) Radial Thin Layer Chromatography of  
4,4'-bisdimethylaminobenzophenone

ADSORBENT : As Table (3-1)

SOLVENT :

RUNNING TIME :

No	Colour	Size	* Mean Rf	+ Experimental $\lambda$ max (nm)	Comments
1	Yellow	L	0.93	366	
2	Blue	S	0.51	591	
3	Blue	M	0.47	594	

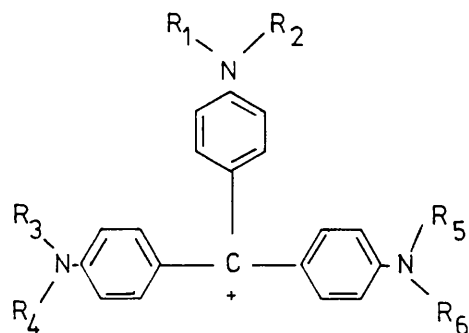
Table (3-7) Radial Thin Layer Chromatography of CV dissolved in  
Methanol and Exposed to Light for 20 days at 20<sup>o</sup>C

ADSORBENT : As Table (3-1)

SOLVENT : "

RUNNING TIME : "

No	Colour	Size	Mean Rf	Experimental $\lambda$ max (nm)	Comments
1	Red	M	0.73	542	Pararoseaniline
2	Blue	M	0.69	548	
3	Blue	M	0.61	558	
4	Violet	L	0.55	564	
5	Violet	L	0.49	594	CV
6	red/brown	S	0.41		
7	red/brown	S	0.33		



$R_1$  to  $R_6$  = Me = Crystal Violet

$R_1$  to  $R_6$  = H = pararoseaniline

Table (3-8) Structures of Triarylmethane dyes

R groups refer to diagram above

No	Methyl Groups	$R_1$	$R_2$	$R_3$	$R_4$	$R_5$	$R_6$	$H_2O$ $\lambda$ max (nm)
1	6	Me	Me	Me	Me	Me	Me	590
2	5	H	Me	Me	Me	Me	Me	587
3	4	H	H	Me	Me	Me	Me	
4	4	H	Me	H	Me	Me	Me	
5	3	H	H	H	Me	Me	Me	
6	3	H	Me	H	Me	H	Me	
7	2	H	H	H	H	Me	Me	
8	2	H	H	H	Me	H	Me	
9	1	H	H	H	H	H	Me	
10	0	H	H	H	H	H	H	541

No band had a  $\lambda$  max = 587nm therefore No.2 Table (3-8) can be ruled out, this has 5 methyl groups and is commonly known as methylviolet, although it is possible that this species was present but was unresolved. The seven remaining compounds can be divided into two groups:-

No. of methyl groups	Series (a)				Series (b)			
	4	3	2	1	2	3	4	
	H	H	H	H	H	H	H	
	H	H	H	H	H	R <sub>2</sub>	R <sub>2</sub>	
	R <sub>3</sub>	H	H	H	H	H	H	
	R <sub>4</sub>	R <sub>4</sub>	H	H	R <sub>4</sub>	R <sub>4</sub>	R <sub>4</sub>	
	R <sub>5</sub>	R <sub>5</sub>	R <sub>5</sub>	H	H	H	R <sub>5</sub>	
	R <sub>6</sub>	R <sub>6</sub>	R <sub>6</sub>	R <sub>6</sub>	R <sub>6</sub>	R <sub>6</sub>	R <sub>6</sub>	

The dyes in series (a) are less symmetrical than those in series (b). Loss of symmetry, as well as electron donating power would tend to produce x and y transitions, analogous to malachite green. The electron donating ability of amines are in the order tertiary > secondary > primary, but the differences are small and are unlikely to be large enough to produce x and y transitions. Therefore it is not possible to distinguish between the two series by their  $\lambda$  max values. Only three species are resolved out of a possible seven. Resolution was very good in this system and it should have been possible to detect not only species that differ by one methyl

group, but also structural isomers, c.f. Azure A/ symmetrical dimethylthionine page 226 Chapter 4.

If an empirical value is placed upon the hypsochromic shift caused by removal of one methyl group, a value of 9nm is obtained, Table (3-9).

Table (3-9) Predicted  $\lambda$  max values of Triarylmethane Dyes

No. Methyl Groups	H <sub>2</sub> O $\lambda$ max Literature values *	Predicted +	Observed	Rf of Band
6	590	592	594	0.52
5	584	583	-	-
4	-	574	-	-
3	-	565	564	.61
2	-	556	557	.67
1	-	547	548	.74
0	538	538	542	.77

+ The empirical values were calculated by:-

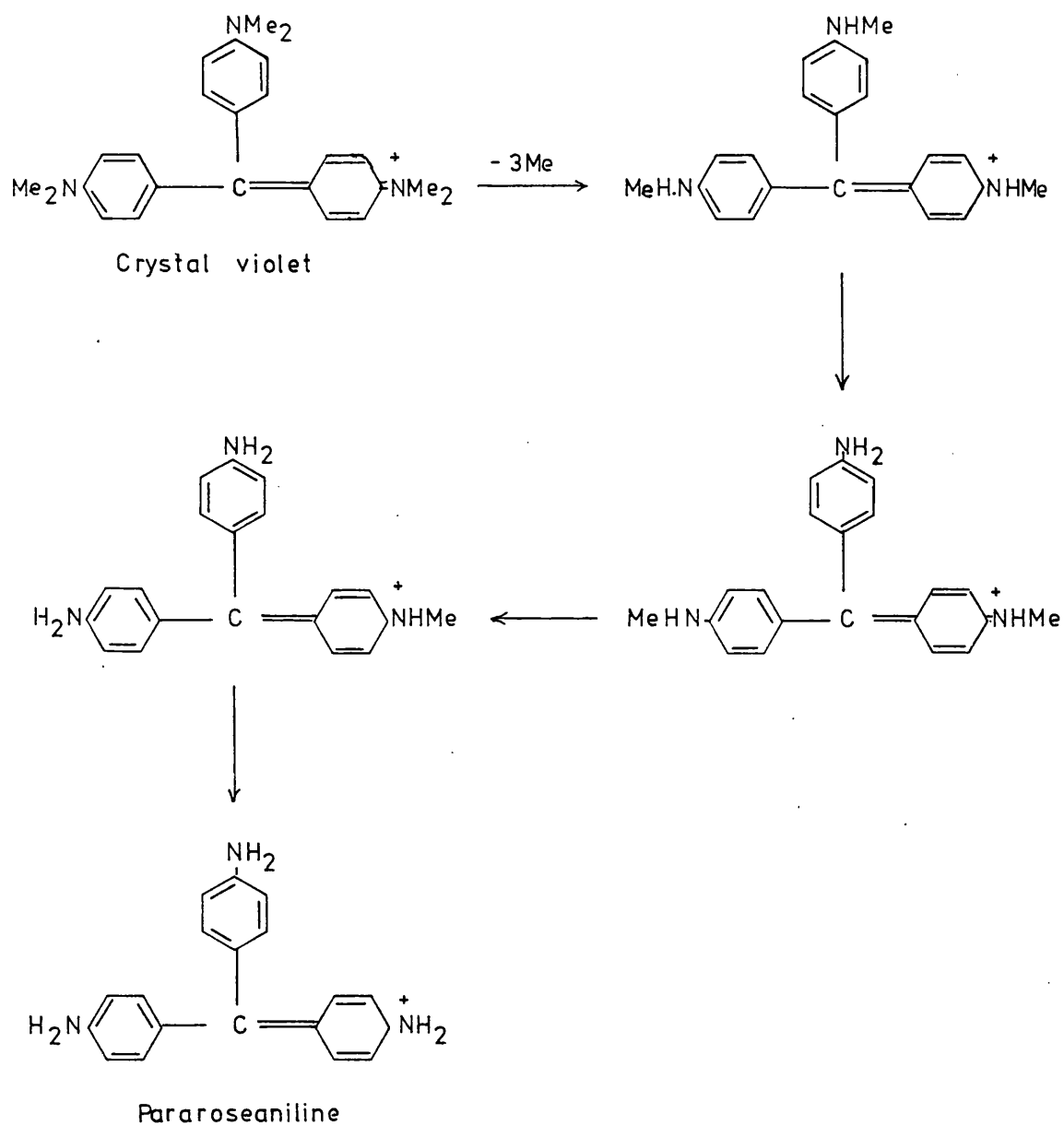
(  $\lambda$  max CV -  $\lambda$  max pararoseaniline)  $\div$  6 = hypsochromic shift/Me group.

(592 - 538 = 54  $\div$  6 = 9nm/me).

\* No literature values could be found for the dyes with 4,3,2 and 1 methyl groups. The observed max for bands 4,5 and 6 Table (3-1) most closely fit the predicted values for 3,2 and 1 methyl groups. Since there is only one structure for the dye with, one methyl group, Table (3-9), only the distinction between series (a) and (b) for the dyes with 2 and 3 methyl groups is necessary.

From the data no distinction can be made. But series (b), where the molecules are more symmetrical would suggest it is the more likely pathway.

Summarizing the possible demethylation as:



### 3.3.3 Radial Thin Layer Chromatography of Crystal Violet Lactone

A solution of crystal violet lactone in ethanol which was unprotected from light rapidly turned blue. The  $\lambda$  max of the solution was 596nm. The intensity of the colour increased with time. Table (3-10) shows the RTLC separation of such a solution, 13 watts/m<sup>2</sup> light at 20°C for 20 days. Comparing this with Table (3-2) it becomes apparent that several coloured species are produced. Any species which possesses a carboxyl group on the C<sub>2</sub> atom travels in the TLC solvent as a lactone and is therefore colourless. Such species would travel on the solvent front because they are not charged. It can therefore be concluded that the bands 3-11 in Table (3-10) show CVL has been decarboxylated.

Table (3-10) Radial Thin Layer Chromatography of CVL dissolved in Ethanol and Exposed to Light for 20 days at 20°C

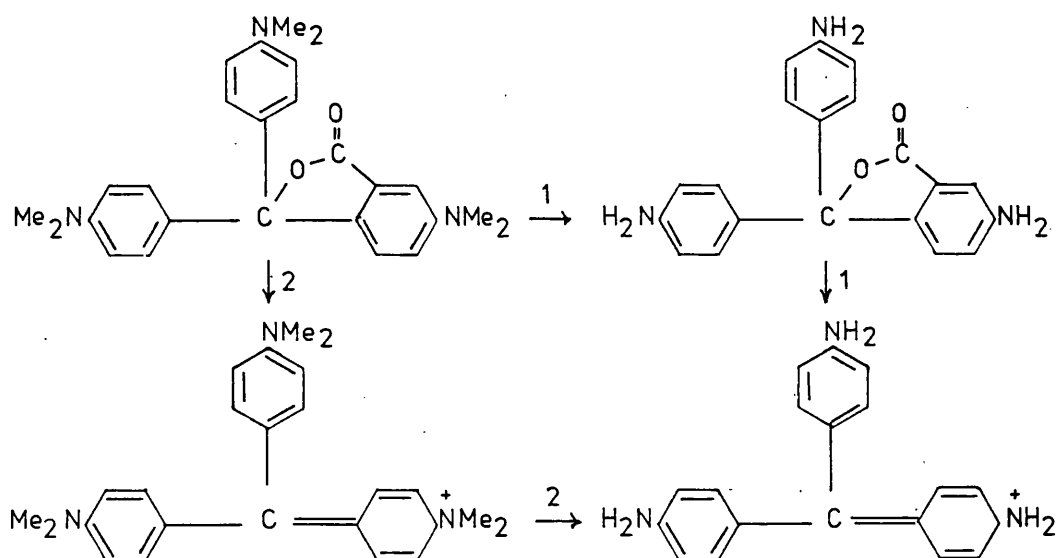
ADSORBENT : As Table (3-1)  
 SOLVENT :  
 RUNNING TIME :

No.	Colour	Size	Mean Rf	Experimental $\lambda$ max (nm)	Comments
1	Violet	L	0.95		CVL
2	Red	S	0.88		
3	Red	S	0.77	542	Pararoseaniline
4	Blue	S	0.75	548	
5	Blue	vS	0.72		
6	Blue	vS	0.66		
7	Blue	M	0.63	574	
8	Blue	vS	0.58		
9	Violet	M	0.53	594	CV
10	Blue	S	0.46		
11	Blue	S	0.42		



Components No.3 and 9, Table (3-10) have been identified, by  $R_f$  and  $\lambda_{max}$ , as pararoseaniline and crystal violet respectively. Again, it is highly likely that bands 4 to 8 are demethylated derivatives of crystal violet. But in this case there are five bands separated compared with three for CV. Not all bands were in sufficient quantity to permit identification. But those that were, seemed to suggest that all the demethylated species were present.

There are two routes to produce demethylated derivatives of CV from CVL, (1) demethylation followed by decarboxylation; (2) decarboxylation followed by demethylation, see below:

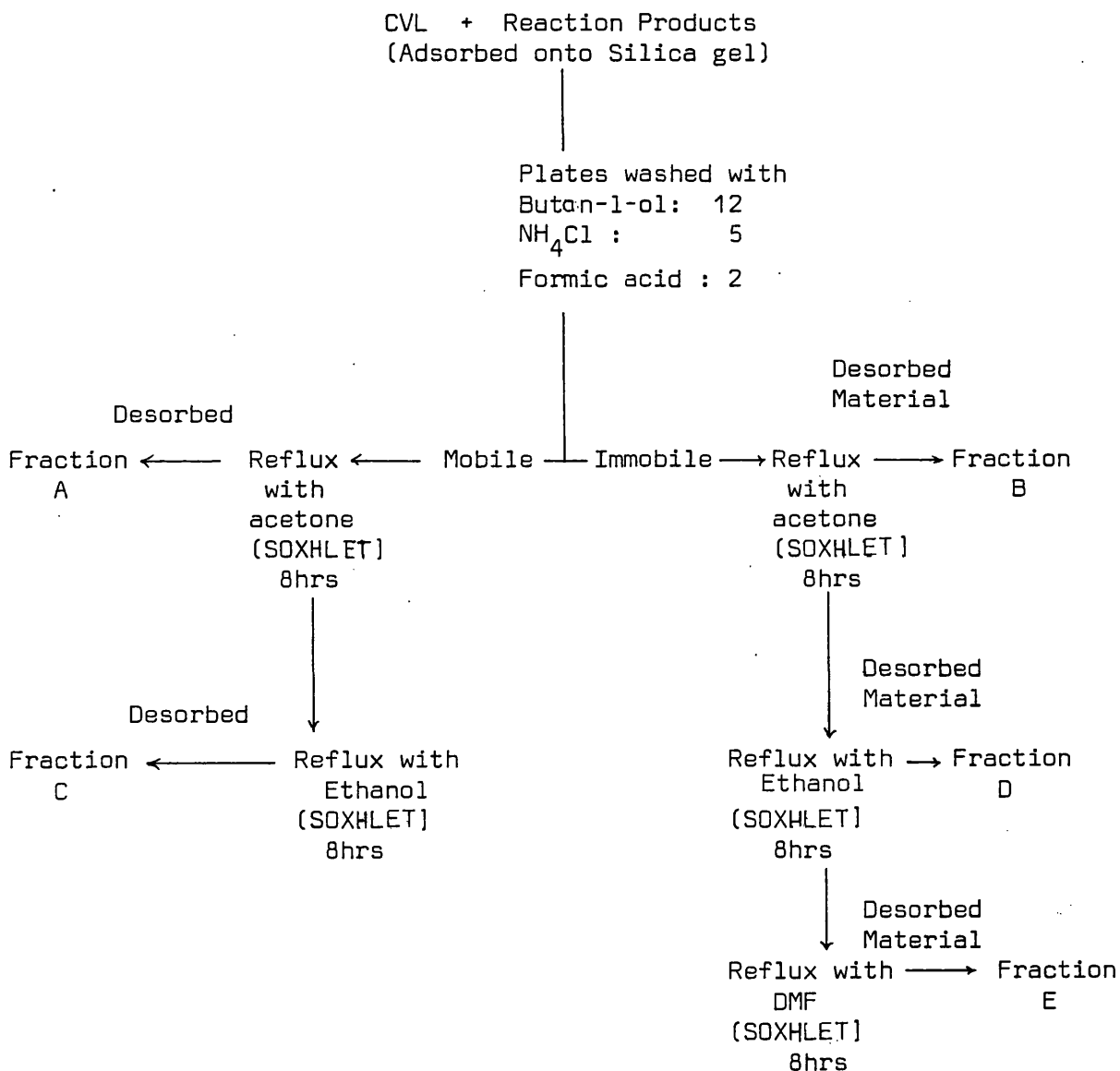


If route (2) was the major pathway, CV would be formed and the demethylation products would be the same as those formed from the irradiation of CV Table (3-7), this was not observed. All the demethylated products were formed and this would suggest that crystal violet lactone is more susceptible to photodegradation than CV.

3.3.4. Thin Layer Chromatography of Crystal Violet Lactone  
Irradiated on Silica Gel.

The reaction products of CVL, which had been exposed to light, were crudely separated using the following scheme:-

Scheme to Separate Breakdown Products of CVL



The components of Fractions A to E were further separated by RTLC.

The butan-1-ol :  $\text{NH}_4\text{Cl}$  2% aq : formic acid 1% aq (12:5:2) was intended to separate the mixture into 2 broad fractions of high and low Rf.

The acetone extraction removed almost all of the unreacted CVL, Fraction A; Table (3-11), plus some CV. The alcohol extraction Fraction C; Table (3-13) contained no major band. There were 13 components resolved, components 1 and 7 were identified as CVL and CV respectively.

Fractions B and D, Tables (3-12 and 3-14) were resolved into 6 and 5 bands respectively. Bands 2 and 4, Table (3-14) were identified as CV demethylation products.

Radial Thin Layer Chromatographs of the Reaction Products of CVL  
upon Silica gel at 40°C

Table 3-11)      Fraction A  
ADSORBENTS : As Table (3-1)  
SOLVENT :  
RUNNING TIME :

No	Colour	Size	Mean Rf	Experimental $\lambda$ max (nm)	Comments
1	Violet	VL	0.96		CVL
2	"	S	0.58		
3	"	S	0.54	594	CV
4	"	S	0.48		

Table (3-12)

Fraction B

ADSORBENT : As Table (3-1)

SOLVENT :

RUNNING TIME :

---

No	Colour	Size	Mean Rf	Experimental $\lambda$ max (nm)	Comments
1	brown/orange	L	0.98		
2	blue	S	0.89		
3	brown/orange	L	0.80		
4	brown/orange	L	0.78		
5	brown/orange	L	0.61		A large %
6	orange	vL	origin		did not move.

---

Table (3-13)                      Fraction C

ADSORBENT        :    As Table (3-1)

SOLVENT            :

RUNNING TIME    :

NO	Colour	Size	Mean Rf	Experimental $\lambda$ max (nm)	Comments
1	blue	m	0.94		CVL
2	blue	m	0.84		(blue when absorbed colourless in ETOH)
3	blue	s	0.69	557	
4	brown	m	0.63		
5	blue	s	0.61	564	
6	amber	s	0.61		
7	blue	m	0.56	594	CV
8	pink	m	0.49		
9	pink	s	0.40		
10	blue	m	0.33		
11	brown	s	0.29		
12	brown	s	0.20		
13	brown	s	0.12		

Table (3-14) : Fraction D

ADSORBENT : As Table (3-1)

SOLVENT :

RUNNING TIME :

No	Colour	Size	Mean Rf	Experimental $\lambda$ max (nm)	Comments
1	brown	S	0.81		
2	blue	S	0.74	548	
3	orange	S	0.70		
4	blue	S	0.63	564	
5	amber	M	0.30		

Table (3-15) Fraction E

ADSORBENT : As Table (3-1)

SOLVENT :

RUNNING TIME :

No	Colour	Size	Mean Rf	Experimental $\lambda$ max (nm)	Comments
1	Yellow	S	0.98	338	
2	Yellow	S	0.78		
3	Yellow	S	0.56		

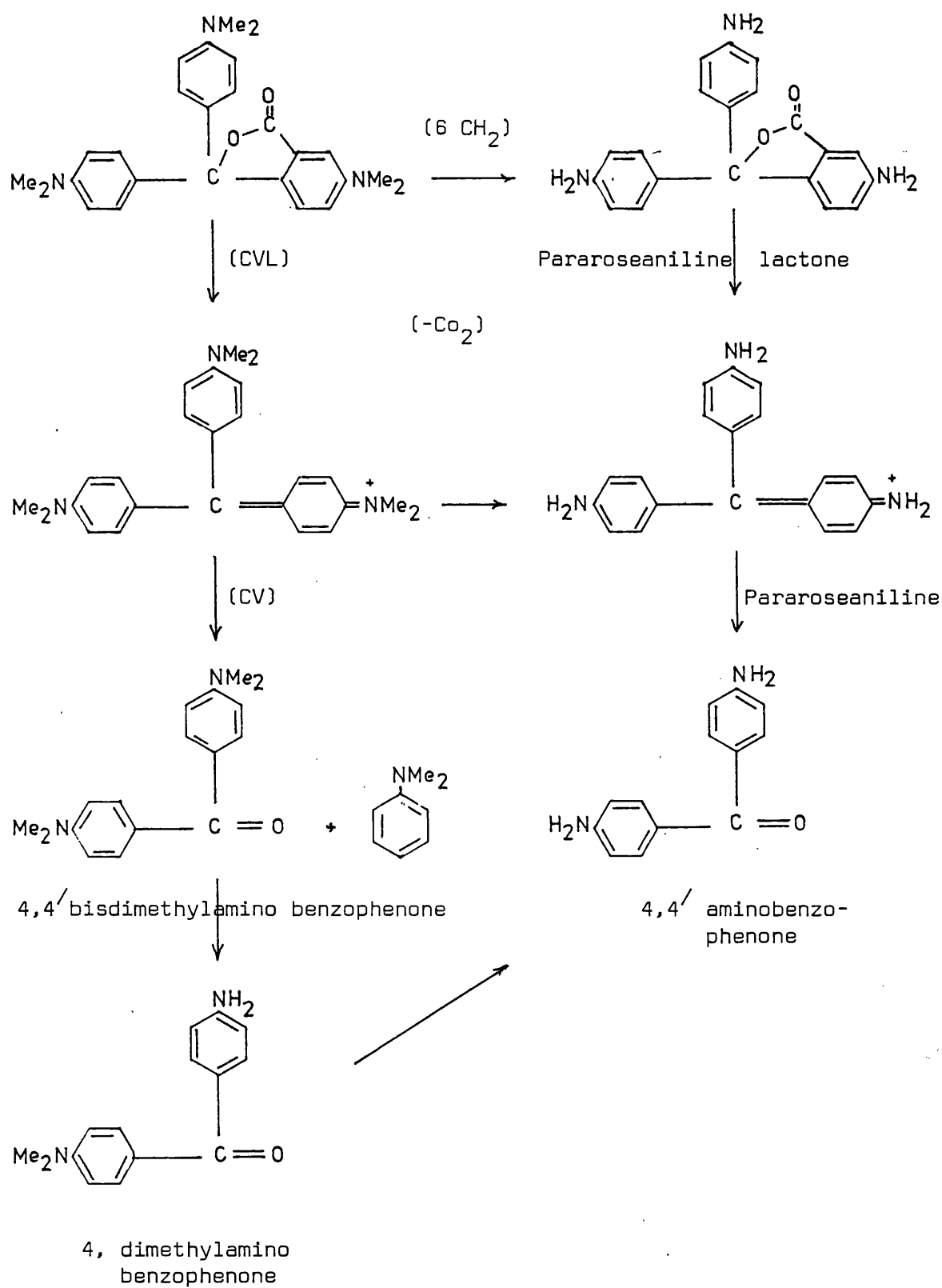
Fraction E, Table (3-15) resolved yellow and orange components. Band 1 had a  $\lambda_{\max}$  338nm. The Rf of 4,dimethylaminobenzophenone and 4,4 bisdimethylaminobenzophenone are shown in Tables (3-5 and 3-6), both with Rf 0.93. The  $\lambda_{\max}$  of 4,dimethylaminobenzophenone is 330nm. This would tentatively identify band 1 Table (3-15) as 4,dimethylamino-benzophenone.

Many components were separated in quantities too small to allow identification. In order to identify these components preparative layer chromatography was attempted, but the separations were poor.

The RTLC showed the presence of CV and benzophenone was tentatively identified, indicating degradation of the tri-arylmethane nucleus. Benzophenones are known to be free radical sources when irradiated with light, i.e. 4,4bisdimethylaminobenzophenone (Michlers Ketone) are free radical sources in u/v ink drying, this in turn would further accelerate CVL decomposition.

A possible scheme for the decomposition of CVL on silica gel is shown below.

Scheme for the Degradation of CVL upon Silica Gel

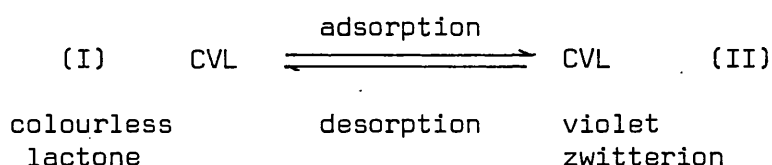




3.3.5. Diffuse Reflectance Studies of Crystal Violet and  
Crystal Violet Lactone Adsorbed upon Silica Gel

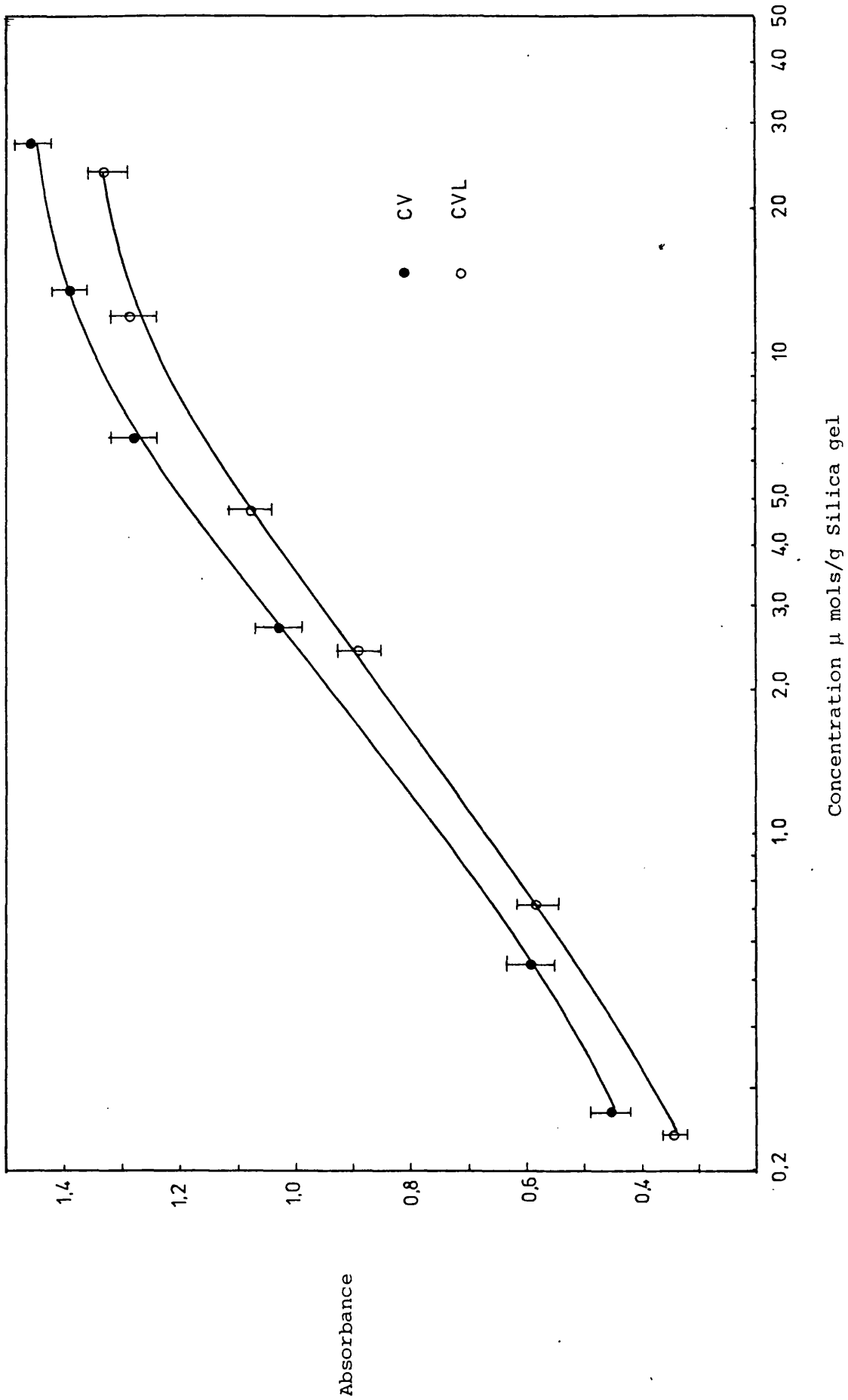
(i) The Effect of Concentration

The absorbance of CV and CVL, adsorbed upon silica gel, as a function of concentration is shown in Figure (3-7). The relationship was linear over a wide range of concentrations. The absorbance of CVL was 80% of the absorbance of CV at the same concentration. CVL reacts on the surface to form a coloured zwitterion,  
page 77 Chapter 3.



Only if the reaction goes completely to the right hand side of the equilibrium can the absorbance of the CVL zwitterion equal that of CV, (mono cationic violet form). This presumes that the extinction of  $\text{CVL}(\pm) = \text{CV}(+)$ . But this presumption is incorrect since substituents in an ortho position to the central carbon atom of triarylmethane dyes tends, by steric hinderance, to twist the rings further out of the plane and hence reduce  $\pi$  orbital overlap. This will reduce the intensity of the visible band, Barker, C.C. Bride, M.H. and Stamp, A. (1959). At lower coverage the curves tend to converge. This is expected because the colour change can only occur in the monomolecular layer at the surface of the adsorbent. Hence virtually all the CVL present will be in the zwitterionic form (II), when the coverage is low, and at high concentrations the absorbance will reach a limiting value. Such reactions give Langmuir type adsorption isotherms, and the surface area of an adsorbent can be

FIGURE. (3—7) The Absorbance of Crystal Violet and Crystal Violet Lactone on silica gel



predicted accurately when compared with BET surface area determinations, Kortum, G., and Delkrug, D., (1962).

(ii) The Effect of Moisture and Light upon Adsorbed Crystal Violet

There are several causes which can account for the loss in intensity of the visible band of CV, when adsorbed onto a solid surface. These can broadly be divided into two types, (1) hydration and dehydration, (2) photochemical. Hydration and dehydration are essentially reversible changes whereas photochemical processes are generally irreversible. If there was essentially no difference between the samples kept in the dark compared to those irradiated, the reaction was assumed to be one of hydration or dehydration. If there were differences, the change in intensity was essentially caused by a photochemical process.

The zero time absorbance ( $A_0$ ), was the absorbance of the sample directly after preparation, and as such was air dry ( $\sim 60\%$  RH). Therefore large differences can be seen in the first 24hrs, due to equilibration, when the RH was greatly different to 60%. The spectra of CV adsorbed upon silica gel, at three different humidities, as a function of time is shown in Figures (3-8 to 3-13). Crystal violet was adsorbed as the monocation ( $B^+$ ) at all humidities.

100% Relative Humidity

The absorbance of CV with time, at 100% RH is shown in Figure (3-14). The intensity of the visible band decreased in the irradiated and non-irradiated samples. The intensity after 24hrs was  $\sim 40\%$  of the  $A_0$  value, after which it remained constant (1 to 43 days). The loss of intensity in the presence of water vapour

FIGURE (3-8). The Diffuse Reflectance Spectra of Crystal Violet on Silica, at 100% RH, as a function of time without irradiation (2.5 mg CV/g Silica)

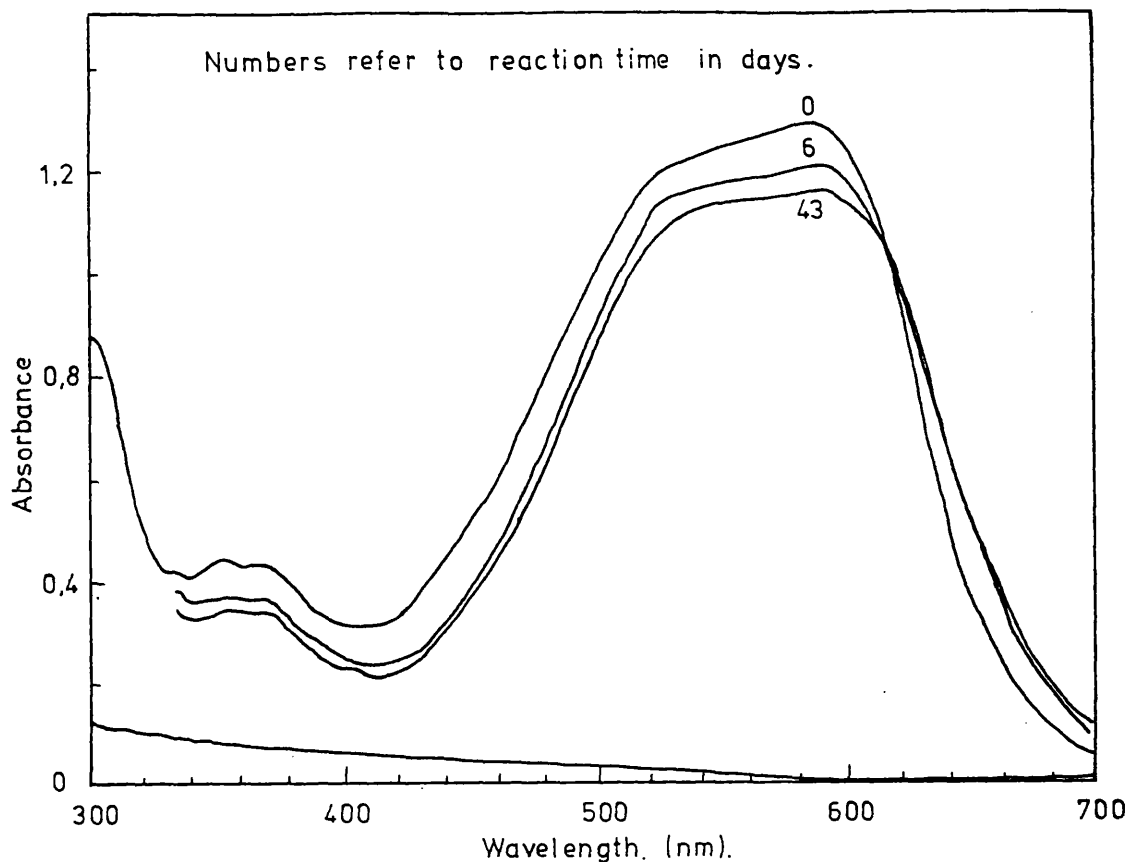


FIGURE (3-9). The Diffuse Reflectance Spectra of Crystal Violet on Silica, at 100% RH, as a function of time with irradiation (2.5 mg CV/g Silica)

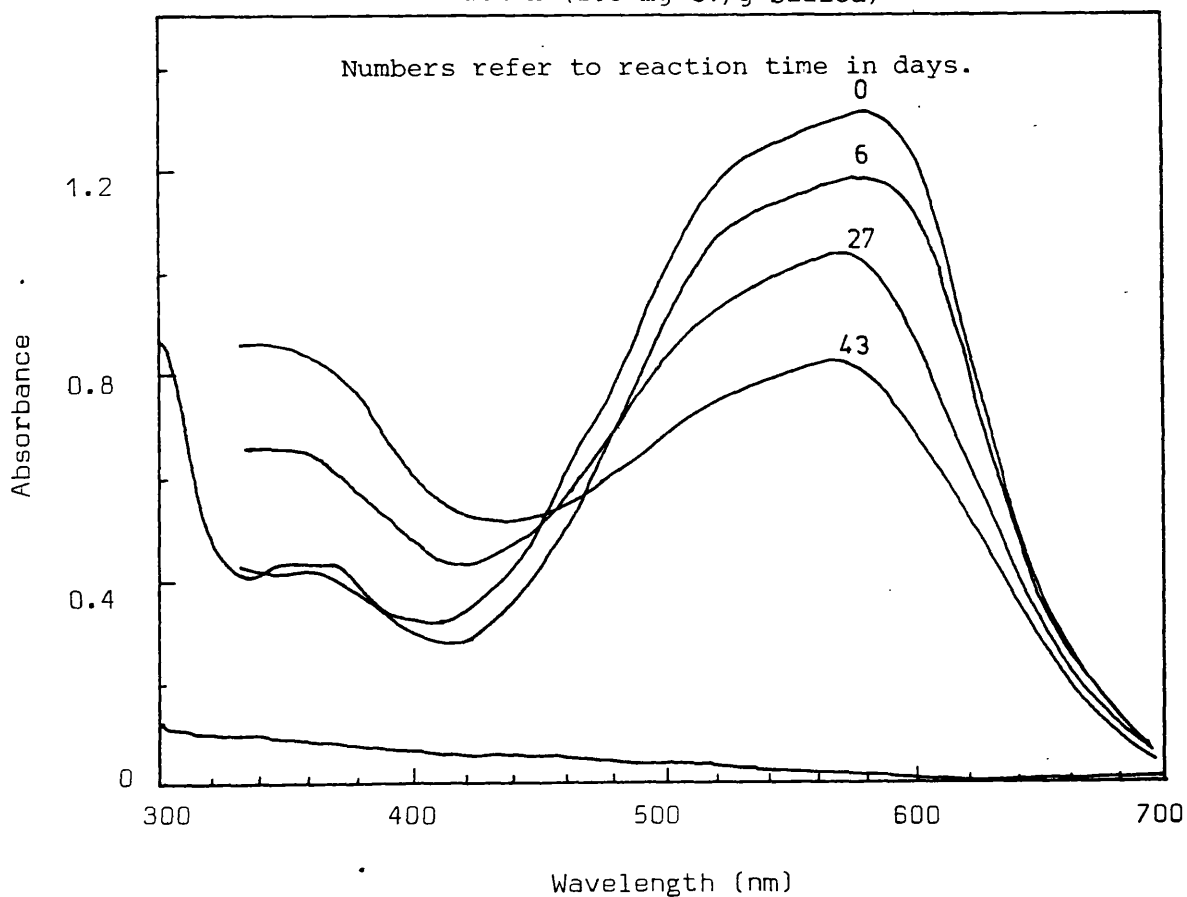


FIGURE (3-10). The D.R. Spectra of Crystal Violet on Silica at 62.5% RH, as a function of time, without irradiation (2.5 mg CV/g Silica)

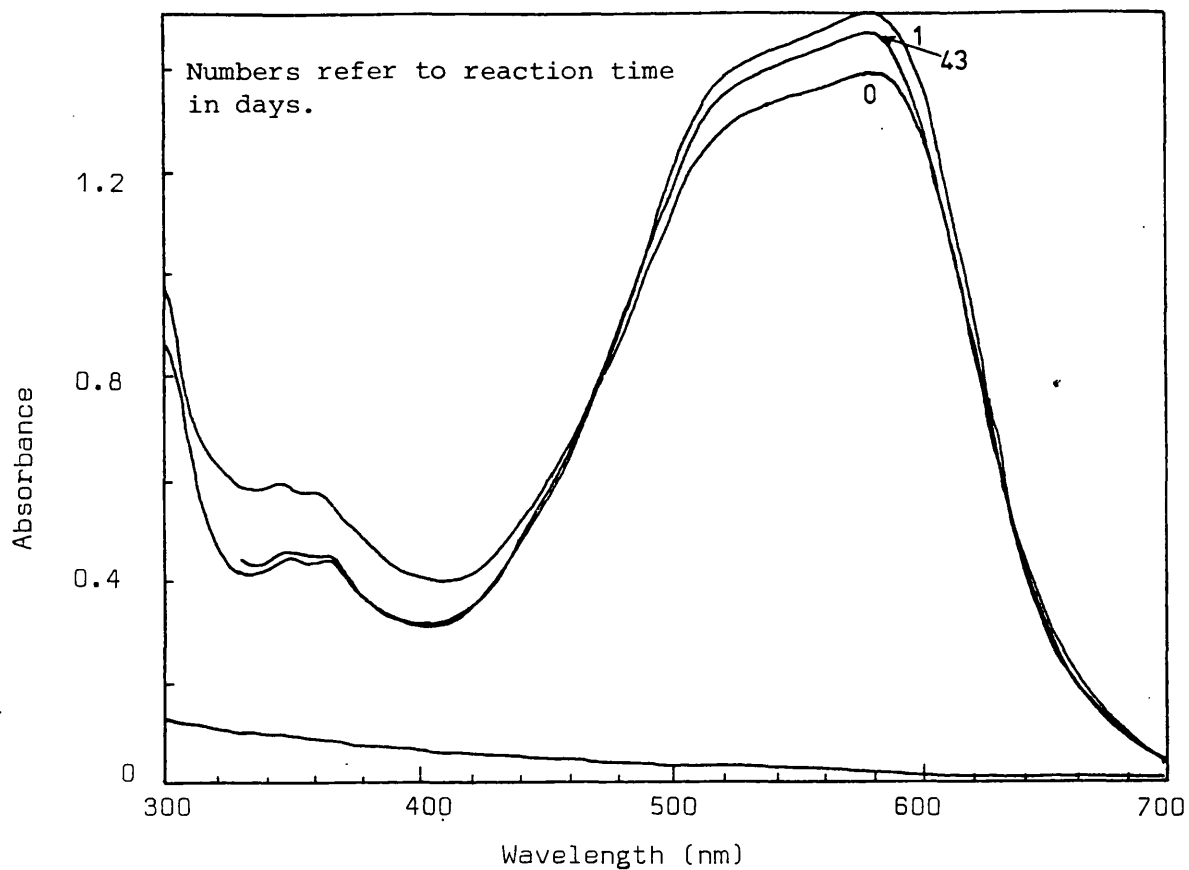


FIGURE (3-11). The D.R. Spectra of Crystal Violet on Silica at 62.5% RH, as a function of time, with irradiation (2.5 mg CV/g Silica)

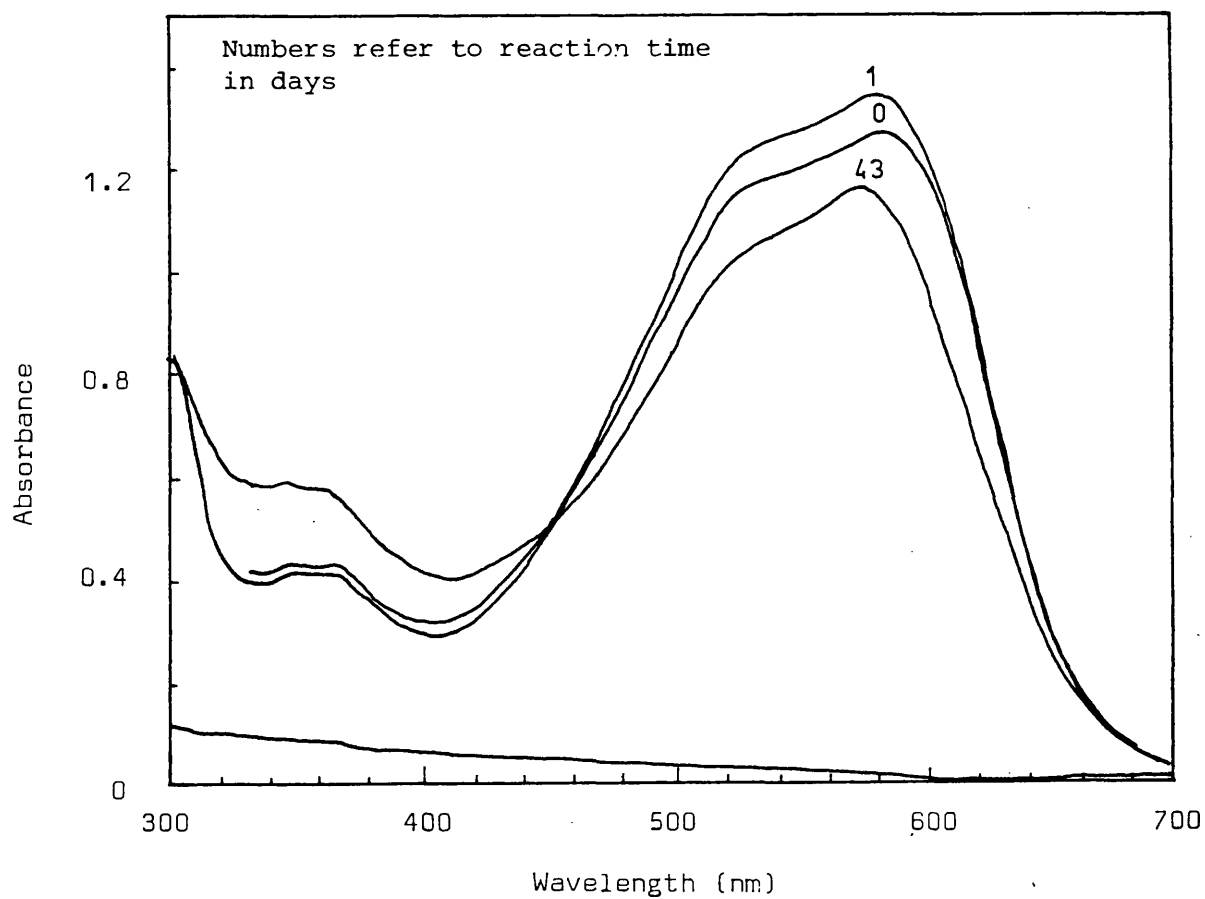


FIGURE (3-12). The D.R.S. of Crystal Violet on Silica at 0% RH, as a function of time, without irradiation (2.5 mg CV/g Silica)

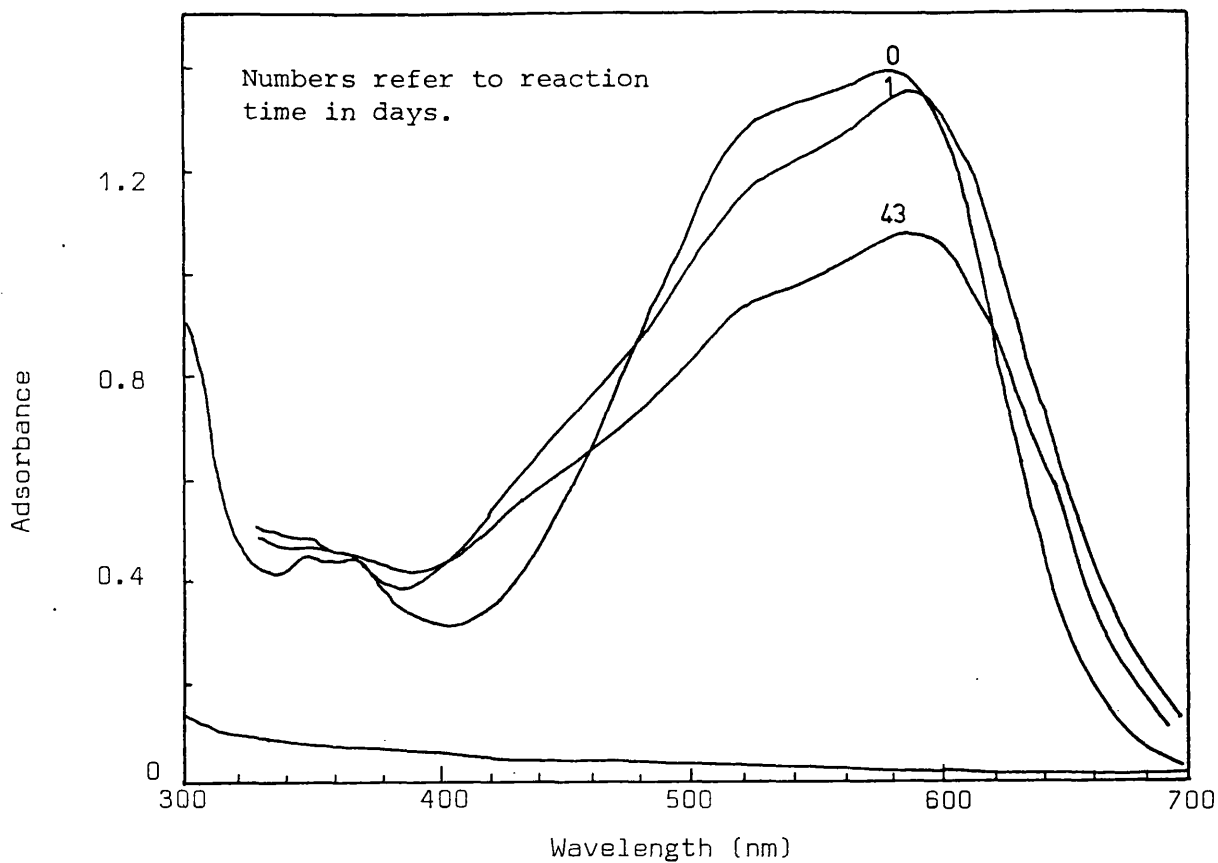
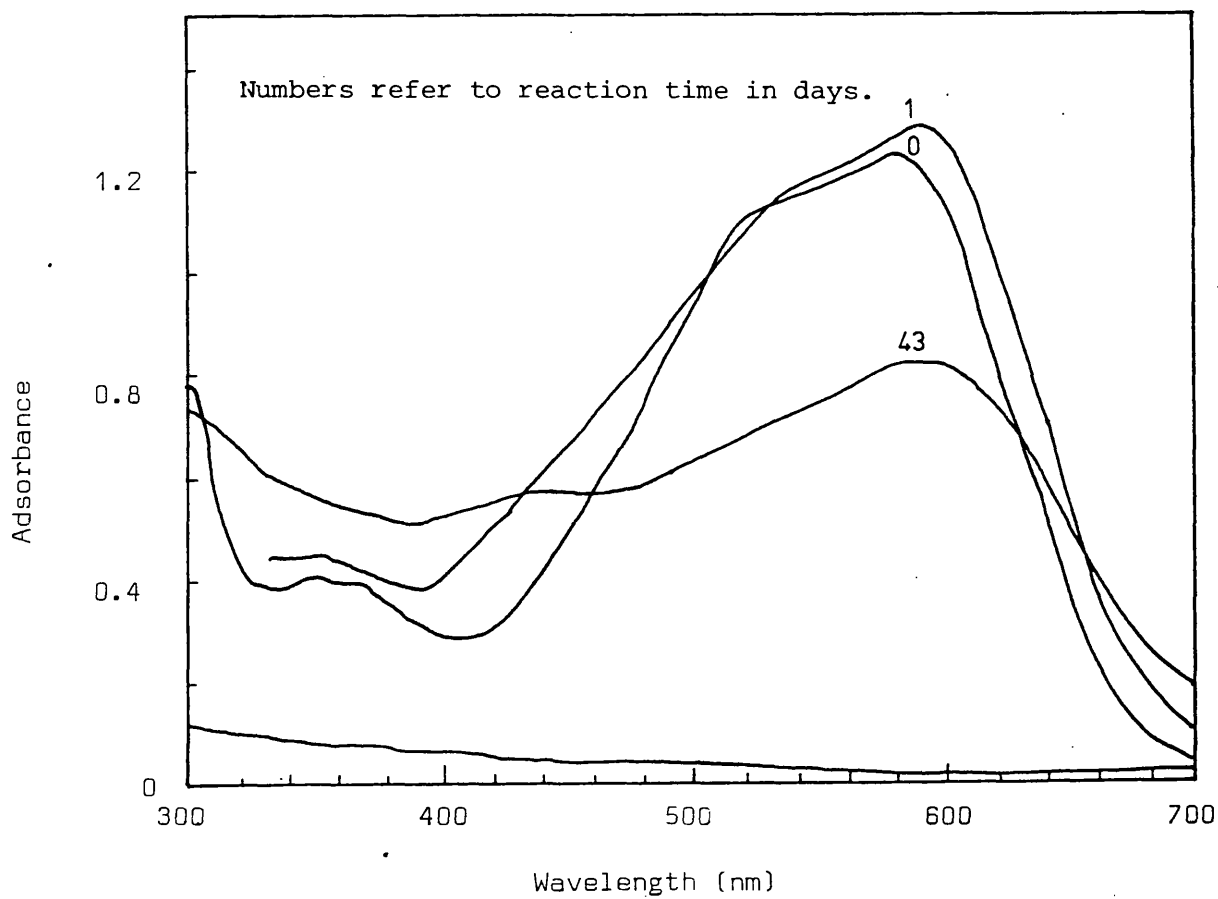


FIGURE (3-13). The D.R.S. of Crystal Violet on Silica at 0% RH, as a function of time, with irradiation (2.5 mg CV/g Silica)



(moist air) can be attributed to the displacement of CV from the surface by water, and the formation of the colourless form  $S_1$ , see page 72 Chapter 3. The intensity of the visible absorption band was the same for the irradiated and non-irradiated samples, within experimental error. But the position of the  $\lambda$  max was substantially different, Figures (3-17 and 3-18). The  $\lambda$  max of the non-irradiated sample was constant at 592nm, whereas the irradiated sample showed a pronounced hypsochromic shift of 20nm. Thus indicating that the remaining coloured CV undergoes demethylation.

#### 62.5% Relative Humidity

The intensity of the visible absorbance of the non-irradiated sample increased to 150% of the  $A_0$  value, Figure (3-15). The irradiated sample initially increased to 120%  $A_0$  but thereafter decreased (40%  $A_0$  after 43 days). An increase in intensity can be explained in terms of three effects:-

(i) An increase in humidity can reduce the scattering coefficient of the sample, because there is a reduction in the ratio of refractive indices of the sample and surrounding medium, i.e. when air is replaced by water vapour. This causes a reduction in the scattering coefficient and hence an increase in  $(FR_\infty)$ , or absorbance, Kortum, G. et al., (1963); Kubelka, P and Monk, F. (1931) and Kubelka, P. (1948).

(ii) An increase in humidity reduces the acidity of the surface and any CV which was in the dicationic form would be converted to the monocationic form, and there would be a corresponding increase at 592nm.

FIGURE.(3-14). The Percentage of the Zerotime absorbance of Crystal Violet, on Silica gel, remaining with time  
(Solid symbols refer to non-irradiated samples)

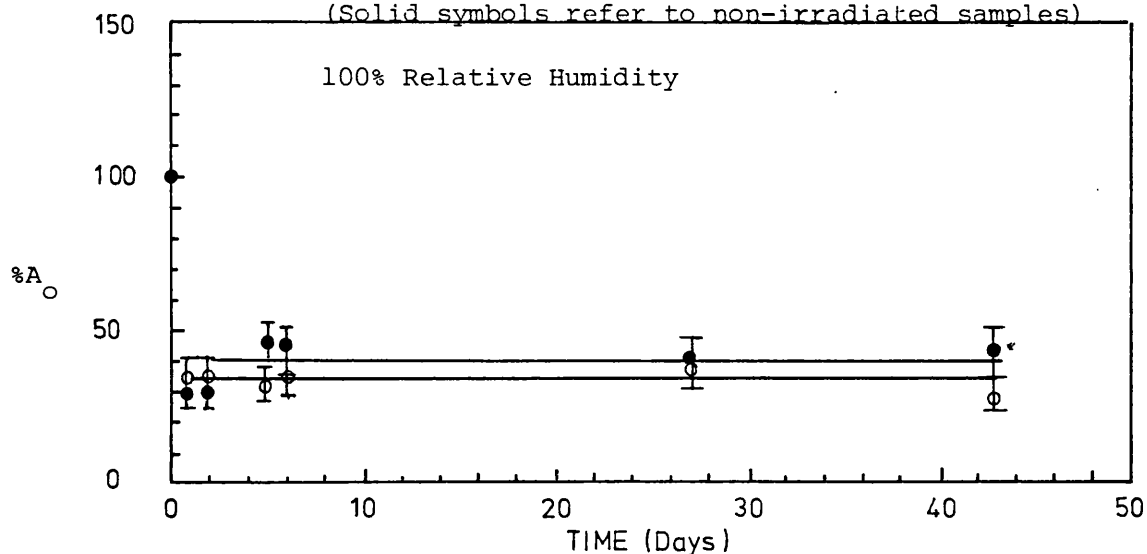


FIGURE.(3-15). 62.5% Relative Humidity  
(Solid symbols refer to non-irradiated samples)

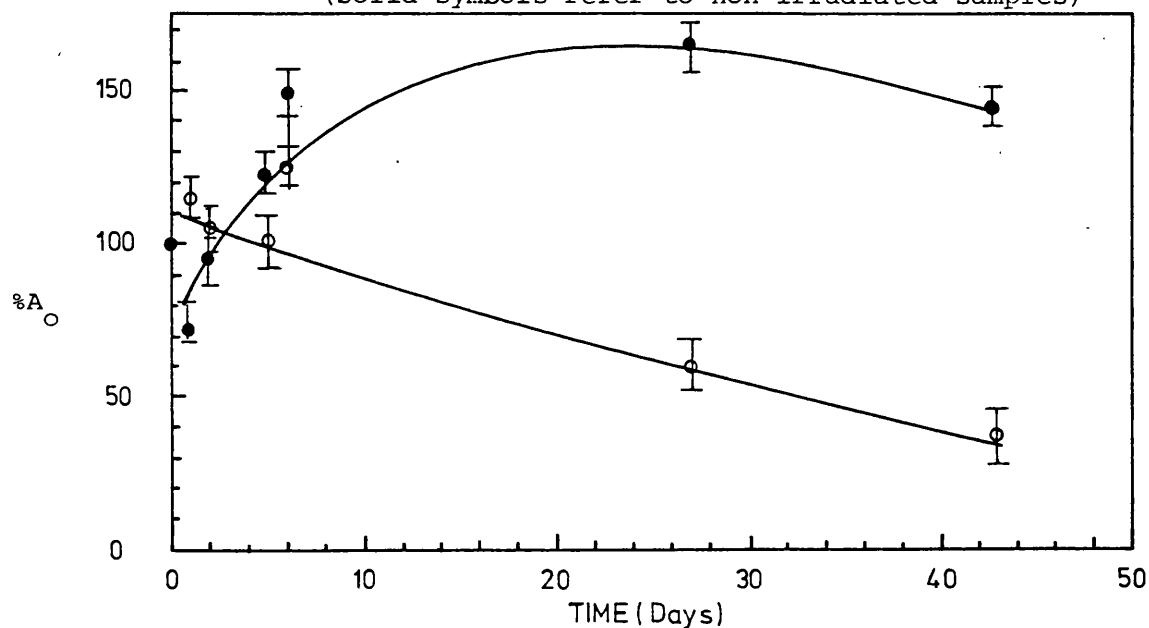
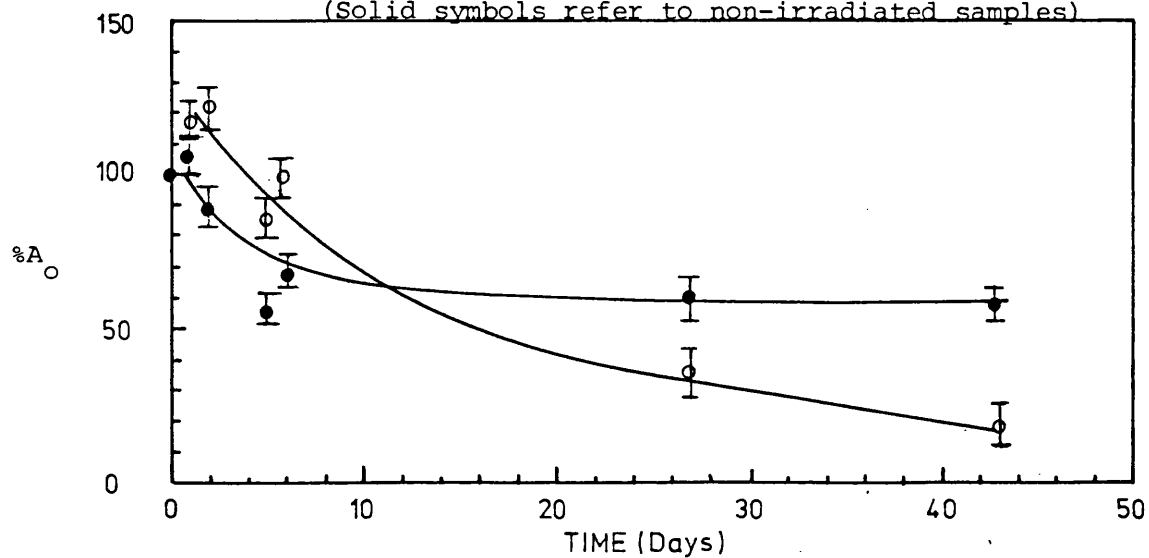


FIGURE.(3-16). 0% Relative Humidity  
(Solid symbols refer to non-irradiated samples)





The Position of  $\lambda$  max of Crystal Violet on Silica gel as a function

FIGURE (3-17). Non-irradiated

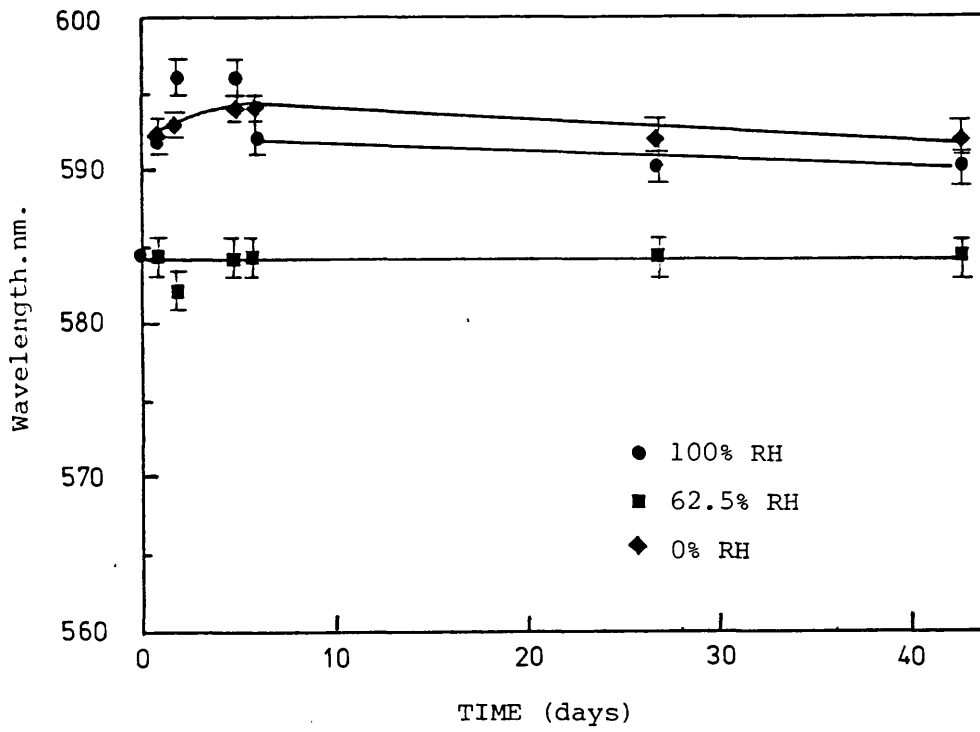
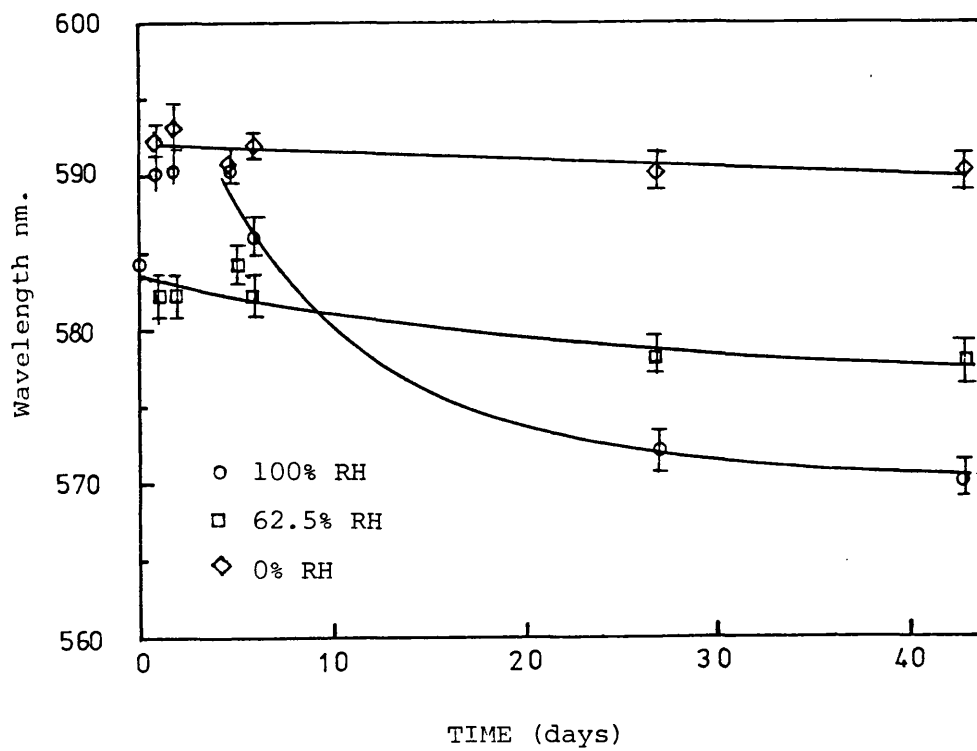
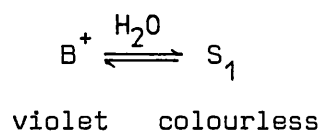


FIGURE (3-18). Irradiated



(iii) A decrease in humidity could cause the equilibrium:-



to be shifted to the left.

It is unlikely that [iii] is the correct reason as there should be an increase in relative humidity, not a decrease. But no distinction can be made between (i) and (ii).

The position of the  $\lambda$  max for the irradiated sample decreased with time, 584 to 578nm over 43 days. But the position of the  $\lambda$  max for the non-irradiated sample remained constant at 584nm, Figures (3-17) and (3-18).

Therefore there is photo-decomposition at this relative humidity.

#### 0% Relative Humidity

At 0% relative humidity both irradiated and non-irradiated samples decreased to 60%  $A_0$ , after 10 days, Figure (3-16). After this the dark sample remains at a constant level, but the irradiated sample was further reduced to 20%  $A_0$  after 43 days. The initial reduction in intensity was caused by removal of water from the silica surface. This process is much slower than hydration because water is tightly bound to the silica surface which is hygroscopic. An examination of the spectra, Figures (3-12 and 3-13), shows an increase in intensity at 650nm and 450nm. This indicates the presence of the dication ( $G^{++}$ ), and possibly the trication ( $Y^{+++}$ ). The dehydration of the surface causes an increase in acidity of the silica and hence causes an increase in the di and tricationic forms.

The absorbance decreases because the molar extinction of the green and yellow species are less than the violet, Cigen, R. (1958). Irradiation causes a further reduction in intensity, but only a small hypsochromic shift (-2nm), Figures (3-17 and 3-18).

(iii) The Effect of Humidity and Light upon CVL Adsorbed upon Silica Gel

The spectra of CVL adsorbed upon silica gel at three humidities, (100, 62.5 and 0 RH), are shown in Figures (3-19 to 3-24). CVL was adsorbed at all humidities as the monocationic (B<sup>+</sup>) zwitterion. ( $\lambda_{\text{max}} = 596\text{nm}$ ).

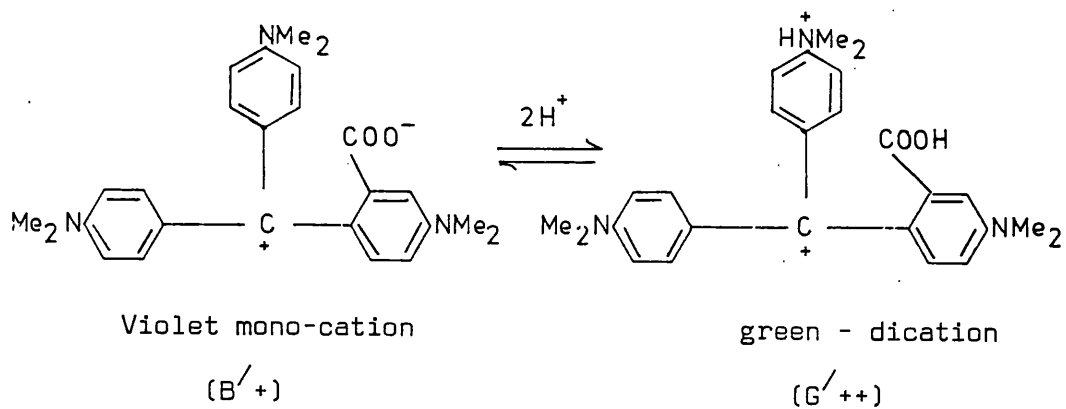


FIGURE (3-19). The Diffuse Reflectance Spectra of Crystal Violet Lactone on Silica gel, at 100% RH as a function of time, without irradiation (1.0 mg CVL/g Silica)

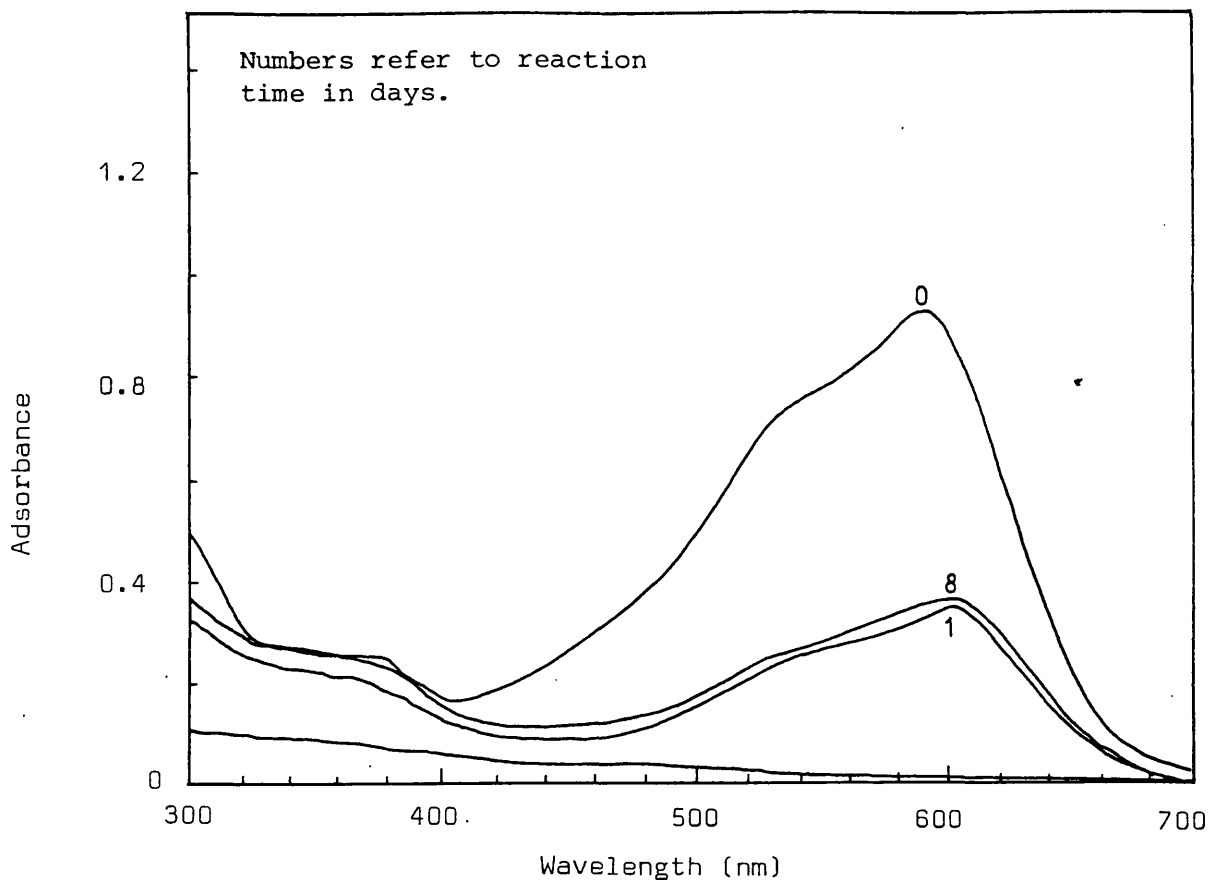


FIGURE (3-20). The Diffuse Reflectance Spectra of Crystal Violet Lactone on Silica gel, at 100% RH as a function of time with irradiation (1.0 mg CVL/g Silica)

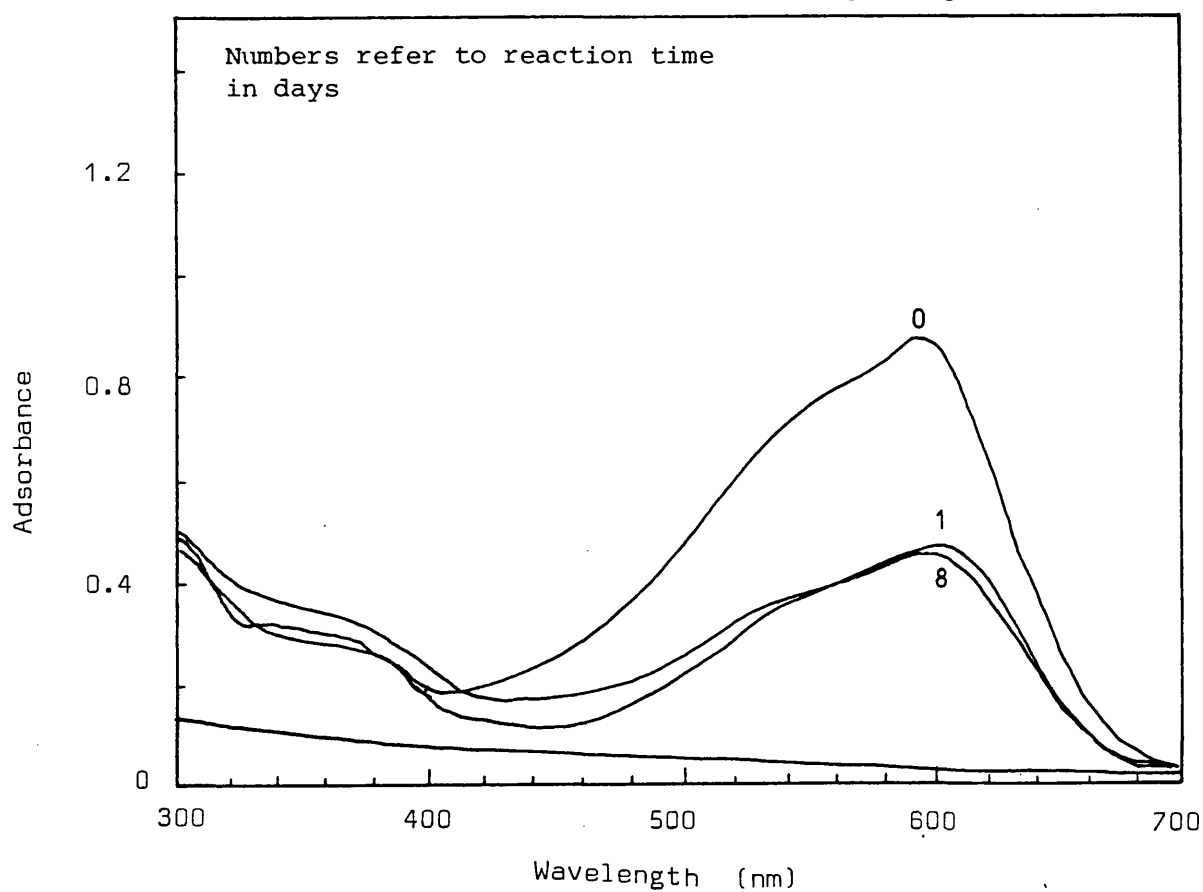
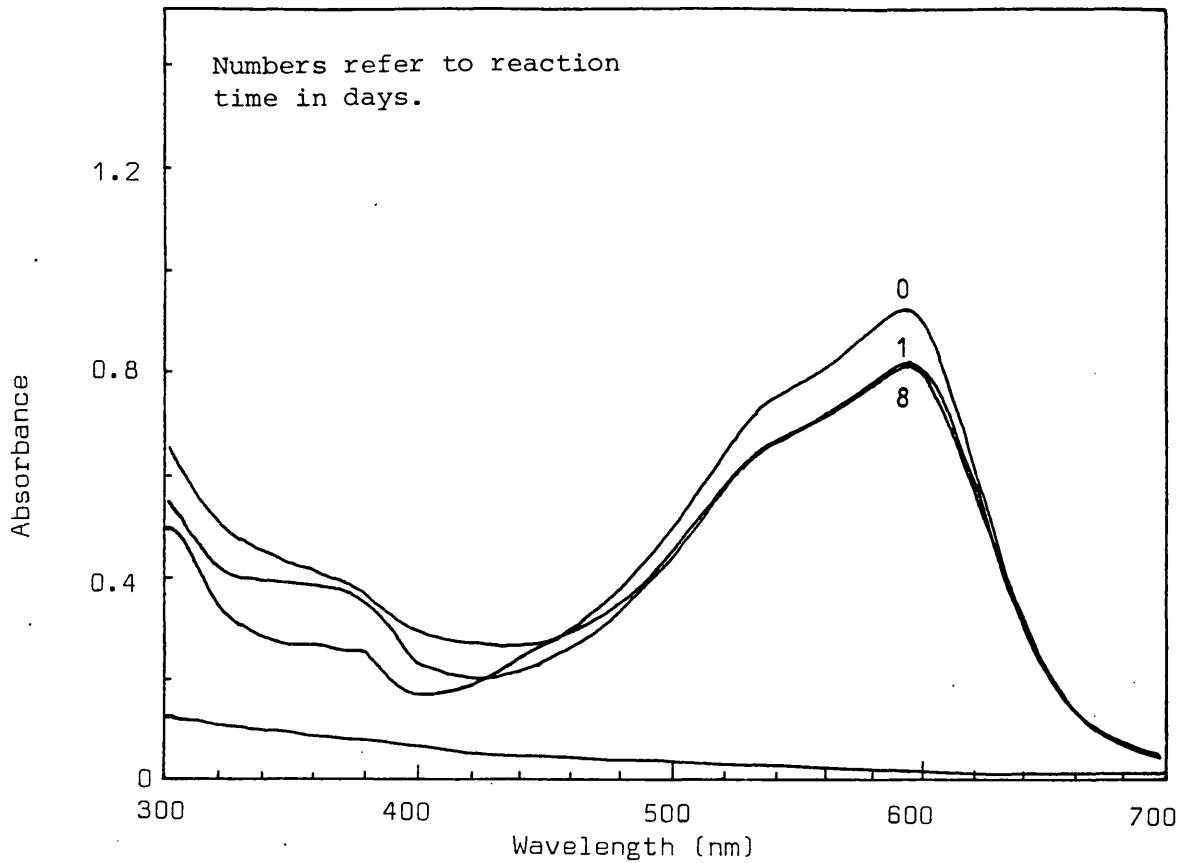


FIGURE (3-21). The D.R.S. of CVL on Silica gel at 62.5% RH as a function of time, without irradiation (1.0 mg CVL/g Silica)



FIGURE, (3-22). The D.R.S. of CVL on Silica gel at 62.5% RH as a function of time, with irradiation (1.0 mg CVL/g Silica)

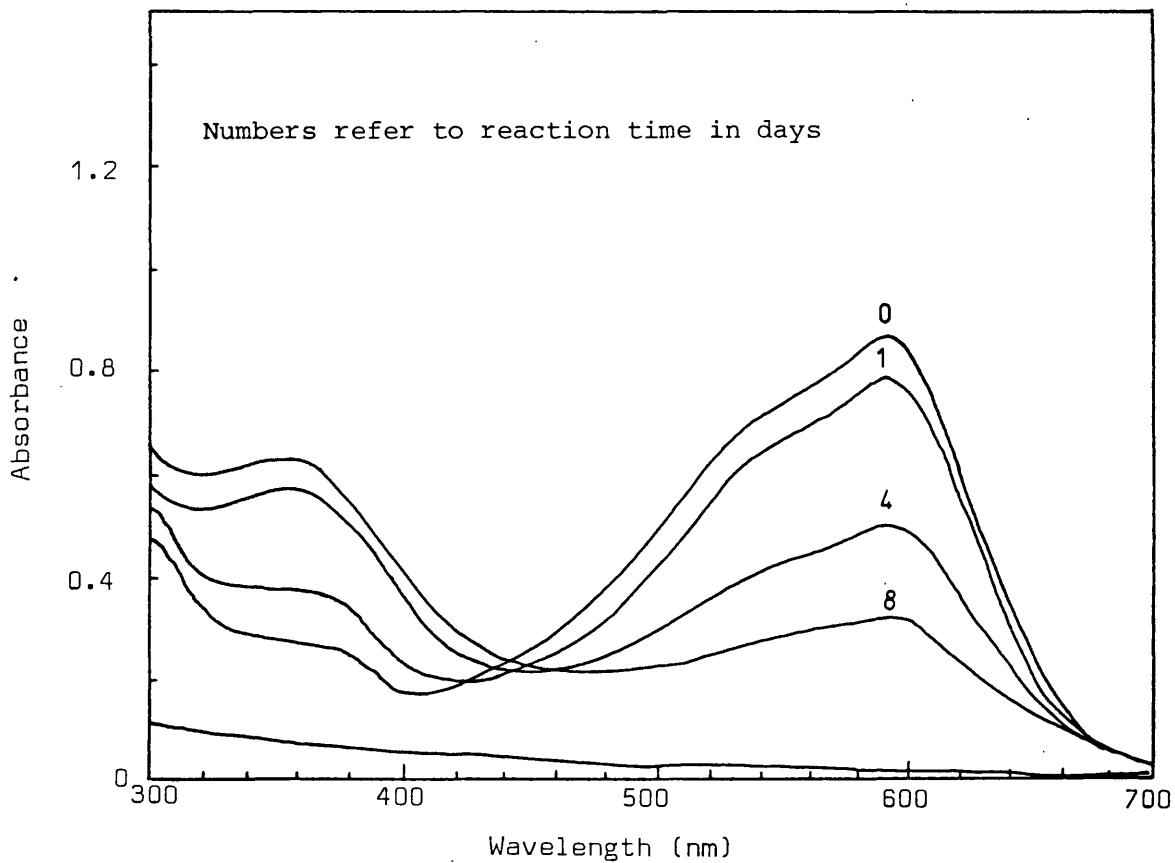


FIGURE.(3-23). The D.R.S. of CVL on Silica gel at 0% RH as a function of time, without irradiation (1.0 mg CVL/g Silica)

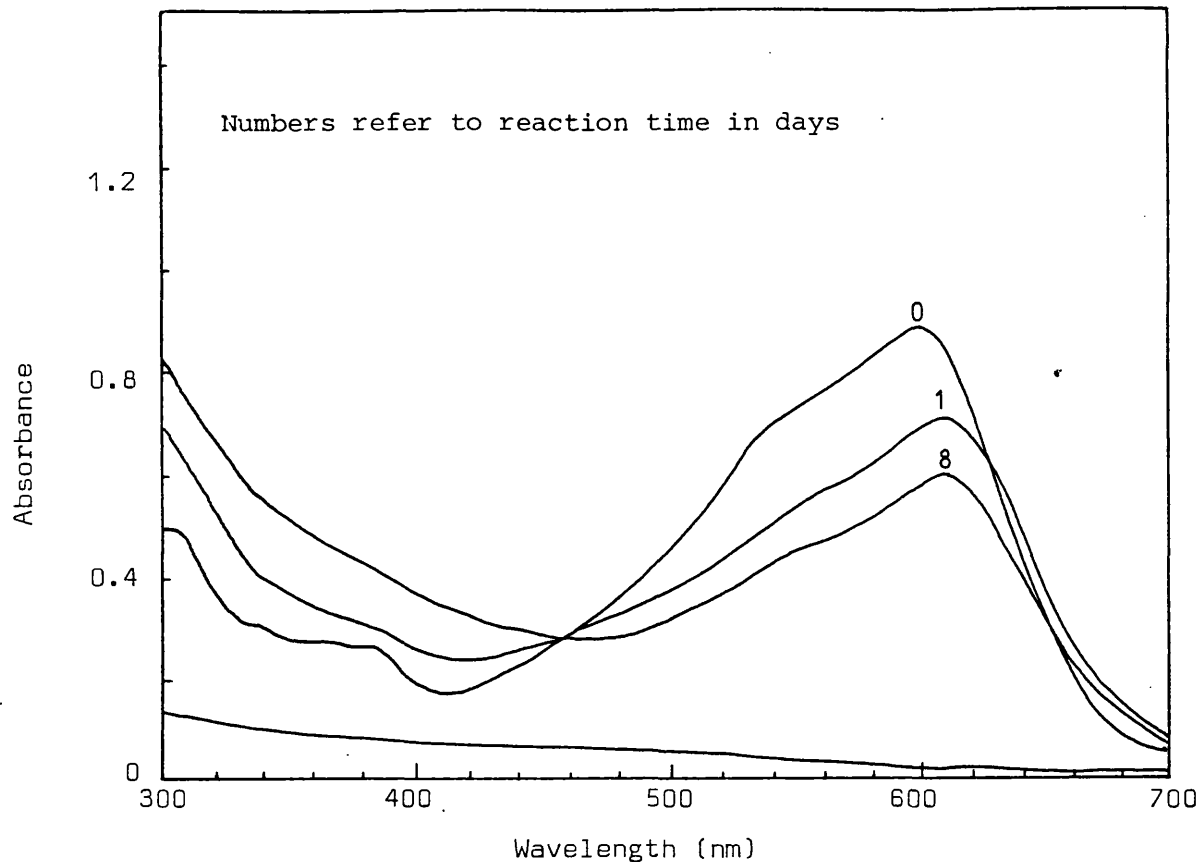
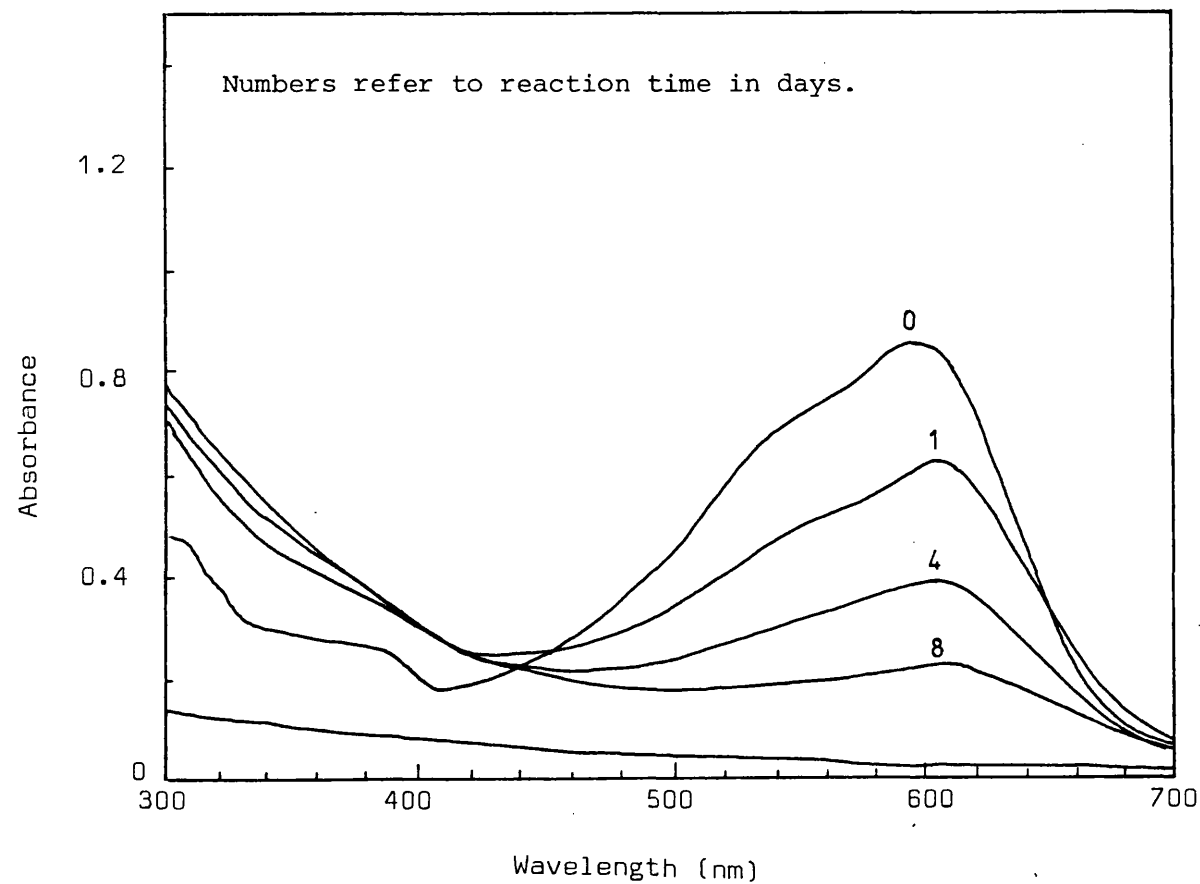


FIGURE.(3-24). The D.R.S. of CVL on Silica gel at 0% RH as a function of time, with irradiation (1.0 mg CVL/g Silica)



The zwitterion  $B'^+$  can undergo the same acid-base equilibria that the parent dye  $CV^+$  can undergo, see page 72, Chapter 3. Therefore  $B'^+$  can be hydrated to a colourless species as can the di protonated species ( $G'^{++}$ ). Also if  $B'^+$  is displaced from the surface the lactone ring will reform, and the violet colour will be discharged.

#### 100% Relative Humidity

The absorbance of CVL as function of time, at 100% RH is shown in Figure (3-25). The absorbance after 24hrs decreased to 10% of  $A_0$  value, for both the irradiated and non-irradiated samples. This showed that the zwitterion was displaced from the surface by water to form the colourless lactone.

The position of the  $\lambda$  max for irradiated and non-irradiated samples is shown in Figures (3-28 and 3-29). A small hypsochromic shift was observed for the irradiated sample and no shift was observed for the non-irradiated sample.

#### 62.5% Relative Humidity

The irradiated sample shows a large decrease in intensity, 10%  $A_0$  after 8 days; Figure (3-26). But the non-irradiated sample shows only a small loss of intensity, 80%  $A_0$  after 8 days, Figure (3-26). Again the irradiated sample showed a small hypsochromic shift (5nm), Figure (3-29). Therefore the reduction in intensity was caused by photodegradation of CVL.

The Percentage of the Zerotime absorbance of Crystal Violet Lactone on Silica gel, remaining with time

FIGURE (3-25). 100% Relative Humidity

(Solid symbols refer to non-irradiated samples)

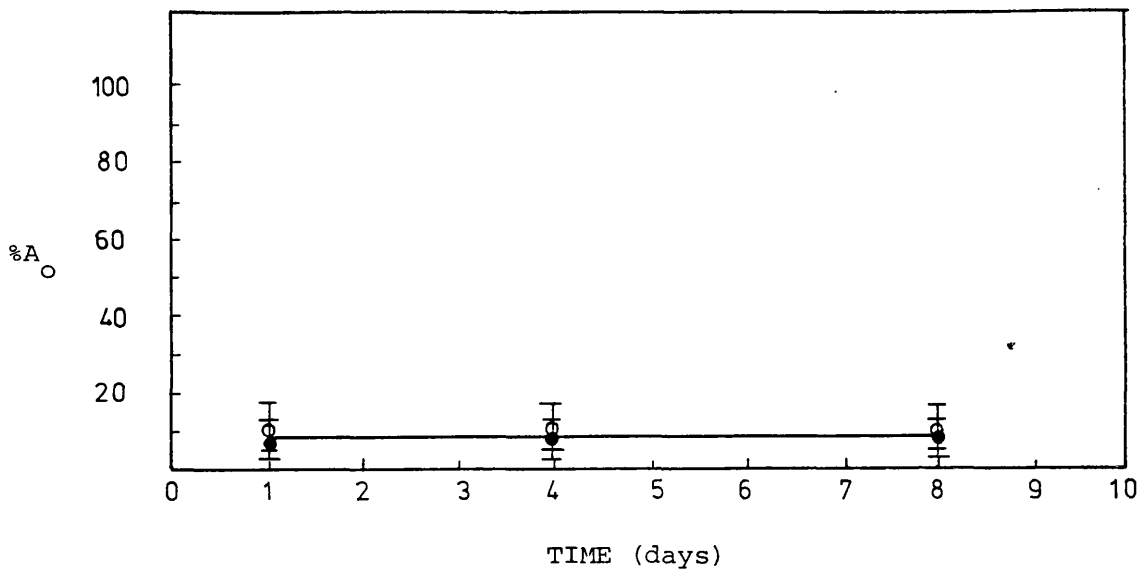


FIGURE (3-26) 62.5% Relative Humidity

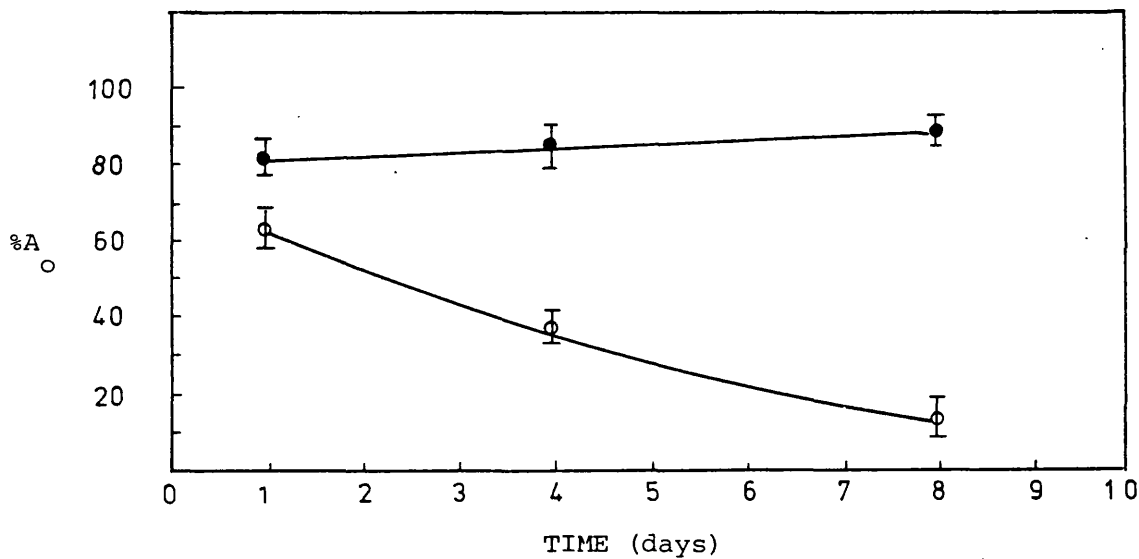
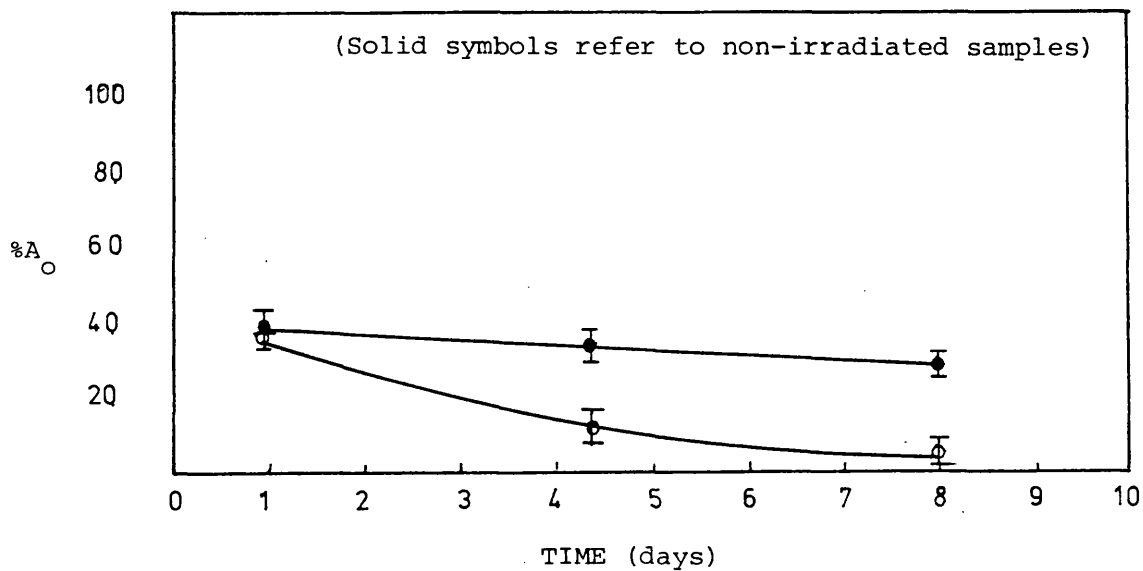


FIGURE (3-27). 0% Relative Humidity

(Solid symbols refer to non-irradiated samples)





The position of the  $\lambda_{\max}$  of Crystal Violet Lactone, on Silica gel, with time.

FIGURE (3-28). Non-irradiated

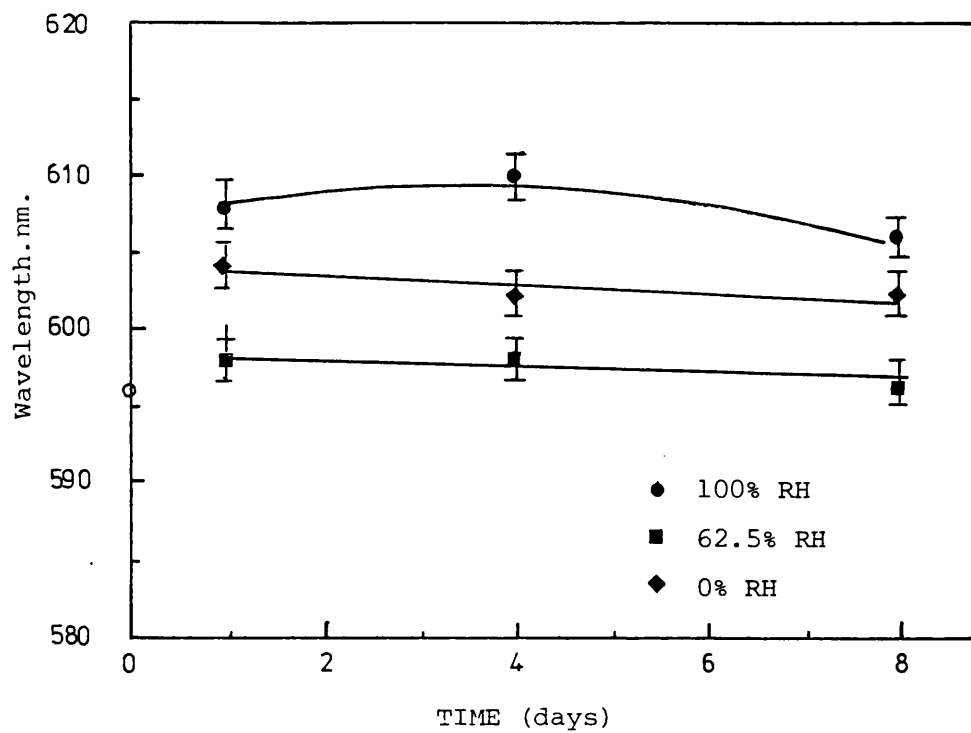
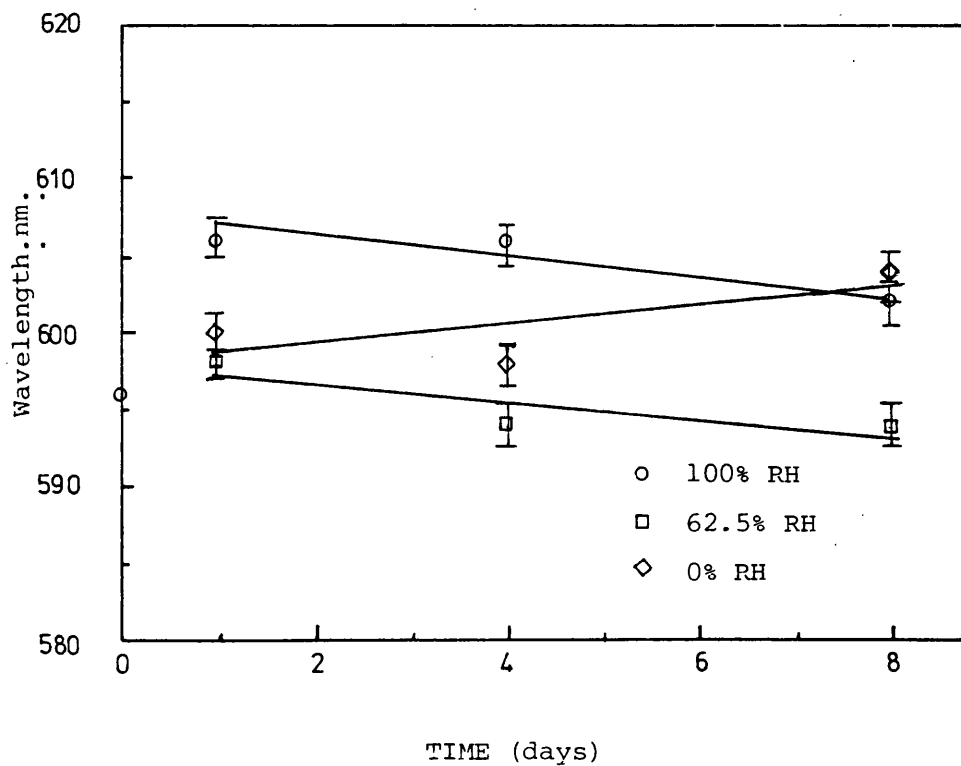


FIGURE (3-29). Irradiated



### 0% Relative Humidity

The intensity of the non-irradiated sample decreases to 40%  $A_0$  after 24hrs, and remains constant thereafter, Figure (3-27). The irradiated sample showed a decrease to 30%  $A_0$  after 24hrs, and slowly decreased thereafter to 5%  $A_0$ . It can be seen from the spectrum that the peak at 596nm decreases, and the absorbance at 650nm and 450nm increases, Figure (3-26). This indicates that dehydration of the surface has caused an increase in the acidity, and the concentration of ( $G^{++}$ ) has increased, with a loss of intensity of ( $B^+$ ). Irradiation has caused further degradation, and results in a 6nm bathochromic shift.

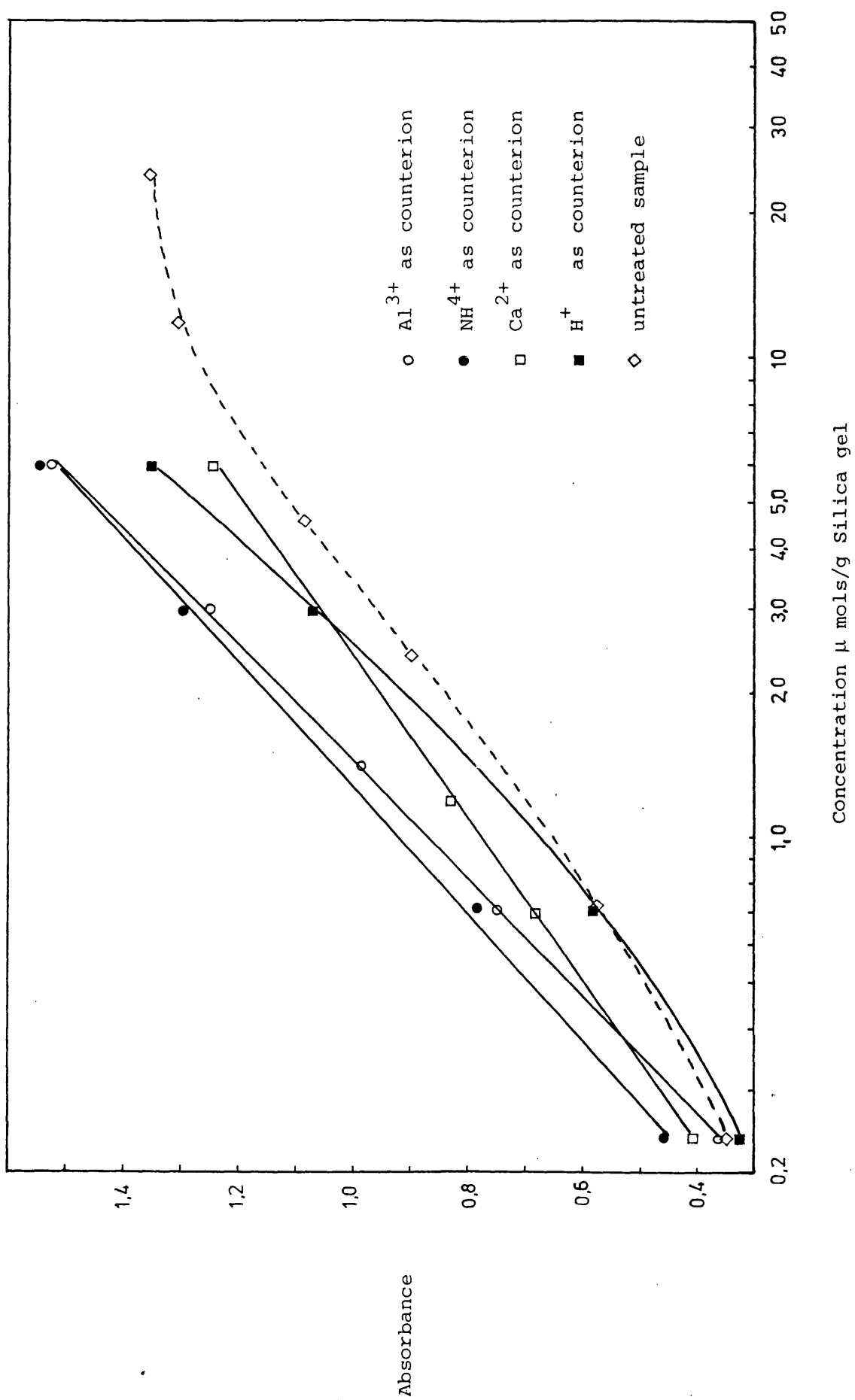
#### (iv) The Effect of Counterions upon the Fading of CVL Adsorbed upon Silica Gel

The effect of exchangeable counterions upon the fading processes of CVL was measured as a function of the loss in intensity and shift in  $\lambda$  max of the adsorbed species. Four counterions were used,  $Al^{3+}$ ,  $Ca^{2+}$ ,  $H^+$  and  $NH_4^+$ . All samples were maintained at 62.5% RH. Treatment of silica with the four counterions caused an increase in the intensity of the absorbed CVL, compared to an untreated sample, Figure (3-30). The absorbance of CV was also affected by the presence of counterions, Figure (3-30). The hydration energies for the counterions vary from 1149 Kcals/g.ion for  $Al^{3+}$  to 87 Kcals/g.ion, for  $NH_4^+$ , Norrish, K., (1954).

#### $Al^{3+}$ as Counterion

A loss of intensity to 20%  $A_0$  after 13 days was observed for, both irradiated and non-irradiated samples, Figure (3-31).

FIGURE. (3-30). The Effect of Counterions on the Absorbance of Crystal Violet Lactone on Silica gel



In contrast the untreated sample maintained a high intensity when not irradiated.

CVL was adsorbed as the ( $B^+$ ) monocation. Both irradiated and non-irradiated samples exhibited a small bathochromic shift, Figure (3.35). Analysis of the spectrum shows a new peak developing at 350-360nm, when irradiated. No peak developed unless irradiated.

$Al^{3+}$  as a counterion will cause an increase in the acidity of the surface, due to its ability to polarize water molecules, Russell, J.D. et al., (1968). This will shift the lactone zwitterion equilibrium further toward the zwitterion. Hence the increase in intensity of the visible band was caused by an increase in the acidity of the surface. The subsequent loss of intensity must be caused by hydration of the surface, because there was no requirement for light. Hydration of the surface would reduce the polarity and cause the displacement of the zwitterion by water.

#### Ca<sup>2+</sup> as Counterion

The intensity of CVL, adsorbed upon  $Ca^{2+}$  treated silica, falls rapidly to 4%  $A_0$  after 8 days irradiation, Figure (3-32); c.f. untreated sample 10%  $A_0$ , 8 days exposure. The intensity of the non-irradiated sample 45%  $A_0$ , 8 days storage, also falls below the untreated control sample of 80% after 8 days storage. The loss in intensity of the non-irradiated sample can be attributed to hydration of the surface causing a reduction in the polarity of the surface and a displacement of the zwitterion by water. The effect was more pronounced when  $Al^{3+}$  was counterion, because the hydration energy of

The Effect of Counterions on the percentage of the Zerotime absorbance of Crystal Violet Lactone, on Silica gel, remaining with time. 62,5% RH.

FIGURE (3-31)  $Al^{3+}$  as Counterion  
(Solid symbols refer to non-irradiated samples)

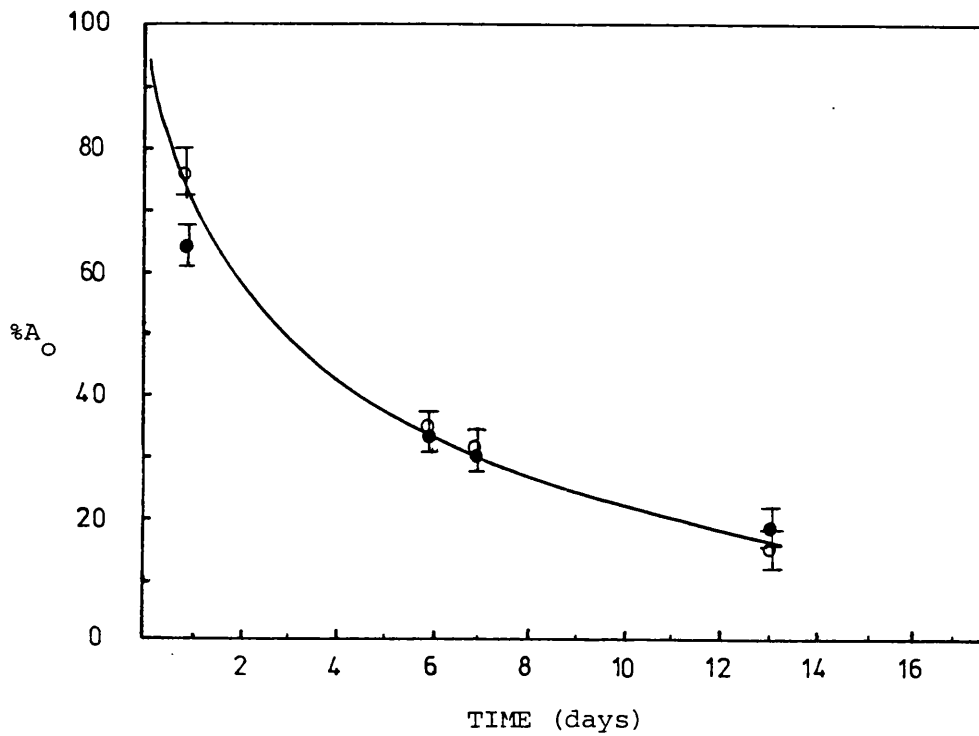
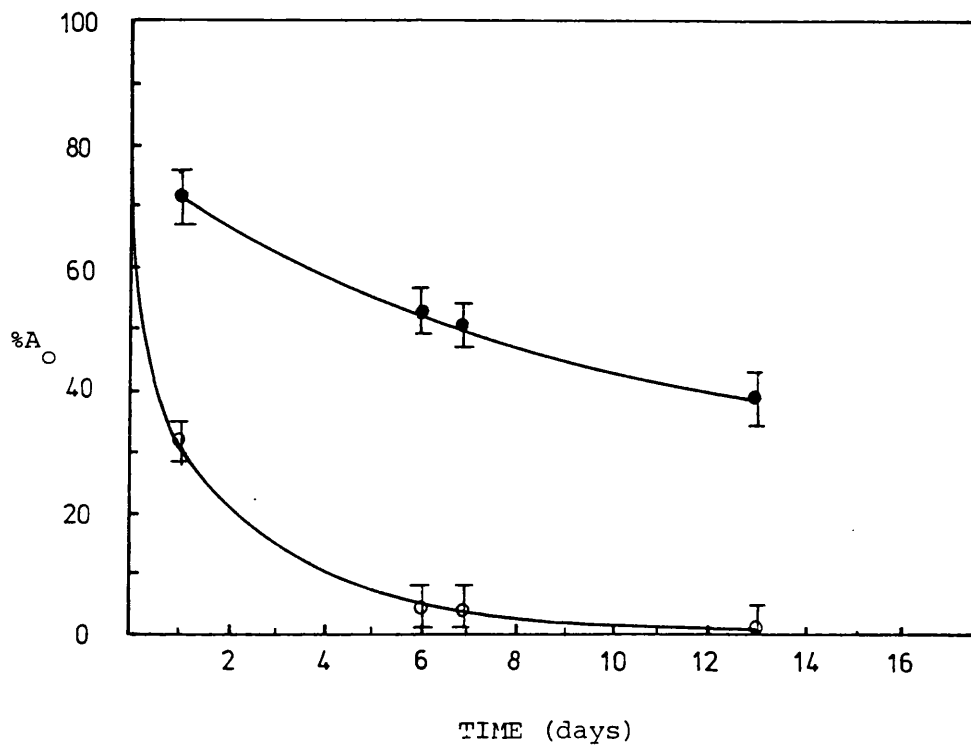


FIGURE (3-32).  $Ca^{2+}$  as Counterion  
(Solid symbols refer to non-irradiated samples)



The Effect of Counterions on the Percentage of zerotime absorbance of Crystal Violet Lactone remaining, on Silica gel, as a function of time (62.5% RH).

FIGURE (3-33).  $H^+$  as Counterion  
(Solid symbols refer to non-irradiated samples)

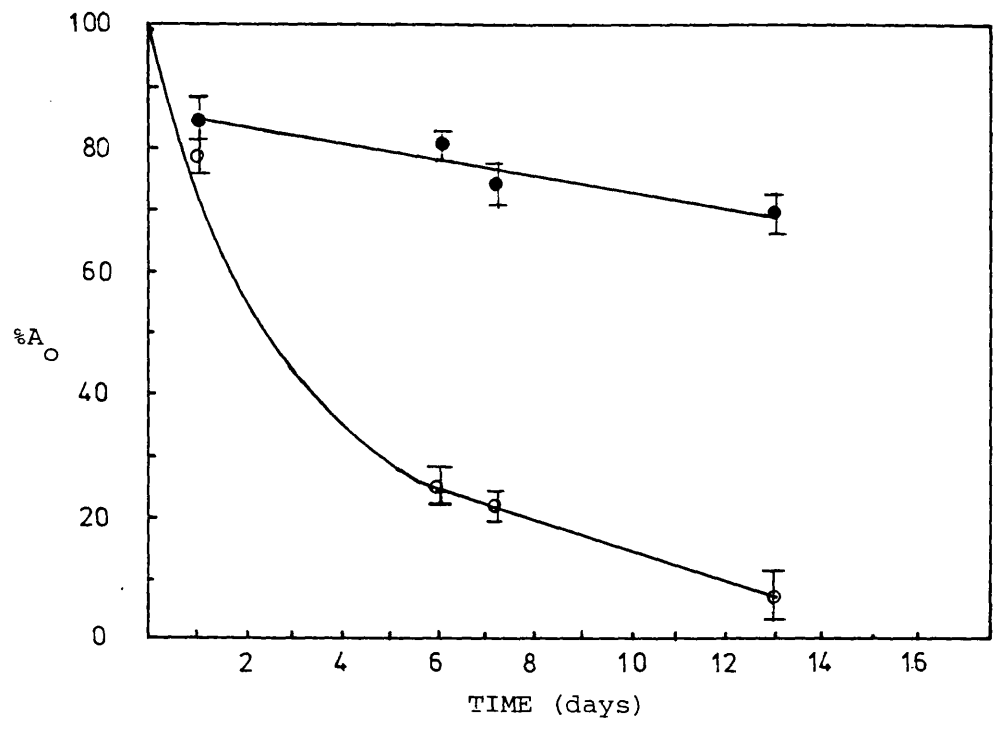
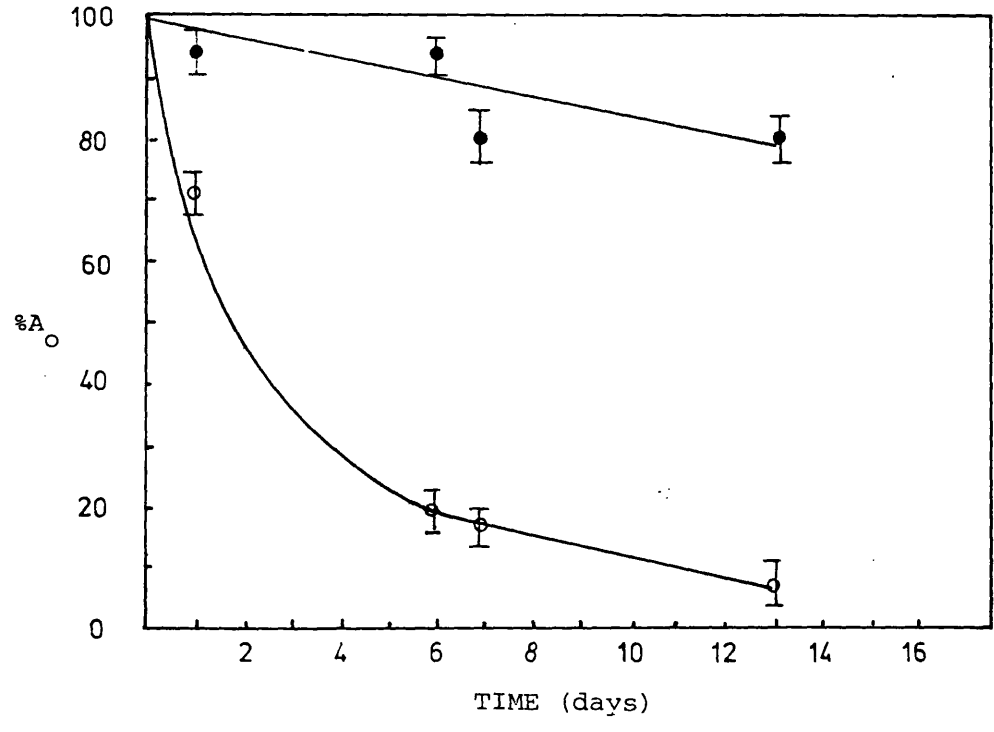


FIGURE (3-34).  $NH_4^+$  as Counterion  
(Solid symbols refer to non-irradiated samples)



The Effect of Counterions on the position of  $\lambda_{\text{max}}$  of Crystal Violet Lactone on Silica gel, (62.5% RH)

FIGURE (3-35). (Solid symbols refer to non-irradiated samples)

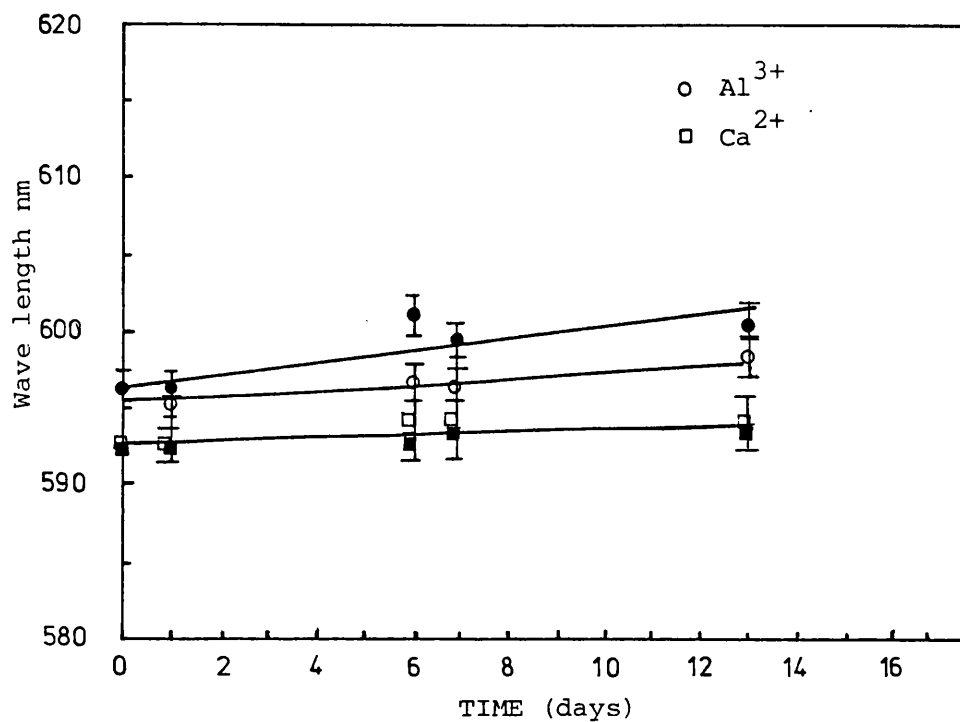
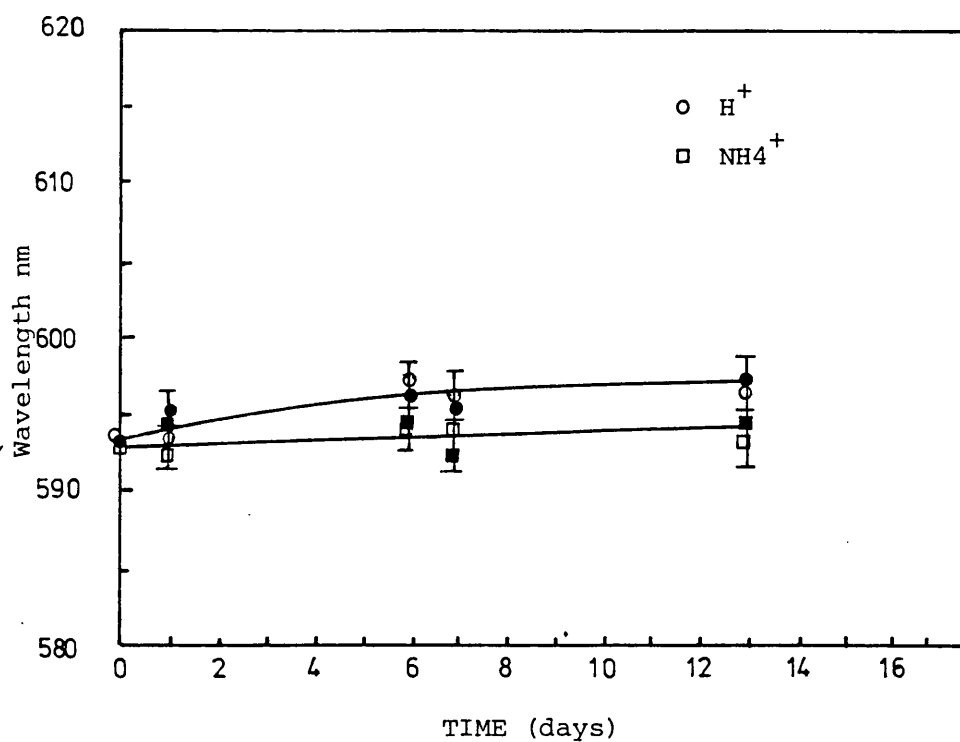


FIGURE (3-36). (Solid symbols refer to non-irradiated samples)



$Al^{3+} > Ca^{2+}$ . Hence the greater the hydration energy the more water the counterion abstracts from the atmosphere. Small bathochromic shifts were observed for irradiated and non-irradiated samples Figure (3.35). The irradiated sample undergoes displacement from the surface and photodegradation.

#### $H^+$ as Counterion

There was essentially no difference between the  $H^+$  treated silica and an untreated sample, Figures (3-33 and 3-36). This result was expected since the silica surface would have  $H^+$  counterions in the untreated state.

#### $NH_4^+$ as Counterion

Again no differences were observed between the  $NH_4^+$  treated silica and an untreated sample, Figures (3-34) and (3-36). The production of  $H^+$  from  $NH_4^+$  is possible, and hence the behaviour would be similar to  $H_3O^+$  as counterion.



In general the greater the polarity of the counterion the greater the effect upon the fading process. Considering non-irradiated samples, only the highly polarized cation caused increased adsorption of water on to the silica surface, this displaced the zwitterion causing a large decrease in intensity compared with an untreated sample. This is contrary to the effect of increasing the polarity of cations in the lattice structure, Kortum, G., (1969)



### 3.3.6. The Effects of Humidity and Light upon CVL Adsorbed upon Silton

(i) The absorbance of CV and CVL adsorbed upon Silton as a function of CV and CVL concentration, are shown in Figure (3-37). The ratio of CVL absorbance to CV absorbance tends to 0.8 at low coverages. The spectra of CVL adsorbed upon Silton at 100, 62.5 and 0% RH are shown in Figures (3-38 to 3-43). CVL was adsorbed as the dicationic green species ( $G'^{++}$ ),  $\lambda_{\text{max}} = 666\text{nm}$ . CV adsorbed upon silton was also in the green dicationic form,  $\lambda_{\text{max}} = 650\text{nm}$ . This shows that silton has a more acidic surface than silica gel.

#### 100% Relative Humidity

At 100% RH the green species rapidly turned to the violet species, Figures (3-38 and 3-39). The zero time measurement was made at approximately 60% RH. This causes the green species to predominate. The intensity, measured at two wavelengths corresponding to the  $B'^{+}$ , and  $G'^{++}$   $\lambda_{\text{max}}$  respectively, of CVL adsorbed upon silton as a function of time is shown in Figure (3-44). The absorbance at 610nm, corresponding to the  $B'^{+}$  species, remained constant at 90%  $A_0$  from 1 to 13 days, irradiated and non-irradiated. The absorbance at 666nm corresponding to the  $G'^{++}$  species decreased to 50%  $A_0$  in 24hrs and thereafter remained constant. There are two possible routes for loss of intensity, (i) displacement from the surface by water, (ii) hydration of the adsorbed species to the corresponding colourless species. Preferential displacement of the green species rather than the violet monocation is unlikely. The hydration equilibrium constant for the green species of CV is  $K_5 = [S_2]_{\infty} / [G]_{\infty} = 0.0319$ , which is 200 times greater than the hydration constant for the blue species. Therefore it is probable that the green species is

FIGURE (3-37). The absorbance of Crystal Violet and Crystal Violet Lactone of Silton

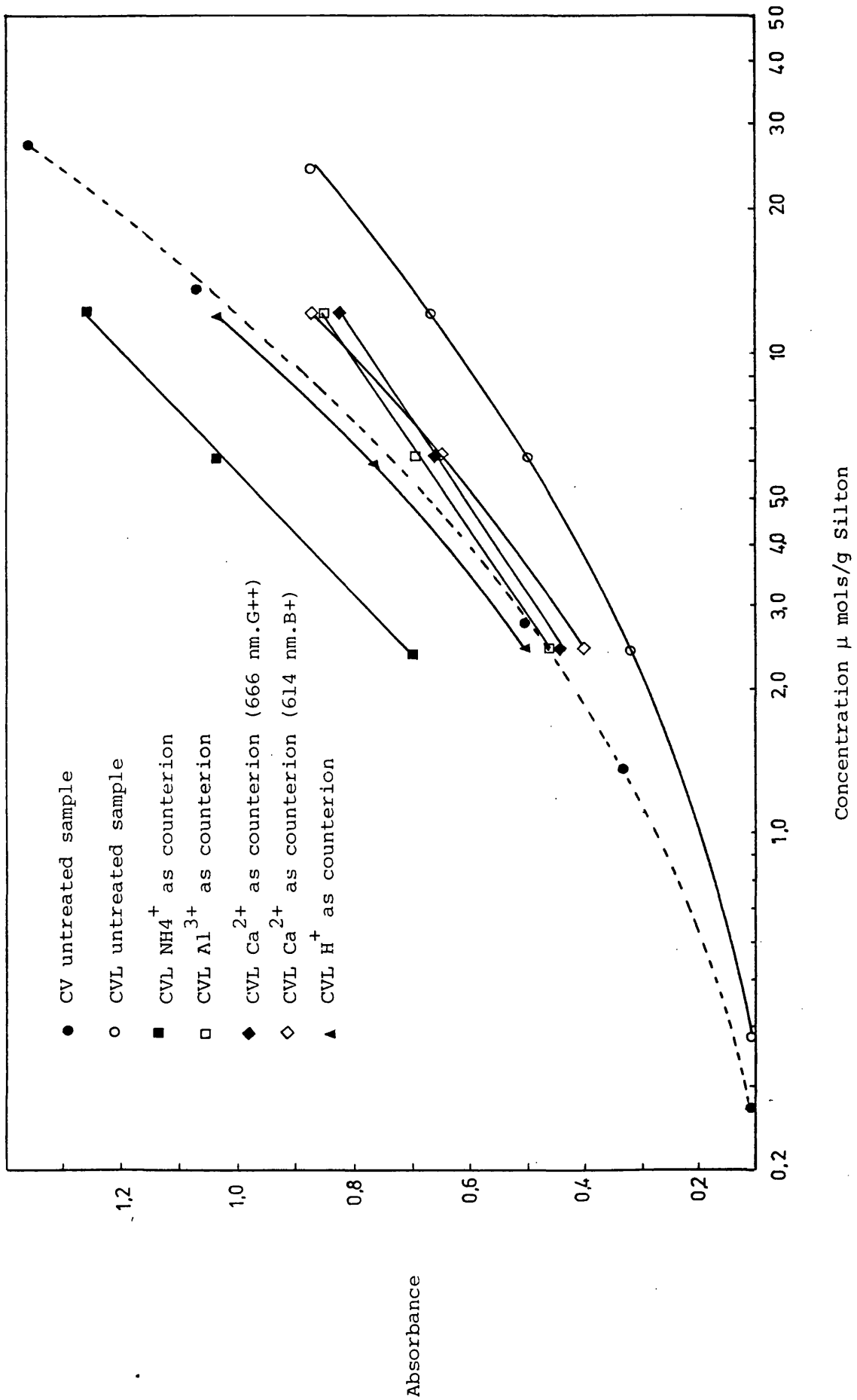


FIGURE (3-38). The Diffuse Reflectance Spectra of Crystal Violet Lactone on Silton, at 100% RH, as a function of time, without irradiation (2.5 mg CVL/g Silton)

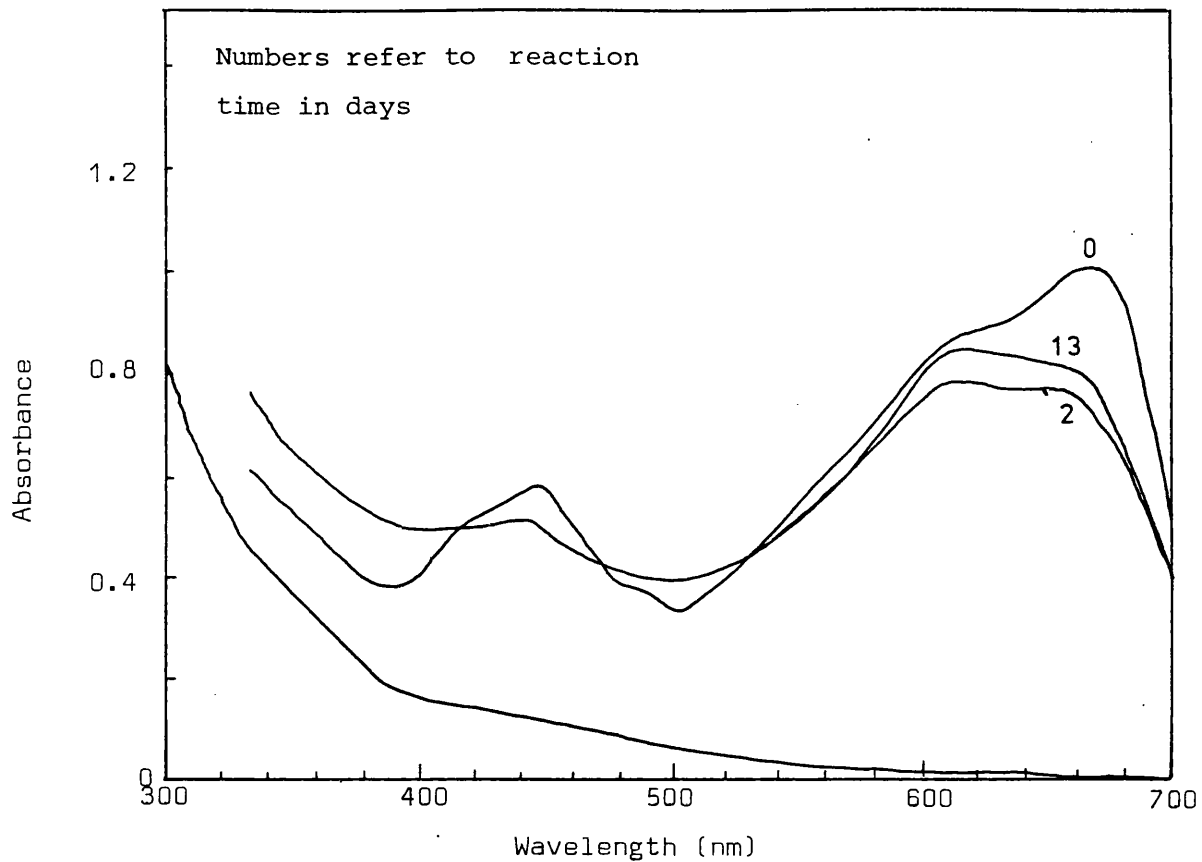


FIGURE (3-39). The Diffuse Reflectance Spectra of Crystal Violet Lactone on Silton, at 100% RH, as a function of time, with irradiation (2.5 mg CVL/g Silton)

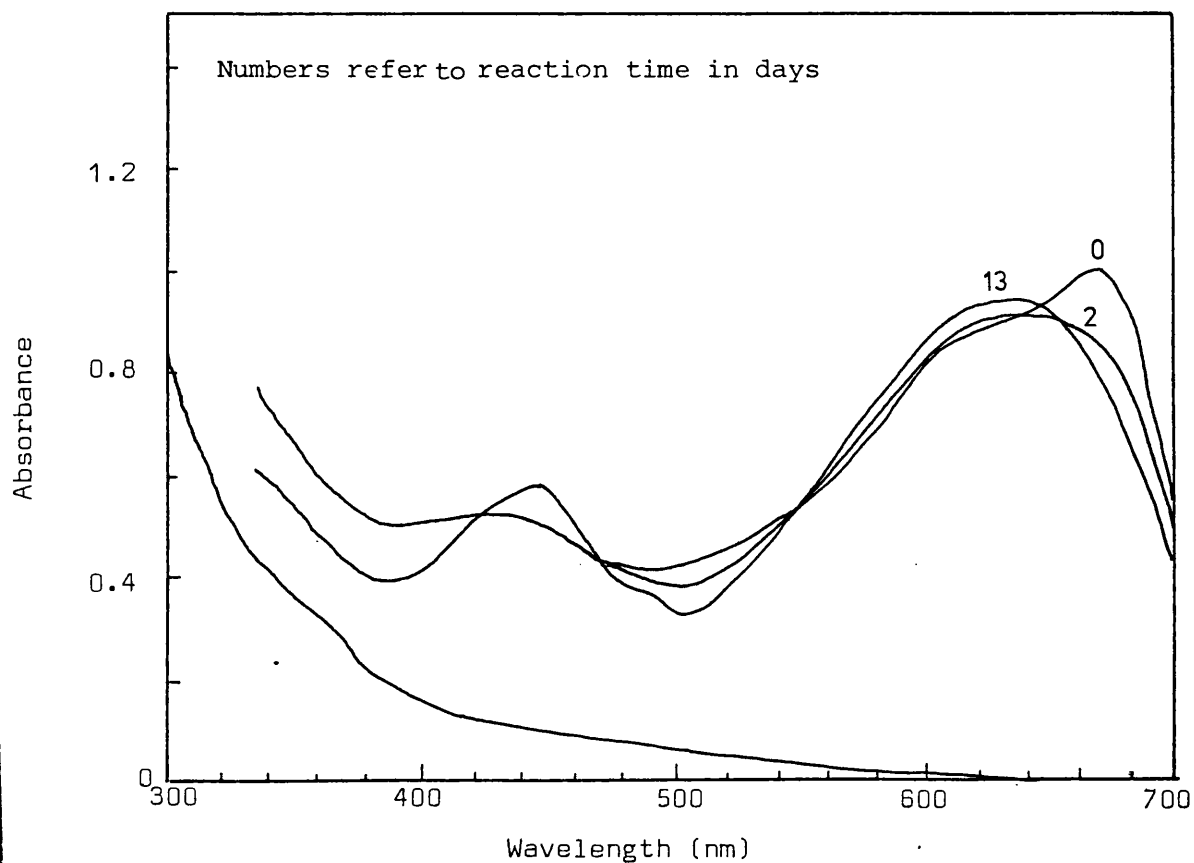


FIGURE. (3-40). The D.R.S. of CVL on Silton, at 62.5% RH, as a function of time, without irradiation (2.5 mg CVL/g Silton)

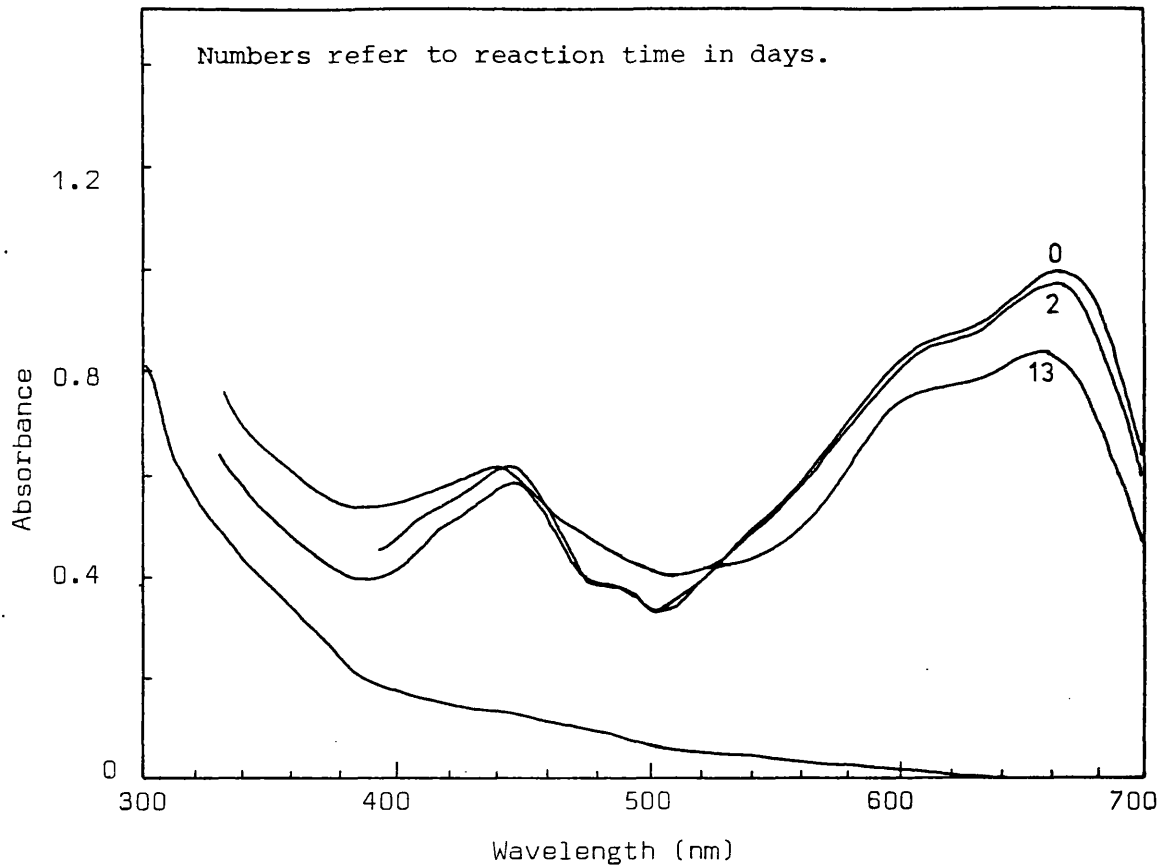


FIGURE. (3-41). The D.R.S. of CVL on Silton, at 62.5% RH, as a function of time, with irradiation (2.5 mg CVL/g Silton)

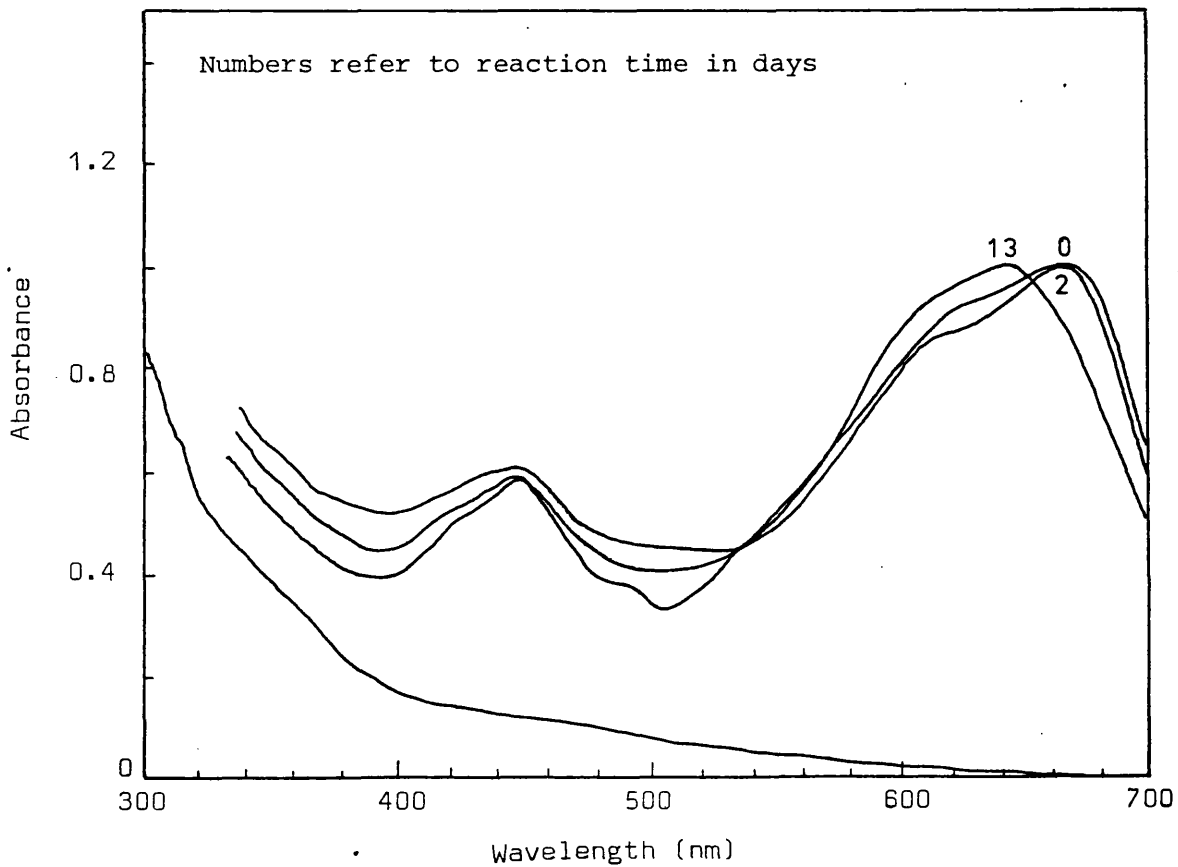


FIGURE.(3-42). The D.R.S. of CVL on Silton, at 0% RH, as a function of time, without irradiation (2.5 mg CVL/g Silton)

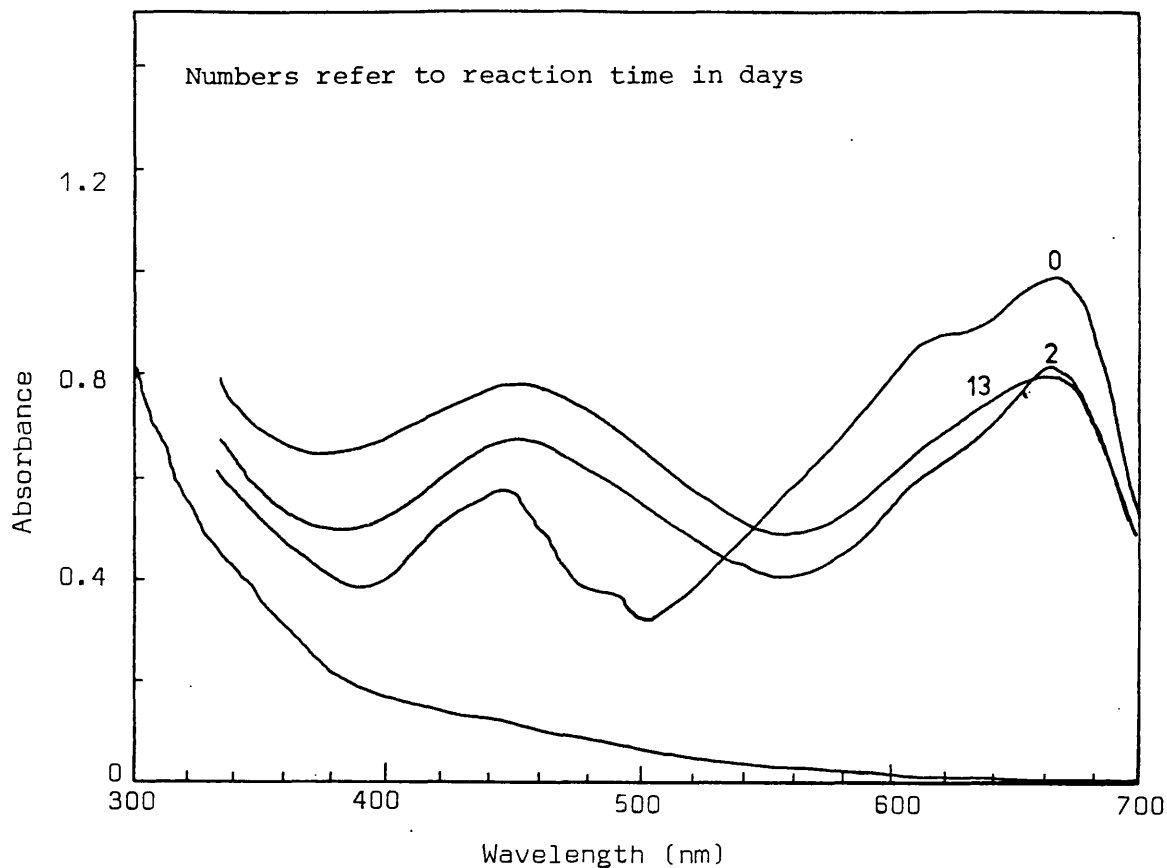


FIGURE .(3-43). The D.R.S. of CVL on Silton, at 0% RH, as a function of time, with irradiation (2.5 mg CVL/g Silton)

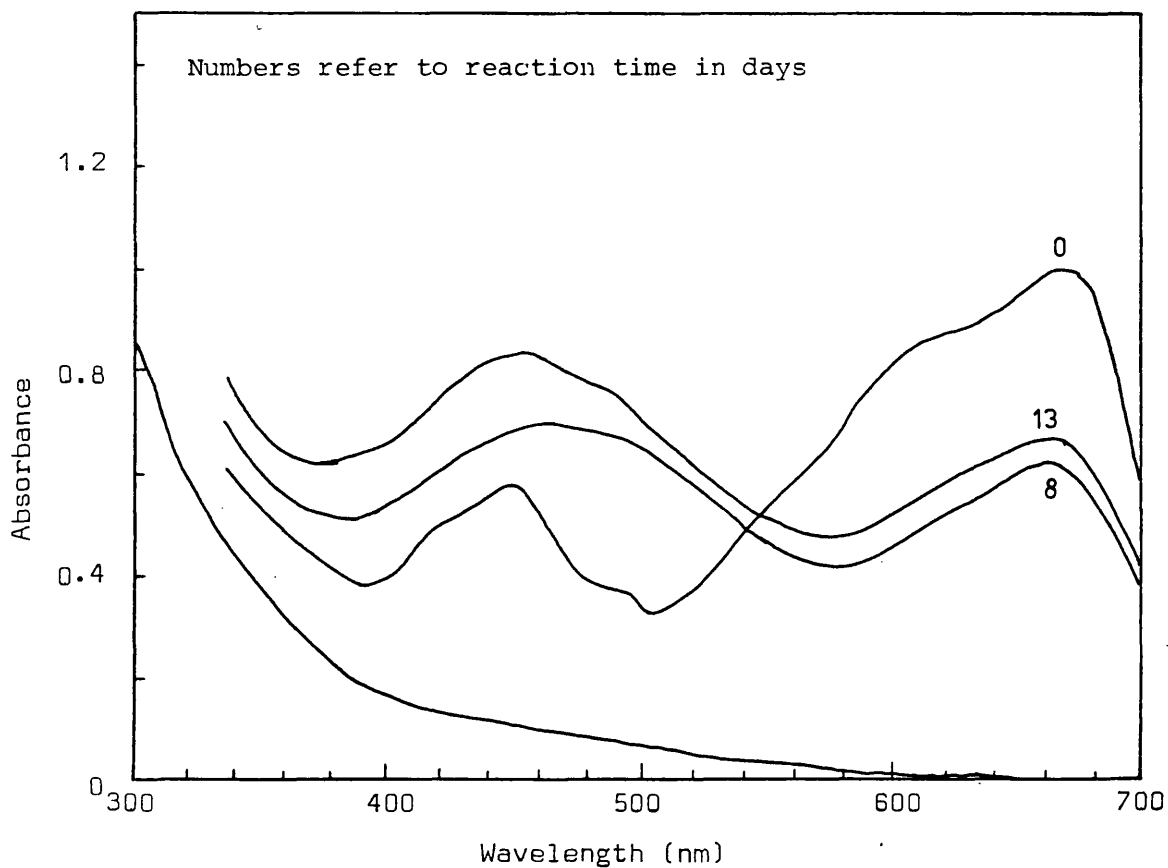


FIGURE (3-44). 100% Relative Humidity  
(Solid symbols refer to non-irradiated samples)

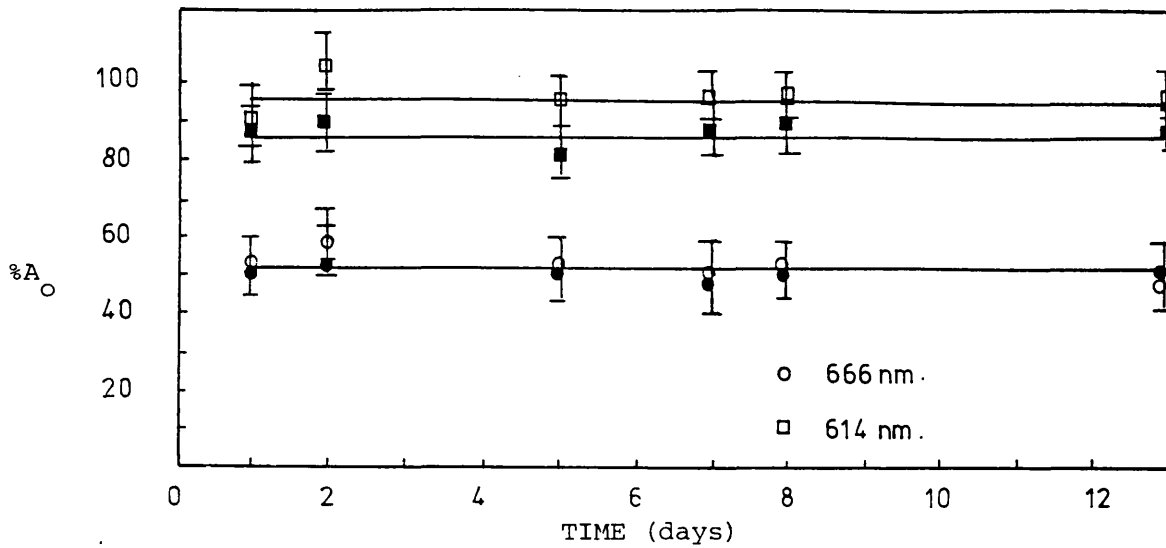


FIGURE (3-45). 62.5% Relative Humidity  
(Solid symbols refer to non-irradiated samples)

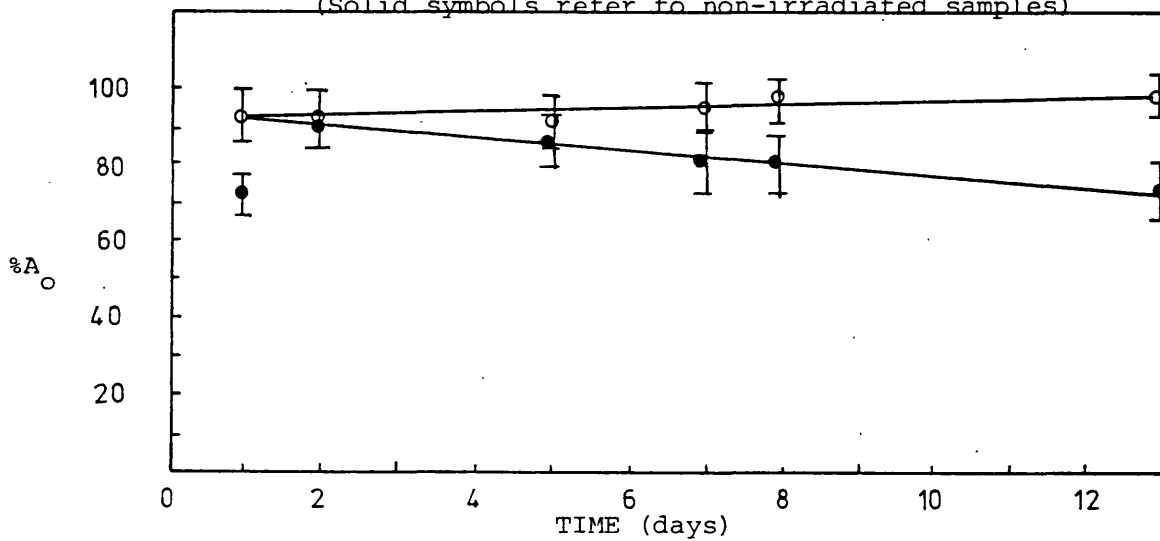
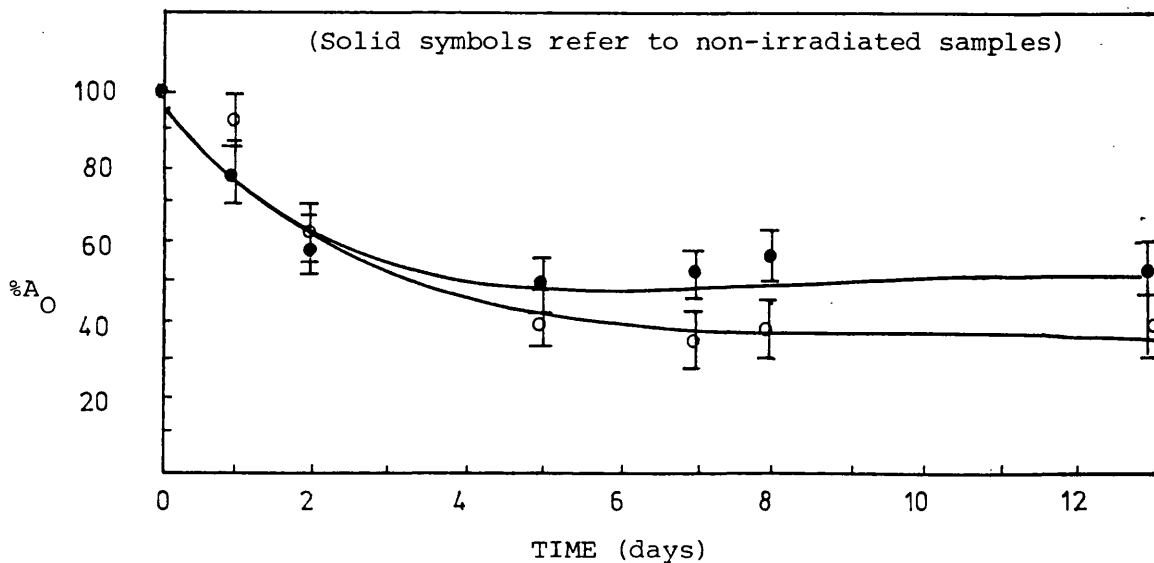


FIGURE (3-46). 0% Relative Humidity



hydrated but still adsorbed to the silt. The  $\lambda$  max for irradiated and non-irradiated samples as a function of time are shown in Figures (3-47 and 3-48). A small bathochromic shift (5nm) was seen for the non-irradiated sample. A large bathochromic shift was seen for the irradiated sample (30nm).

#### 62.5% Relative Humidity

The absorbance of CVL, adsorbed upon Silt at 62.5% RH remained high (80-90%  $A_0$ ), after 13 days, for both irradiated and non-irradiated samples Figure (3-45). The irradiated sample also showed a large (20nm) hypsochromic shift, but no shift was observed for the non-irradiated sample, Figures (3-47 and 3-48). The large shift combined with only a small reduction in absorbance indicate that the degradation products are probably dimethylated CVL or dimethylated CV.

#### 0% Relative Humidity

The absorbance of CVL decreased with time at 0% RH, Figure (3-46), for both irradiated and non-irradiated samples. The absorbance decreased to 50%  $A_0$  and thereafter remained constant. Examination of the spectra, Figures (3-42 and 3-43) showed an increase in absorbance at 450nm. The surface had been dehydrated, and as a consequence the surface acidity increased, thus causing the equilibrium to shift towards the yellow tricationic species ( $Y^{+++}$ ). No shifts in  $\lambda$  max were observed, Figures (3-47 and 3-48).

The Position of the  $\lambda$  max of Crystal Violet Lactone, on Siltan, as a function of time.

FIGURE (3—47) Non-irradiated samples

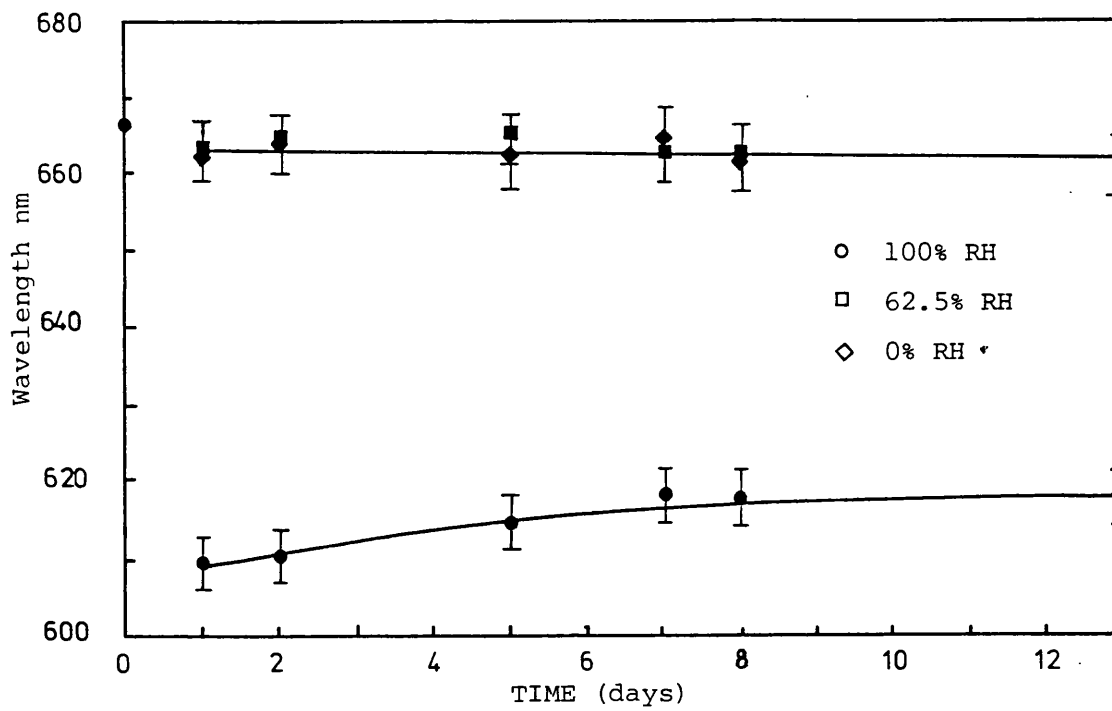
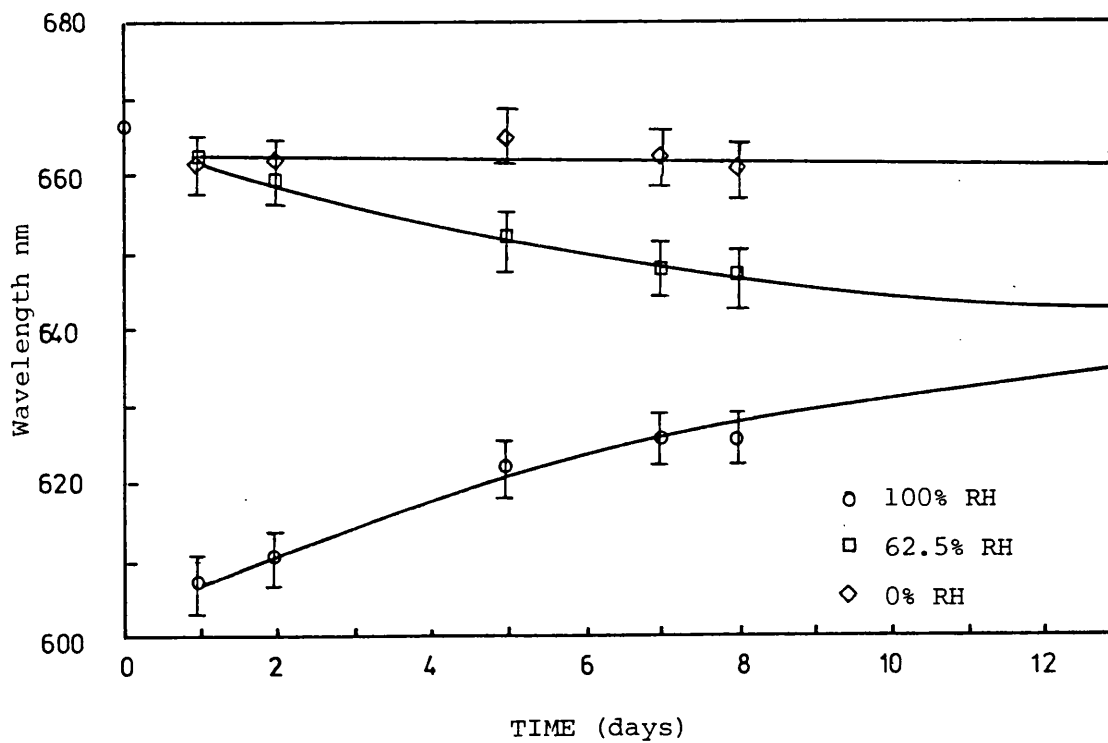


FIGURE (3—48) Irradiated samples





(ii) The Effect of Counterions upon the Fading of CVL  
Adsorbed upon Silton

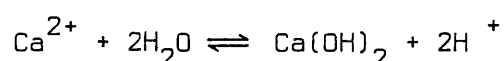
The fading process was measured by monitoring the shift in  $\lambda$  max, and changes in absorbance with time, relative to an untreated sample. All samples were maintained at 62.5% RH, 40°C. The original absorbance for the treated samples was higher than the corresponding untreated sample, Figure (3-37).

Al<sup>3+</sup> as Counterion

The behaviour of CVL upon Al<sup>3+</sup> treated silton was identical in all respects to the untreated sample, Figures (3-49 and 3-51).

Ca<sup>2+</sup> as Counterion

CVL was absorbed as a mixture of the mono and dicationic forms upon Ca<sup>2+</sup> Silton. Amounts of both forms were determined at 614 and 666nm respectively. The absorbance of the (B<sup>+</sup>) blue cation, after decreasing initially, slowly increased over the 16 day period, for irradiated and non-irradiated samples, (70-80% A<sub>0</sub>, and 80-100% A<sub>0</sub>), respectively. But the dication only increased in the dark and decreased in intensity when irradiated, Figure (3-50). These changes are consistent with a rapid hydration followed by a slow dehydration of the surface. The change could be a reflection of the state of the counterion, i.e.



The blue species exhibited a small bathochromic shift (5nm) for both samples. The green species showed a large hypsochromic shift when irradiated and a small hypsochromic

The Effect of Counterions on the percentage of zero time absorbance of Crystal Violet Lactone remaining, on Silton, as a function of time (62.5% RH)

FIGURE (3-49).  $\text{Al}^{3+}$  as Counterion  
(Solid symbols refer to non-irradiated samples)

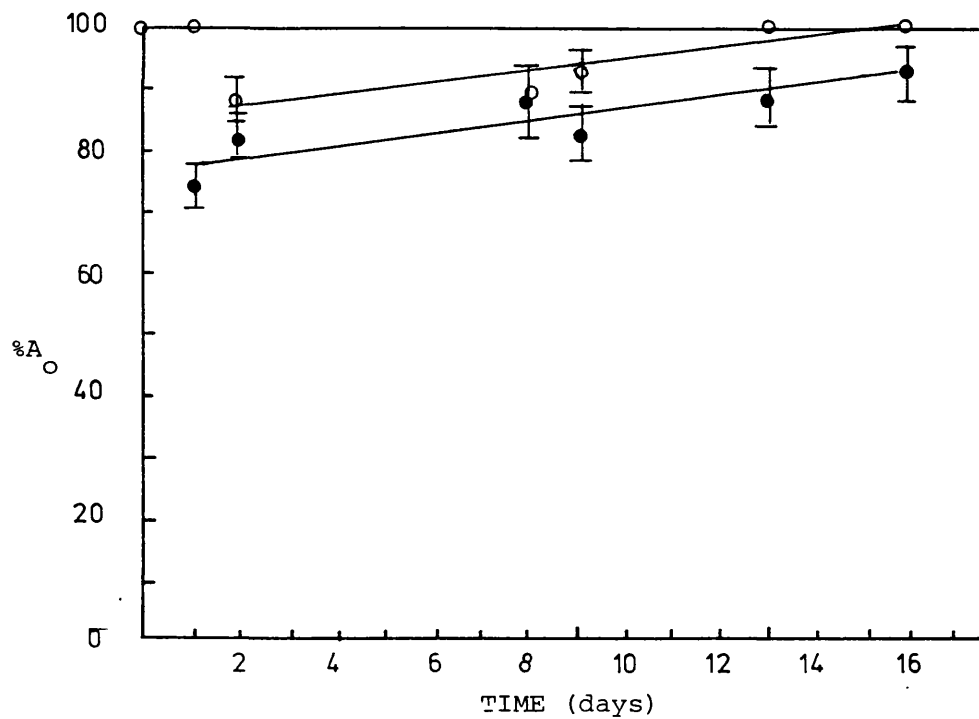


FIGURE (3-50).  $\text{Ca}^{2+}$  as Counterion  
(Solid symbols refer to non-irradiated samples)

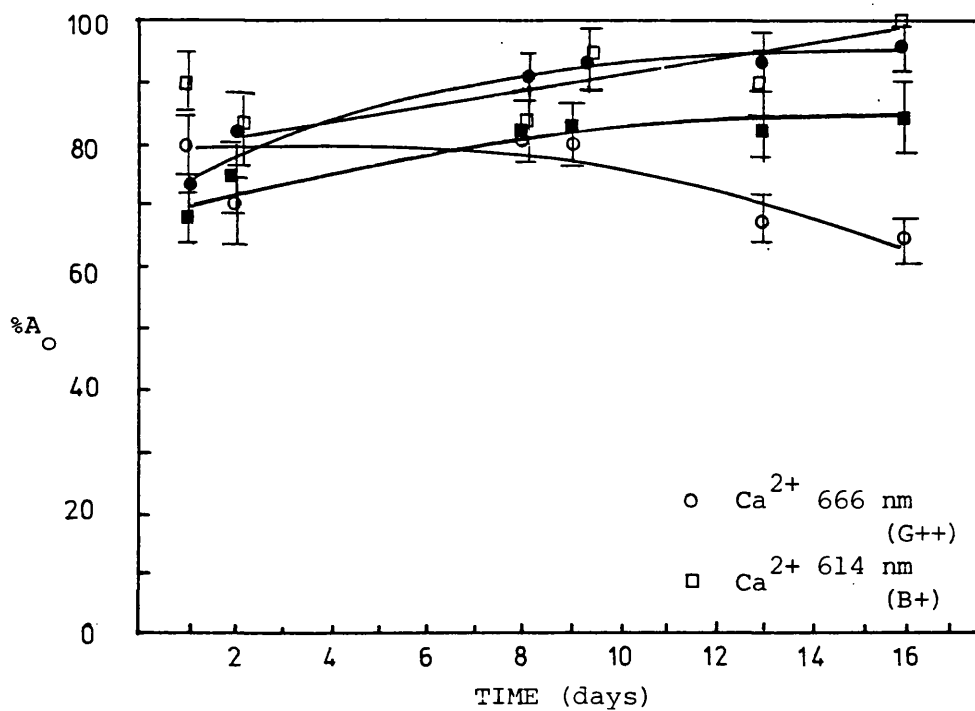


FIGURE (3-51)  $Al^{3+}$  as Counterion  
(Solid symbols refer to non-irradiated samples)

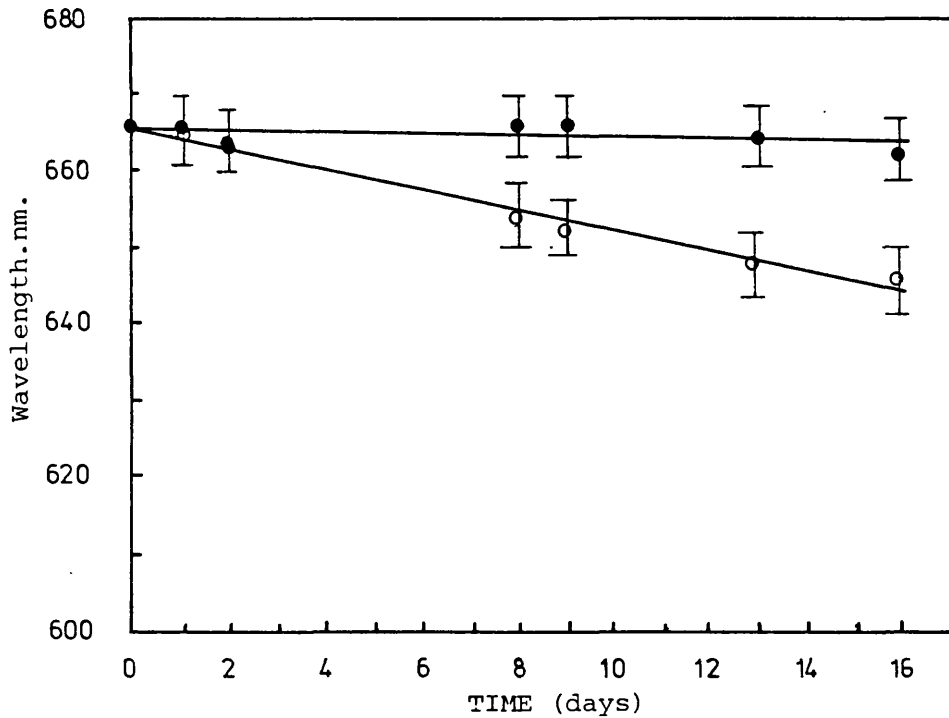
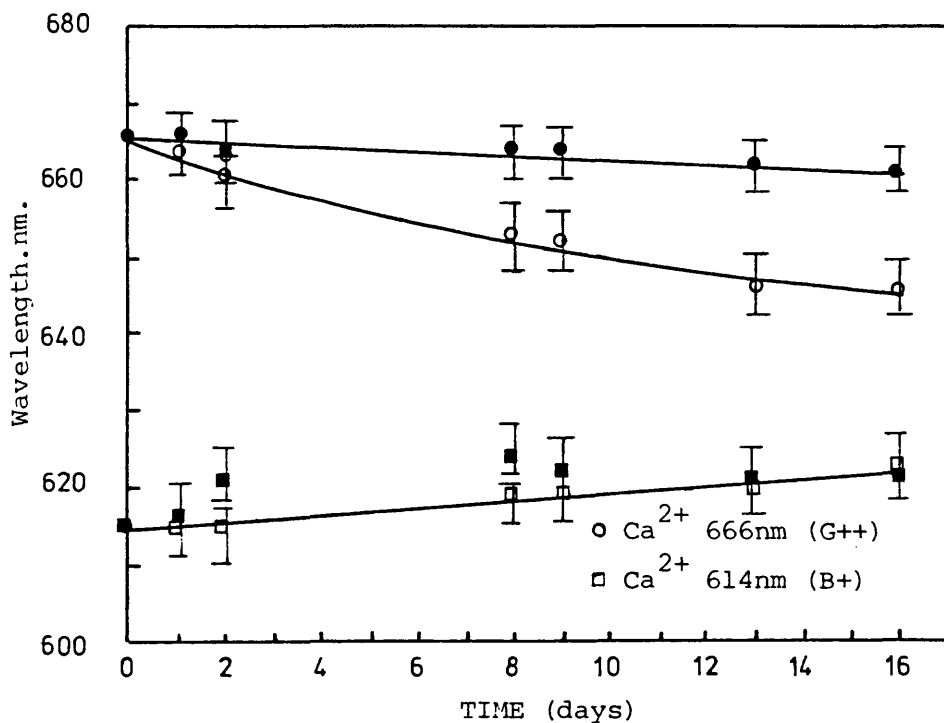


FIGURE (3-52)  $Ca^{2+}$  as Counterion  
(Solid symbols refer to non-irradiated samples)



shift when not, Figure (3-52). This indicates that the green species is more susceptible to photodegradation than the blue species.

#### H<sup>+</sup> as Counterion

When CVL was adsorbed upon H<sup>+</sup> treated Silton, it behaved as it did on untreated Silton, Figure (3-53), and Figure (3-55) with respect to intensity and changes in  $\lambda$  max.

#### NH<sub>4</sub><sup>+</sup> as Counterion

CVL was adsorbed upon NH<sub>4</sub><sup>+</sup> - Silton as the blue monocation (B<sup>+</sup>). The absorbance decreased over the first 24 hrs to 50% A<sub>0</sub>. The absorbance was then constant, Figure (3-54). No change in the position of the  $\lambda$  max (608nm) for the irradiated or non-irradiated sample was observed, Figure (3-56). The above results are a clear indication that the surface acidity of Silton is determined by the counterions present. In order of increasing acidity NH<sub>4</sub><sup>+</sup> > Ca<sup>2+</sup> > untreated > H<sup>+</sup> > Al<sup>3+</sup>. A reduction in surface acidity, (NH<sub>4</sub><sup>+</sup> treatment), can result in an increase in intensity because only the blue monocation is formed, which has a high extinction compared to the green or yellow forms.

FIGURE (3-53)  $H^+$  as Counterion  
(Solid symbols refer to non-irradiated samples)

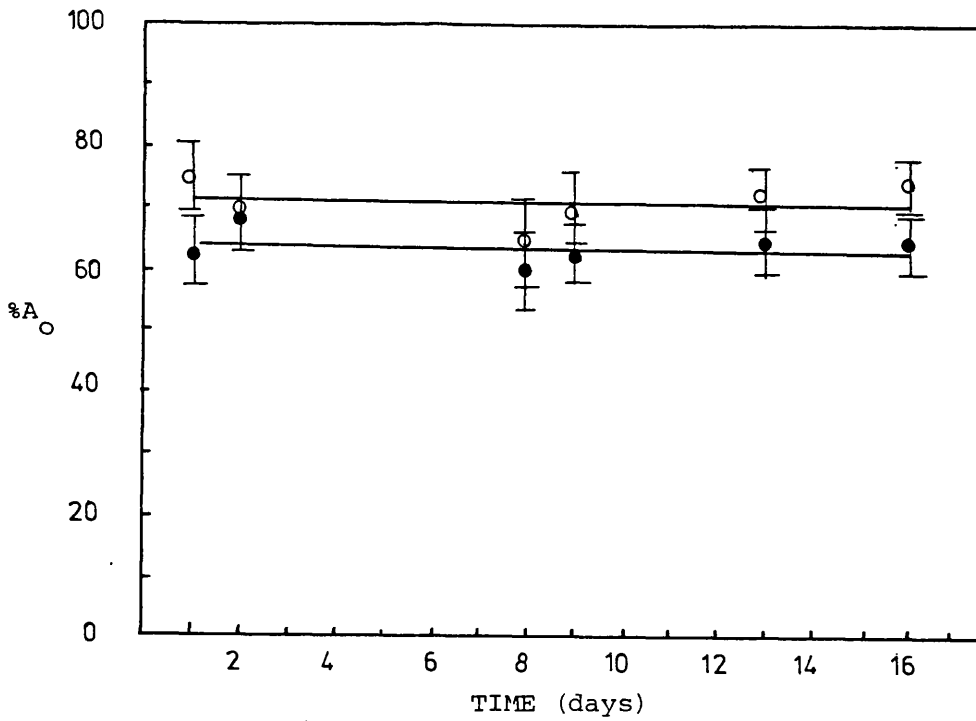


FIGURE (3-54)  $NH_4^+$  as Counterion  
(Solid symbols refer to non-irradiated samples)

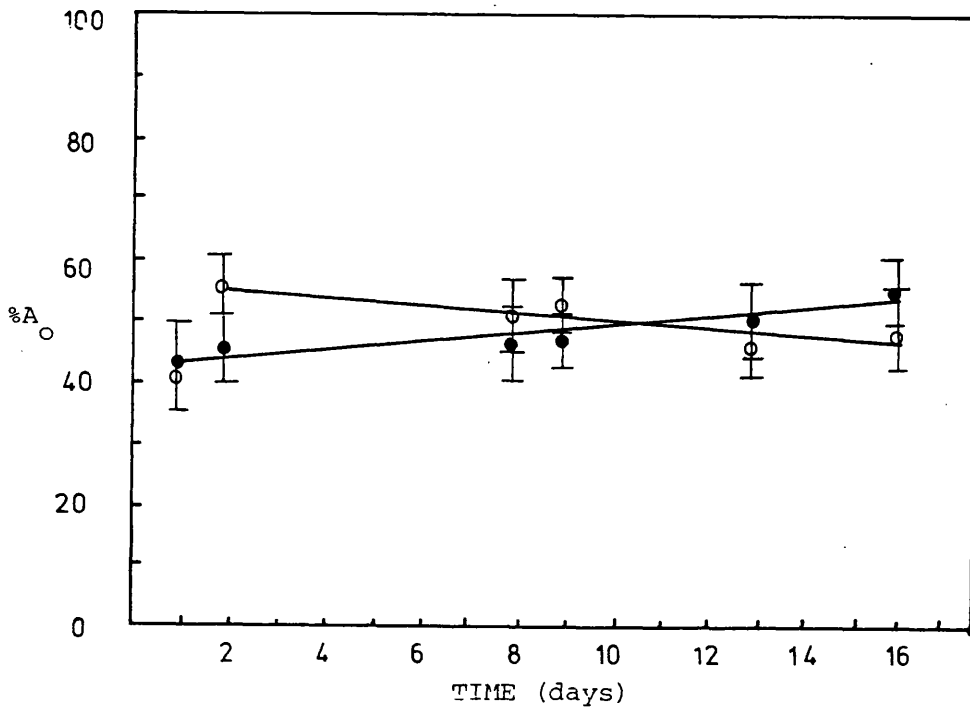


FIGURE (3-55).  $\text{H}^+$  as Counterion  
(Solid symbols refer to non-irradiated samples)

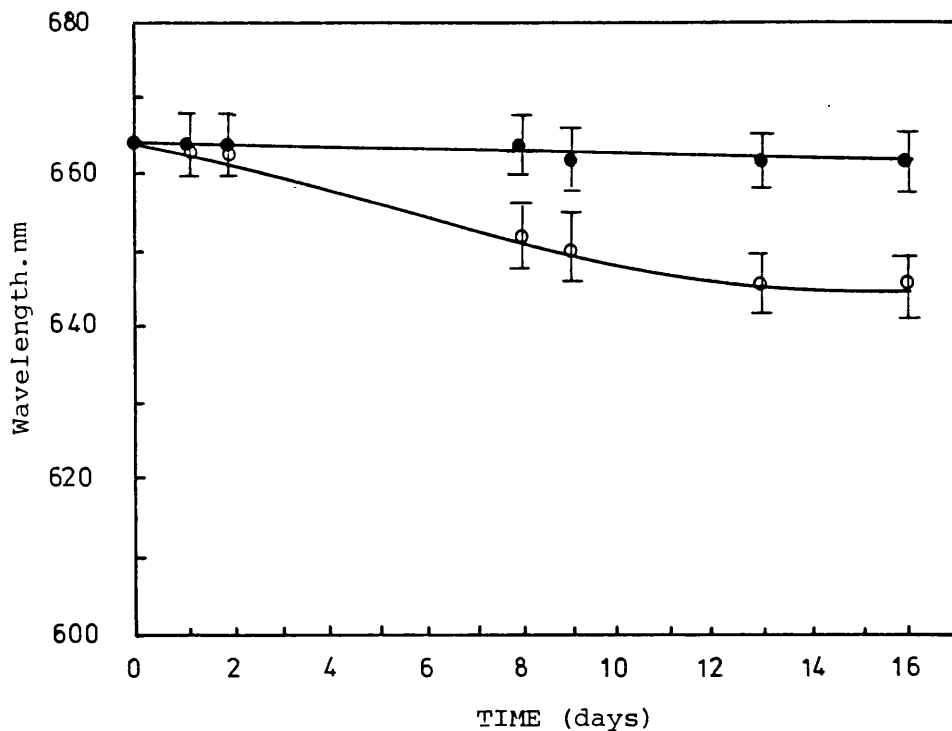
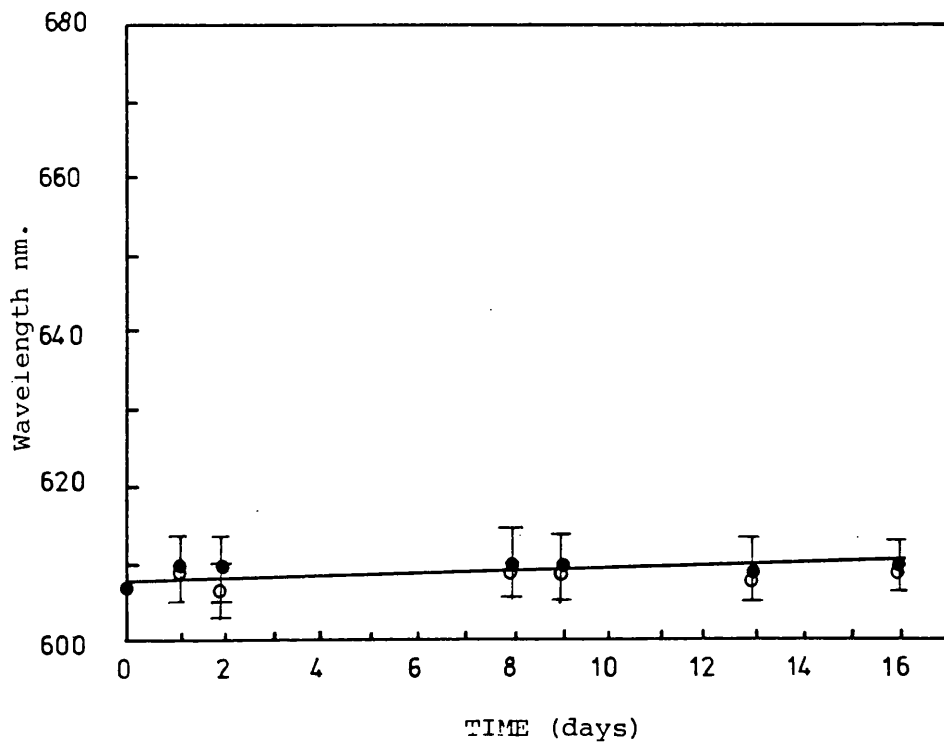


FIGURE (3-56).  $\text{NH}_4^+$  as Counterion  
(Solid symbols refer to non-irradiated samples)



### 3.3.7 The Effect of Humidity and Light upon CVL Adsorbed upon Wyoming Bentonite

(i) The absorbance of CVL, adsorbed upon Wyoming bentonite as a function of the concentration applied is shown in Figure (3-57). CVL was adsorbed as the blue monocation. The reflectance spectra of CVL adsorbed upon bentonite are shown in Figures (3-58 to 3-63).

#### 100% Relative Humidity

At 100% RH the absorbance of the irradiated and non-irradiated samples fell rapidly, due to hydration, over the first 24hrs to 30%  $A_0$  Figure (3-64).

#### 62.5% Relative Humidity

At 62.5% RH the absorbance decreased rapidly for the irradiated and non-irradiated samples. Over the first 24hrs the absorbance fell to 40%  $A_0$ , Figure (3.65).

#### 0% Relative Humidity

At 0% RH the absorbance increased after 24hrs to 200%  $A_0$  for both samples, Figure (3-66). The irradiated sample showed a subsequent decrease, until 70%  $A_0$  remained (16 days). The non-irradiated sample remained constant at 200%  $A_0$ , over the period of the experiment. When irradiated a shoulder appears at 650nm on the spectra, and a new peak appears at 450nm, Figure (3-63). No changes are observed for the sample in the dark, Figure (3-61). Also no change is observed in the position of  $\lambda$  max for either sample, Figures (3-67 and 3-68).

FIGURE (3-57). The Absorbance of Crystal Violet and Crystal Violet Lactone on Wyoming Bentonite

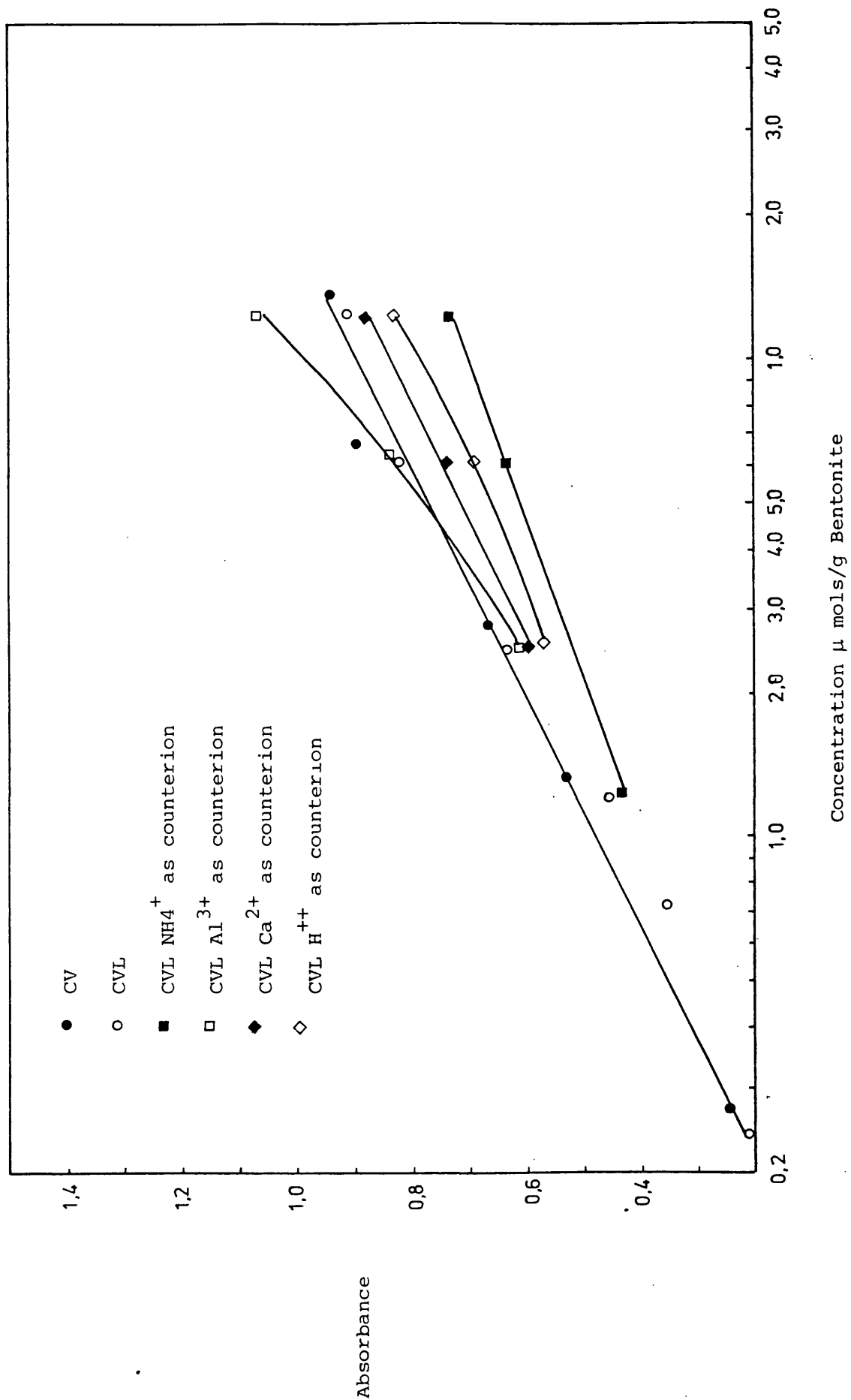




FIGURE.(3-58). The Diffuse Reflectance Spectra of Crystal Violet Lactone on Wyoming Bentonite, at 100% RH, as a function of time without irradiation (2.5 mg CVL/g Bentonite)

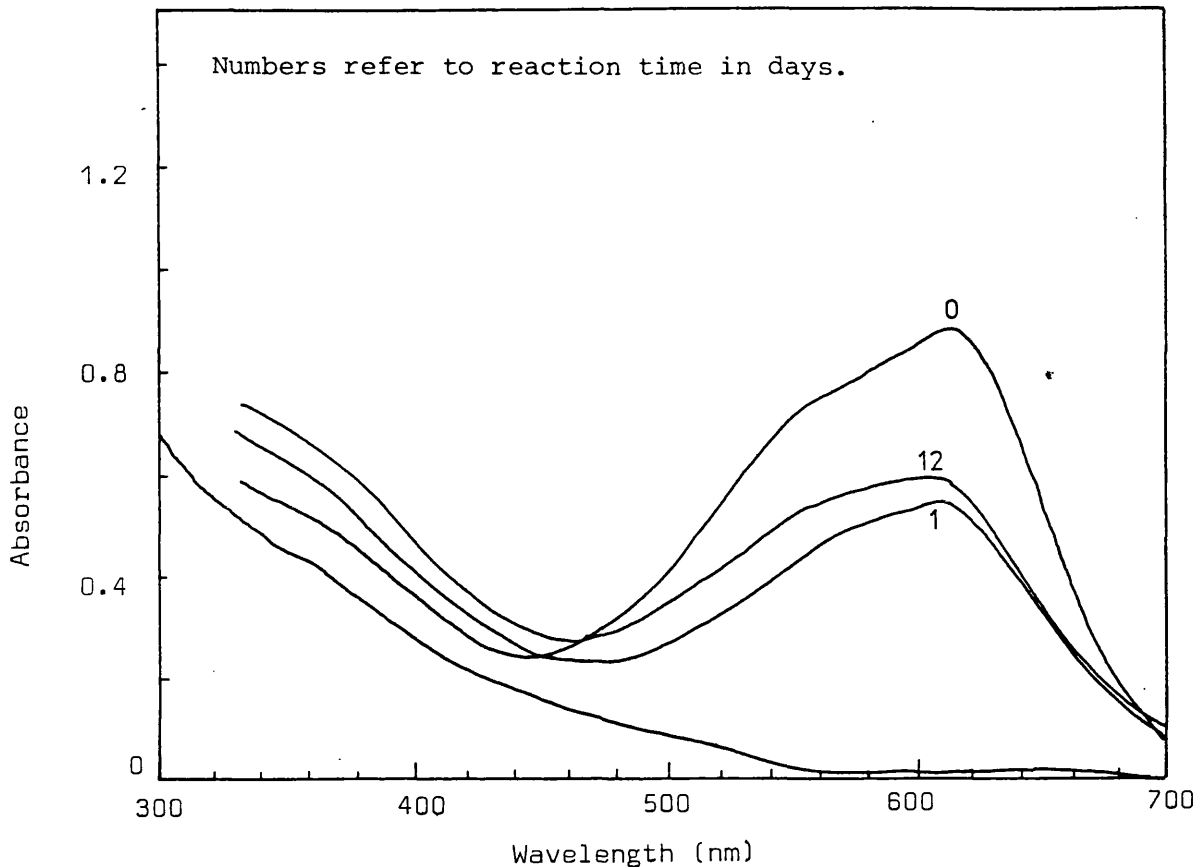


FIGURE.(3-59). The Diffuse Reflectance Spectra of Crystal Violet Lactone on Wyoming Bentonite, at 100% RH, as a function of time with irradiation (2.5 mg CVL/g Bentonite)

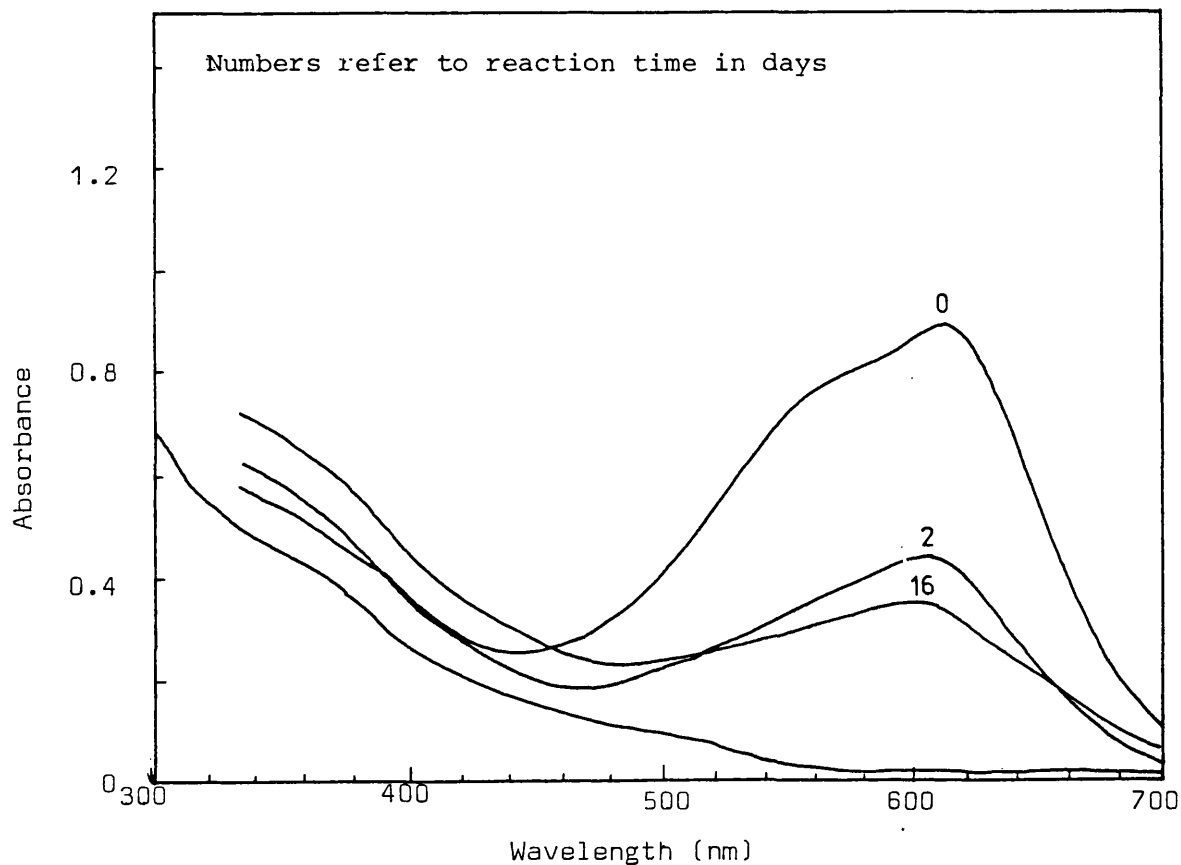


FIGURE.(3-60). The D.R.S. of CVL on Wyoming Bentonite at 62.5% RH, as a function of time without irradiation, (2.5 mg CVL/g Bentonite)

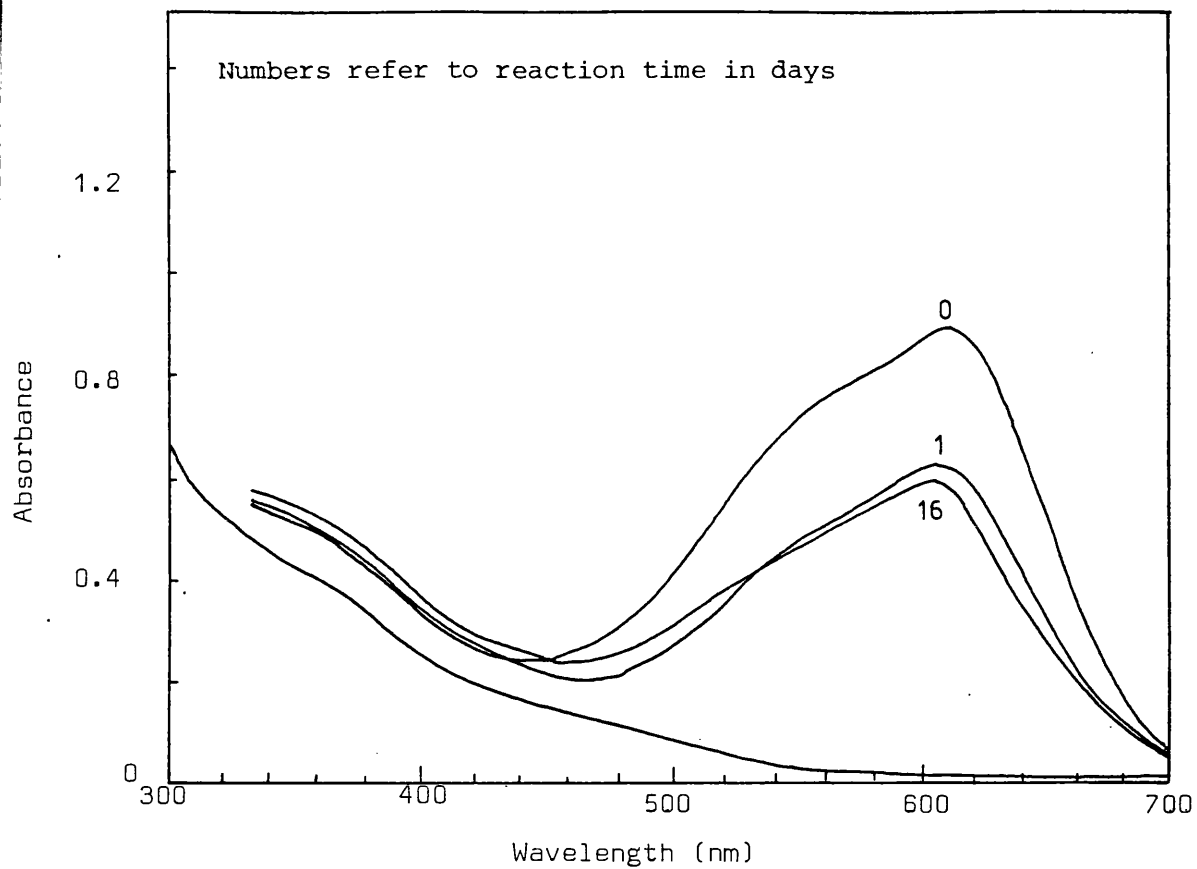


FIGURE.(3-61). The D.R.S. of CVL on Wyoming Bentonite at 62.5% RH, as a function of time with irradiation, (2.5 mg CVL/g Bentonite)

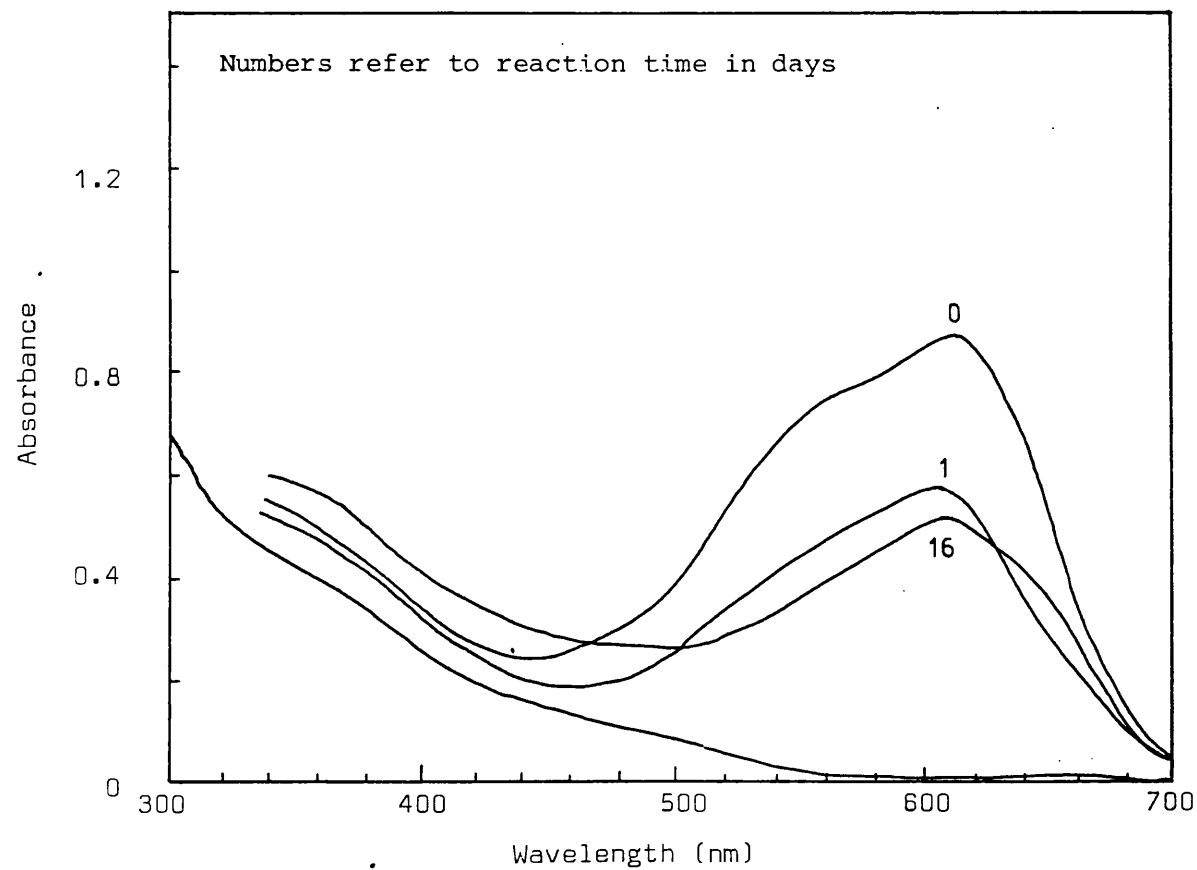


FIGURE (3-62). The D.R.S. of CVL on Wyoming Bentonite at 0% RH, as a function of time without irradiation, (2.5 mg CVL/g Bentonite)

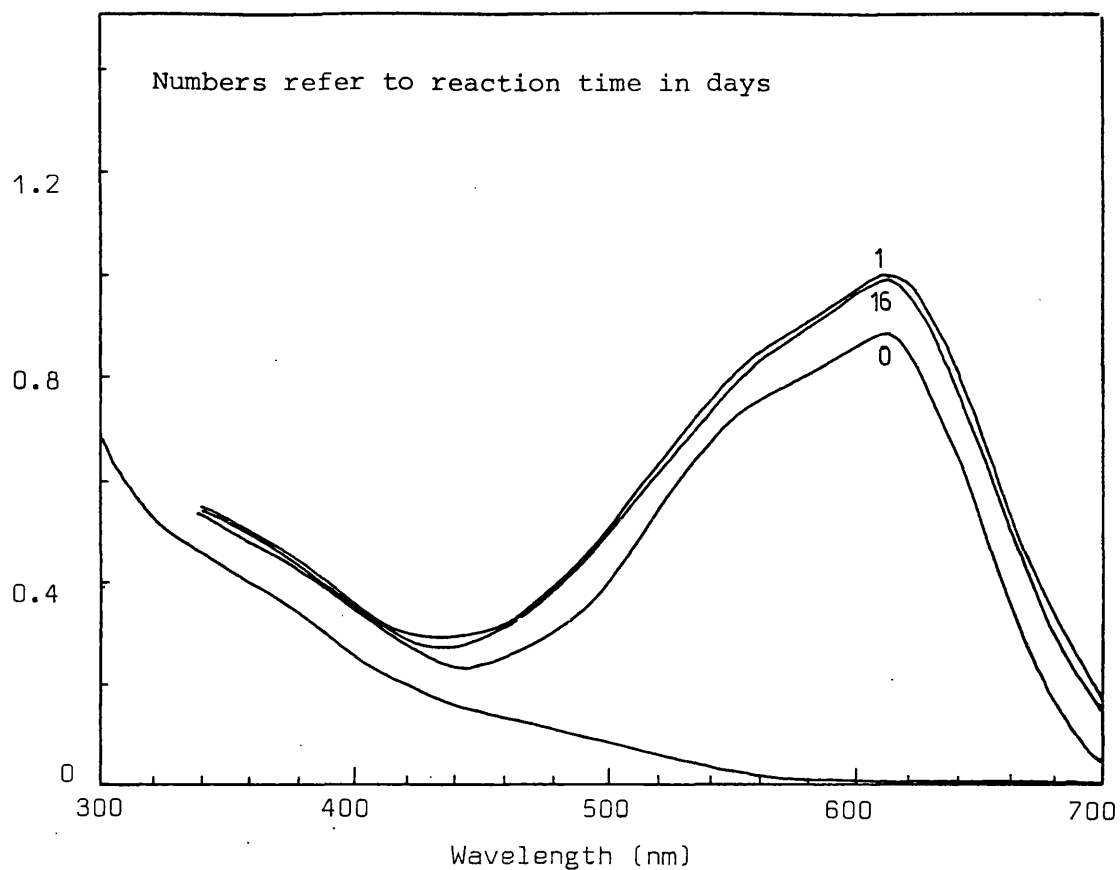


FIGURE (3-63). The D.R.S. of CVL on Wyoming Bentonite at 0% RH, as a function of time with irradiation, (2.5 mg CVL/g Bentonite)

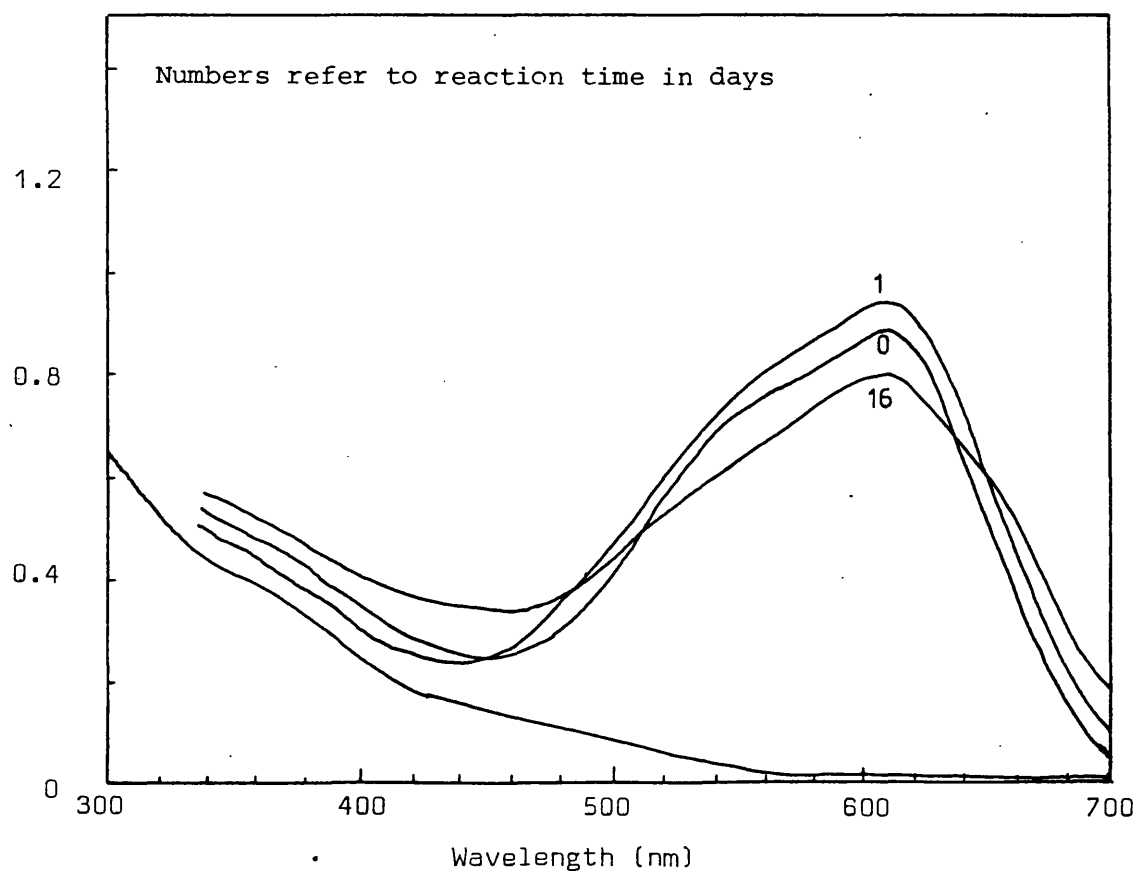


FIGURE (3-64). 100% Relative Humidity  
(Solid symbols refer to non-irradiated samples)

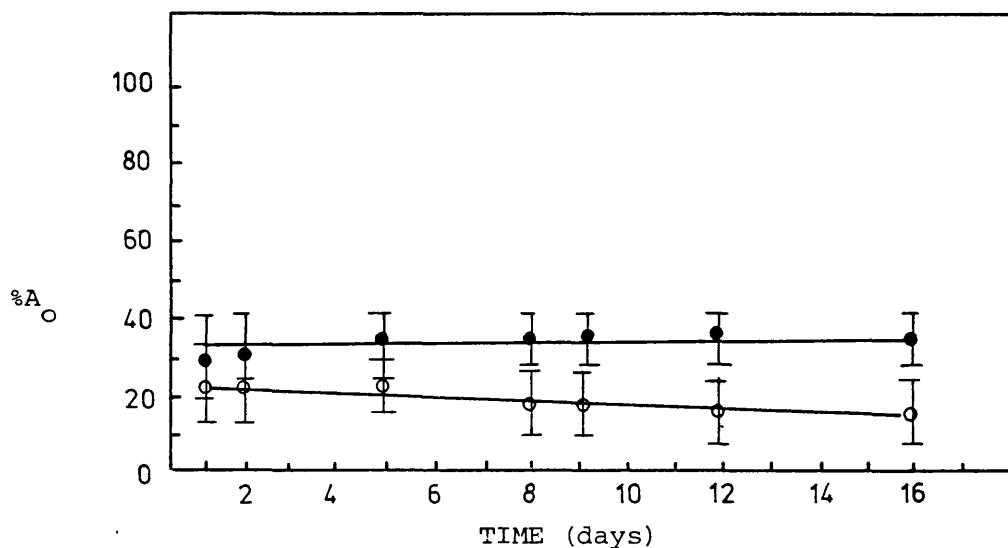


FIGURE (3-65). 62.5% Relative Humidity  
(Solid symbols refer to non-irradiated samples)

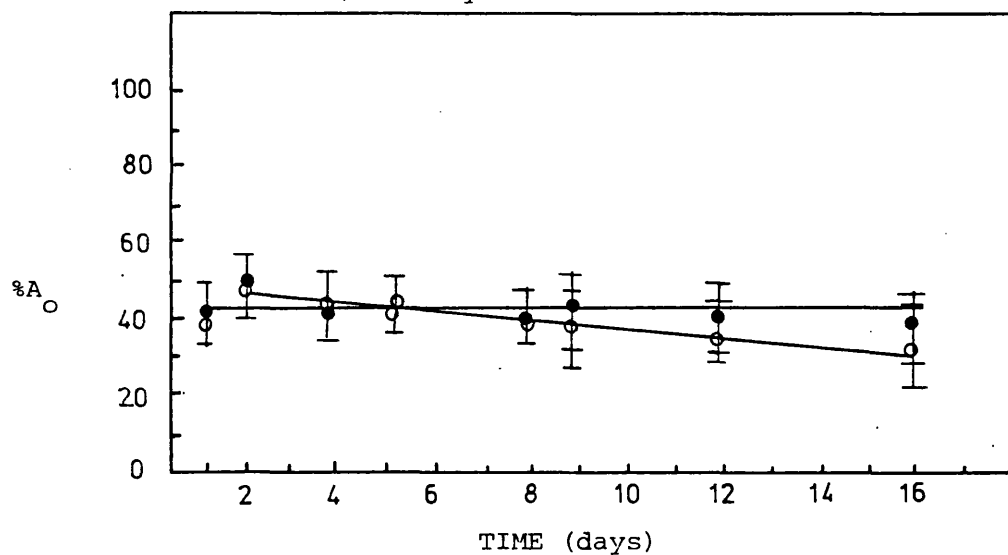


FIGURE (3-66). 0% Relative Humidity  
(Solid symbols refer to non-irradiated samples)

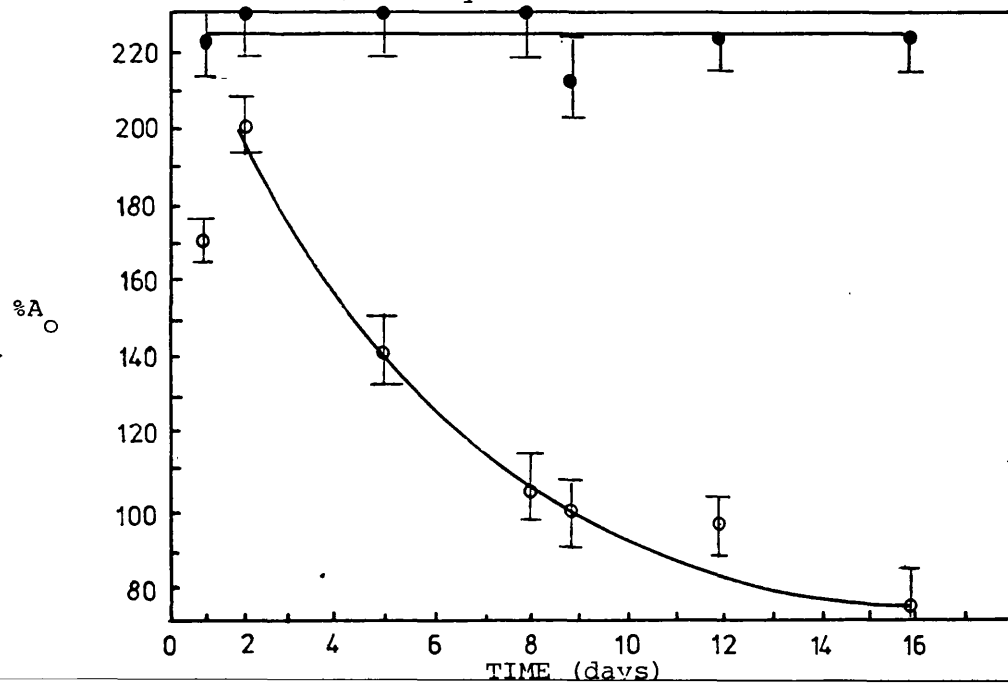


FIGURE (3-67). Non-irradiated samples

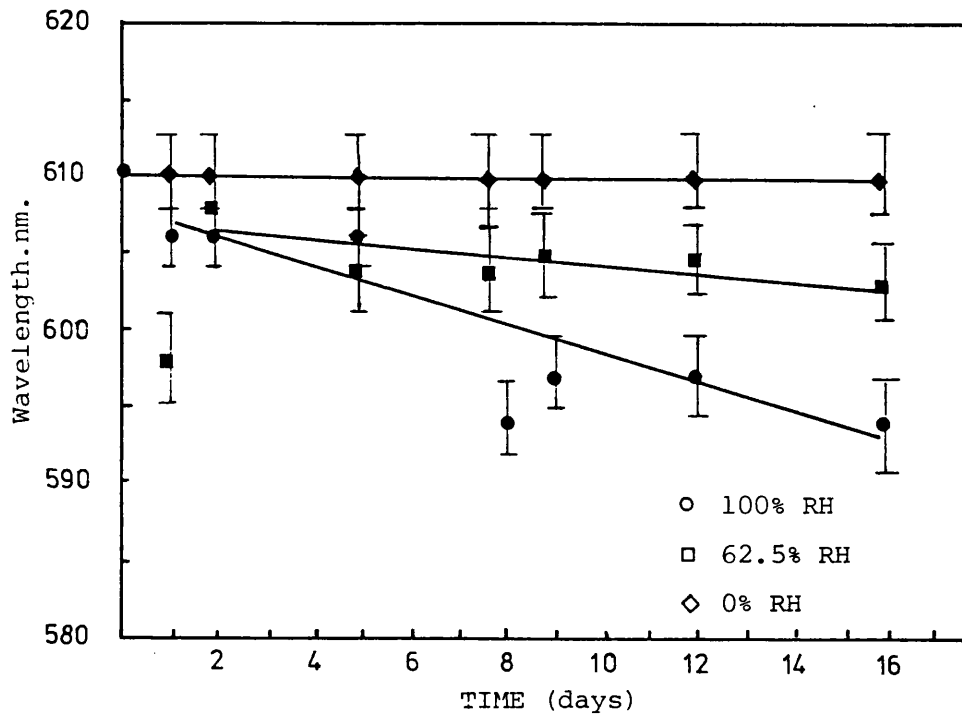
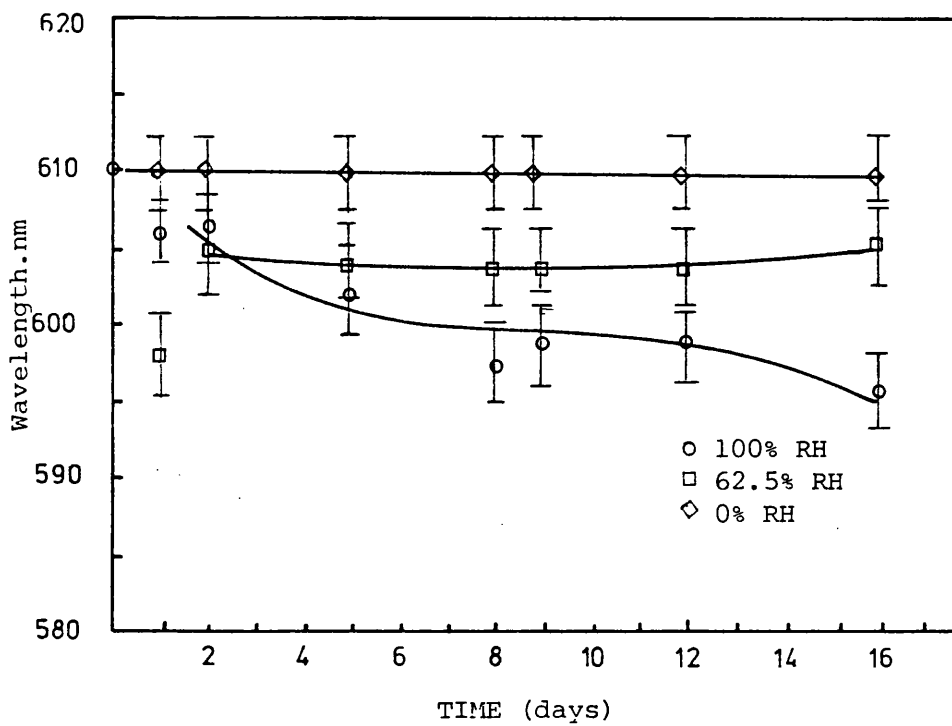


FIGURE (3-68). Irradiated samples



The reduction in absorbance of the irradiated sample could be caused either by an increase in temperature at the surface of the irradiated sample, (light can increase the temperature of a solid surface by as much as  $10^{\circ}\text{C}$ , Egerton, G.S. and Morgan, A.G., (1970)), or the blue zwitterion was unsymmetrically demethylated, producing malachite green or one of its derivatives.

(ii) The Effect of Counterions upon the Fading of CVL  
Adsorbed upon Wyoming Bentonite

$\text{Al}^{3+}$  as Counterion

The presence of  $\text{Al}^{3+}$  as counterion caused CVL to be adsorbed as the green dication. Both samples were 80%  $A_0$  after 24hrs and steadily increased to 85%  $A_0$  after 15 days, Figure (3-69). The position of  $\lambda$  max for the dark sample remained constant at 666nm, but the irradiated sample exhibited a - 8nm hypsochromic shift, Figure (3-71). The irradiated sample was probably demethylated because of the hypsochromic shift and no change in absorbance.

$\text{Ca}^{2+}$  as Counterion

CVL adsorbed upon  $\text{Ca}^{2+}$  - bentonite was in the blue monocationic form. The absorbance of the non-irradiated sample decreased to 30%  $A_0$  after 24hrs and decreased further to 20%  $A_0$  over the 15 day period, Figure (3-69). The irradiated sample decreased to 20%  $A_0$  after 24hrs and decreased to 10%  $A_0$  over the 15 day period, Figure (3-69). The position of the  $\lambda$  max for dark and irradiated changed from 608 to 598nm and 594 to 610nm respectively, Figure (3-72).

The Effect of Counterions on the Percentage of the Zerotime absorbance of Crystal Violet Lactone, on Wyoming Bentonite as a function of time (62.5% RH).

FIGURE (3-69).  $\text{Al}^{3+}$  and  $\text{Ca}^{2+}$  as Counterions  
(Solid symbols refer to non-irradiated samples)

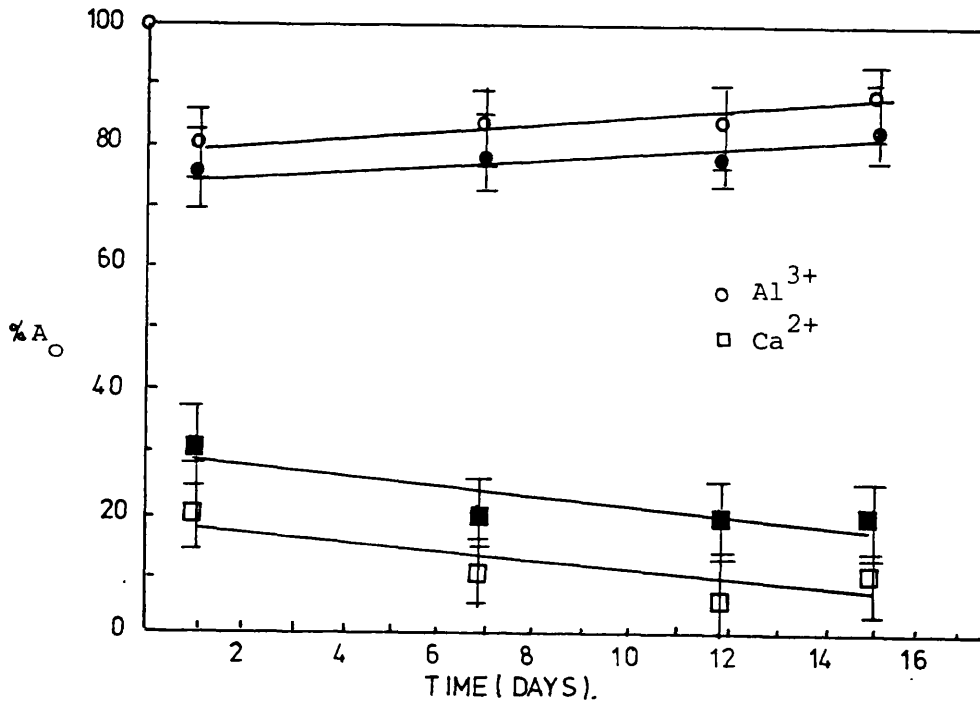


FIGURE (3-70).  $\text{H}^+$  and  $\text{NH}_4^+$  as Counterions  
(Solid symbols refer to non-irradiated samples)

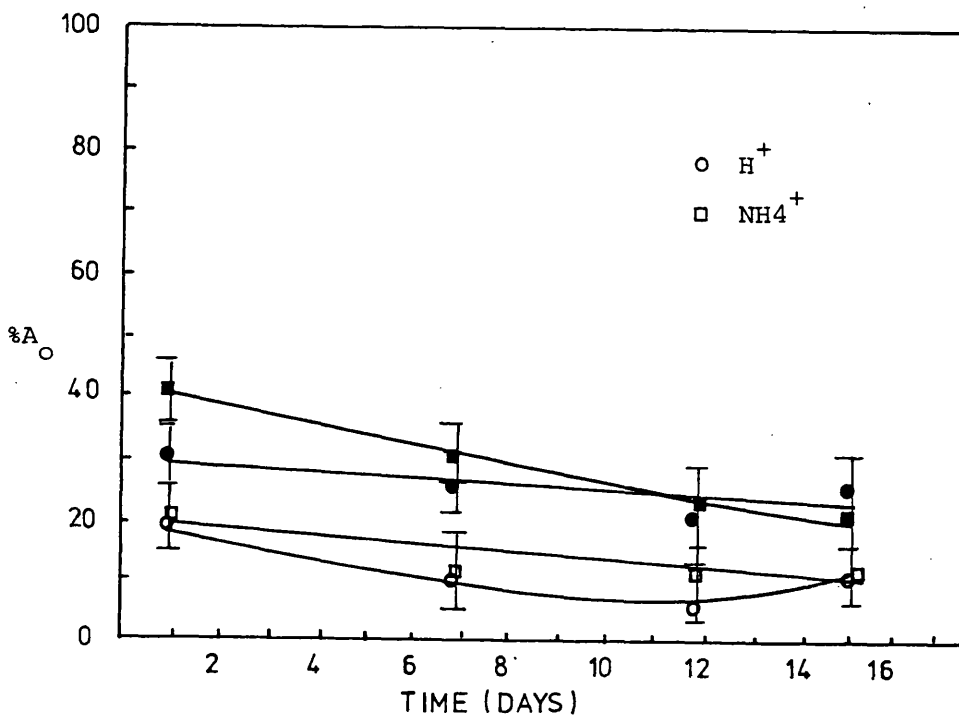


FIGURE (3-71).  $Al^{3+}$  as Counterion  
(Solid symbols refer to non-irradiated samples)

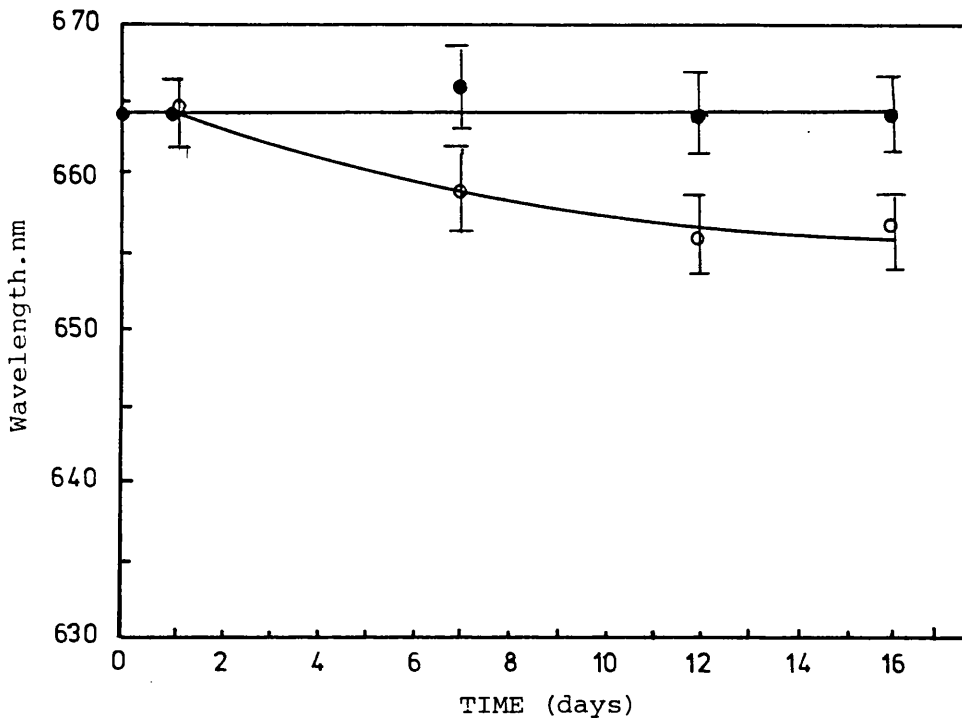
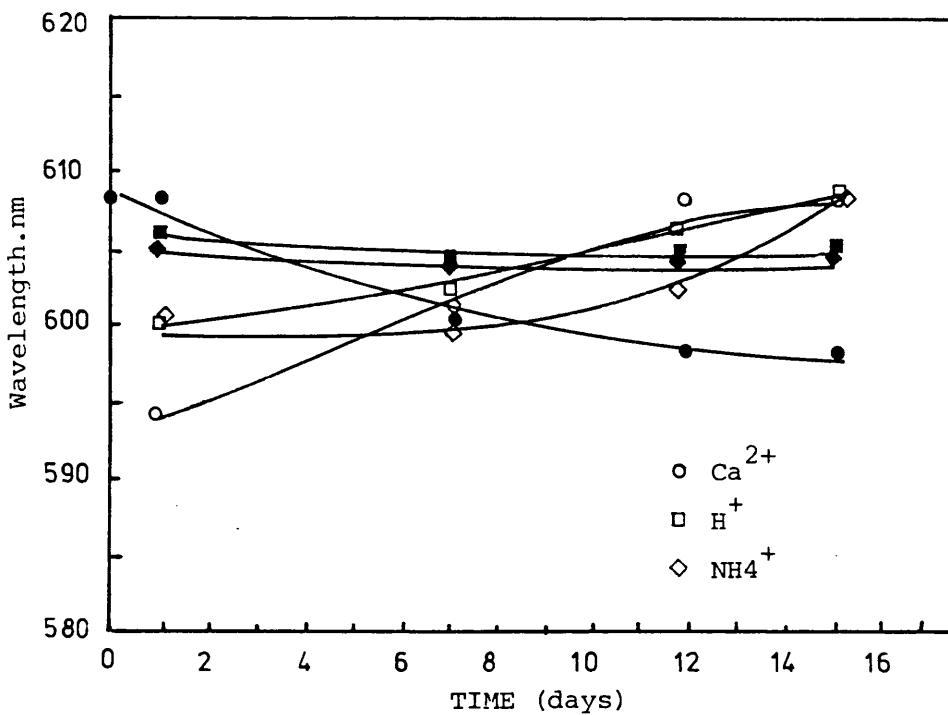


FIGURE (3-72).  $Ca^{2+}$ ,  $H^{+}$  and  $NH_4^{+}$  as Counterion  
(Solid symbols refer to non-irradiated samples)





H<sup>+</sup> as Counterion

The blue monocationic form of CVL was formed when it was adsorbed upon H<sup>+</sup> - bentonite. Both the intensity and position of  $\lambda$  max changed in similar manner to CVL upon Ca<sup>2+</sup> - bentonite, Figures (3-70 and 3-72).

NH<sub>4</sub><sup>+</sup> as Counterion

As with Ca<sup>2+</sup> and H<sup>+</sup> bentonite CVL was adsorbed as the blue monocation. The change in absorbance with time is shown in Figure (3-70). Again the changes in absorbance are similar to those occurring upon Ca<sup>2+</sup> and H<sup>+</sup> bentonite. Also the changes in position for dark and irradiated samples were similar to those upon Ca<sup>2+</sup> and H<sup>+</sup> bentonite, Figure (3-72).

### 3.3.8 Reflectance of CV and CVL Adsorbed upon Kaolinite

CV was adsorbed upon kaolinite as the blue, and green mono and dicationic species, Figure (3-73). The ratio of the two forms remained constant, with varying coverage, see page 52 Chapter 2. This provided a simple method to measure the surface acidity as has been outlined earlier. When CVL was adsorbed upon kaolinite it was adsorbed as the blue monocation, with a small percentage of the green dication. This was seen as a small shoulder at 650nm, Figures (3-75 to 3-80). The absorbance of CV and CVL as a function of concentration are shown in Figure (3-74).

#### (i) The Effect of Humidity and Light upon CVL Adsorbed upon Kaolinite

The adsorbance of the non-irradiated samples decreases proportionally with the relative humidity (absorbance after 24hrs; 55%  $A_0$ , 100% RH; 70%  $A_0$ , 62.5% RH, and 90%  $A_0$ ; 0% RH), Figures (3-81 to 3-83). The absorbance remained constant after 24hrs for the period the experiment.

The absorbance of the irradiated samples slowly decreased over 13 days, to 50-60%  $A_0$ , for all humidities. All non-irradiated samples exhibited a bathochromic shift over the first 48hrs, (100% RH, + 8nm to 610nm; 62.5% RH, + 2nm to 604nm and 0% RH, + 12nm to 614nm). This represented an equilibration of the surface to the specified humidity, Figures (3-84 to 3-85).. Irradiation causes a small (+3nm) bathochromic shift, at 100 and 0% RH. At 62.5% RH, a large +30nm bathochromic shift was observed.

FIGURE (3—73). The Absorbance Spectra of Crystal Violet on Kaolinite

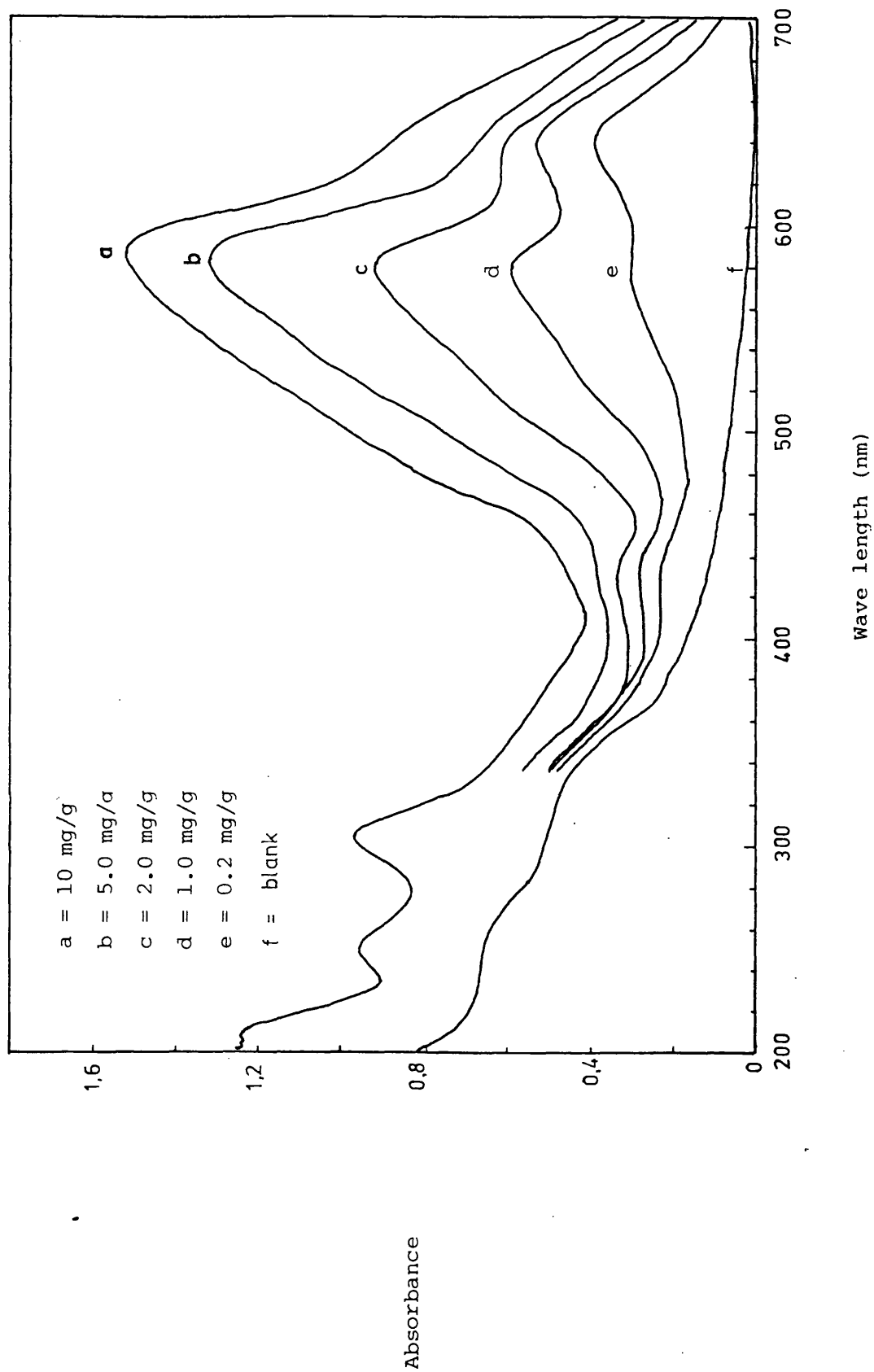


FIGURE (3—74). The Absorbance of Crystal Violet and Crystal Violet Lactone on Kaolinite

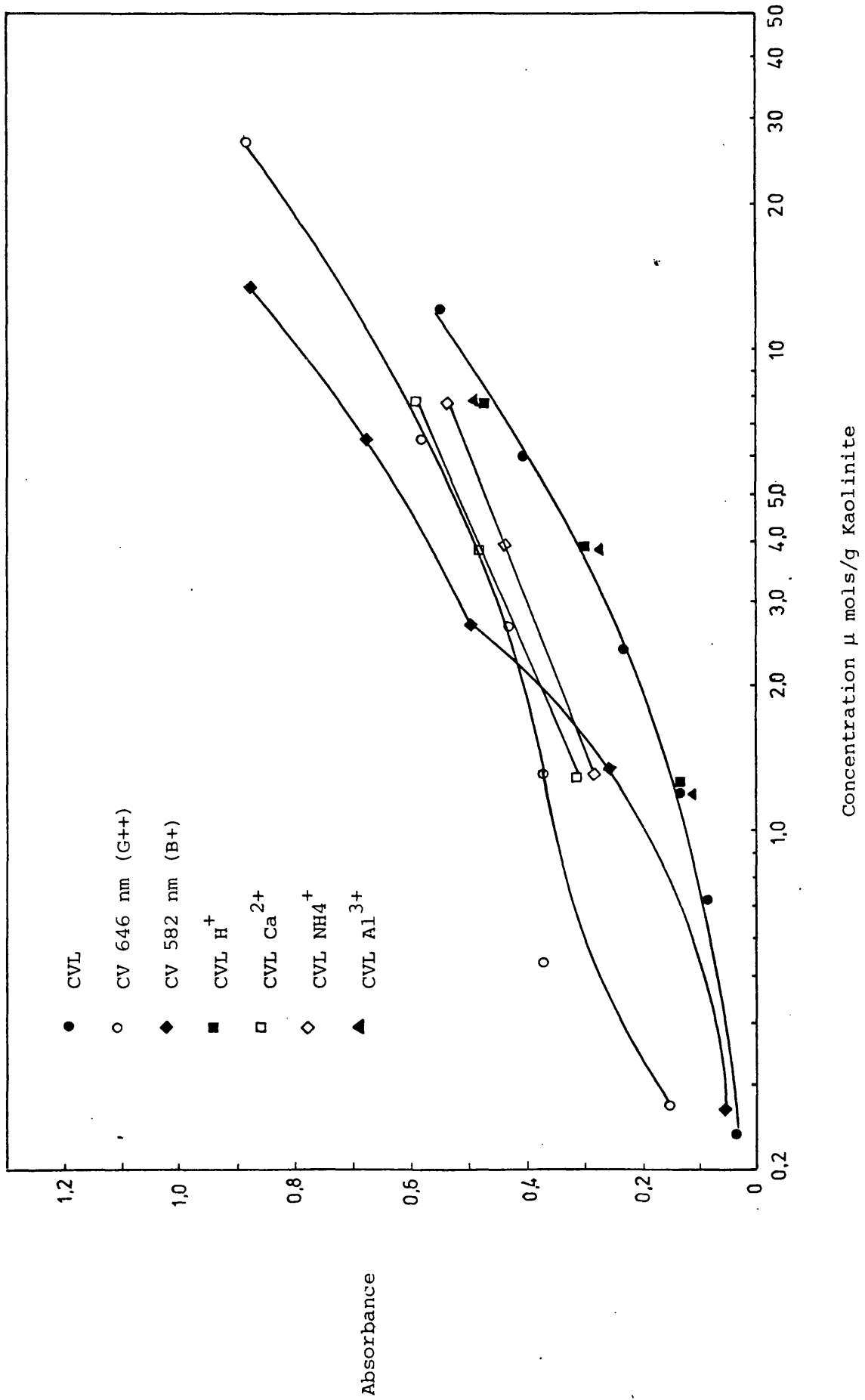


FIGURE (3-75). The Diffuse Reflectance Spectra of Crystal Violet Lactone on Kaolinite, at 100% RH as a function of time, without irradiation (2.5 mg CVL/g Kaolinite)

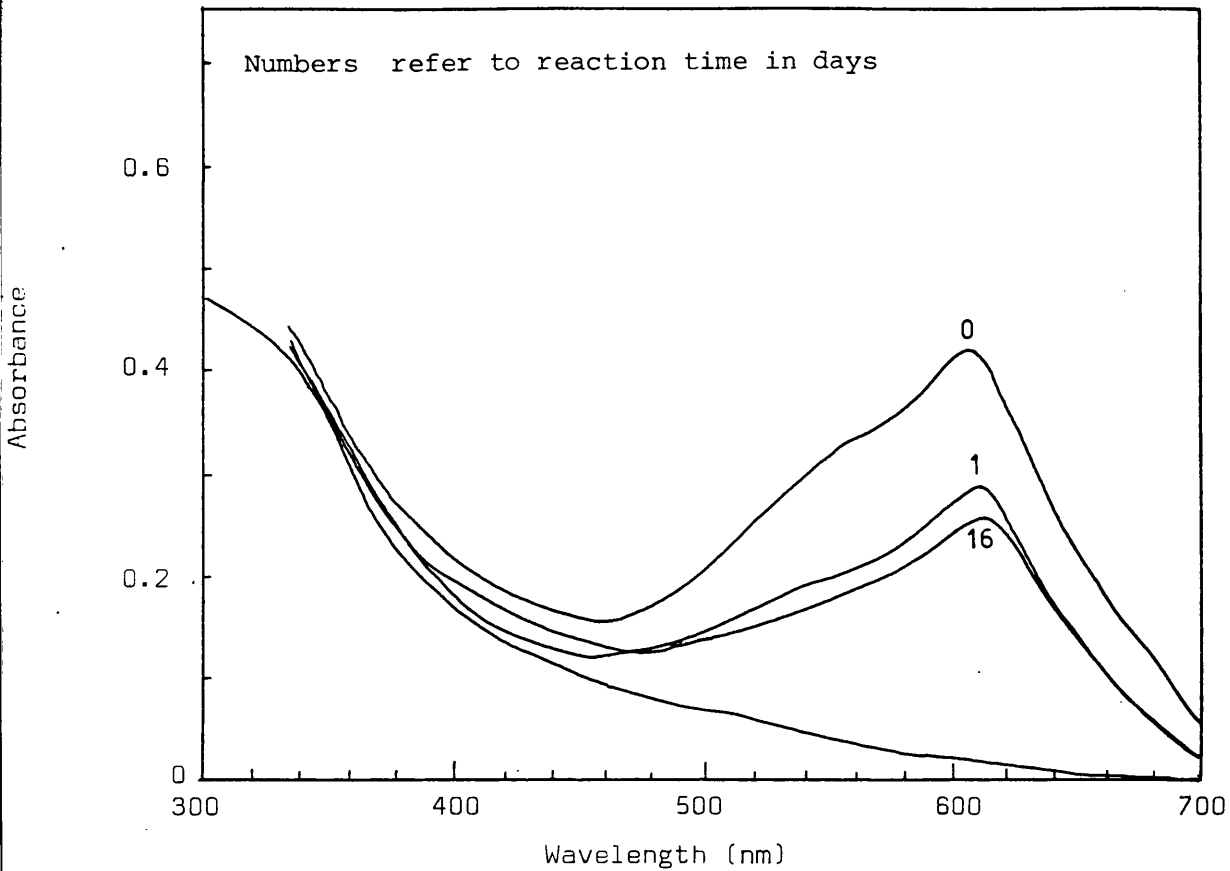


FIGURE (3-76). The D.R.S. of CVL on Kaolinite, at 100% RH as a function of time, with irradiation, (2.5 mg CVL/g Kaolinite)

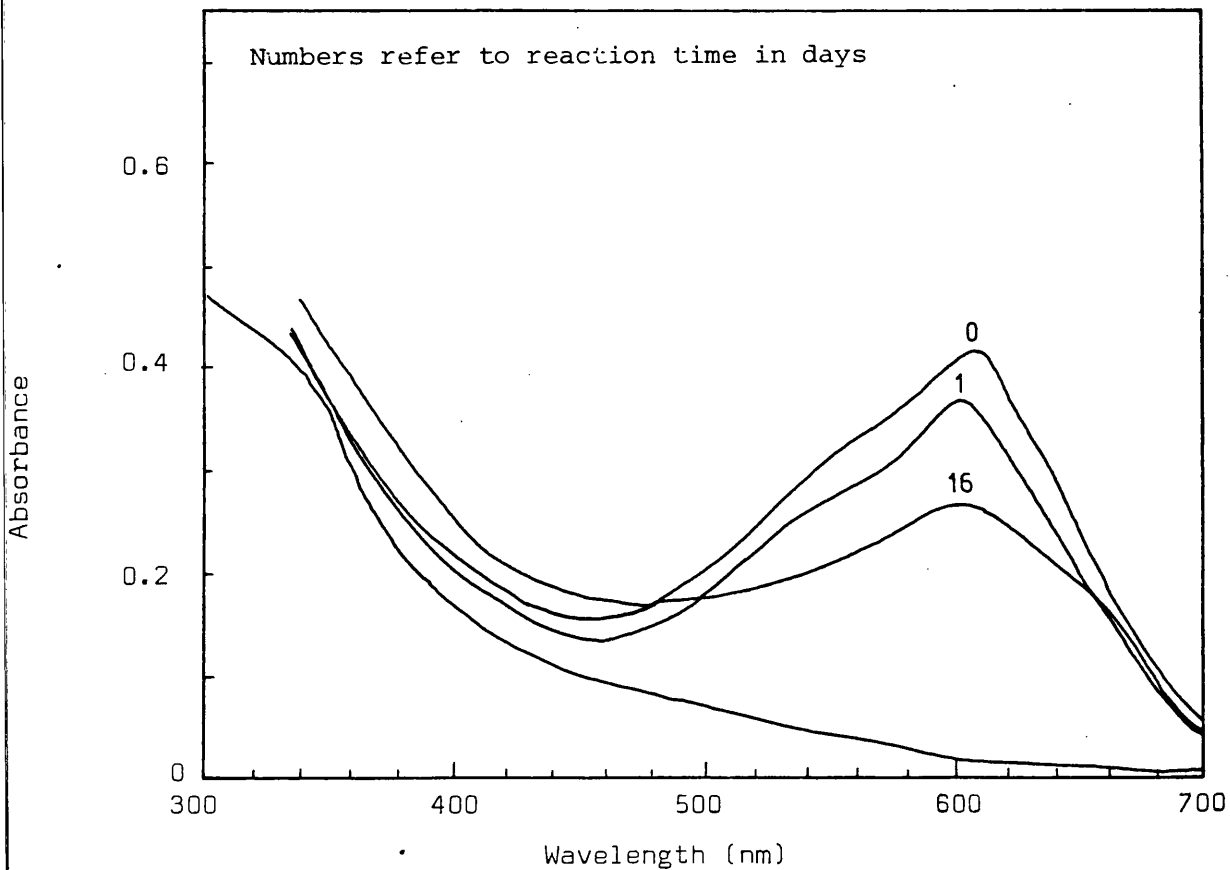


FIGURE (3-77). The D.R.S. of CVL on Kaolinite at 62.5% RH as a function of time, without irradiation, (2.5 mg/g Kaolinite)

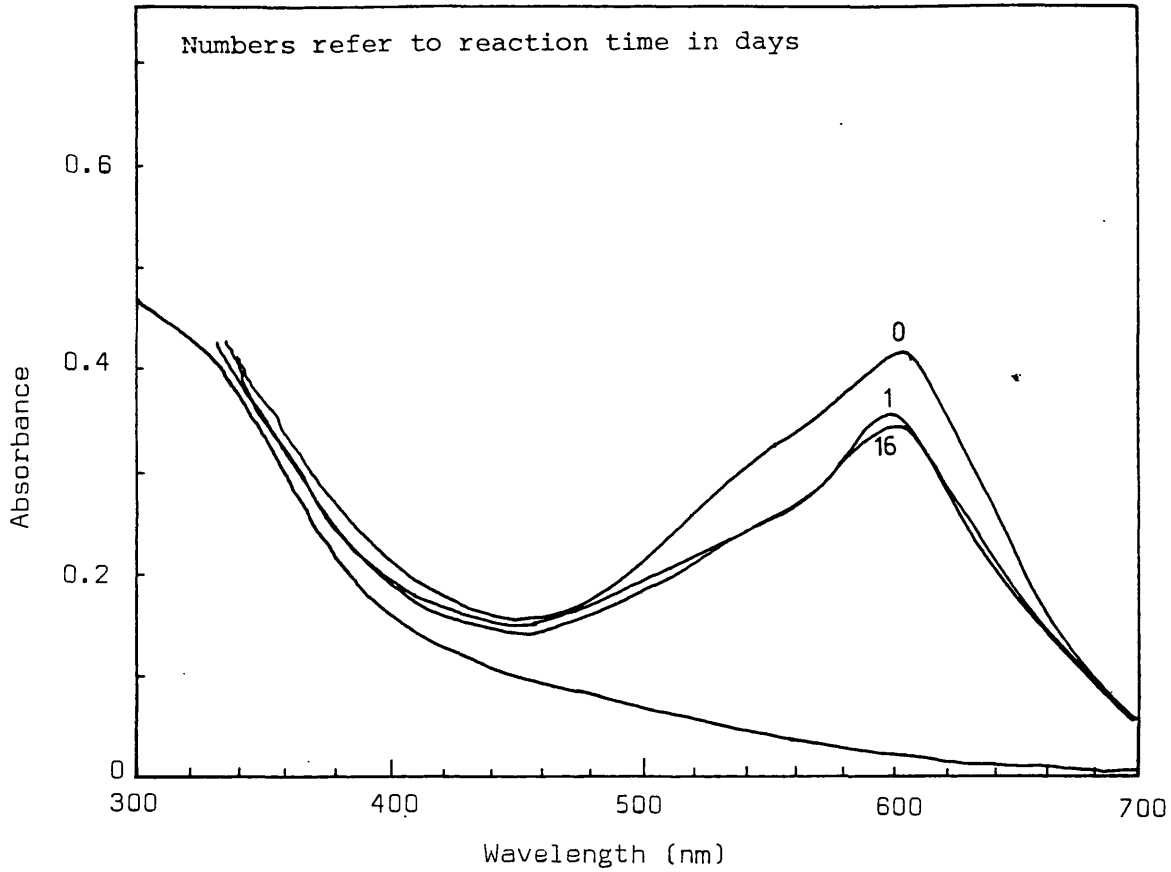


FIGURE (3-78). The D.R.S. of CVL on Kaolinite at 62.5% RH as a function of time, with irradiation, (2.5 mg/g Kaolinite)

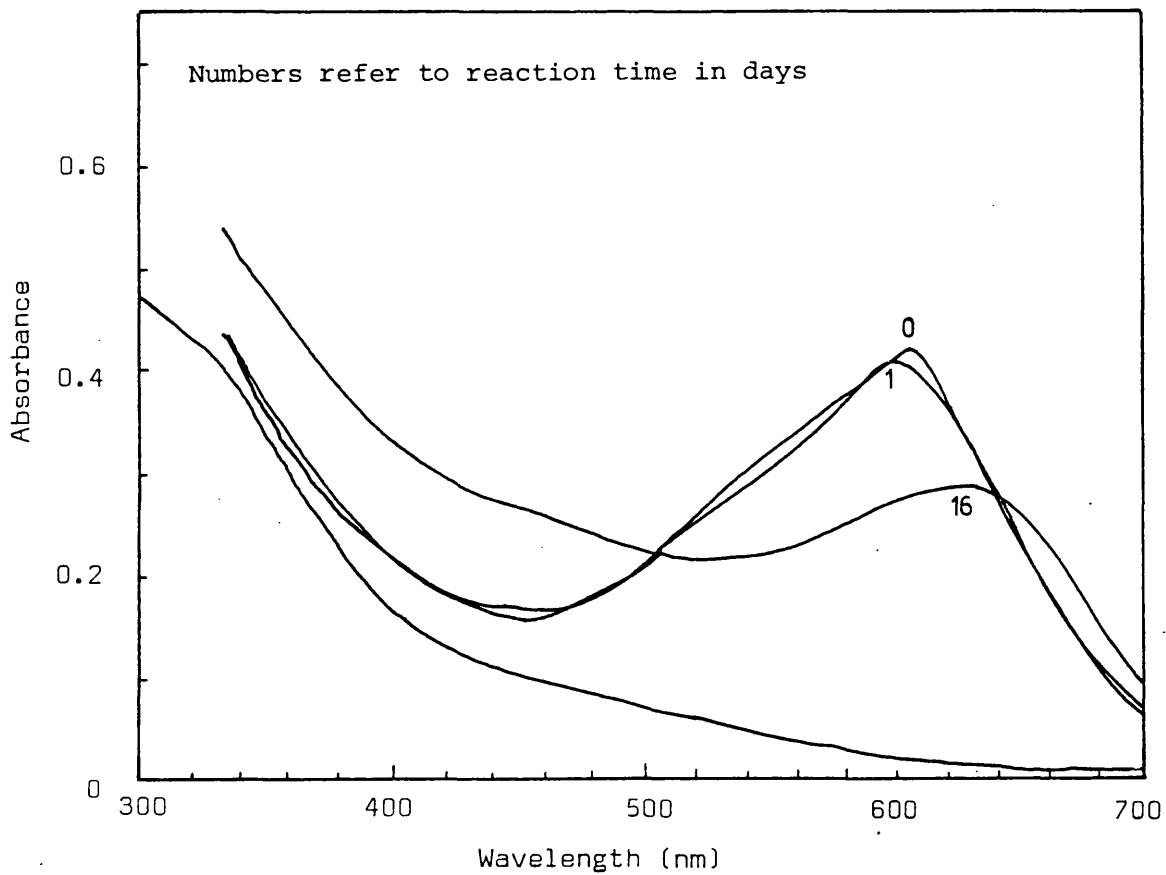


FIGURE (3-79). The D.R.S. of CVL on Kaolinite at 0% RH as a function of time, without irradiation, (2.5 mg/g Kaolinite)

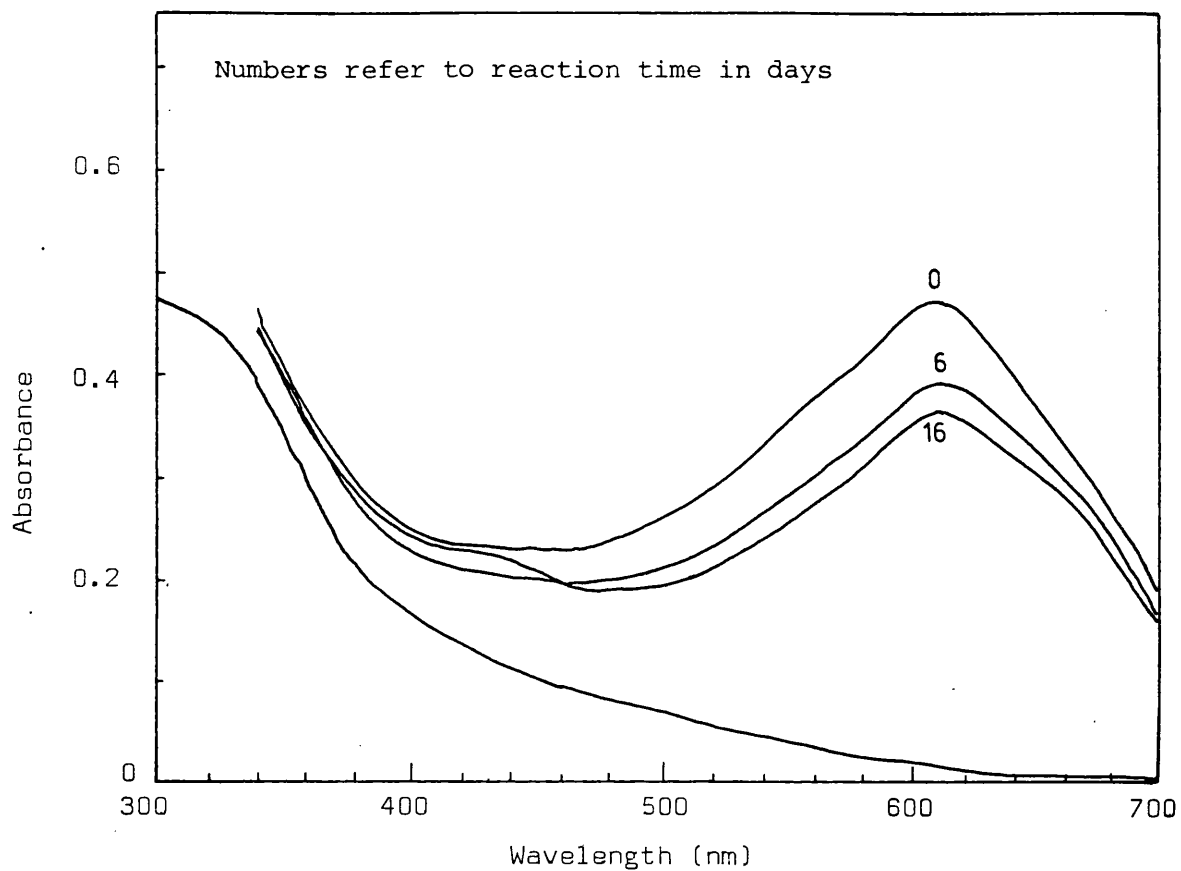


FIGURE (3-80). The D.R.S. of CVL on Kaolinite at 0% RH as a function of time, with irradiation, (2.5 mg/g Kaolinite)

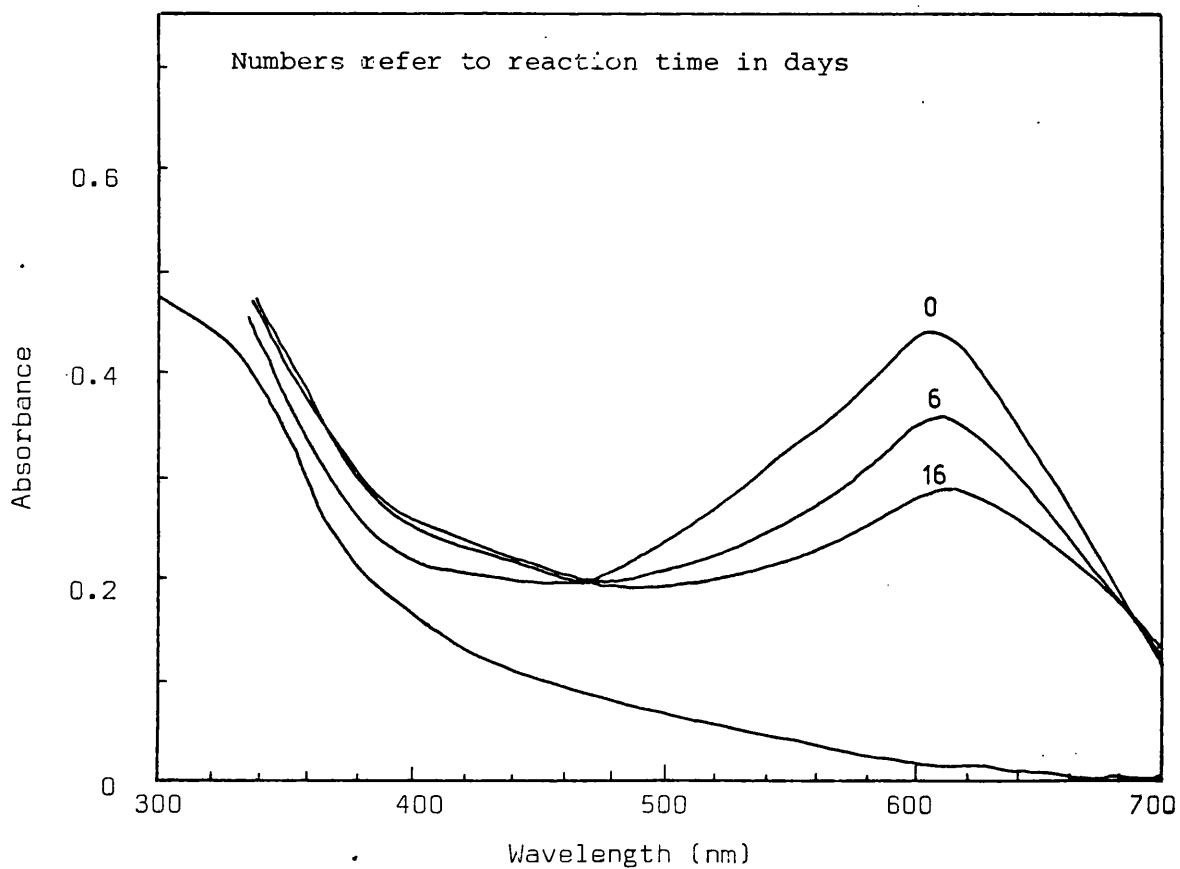


FIGURE (3-81) 100% Relative Humidity  
(Solid symbols refer to non-irradiated samples)

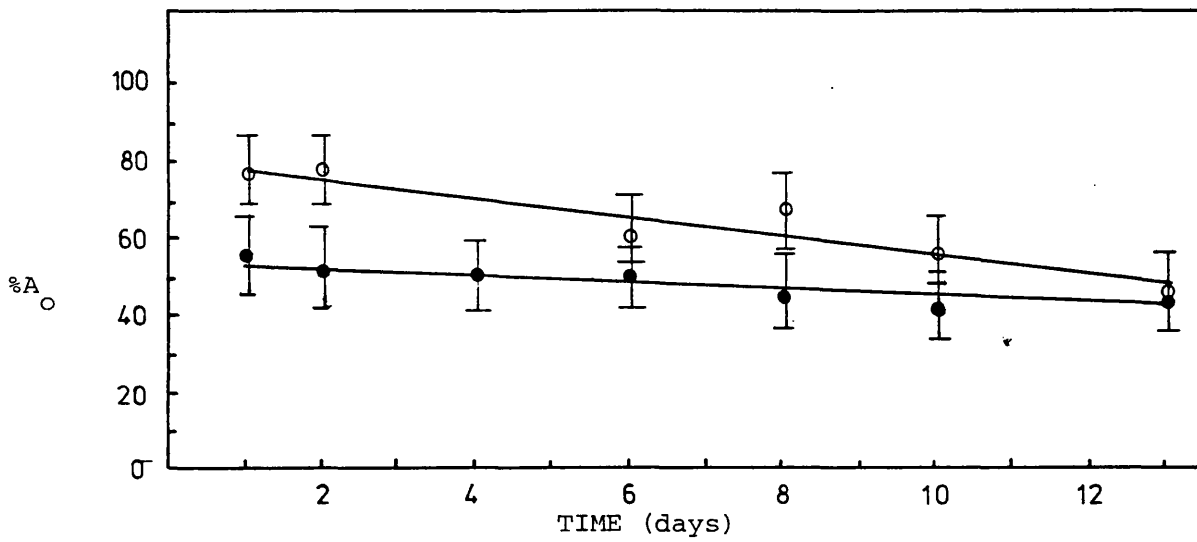


FIGURE (3-82) 62.5% Relative Humidity  
(Solid symbols refer to non-irradiated samples)

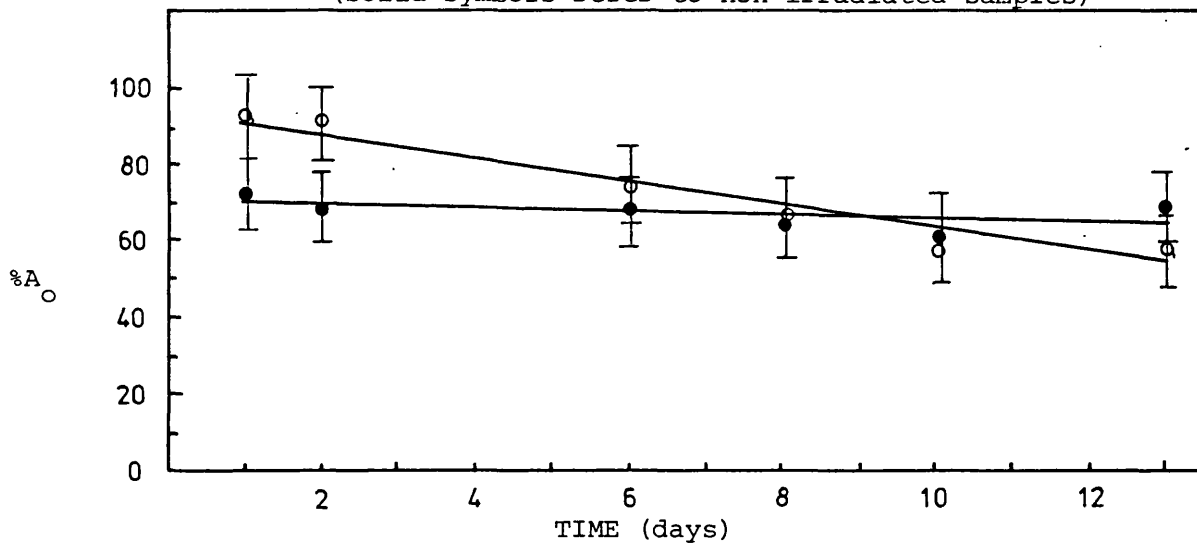
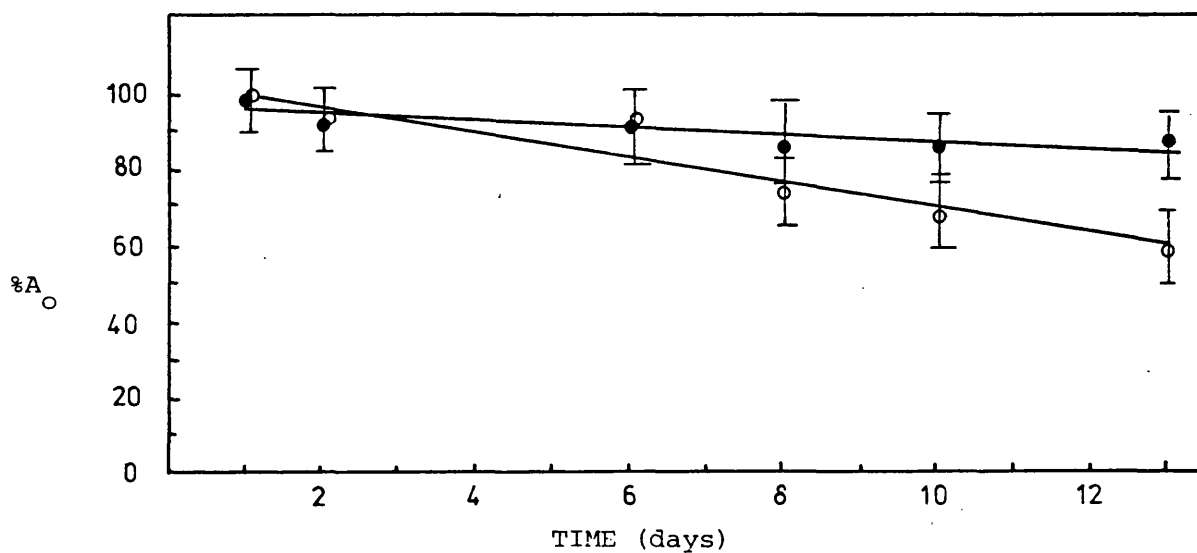


FIGURE (3-83) 0% Relative Humidity  
(Solid symbols refer to non-irradiated samples)





The Position of  $\lambda$  max of Crystal Violet Lactone, on Kaolinite, as a function of time.

FIGURE (3-84) Non-irradiated sample

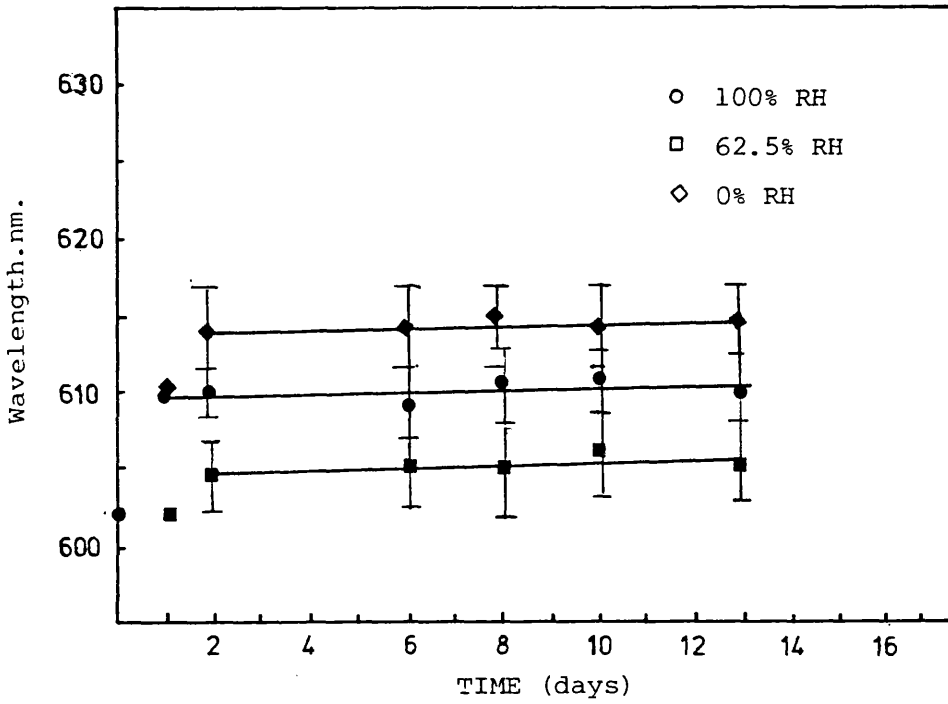
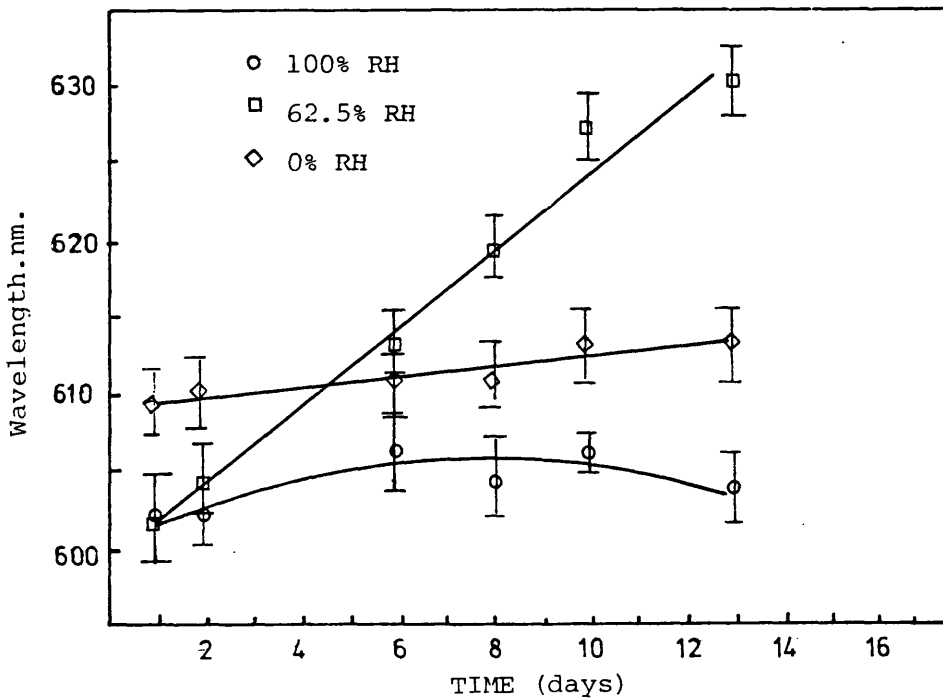


FIGURE (3-85) Irradiated sample



(ii) The Effect of Counterions upon the Fading of CVL  
Adsorbed upon Kaolinite

Al<sup>3+</sup> as Counterion

CVL adsorbed upon Al<sup>3+</sup> - kaolinite was in the blue and green, mono and dicationic forms. The absorbance of the irradiated and non-irradiated samples decreased to 70 and 60% A<sub>0</sub> respectively after 14 days, Figure (3-86). In the dark the λ max remained constant at 602nm, whereas the irradiated sample showed a 40nm bathochromic shift, Figure (3-88). The absorbance of the irradiated sample probably remained higher than the sample in the dark because the surface temperature was probably higher for the irradiated sample. This reduced the amount of water on the surface and this could cause a bathochromic shift.

Ca<sup>2+</sup> as Counterion

CVL was adsorbed upon Ca<sup>2+</sup> - kaolinite as the blue monocation. The absorbance of the irradiated and non-irradiated samples, with time are shown in Figure (3-86). Both samples behaved similarly, but the dark had a higher absorbance. A small bathochromic shift was seen for both samples, Figure (3-88).

H<sup>+</sup> as Counterion

The behaviour of CVL upon H<sup>+</sup> - kaolinite, Figure (3-87) and (3-89), was similar in intensity and position to λ max, for both irradiated and non-irradiated samples, to CVL upon Al<sup>3+</sup> - kaolinite.

The Effect of Counterions on the Percentage of Zerotime absorbance of CVL on Kaolinite as a function of time (62.5% RH)

FIGURE (3-86).  $Al^{3+}$  and  $Ca^{2+}$  as Counterions  
(Solid symbols refer to non-irradiated samples)

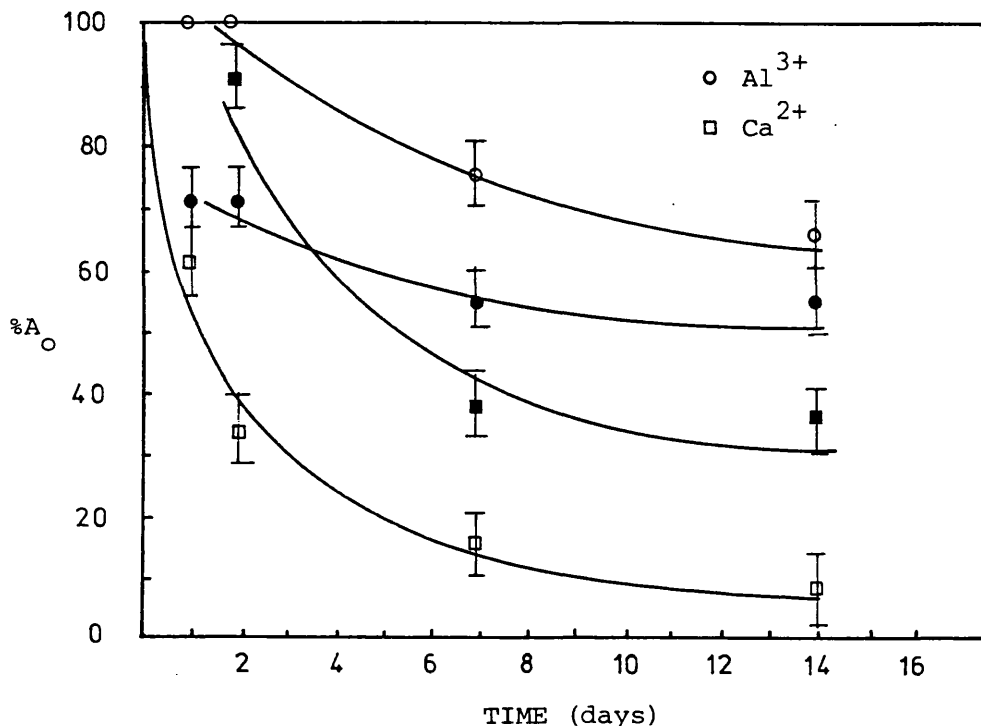
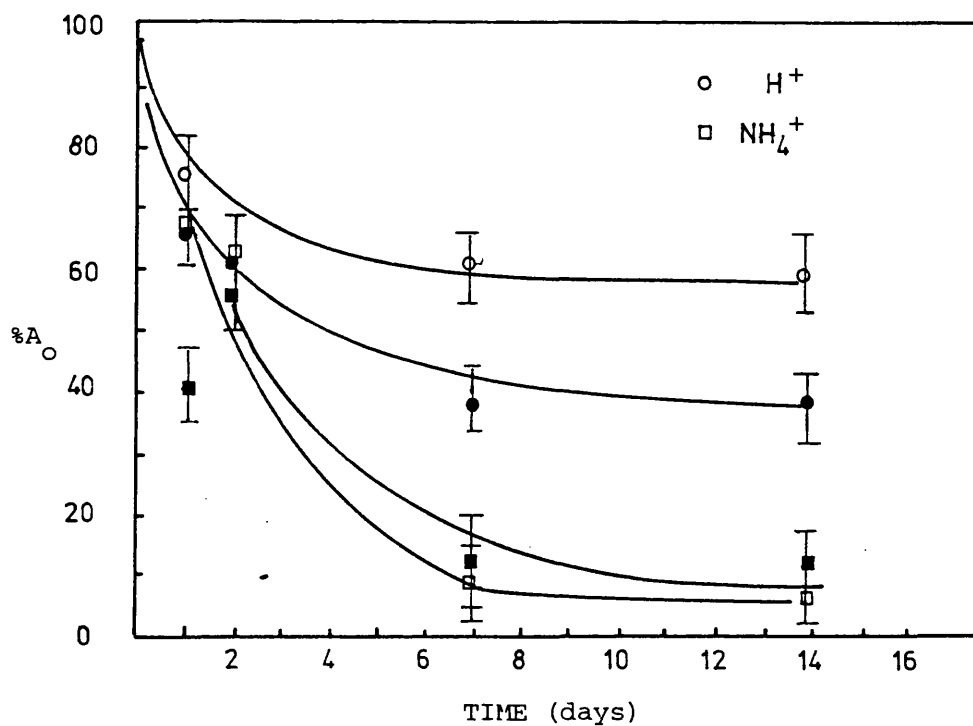


FIGURE (3-87).  $H^+$  and  $NH_4^+$  as Counterions  
(Solid symbols refer to non-irradiated samples)



The Effect of Counterions on the Position of  $\lambda$  max of CVL on Kaolinite as a function of time (62.5% RH)

FIGURE (3-88)  $Al^{3+}$  and  $Ca^{2+}$  ad Counterions  
(Solid symbols refer to non-irradiated samples)

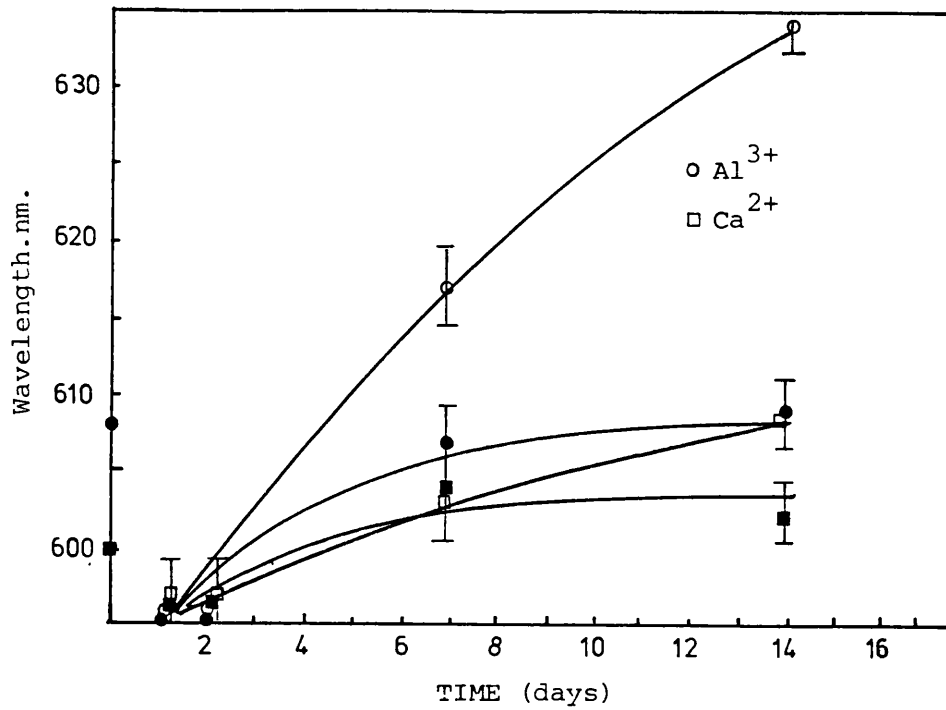
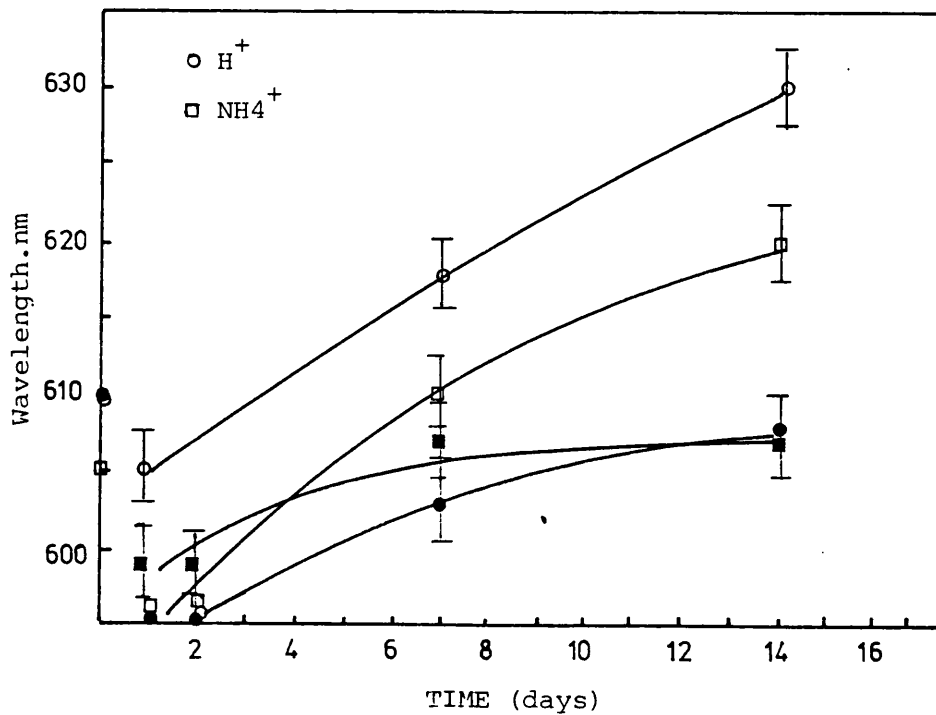


FIGURE (3-89)  $H^+$  and  $NH_4^+$  as Counterions  
(Solid symbols refer to non-irradiated samples)



NH<sub>4</sub><sup>+</sup> as Counterion

CVL adsorbed upon NH<sub>4</sub><sup>+</sup> - Kaolinite was in the blue cationic form. Both irradiated and non-irradiated samples behaved similarly, Figure (3-87). They decreased to 10% A<sub>0</sub> after 7 days remaining constant thereafter. The λ max of the irradiated sample shows a 15nm bathochromic shift compared to a 3nm bathochromic shift for the dark sample, Figure (3-89).

Table (3-16) The Species of Crystal Violet Lactone Formed,  
on Clay Minerals and Oxides

Mineral	Al <sup>3+</sup>	H <sup>+</sup>	No Treatment	Ca <sup>2+</sup>	NH <sub>4</sub> <sup>+</sup>
Silton	G <sup>++</sup>	G <sup>++</sup>	G <sup>++</sup>	G <sup>++</sup> /B <sup>+</sup>	B <sup>+</sup>
Kaolinite	G <sup>++</sup> /B <sup>+</sup>	G <sup>++</sup> /B <sup>+</sup>	G <sup>++</sup> /B <sup>+</sup>	B <sup>+</sup>	B <sup>+</sup>
Bentonite	G <sup>++</sup>	B <sup>+</sup>	B <sup>+</sup>	B <sup>+</sup>	B <sup>+</sup>
Silica	B <sup>+</sup>	B <sup>+</sup>	B <sup>+</sup>	B <sup>+</sup>	B <sup>+</sup>

The behaviour of crystal violet lactone upon clay mineral and oxides is summarized in Tables (3-16 to 3-18). Table (3-16) shows the status of the adsorbed crystal violet lactone. It will be seen that the acid strength of the surfaces decreased as you look down the table, and the order is Siltan > kaolinite > bentonite > silica, for the untreated minerals. Treatment of the minerals also causes changes in the acidity of the surfaces. Treatment with either  $Al^{3+}$  or  $H^+$  causes no change in the status of the adsorbed dye, except for  $Al^{3+}$  treatment of bentonite, which causes an increase in acidity of the surface as shown by the change from  $B^+$  to  $G^{++}$  of the adsorbed CVL. While treatment of either  $Ca^{2+}$  or  $NH_4^+$  reduces the acidity of the surfaces. Table (3-17) shows that at high 100%RH the predominant cause of reduction in intensity, is via the displacement of CVL by water from surface and/or hydration of CVL. Only Siltan maintains a high intensity at this relative humidity. At 0% RH the intensity is reduced on all surfaces except bentonite. Bentonite was the most affected by changes in RH because it is an expanding type mineral. After 14 days exposure to light all the irradiated samples were of lower intensity than the non-irradiated samples. It is a characteristic of the photodegradative processes to be relatively slow, 1 to 14 days. Whereas hydration processes are comparatively fast, less than 24hrs. At 62.5% RH only bentonite showed large changes in intensity due to hydration. Silica and kaolinite showed signs of photodegradation over the 14 day period, whereas Siltan showed none. Treatment with  $Al^{3+}$  caused bentonite to be more resistant to hydration, as is expected because the interactions between CVL and the clay are Coulombic. Treatment of Siltan, and kaolinite with  $NH_4^+$  caused a reduction in the intensity after 24hrs showing that the CVL-clay interactions had been reduced, hence the CVL was more easily displaced from the surface after treatment. Table (3-18) summarises the spectral changes observed for CVL on the minerals.

Table (3-17) A Summary of the Intensity of Crystal Violet Lactone  
upon Clay Minerals and Oxide

Mineral	% RH	Irradi- ation	% A <sub>o</sub> after t days		Al <sup>3+</sup>		Ca <sup>2+</sup>		H <sup>+</sup>		NH <sub>4</sub> <sup>+</sup>	
			A <sub>o</sub> (1)	A <sub>o</sub> (14)	1	14	1	14	1	14	1	14
S I L I C A	100	NO	10	10								
		YES	10	10								
	62.5	NO	85	80	75	20	70	45	85	75	95	80
		YES	85	10	75	20	30	4	80	10	70	10
	0	NO	40	40								
		YES	30	5								
S I L T O N	100	NO	50 (85)*	50 (85)*								
		YES	50 (95)*	50 (95)*								
	62.5	NO	95	80	70	90	80	90	65	65	40	50
		YES	95	100	100	100	80	60	70	70	50	55
	0	NO	80	50								
		YES	80	40								
B E N T O N I T E	100	NO	35	35								
		YES	20	15								
	62.5	NO	40	40	75	80	30	20	30	25	40	30
		YES	40	30	80	85	20	15	20	10	20	10
	0	NO	200	220								
		YES	200	75								
K A O L I N I T E	100	NO	55	40								
		YES	75	40								
	62.5	NO	70	70	70	55	90	40	65	40	50	10
		YES	92	50	100	70	60	10	75	60	60	10
	0	NO	100	85								
		YES	100	60								

\* Refers to B<sup>+</sup> measured at 614nm





### 3.4 Conclusions

A methanolic solution of crystal violet will decompose when irradiated by day light. The products of the photodecomposition are pararoseaniline, and the demethylated derivatives of crystal violet with 3,2 and 1 terminal methyl groups. Crystal violet lactone decomposes in ethanolic solution, with irradiation to yield crystal violet, pararoseaniline and demethylated derivatives of crystal violet with 5,4,3,2 and 1 terminal methyl groups.

Crystal violet lactone undergoes lactone ring cleavage when adsorbed upon clay minerals and oxides, to form the coloured zwitterion. This process is reversible, and the coloured zwitterion can be displaced from the surface by water vapour. The species of zwitterion formed, blue or green depends upon the nature of the mineral on which the CVL is adsorbed, and/or the nature of the counterion on the mineral surface. The surface acidity of the clay minerals and oxides used were in the order : Siltan > kaolinite > bentonite > silica, as judged by the species of zwitterion formed.

The loss in intensity of the adsorbed zwitterion can either be a reversible or an irreversible process. The irreversible process being due to photodecomposition, and the reversible process, as mentioned above, is due to displacement of the zwitterion from the mineral surface by water vapour. The minerals with the strongest surface acidity, e.g. Siltan, are the least affected by displacement of the zwitterion by water vapour. The Coulombic attractions between the carboxyl group on the zwitterion, and the positive charge on the surface counterion being greatest for these minerals, and the minerals with the weakest surface acidity, e.g. silica, are the minerals

where the zwitterion is readily displaced. Exchanging the counterion on the mineral surface can also affect the stability of the zwitterion.  $\text{Al}^{3+}$  treatment caused a slight increase in surface acidity and hence reduced the displacement of the zwitterion by water.

The products of the photodegradation of CVL on silica are the same as those for the photodegradation in ethanolic solution. Also 4-dimethylaminobenzophenone was identified. The extent of photodegradation was greatest on silica.

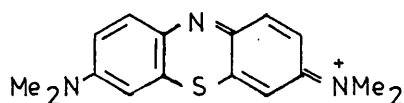
CHAPTER 4

REACTION OF METHYLENE BLUE, AND BENZOYL  
LEUCO METHYLENE BLUE ON CLAY MINERALS  
AND OXIDES

Reactions of Methylene Blue, and Benzoyl leuco Methylene Blue  
on Clay Minerals and Oxide Surfaces

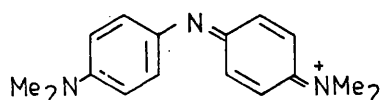
4.1 Introduction

Methylene blue and benzoyl leuco methylene blue are cyanine-type chromogens. In this respect they are related to crystal violet. Methylene blue is a hetero-cyclic analogue of the diarylmethane dyes. Methylene blue, (MB), (1), can be regarded as being formed by bridging the 2-2' positions of the diarylmethane dye, Bindschedler's Green (2), with a sulphur atom.



(1)

Methylene Blue



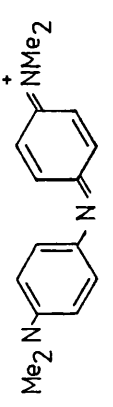
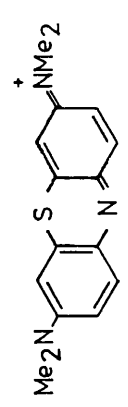
(2)

Bindschedler's Green

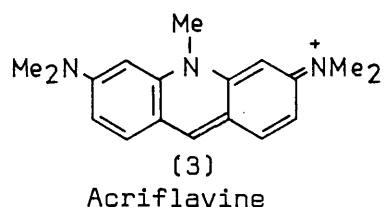
The bridging sulphur atom can be regarded as a mesomeric electron donating group attached simultaneously to two unstarred positions of a diarylmethane dye.

Perturbational theory predicts a large hypsochromic shift of the visible band due to the heteroatom and this is observed, (see Table (4-1)).

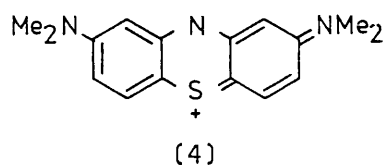
Table (4-1) The Hypsochromic Shift Produced by the Introduction of a Sulphur Atom into a Diarylmethane Dye Structure

Structure	Common Name	$\lambda$ max (nm)	Solvent	Reference
	Bindschedler Green	725	H <sub>2</sub> O	Lewis, G.N., and Bigeleisen, J., (1943)
	Methylene Blue	665	H <sub>2</sub> O	"

Therefore all heterocyclic analogues of diarylmethane dyes absorb at shorter wavelengths than does the parent dye. The more electron donating the heteroatom of the bridging group the larger the shift, with the exception of the sulphur atom, which exerts the smallest shift. Thus the hypsochromic shift produced by the bridging heteroatom is in the series  $-NR \rangle -NH \rangle O \rangle S$ . Hence dyes with sulphur as the bridging atom, such as methylene blue, will generally be deeper in colour than those with  $-NR$  as the bridging group, the latter will be yellow. An example is acriflavine (3),

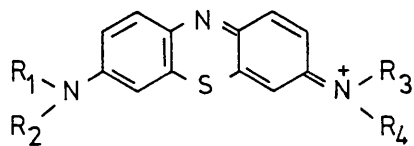


The methylene blue cation (1) can be represented by an alternative resonance structure (4), in which the positive charge is localised on the bridging heteroatom.



This shows that the heteroatom is involved in the electron system of the chromogen. However they are best treated as perturbed odd alternants where the positive charge is largely associated with the terminal amino groups.

The group of dyes with cyanine type chromogens which have similar structural characteristics to methylene blue, can be further classified as the thiazine group of dyes. They have the general formula (5)



(5)

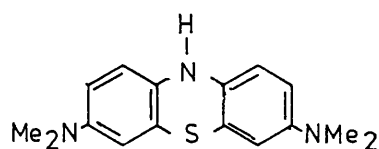
Where:-

	MB	Azure B	Symdi-methyl-thionine	Azure A	Azure C	Thionine
R <sub>1</sub>	Me	Me	Me	Me	Me	H
R <sub>2</sub>	Me	Me	H	Me	H	H
R <sub>3</sub>	Me	Me	Me	H	H	H
R <sub>4</sub>	Me	H	H	H	H	H

The standard redox potentials for the thiazine dyes are about +0.5 volts, with respect to the hydrogen electrode, Meyer, H.W. and Treadwell, W.D. (1953).

4.1.2. Photochemistry of Methylene Blue

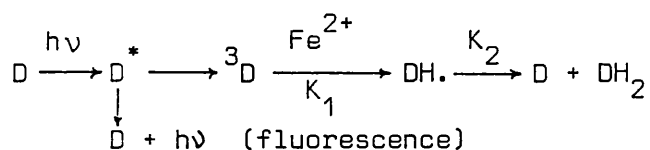
When methylene blue is dissolved in dilute  $H_2SO_4$ , in the absence of oxygen, the colour is bleached on exposure to light, and the colourless leuco form is produced (6).



(6)

Leucomethylene Blue

In flash photolysis experiments, when orange-red light is used to irradiate samples of methylene blue, the spectrum shows a new band with a mean lifetime of less than 30  $\mu$ secs. This is assumed to be the triplet state formed from the singlet excited molecule initially produced by the flash; Parker, C.A. (1958)a, Parker, C.A., (1958)b; Parker, C.A. (1959); Hatchard, C.G. and Parker, C.A. (1961). The photo chemical reactions of methylene blue and the thiazine dyes are similar, and the group of dyes can therefore be designated D. In the presence of ferrous sulphate this spectrum is no longer observed, but that of the free radical DH., analogous to the semiquinone free radical is seen. This has a much longer lifetime than the triplet state. It is not formed from the singlet excited state for its concentration is not correlated with the quenching of fluorescence by  $Fe^{2+}$ , but presumably it is formed from the triplet state, Caldin E.F., (1964).





Where:-  
 D = ground state  
 D\* = excited state  
 $^3D$  = triplet state  
 DH. = semi-quinone 'type' radical  
 DH<sub>2</sub> = leuco form

The semiquinone free radical's disappearance, which has been studied by following the adsorption at various wavelengths in the presence of various concentrations of Fe<sup>2+</sup>, was attributed to the disproportionation into the original dyestuff, D, and the leuco form DH<sub>2</sub>.

The rate constants have been determined for thionine, Hatchard C.G., and Parker, C.A., (1961), for the quenching of the triplet state by Fe<sup>2+</sup>,  $K_1 = 3 \times 10^7 \text{ l mol}^{-1} \text{ sec}^{-1}$ , and for the dismutation,  $K_2 = 2.4 \times 10^9 \text{ l mol}^{-1} \text{ sec}^{-1}$

Quenching of the triplet state by Fe<sup>3+</sup> has a rate constant of  $3 \times 10^7 \text{ l mol}^{-1} \text{ sec}^{-1}$ . The rate constants for the oxidation by Fe<sup>3+</sup>, of the semiquinone, and the leuco form, which are responsible for the reversal of bleaching in the dark, are  $7.9 \times 10^4$  and  $2.6 \times 10^2 \text{ l mol}^{-1} \text{ sec}^{-1}$  respectively.

According to other workers, Koizumi, M., and Usin, Y., (1972), the primary photochemical process at concentrations of  $< 10^{-5} \text{ M}$  methylene blue in water and ethanol are the interactions of the triplet dye  $^3D$  and oxidising or reducing agents; the dye-oxidizing agent (D-O) and dye-reducing agent (D-R) mechanisms. At higher dye concentrations the reaction proceeds by the interaction of the triplet and ground state dye; the dye-dye (D-D) mechanism.

There is also evidence for the formation of molecular complexes of the ion pair type, such as  $D^+$ ,  $O_2^-$  and  $D^+$ ,  $D^-$ . The oxidation and the reduction reactions occur via different pathways, and the oxidation reverse of bleaching occurs via oxygen, through the  $D^+$   $O_2^-$  pathway.

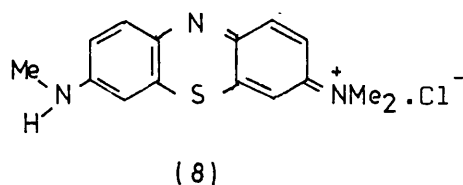
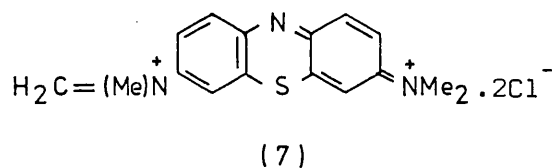
Thiazine dyes, in the presence of polymethyl-acrylic acid or polyacrylic acid, undergo a spectral shift when irradiated with visible light, Wotherspoon, N., and Oster, G., (1957). Two photo-products were formed, one in the absence of oxygen and the second by the photochemical oxidation of the first. The rate of formation of the second was retarded by small amounts of paraphenylene-diamine, or by KI, suggesting that long lived excited states are involved. The final photo product was the same for all thiazine dyes and was identical to thionine. The reaction requires a polyacrylic acid but does not take place in the presence of other high polymeric acids. It is known that methylene blue may be demethylated by non-photochemical oxidation in alkali, to give dyes with fewer methyl substituents, Conn. H.J., (1946). The highly specific nature of the polymer required for the reaction implies that the polyacrylic acids serve as substrates for a special type of dye binding. In the dye-polymer complex the transition from the ground state to the first excited state did not drastically differ from the free dye since the absorption spectra were similar. But transitions from the first excited state to other excited states must be profoundly affected by complexation with specific polymers. The carboxyl groups or polyacrylic acids are particularly well suited to complexing with the thiazine dyes via their terminal amino groups. Other workers have reported photodegradation of methylene blue in various solvents, such as  $H_2O$ , MeOH, EtOH and propan-2-ol, Yoshida,

Z., and Kazama, K., (1956); Yoshida, A., and Kazama, K., (1957). They reported that methylene blue was not only demethylated by also N-C bond breaking occurred in the dimethylamino radical with the formation of a 2-mercapto-diphenylamine derivative. Breaking of the C-5 bond in the thiazine radical was also observed and this mechanism predominated in propan-2-ol. The existence of Azure A, AzureB and Azure C as breakdown products were all shown by paper chromatography. Atmospheric oxygen retarded the photodegradation of methylene blue considerably, probably owing to the high reactivity of free radicals with oxygen.

4.1.3. Reactions of Thiazine Dyes

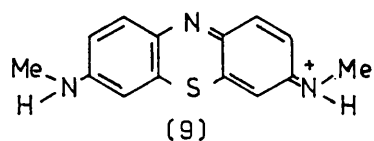
As mentioned above thiazine dyes are particularly sensitive to oxidative demethylation in alkali media; adsorbed onto specific polymers or on clay minerals. It has been shown by Schaefer, F.C., and Zimmermann, W.D., (1968), that methylene blue is oxidised in the dark when in organic solvents containing amines.

The mechanism was rationalised as base-catalysed self oxidation or disproportionation of methylene blue followed hydrolysis of the oxidised species, (7), to the demethylated dye Azure B, (8).



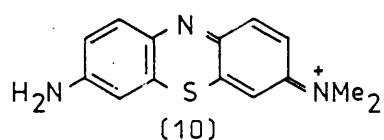
Azure B

It was found that for all the amines that were used, the reaction proceeded in a similar manner; firstly degradation of methylene blue, which takes place rapidly, followed by a slower demethylation of Azure B to form symmetrical-dimethylthionine (9)



Sym-dimethylthionine (SDMT)

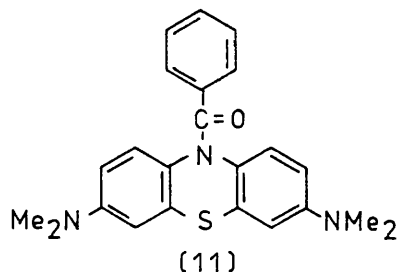
This type of demethylation is comparable with base-catalysed oxidation of methylene blue in aqueous solution at pH 11.0 which is a common mode of amine oxidation, Barnes, K.K., and Mann C.K., (1967); Smith P.A.S., and Loeppks, R.N., (1967); Bacon R.G.R., and Stewart D., (1966). The observed series of demethylation, methylene blue  $\rightarrow$  Azure B  $\rightarrow$  Sym-dimethylthionine. (Schaefer, F.C. and Zimmermann, W.D., 1968) contradicts previous evidence by Kehrmann, F., (1906), his work strongly supported the series methylene blue  $\rightarrow$  Azure B  $\rightarrow$  Azure A(10)



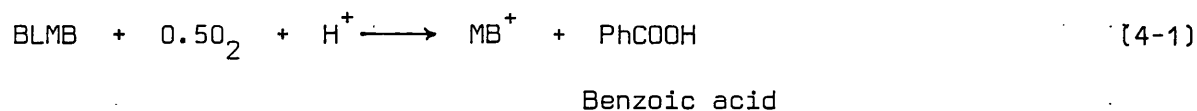
Azure A

4.1.4. Reactions of Benzoyl-leuco-Methylene Blue

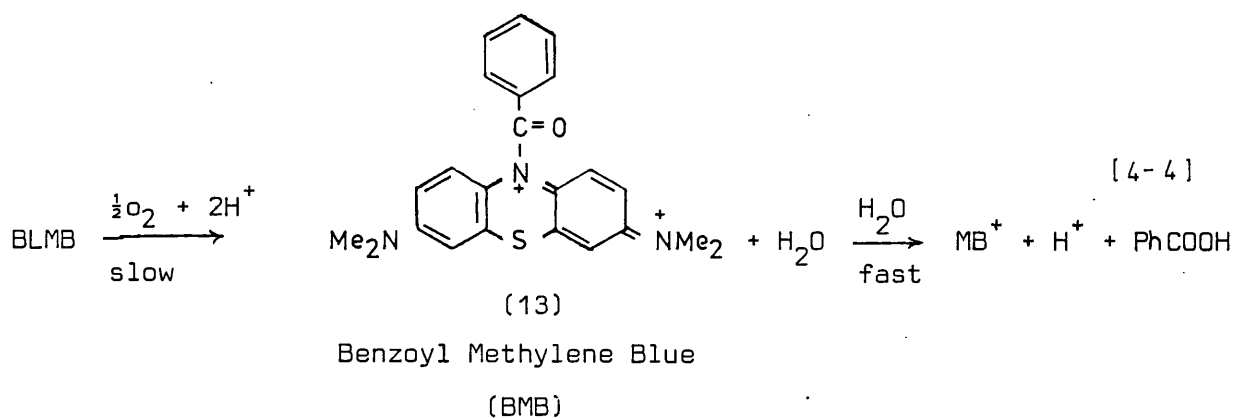
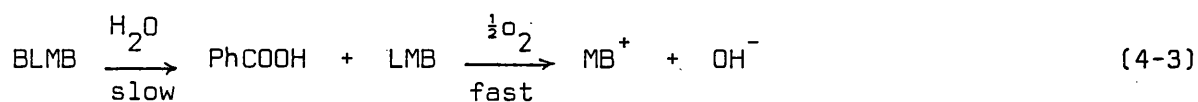
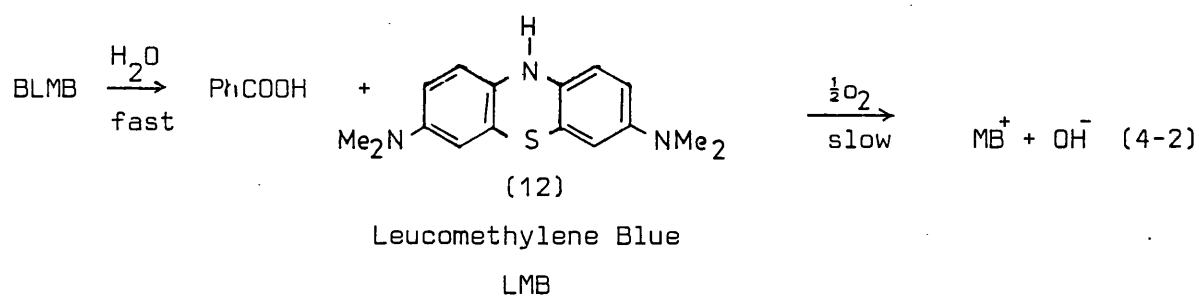
A colourless solution of Benzoyl leuco methylene blue, BLMB (11), in aqueous sulphuric acid turns blue on exposure to air.



Gensler, W.J., et al., (1966), have shown that the overall process can be summarised by reaction (4-1)



There are three possible sequences for the conversion of BLMB to methylene blue, these are shown as reactions (4-2), (4-3), and (4-4)



The results presented by Gensler W.J., et al (1966) were consistent with mechanism (4-3). The reaction was first order and the rate constant at 50°C was  $K_{50} = 3.0 \times 10^{-6} \text{ sec}^{-1}$ . The above workers also found that several oxidants other than oxygen, e.g. Ceric ion, lead dioxide, bromine or ferrous ion-hydrogen peroxide (Fenton's reagent) were also capable of converting BLMB to MB. But in all cases the rate of colour formation was faster than the hydrolysis of BLMB. It is therefore likely that these reagents can somehow attack BLMB directly without a preliminary hydrolysis step. One way in which this could be described would be via reaction (4-4). BLMB has been used as a reagent for the quantitative determination of organic peroxides, Eiss, M.I. and Giesecke, P., (1959). BLMB is also known to produce a blue colour when a solution in benzene is applied to silica gel or certain clay minerals, and exposed to light. The coloured product has been identified as methylene blue, Potts, H.A., et al., (1972). A simple hydrolysis step followed by an oxidation of leucomethylene blue to give a coloured product is not a tenable theory, as neither of the steps require light. Also the rate of colour formation was greater than the rate of hydrolysis of BLMB. It was suggested by Potts, H.A., et al., (1972) that a photoinduced free radical mechanism was operative. This was supported by the fact that Fenton's reagent, (ferrous sulphate and 5% hydrogen peroxide), a known free-radical source, caused immediate colouration of a BLMB solution. It was therefore likely that a direct attack by these reagents upon BLMB was the mechanism of the reaction. A possible reaction scheme is equation (4-4).

Potts, H.A. et al., (1972) have also shown that the methylene blue produced was subsequently demethylated and that all the demethylated species including thionine were present.

#### 4.1.5. Uses of Thiazine Dyes and their Derivatives

Thiazine dyes including methylene blue have for many years been used as biological stains as well as textile dyes. Their use as biological stains has produced much work on identification and purification of the thiazine group. The need to do so was caused by dyes such as Azure A, having differing staining properties from batch to batch. It was found that most of the commercial thiazine dyes were mixtures of the whole thiazine group of dyes, and such mixtures were referred to as, metachromic methylene blue. This was not a surprising fact since the thiazine dyes with fewer methyl groups than methylene blue are generally prepared by the oxidation of methylene blue in alkali media. The products are then crudely separated. Also insufficient care when using thiazine dyes, can result in demethylation. For instance if a solution of MB is exposed to light for a short period of time, 2-4hrs, the resulting solution will contain Azure A;B; C and thionine. Therefore in order to rationalise staining procedures many workers attempted to produce a rapid way of separating the thiazine dyes, Stotz, E., et al., (1950); Ball, J., and Jackson, D.S. (1953); Loach, K.W., (1971); Lohr, W., et al., (1974); Lohr, W., et al., (1975); Marshall, P.N., and Lewis, S.M. (1974)a; Marshall, P.N. and Lewis, S.M., (1974)b; Marshall, P.N., et al., (1975); Marshall, P.N., and Lewis, S.M., (1975).

All the solvent systems used by the above workers were tried in the course of this work, but the solvent system used by Marshall, P.N., and Lewis, S.M., (1974)a gave exceptionally good resolution, definition and speed, particularly when using a radially developed chromatogram.



As previously stated, page 195 Chapter 4, BLMB has been used as a reagent for the quantitative determination of organic per-oxides. The ability to produce a blue colour when reacted on oxides, or clay minerals has been utilized in the carbon-less copying process. In this process the underside of the top sheet has BLMB or a similar MB derivative encapsulated in gelatin or synthetic polymer. The upper surface of the next sheet has a clay mineral coating. When pressure is applied on the top sheet, i.e. when writing, the capsules are ruptured and the BLMB is released., this slowly reacts (1-4 weeks), with the clay mineral surface to produce a lasting copy. c.f. page 82 Chapter 3.

## 4.2 Experimental

### 4.2.1. Materials

(i) The silica gel used, silica gel G (type 60) acc to Stahl, was obtained from E. Merck, Darmstadt, Germany. The silica as characterised by the manufacturer, also contained:-

Gypsum, 13%; Iron (fe), 0.02% and Chloride, 0.02%.

The physical data for type 60 silica gel G, also supplied by the manufacturer, are:-

Pore volume (ml/g) = 0.75

Specific Area ( $m^2/g$ ) = 500

Mean Pore Diameter (A) = 60

pH of a 10% aqueous slurry = 7.0

The pore volume is determined using the Mottlam and Fisher Method; the specific surface area using the B.E.T.  $N_2$  adsorption method.

Silica gel GF 254 acc. to Stahl (type 60) for TLC has the same characteristics as silica gel G, but contains an insoluble inorganic fluorescent indicator which under short wave u/v light (254 nm) produces a uniform greenish fluorescence of the layer.

(ii) The Silton used was the same material as described on page 83 Chapter 3.

(iii) Water and other chemical reagents used were the same as those on page 84 Chapter 3.

(iv) The methylene blue, (3,7 dimethylamino-phenothiazonium salt), used was supplied by Hopkin and Williams ( $C_{16}H_{18}N_3Cl \cdot S \cdot 2H_2O$  m.wt = 355.89). The methylene blue chloride was twice recrystallized from distilled water and dried over  $P_2O_5$  at room temperature. Absorbance values were determined at the maximum, 668nm in 0.5 Molar  $H_2SO_4$ .

(v) The benzoyl leuco methylene blue (BLMB), 10 benzoyl, 3,7, bis(dimethylamino) phenothiazine used was a gift from English Clays, Lovering, Pochin and Co., Ltd. The pale green solid (BLMB) was warmed with c.a. 100mls redistilled acetonitrile. All subsequent steps were performed in a nitrogen atmosphere. Before filtration the mixture was decolourized with a small amount of attapulgitic clay. The filtrate was cooled and deposited faintly yellow crystals, which were collected and washed with cold acetonitrile.

The pale benzoyl leuco methylene blue was then dried in vacuo at  $80^{\circ}C$  over  $P_2O_5$ . This material in a sealed capillary, showed a melting point of  $194^{\circ}C$ . BLMB has a reported melting point of  $194-196^{\circ}C$ , Chalkley, L., (1925);  $185-187^{\circ}C$ , Moriga, H., and Oda, R., (1964). BLMB was also subjected to TLC, using silica gel GF 254 as adsorbent and cyclohexane-ethylacetate (3:2) as solvent system. Butan-1-ol :  $NH_4Cl$  2% aq : formic acid, 1% aq (12:5:2), was also used as a solvent to detect any coloured species such as methylene blue. In both solvent systems there was only a faint spot other than the main spot, this showed the presence of a trace impurity, or some hydrolysis of BLMB occurred when the material was applied to the plate.

(vi) The Azure A, B, C and Thionine used were all commercial samples supplied by BDH. These samples were used without further purification.

#### 4.2.2. Methods

##### (i) Analytical Radial Thin Layer Chromatography (RTLC)

The absorbents used were either silica gel G or silica gel GF254. The absorbent layer was prepared as described on page 85 Chapter 3.

All radial TLC was performed using a tank supplied by Schleicher and Schüell Inc. Selecta Sol Chromatography Chamber U.S.A. When in use the tank was wrapped in aluminium foil to exclude light. The developed chromatograms were examined in daylight and under u/v light. The u/v lamp was dual wavelength 254/280nm supplied by Shandon.

Samples were applied using disposable micro-pipettes (Microcaps, Drummond Scientific Co., Broomhall, Pennsylvania, U.S.A.). Two to twenty microlitres of 0.5% w/v methanolic solution of dyes were applied to the plate, each dye in one spot (3mm max diameter) on a concentric circle 1cm radius from the centre of the plate. The developing solvent used was that described by Marshall P.N., and Lewis S.M., (1974) a page 86 Chapter 3.

The chromatogram was developed in the dark at ambient temperature  $\sim 20^{\circ}\text{C}$ . The chromatogram was then dried in a draught of cold air. The spectrum of a component of particular interest was obtained, by scraping the band off the chromatogram. This material was then sucked into a tube which contained ethanol washed cotton wool. Absolute ethanol was run through the tube to elute the component. The sample was made up to 3mls total volume.

(ii) Transmittance Spectrophotometry

All u/v and visible spectrophotometry was performed on a Pye Unicam SP1800 series 2, with an AR25 linear recorder, using a matched pair of quartz cells, 1cm path length.

(iii) Diffuse Reflectance Spectrophotometry of Methylene Blue and Benzoyl leuco Methylene Blue

The silica gel and silton used have all been described above page 198 Chapter 4. The apparatus, and preparation of the sample, have been detailed previously on page 88 Chapter 3. The MB and BLMB were made up to that a final concentration of 0.1 - 10.0 mg/g mineral, was achieved i.e. (0.28 - 28.1  $\mu$ moles/g). All samples were stored at  $40 \pm 0.5^{\circ}\text{C}$ , 0% relative humidity, i.e. stored in vacuo over  $\text{P}_2\text{O}_5$ .

(iv) Melting Point

All melting points were determined using a Gallenkamp automatic melting point apparatus, using a slow rate of heating.

(v) Quantitative Estimation of Methylene Blue and Related Dyes Adsorbed on to Silica Gel

In order to estimate the quantity of MB, and related reaction products on silica gel, the mixture was first separated using RTLC, the details of which are shown on page 201 Chapter 4. All the coloured bands were assigned according to their  $R_f$  and absorbance maximum, relative to standard samples. Each component

was then quantified by scraping the band from the TLC plate and the procedure on page 201 Chapter 4 was followed. The absorbancy at the  $\lambda$  max was measured, and from the extinction coefficients, the quantity of each species was determined. TLC spots can be estimated directly using diffuse reflectance, Frodyma M.M., et al., (1964), but this method was not used due to the relative insensitivity of the method. Also each band on the RTLC was physically too small to size i.e. average area  $20 \text{ mm}^2$ .

(vi) A Method to Determine the Rate of Demethylation of Methylene Blue and Benzoyl leuco Methylene Blue on Irradiated Silica Gel

To determine the quantity of the demethylated species of MB and BLMB with time, a fixed amount of MB and BLMB was applied to a small spot on a TLC plate. Subsequent spots were applied at intervals up to 13 days. The last spot applied was taken as the zero time sample. Six spots were applied to a TLC plate. Therefore the samples ranged from zero to 13 days. The plates were stored at  $40 \pm 0.5^\circ\text{C}$ , over  $\text{P}_2\text{O}_5$  with constant irradiation. The spots were then chromatographed on the plate in situ, and the quantity of each species determined using the procedure on page 201 Chapter 4.

### 4.3. Results and Discussion

#### 4.3.1. Methylene Blue in Aqueous Solution

The  $\lambda$  max of the visible spectrum of methylene blue is 668nm in 0.5 molar sulphuric acid and 657nm in absolute ethanol, Figure (4-1). These values agree with other workers, Formanek, J., (1908), Schubert, M and Levine, A., (1955); Bergmann, K., and O'Konski, C.T., (1963).

The extinction of methylene blue was determined at several concentrations ( $1 \times 10^{-6}$  to  $30 \times 10^{-6}$  M.  $l^{-1}$ ), and the values showed deviations from Beer's law. A calibration curve of the observed absorbances directly related to the concentration of methylene blue in 0.5 M  $H_2SO_4$  is shown in Figure (4-2). The experimental molar extinction coefficients at the  $\lambda$  max (668nm) decreased with increasing concentration, Figure (4-3). This was also true for solutions of methylene blue in 0.1 M  $H_2SO_4$ , but not for solutions in 1.5 M  $H_2SO_4$ , Figure (4-4). Other workers have reported the failure of methylene blue to obey Beer's law; Lewis, G.N., (1943); Hayon, D. et al., (1957); Michaelis, L. and Granick, S., (1945); Rabinowitch, E. and Epstein, L.F. (1941); Schubert, M and Levine, A., (1955) and Holst, S. (1935).

The deviation from Beer's law and the hypsochromic shift on increasing the concentration of methylene blue have been attributed to dimerization; Holst, G., (1938); Rabinowitch, E., and Epstein, L.F. (1941); Lewis, G.N., et al., (1943); and Vickerstaff, T., and Lemin, D.R., (1946).



FIGURE.(4-1). Absorbance Spectra of Methylene blue in Ethanolic and acidic solution

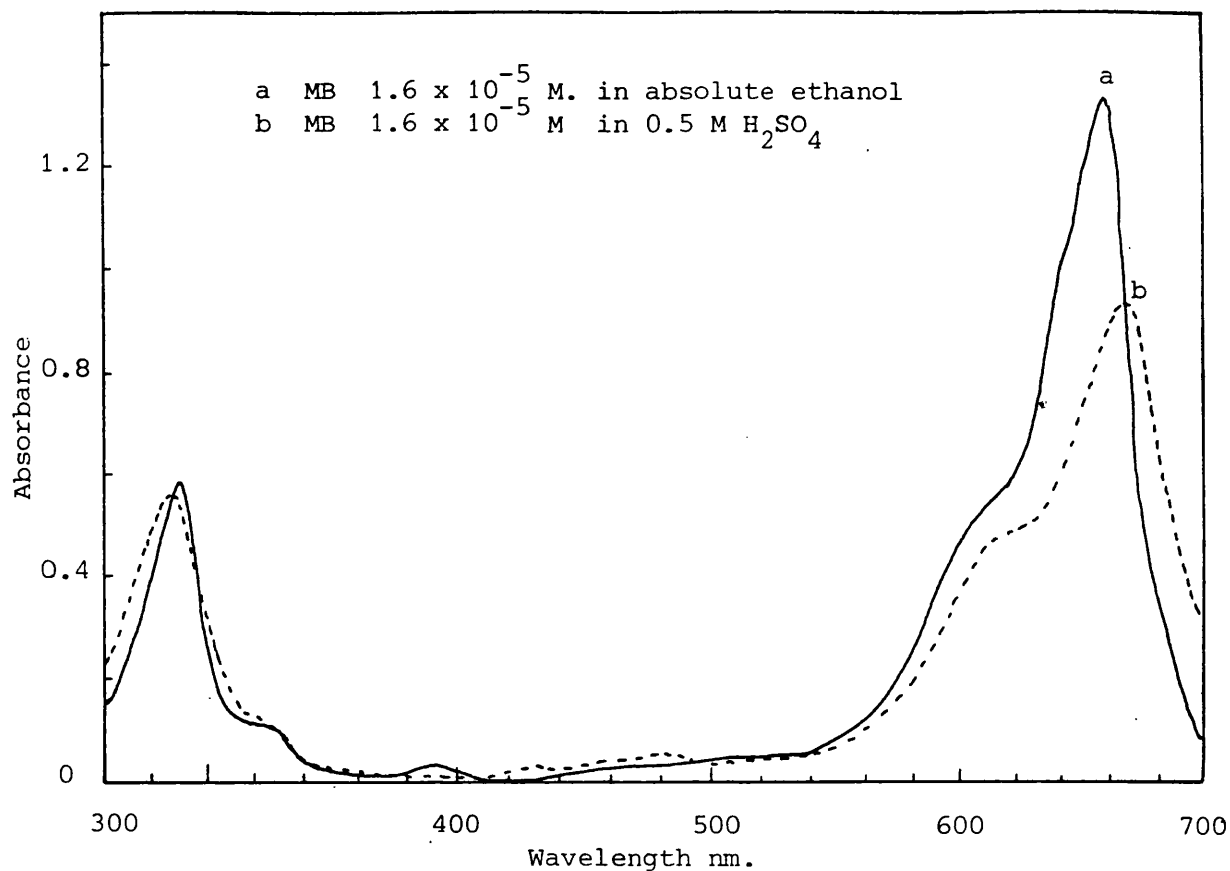


FIGURE.(4-2). Absorbance of Methylene Blue in 0.5 M sulphuric acid at 22°C

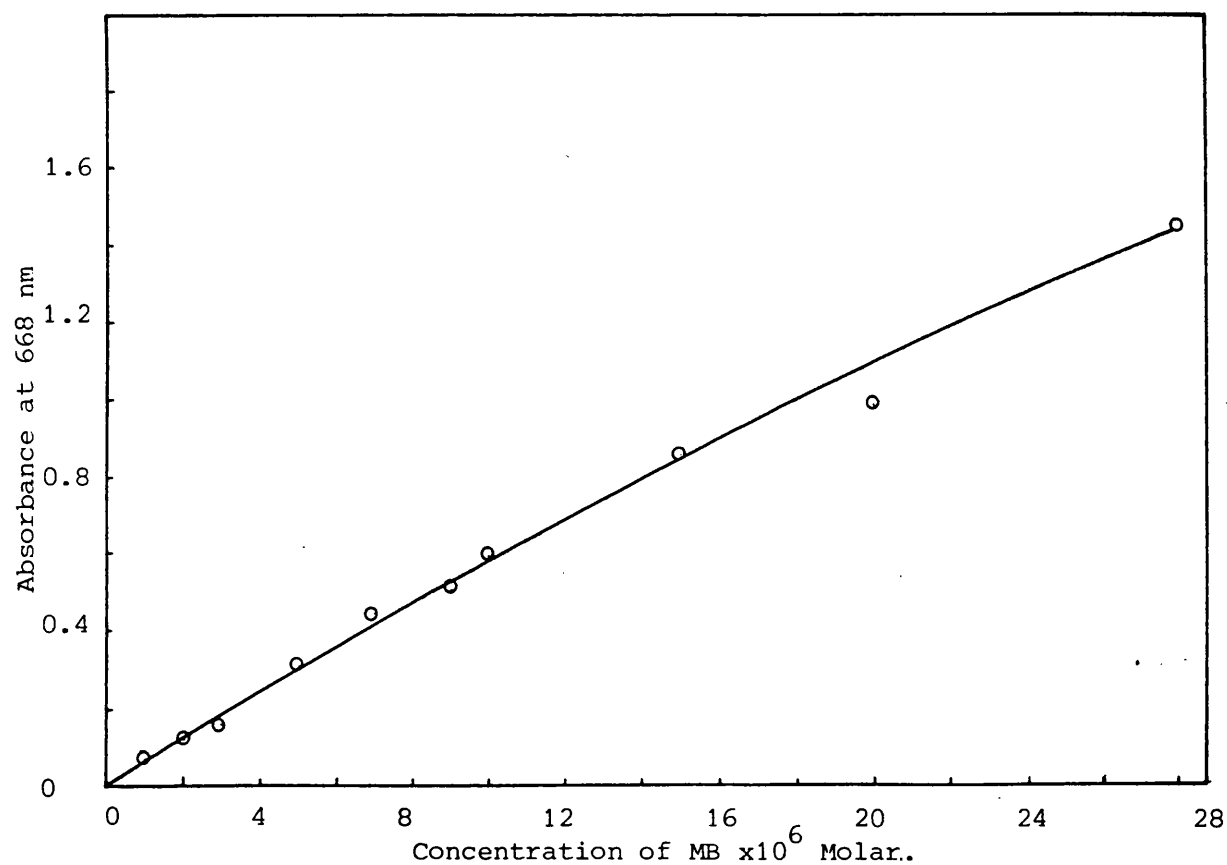


FIGURE (4 - 3). The variation of Molar extinction coefficient with concentration.

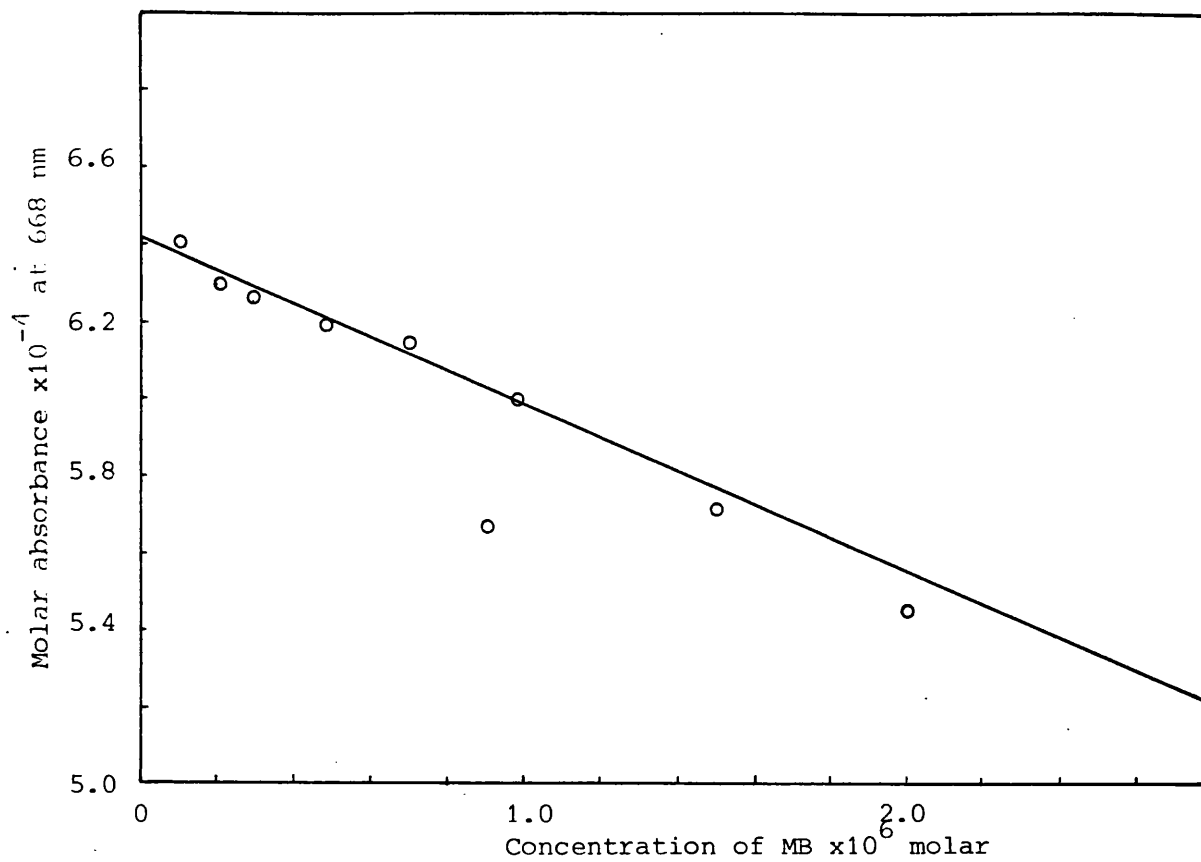
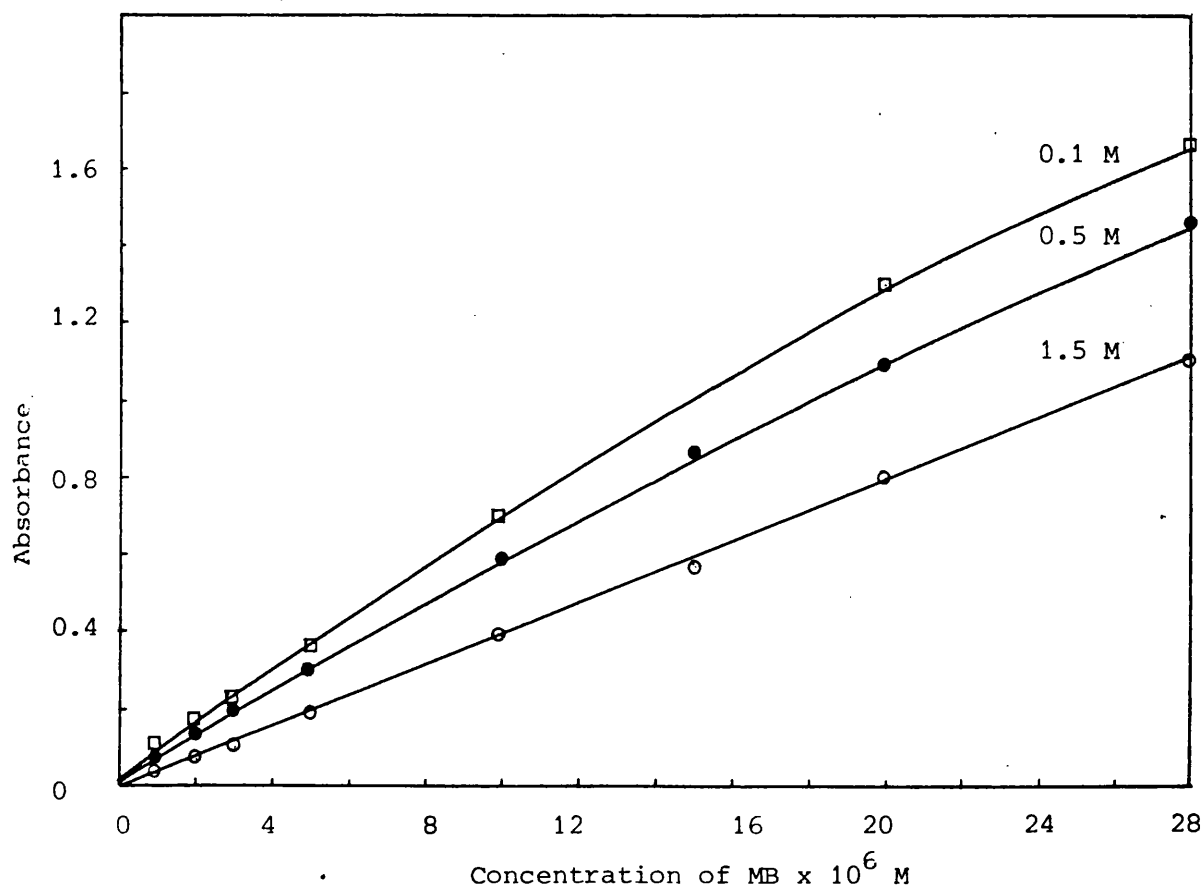
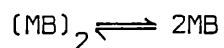


FIGURE (4 - 4). Absorbance of Methylene blue in three concentrations of sulphuric acid.



It has been confirmed that the visible spectra of aqueous methylene blue solutions can be interpreted quantitatively on the assumption of a monomer-dimer equilibrium for concentrations up to  $2.15 \times 10^{-4} \text{ M.l}^{-1}$ ; Rabinowitch, E., and Epstein, L.F. (1941).

In the equilibrium:-



The dissociation constant for the dimer is:-

$$K = \frac{C_m^2}{C_d}$$

Where  $C_m$  and  $C_d$  are the molar concentrations of the monomer and dimer respectively. If higher polymers are neglected, the total molar concentration of methylene blue as monomer is:-

$$C = C_m + 2C_d$$

If  $\alpha$  is the fraction of MB present as monomer then:-

$$\alpha = \frac{C_m}{C}$$

and it follows that

$$K = 2C \alpha^2 / (1-\alpha)$$

The absorbance of a solution of MB at a total concentration of  $C$ , and  $l$  is the pathlength, is  $A$ .

$$E = A/c_l$$

$$\text{If } l = 1\text{cm} \quad E = A/C$$

Assuming Beer's law holds for each component,  
it follows that:

$$E = E_m + (1-\alpha)E_d/2$$

The dissociation constant for the monomer-dimer  
equilibrium has been determined by Bergmann, K., and O'Konski, C.T.,  
(1963) and is:

$$K = (1.7 \pm 0.2) \times 10^{-4} \text{ M. l}^{-1},$$

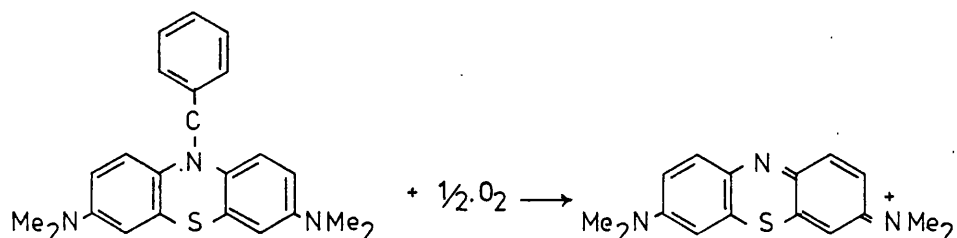
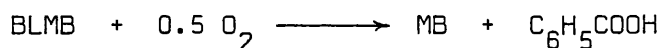
and the standard free energy of dissociation is therefore:

$$\Delta G^{\circ} = -RT \ln K = 5.1 \text{ Kcals. mole}^{-1}$$

#### 4.3.2. Hydrolysis and Autooxidation of Benzoyl leuco Methylene Blue

When a colourless solution of BLMB in 0.5M sulphuric acid is exposed to air the solution turns blue. A thorough qualitative and quantitative study of the reaction mechanism has been performed by Gensler, W.J., et al., (1966).

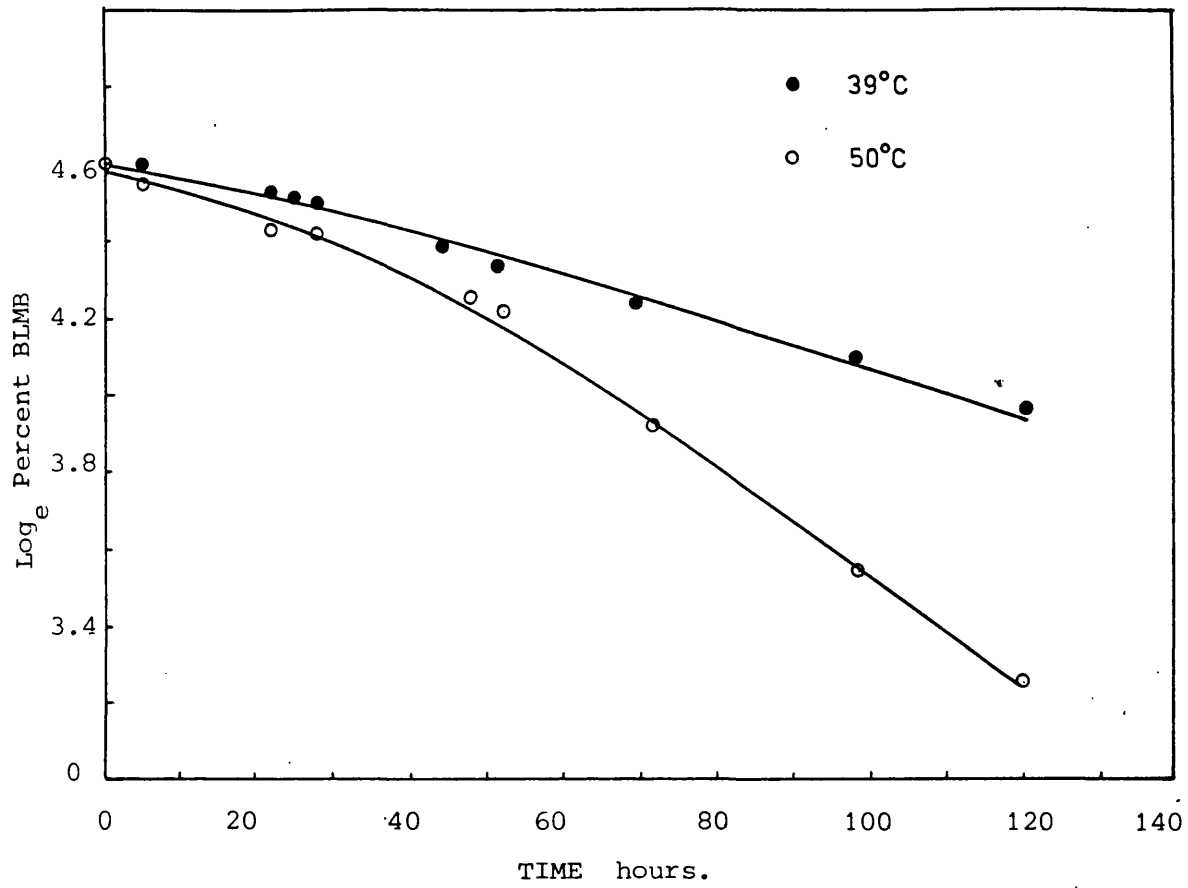
The blue colour formed was methylene blue. Hydrolysis of BLMB in 0.5 M sulphuric acid is a first order reaction ( $k_{50^{\circ}\text{C}} = 2.93 \times 10^{-6} \text{ sec}^{-1}$ ), which is unaffected by, and independent of the concurrent autooxidative development of methylene blue. BLMB reacts in 0.5M  $\text{H}_2\text{SO}_4$  with  $\text{O}_2$  in the molar ratio 1 : 0.5 to form MB and benzoic acid.



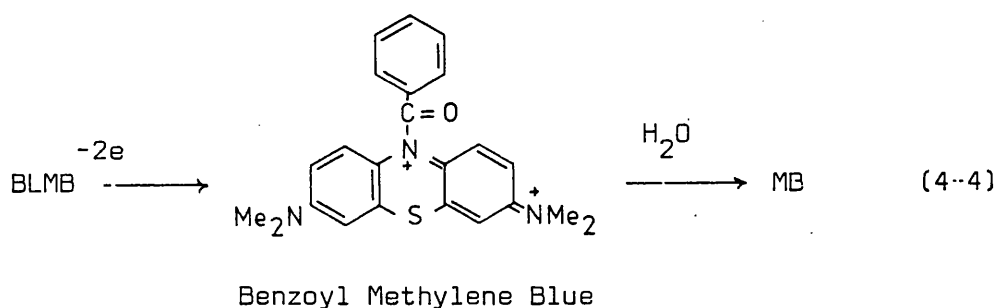
After an initial induction period, the methylene blue formation followed first order kinetics; rate constant at  $50^{\circ}\text{C}$  ( $K = 3.0 \times 10^{-6} \text{ sec}^{-1}$ ). All the data for autooxidation were consistent with a slow hydrolysis of BLMB to leucomethylene blue, followed by rapid oxidation of LMB to MB, reaction (4-3).

Figure (4-5) shows the hydrolysis of BLMB, (sample provided by English Clays Ltd), at 39 and  $50^{\circ}\text{C}$  in 0.5 M  $\text{H}_2\text{SO}_4$ .

FIGURE (4—5). Production of Methylene blue from BLMB in  
0.5 M  $H_2SO_4$



The first order rate constants for methylene blue formation at 39<sup>o</sup> and 50<sup>o</sup>C were, ( $K_{39} = 1.54 \times 10^{-6} \text{ sec}^{-1}$  and  $K_{50} = 3.47 \times 10^{-6} \text{ sec}^{-1}$ ) respectively. These rate constants agree with those of Gensler, W.J. et al., (1966). It has been shown by Gensler W.J., et al., (1966) that the rate of the reaction was dependent upon the concentration of hydrogen ions. If the sulphuric acid concentration was increased to 1.5 molar the first order rate constant was  $8.0 \times 10^{-6} \text{ sec}^{-1}$ . The above workers also found that several oxidants other than oxygen, e.g. ceric sulphate, lead dioxide, bromine or ferrous ion-hydrogen per-oxide (Fenton's reagent) were also capable of converting BLMB to MB. In all cases, however, the initial rates of colour formation were found to be greater than the rate of BLMB hydrolysis, and it was assumed that these agents were somehow capable of directly attacking BLMB, reaction (4-4)



### 4.3.3. The Hydrolysis of BLMB in the Presence of $\text{Co}^{3+}$

It has been discovered in the course of this work that if sodium cobaltinitrite is added to a solution of BLMB in sulphuric acid, a blue colour is rapidly produced. The initial rate of the reaction was dependent upon the concentration of BLMB, Figure (4-6). This indicates that the reaction was first order with respect to BLMB. If the results are plotted as  $\frac{1}{a-b} \ln b \frac{(a-x)}{(b-x)}$  versus time,

Where :

- a =  $(\text{BLMB})_0$  - initial BLMB concentration
- b =  $(\text{Co}^{3+})_0$  - initial  $\text{Co}^{3+}$  concentration
- x = (MB) - Methylene blue concentration during the course of the reaction.

a straight line is produced, Figure (4-7). This indicates that the total reaction order was 2nd order, i.e.  $\text{Rate} = K_2(\text{BLMB})^1(\text{Co}^{3+})^1$ . The rate constant ( $K_2$ ) was determined from the slope of Figure (4-7),  $K_2 = 8.89 \text{ l mol}^{-1} \text{ sec}^{-1}$  at  $25^\circ\text{C}$ . The initial reaction rate was approximately  $10^4$  times faster than without  $\text{Co}^{3+}$  present. By varying the  $\text{Co}^{3+}$  concentration, and holding the BLMB concentration constant, the reaction was confirmed as being first order with respect to the  $\text{Co}^{3+}$  concentration. A second order plot, Figure (4-8), shows the results and the second order rate constant, ( $K_2$ ), was determined from the slope of the line,  $K_2 = 9.01 \text{ l m}^{-1} \text{ sec}^{-1}$ , at  $25^\circ\text{C}$ . This agrees well with the results obtained from Figure (4-7), giving an average rate constant of  $8.95 \text{ l m}^{-1} \text{ sec}^{-1}$ . The  $\text{Co}^{3+}$  used was  $\text{Na}_3\text{Co}(\text{NO}_2)_6$  as this was a stable  $\text{Co}^{3+}$  state. When sodium cobaltinitrite is in 0.5 molar sulphuric acid it is orange in colour; 210nm,  $E = 2 \times 10^4$ ; 272nm,  $E = 1.16 \times 10^4$ ; 360nm,  $E = 0.59 \times 10^4$ .



FIGURE (4—6). The Effect of Initial BLMB concentration on the rate of MB production at 20°C in the presence of  $\text{Co}^{3+}$  and 0.5M Sulphuric acid

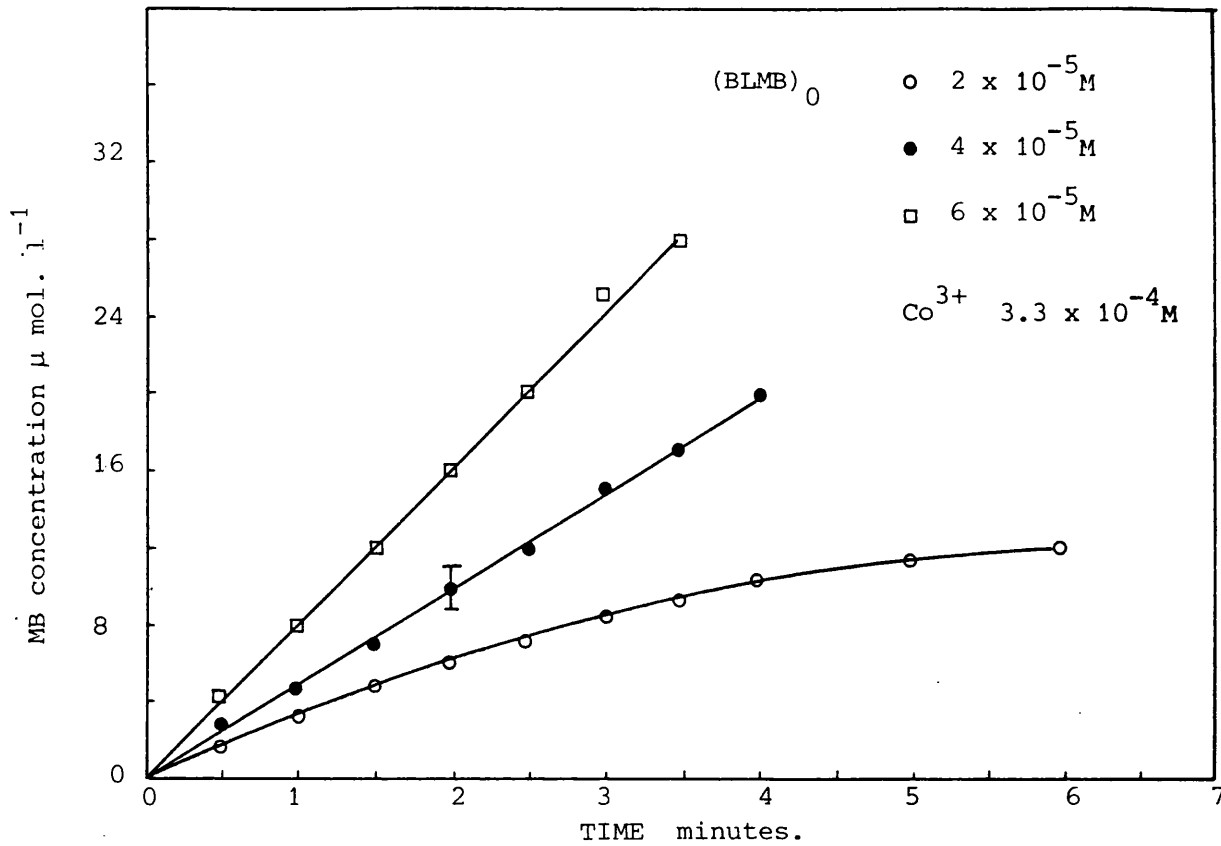
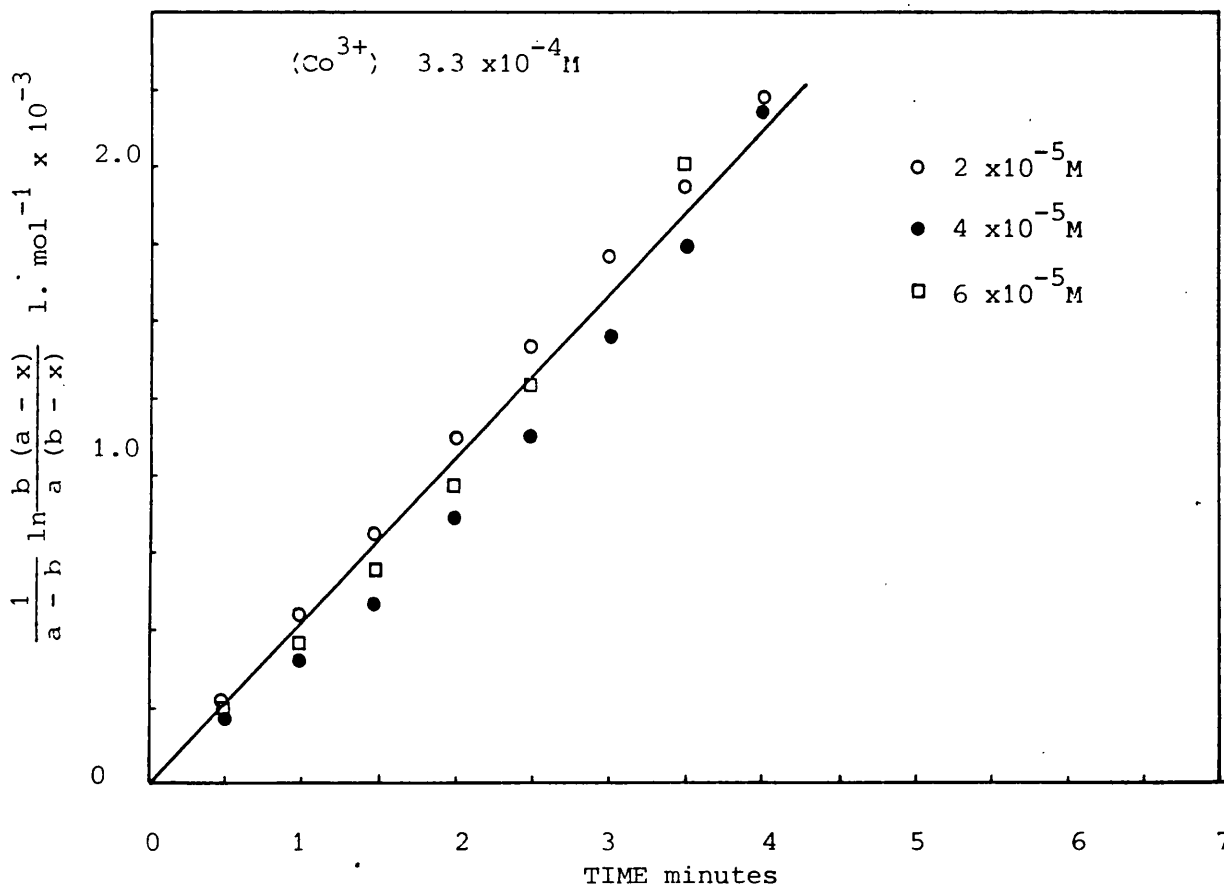
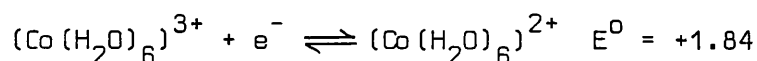


FIGURE (4—7). A second order plot of the production of MB from BLMB in the presence of  $\text{Co}^{3+}$  and 0.5M Sulphuric acid



If the solution of sodium cobaltinitrite was allowed to stand for several hours, the orange colour was discharged, and colourless solution formed. The loss of colour is due to the formation of either  $(\text{Co}(\text{H}_2\text{O})_6)^{3+}$  or  $\text{Co}_2(\text{SO}_4)_3$ . Both of these species are unstable and will readily reduce to  $\text{Co}^{2+}$ , Cotton, F.A. and Wilkinson G. (1972) p. 875-892.



The rate of hydrolysis of BLMB in the presence of colourless sodium cobaltinitrite, prepared 16 hours previously, was measured, Figure (4-8). The rate constant for the reaction was,  $6.94 \text{ l m}^{-1} \text{ sec}^{-1}$ . This value was smaller than the rate constant for the freshly prepared sample and the deviation was larger than experimental error. This indicates that sodium cobaltinitrite is reduced on standing in aqueous sulphuric acid to  $\text{Co}^{2+}$ .  $\text{Co}^{2+}$  is ineffective in oxidizing BLMB and this would be reflected by a fall in the rate constant, as was observed.  $\text{Co}^{2+}$  can exist in aqueous solution in two distinct forms,  $(\text{Co}(\text{H}_2\text{O})_4)^{2+}$ , or  $(\text{Co}(\text{H}_2\text{O})_6)^{2+}$ . Both species have an absorbance in the visible region but the extinction coefficients are small,  $E_{540\text{nm}}^{\text{H}_2\text{O}} = 10$  and  $E_{700\text{nm}}^{\text{H}_2\text{O}} = 600$  respectively.

#### 4.3.4 The Effect of the Hydrogen Ion Concentration upon the Spectral Characteristics of Methylene Blue

The extinction coefficients and the  $\lambda$  max of methylene blue are both affected by changes in the hydrogen ion concentration of the solution Table (4-2). The absorbance of methylene blue at 668nm as a function of concentration in 0.1, 0.5 and 1.5 molar

FIGURE (4-8). A second order plot of the production of MB from BLMB in the presence of  $\text{Co}^{3+}$ , and  $0.5\text{M H}_2\text{SO}_4$ .

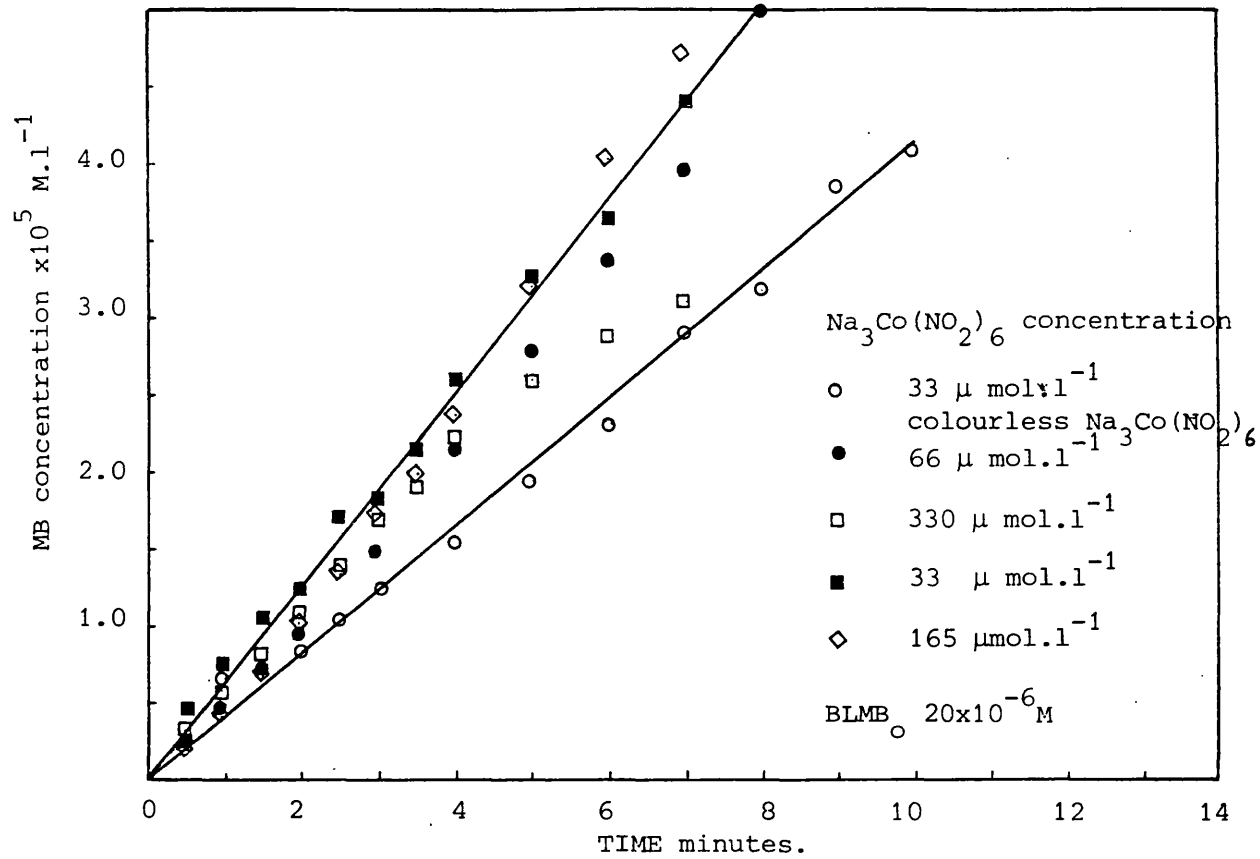


FIGURE (4-9). The production of MB from BLMB in the presence of  $\text{Co}^{3+}$  as a function of sulphuric acid concentration.

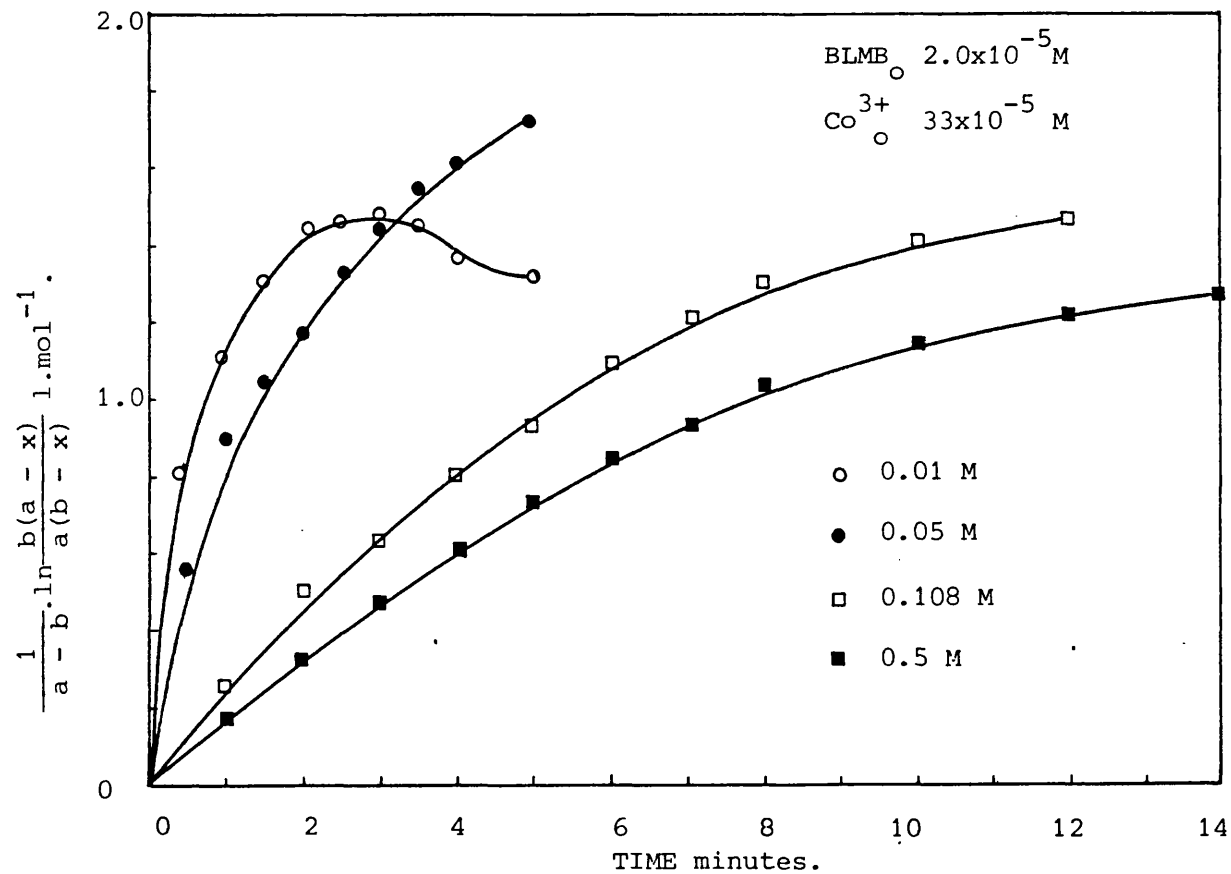


Table (4-2)

The  $\lambda_{\max}$ , and Extinction Coefficients of Methylene Blue in Different Concentrations of Sulphuric Acid

$(\text{H}_2\text{SO}_4)$ moles. $l^{-1}$	Methylene Blue Concentration Moles. $l^{-1}$	$\lambda_{\max}$ (nm)	Extinction Coefficient
$10^{-3}$	$10^{-5} \mu$	666	$6.95 \times 10^4$
$10^{-2}$	"	667	$6.75 \times 10^4$
$10^{-1}$	"	667	$6.65 \times 10^4$
0.5	"	668	$5.65 \times 10^4$
1.0	"	673	$4.1 \times 10^4$
1.5	"	674	$3.9 \times 10^4$
2.0	"	676	$3.25 \times 10^4$
5.0	"	681	$3.50 \times 10^4$
10.0	"	684	$2.0 \times 10^4$

aqueous sulphuric acid is shown in Figure (4-4). When concentrations of methylene blue were calculated from the absorbance values, the position and change in extinction coefficient in different hydrogen ion concentrations were allowed for. The rate of MB production from BLMB with  $\text{Na}_3\text{Co}(\text{NO}_2)_6$  present in various strengths of sulphuric acid, is shown in Figure (4-9). This shows that the rate of colour production was greatest at the lowest ( $\text{H}^+$ ), indicating that when sodium cobaltinitrite was present the role of the acid was different from when none was present, and in some way reduced the activity of the  $\text{Co}^{3+}$ . Since the ( $\text{H}^+$ ) was in excess of the (BLMB) or ( $\text{Co}^{3+}$ ) the kinetics can be regarded as pseudo-second order. When the data were plotted in the form of a second order reaction, several straight lines were produced Figure (4-10). If the reaction was first order with respect to ( $\text{H}^+$ ). the true rate constant can be obtained by dividing the apparent rate constant by the ( $\text{H}^+$ ). The reaction was not first order with respect to ( $\text{H}^+$ ). An approximate method to determine the order of a reaction is by the Van't Hoff method. The log of initial rate is plotted versus  $\log(\text{H}^+)$ , as shown in Figure (4-11) This plot should produce a straight line, and the slope of this line gives the order of the reaction. Figure (4-11) shows deviations from a straight line. The amounts of methylene blue produced at the lowest sulphuric acid concentration (0.01 molar), decreased after reaching a maximum in 1.5 mins. The reduction in colour can be attributed to the greater oxidizing power of  $\text{Co}^{3+}$ , in low sulphuric acid concentrations, causing it to bleach the solution.

All the data for the production of methylene blue from BLMB in the presence of  $\text{Co}^{3+}$  were consistent with a direct attack by  $\text{Co}^{3+}$  on BLMB causing immediate production of a blue colour.

FIGURE (4-10). The Effects of the Sulphuric Acid Concentration on the Production of MB from BLMB in the Presence of  $\text{Co}^{3+}$

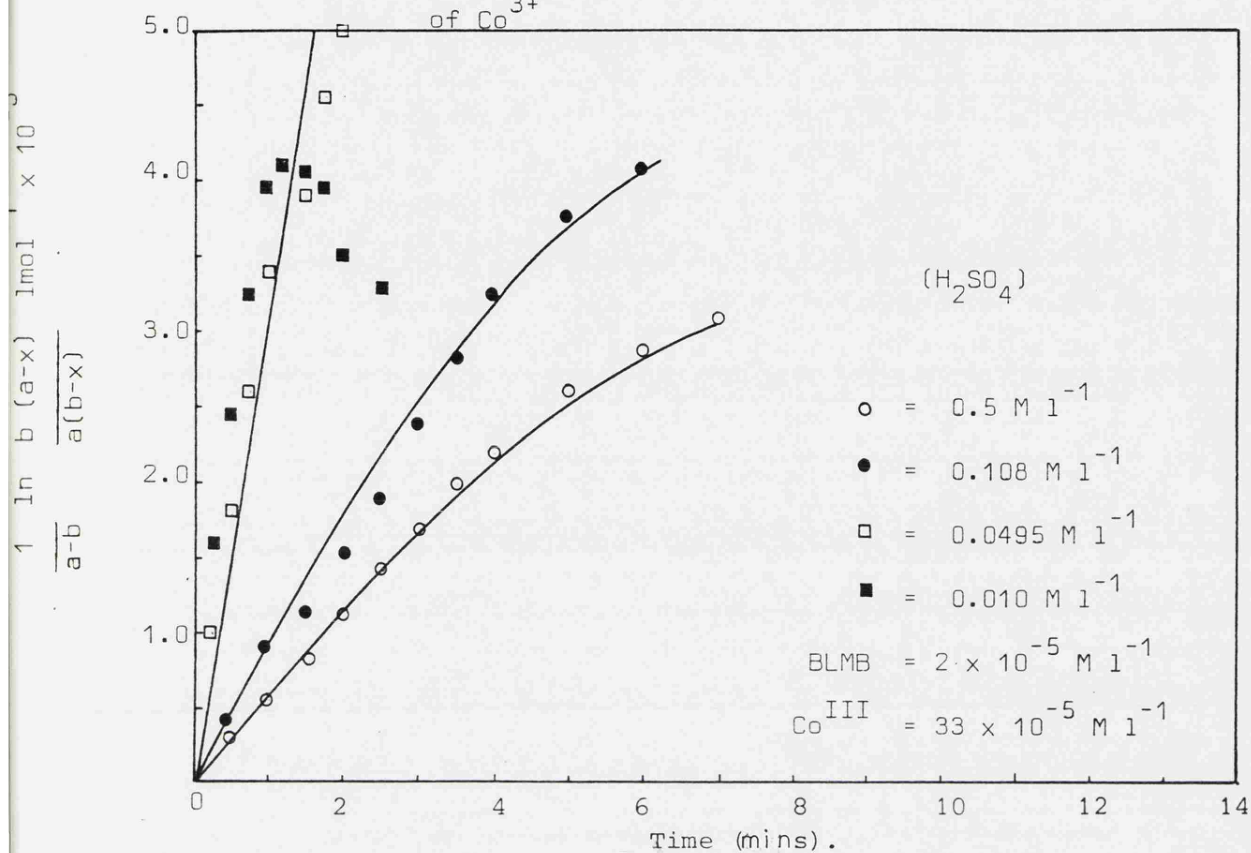
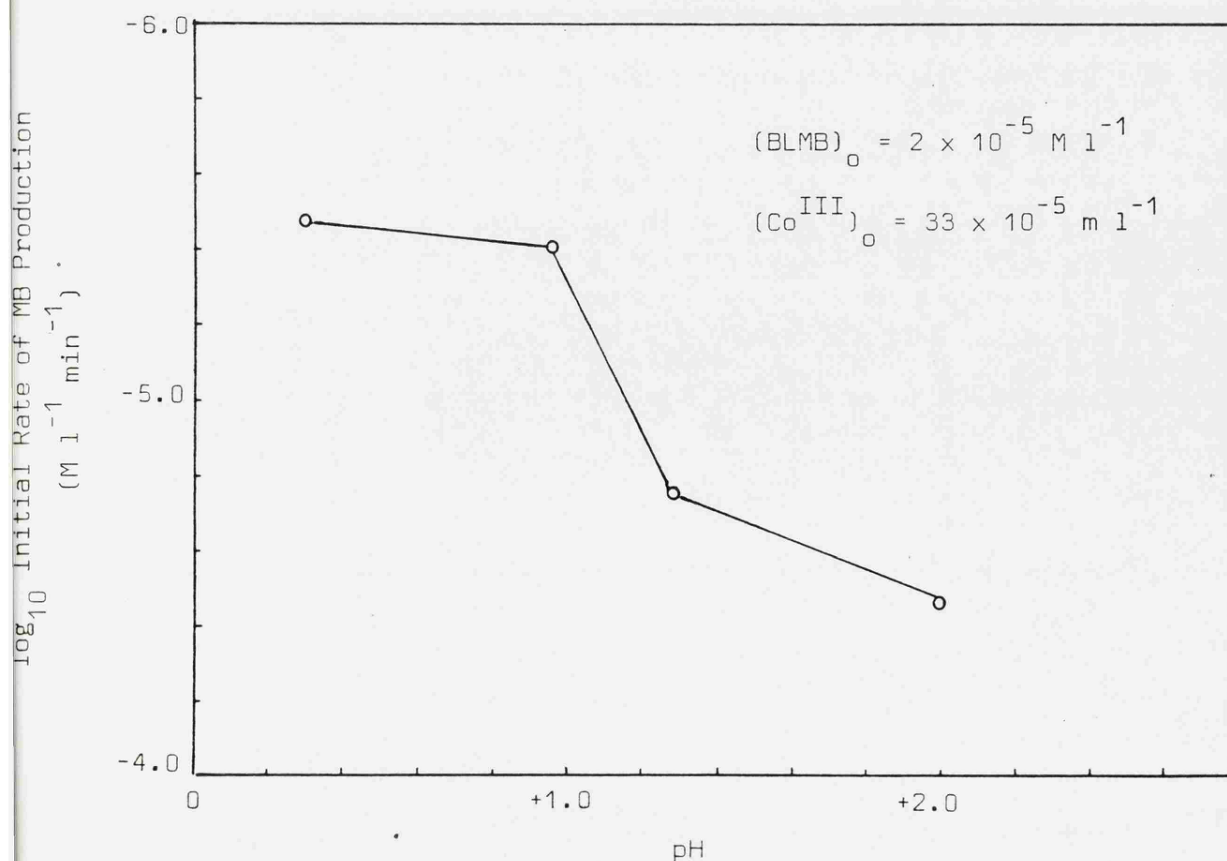
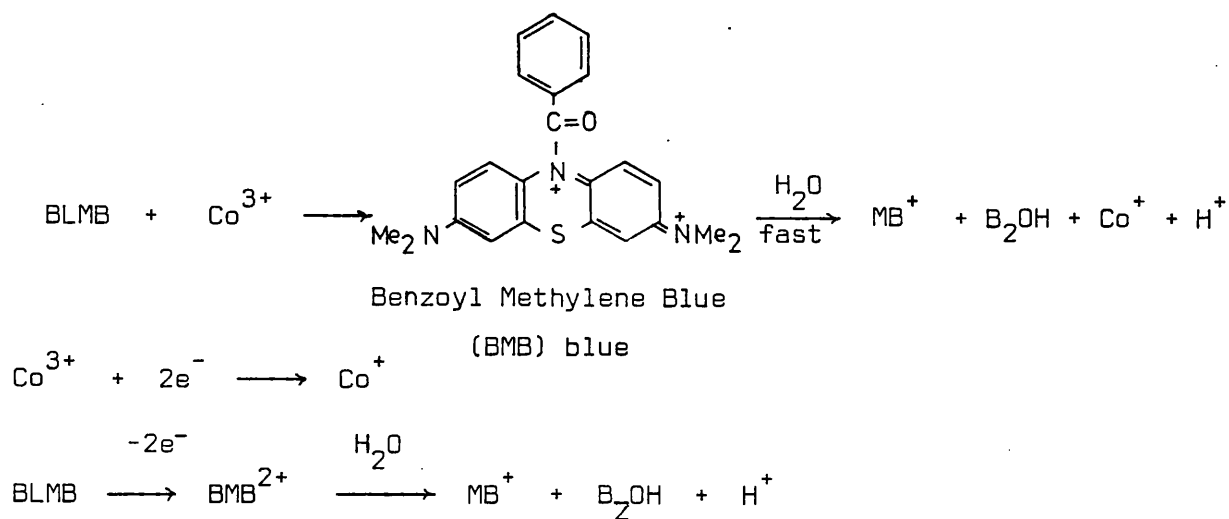


FIGURE (4-11). Hydrolysis of BLMB in the Presence of  $\text{Co}^{3+}$  at Various Hydrogen Ion Concentrations





The sodium cobaltinitrite complex is an effective electron acceptor, with respect to BLMB, but as the chelating nitrite groups are replaced by water the  $\text{Co}^{3+}$  ion is no longer stable, and is reduced to  $\text{Co}^{2+}$ . This is ineffective as an electron acceptor. Since the reaction rate is 1st order with respect to the  $\text{Co}^{3+}$  concentration, it seems likely that both electrons are exchanged simultaneously. The role of sulphuric acid is unclear, but it does have a suppressing effect upon the reaction rate. The sulphuric acid must reduce the ability of the sodium cobaltinitrite complex to accept electrons or reduce the ability of BLMB to donate them.

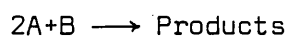
#### 4.3.5. The Hydrolysis of BLMB in the Presence of $Ce^{4+}$

BLMB was rapidly oxidised in 0.5 molar sulphuric acid when  $(NH_4)_2 \cdot (Ce(NO_3)_6)$  was present. A complex form of  $Ce^{4+}$  was used because of its greater stability in aqueous solution. The rate of MB production was greatly enhanced by the presence of  $Ce^{4+}$ . The rate of methylene blue production as a function of  $Ce^{4+}$  concentration as shown in Figure (4-12). If the van't Hoff method was used to determine the order of the reaction, with respect to  $Ce^{4+}$ , as described above, the slope of the line was 2, indicating that the reaction was 2nd order with respect to  $Ce^{4+}$ , Figure (4-13).

$$\text{Rate} = K_3(\text{BLMB})(Ce^{4+})^2$$

The overall reaction was therefore third order.

If the data was presented as a third order reaction:



$$(a-2x)(b-x) \quad x$$

$$\frac{dx}{dt} = K_3(a-2x)^2(b-x)$$

Then

$$\frac{1}{(2b-a)^2} \frac{(2b-a)2x}{a(a-2x)} + \ln \frac{b}{a} \frac{(a-2x)}{(b-x)} \quad \text{vs time}$$

Should yield a straight line, Figure (4-14).

Where:

$$a = (Ce^{4+})_0 \quad \text{initial concentration}$$

$$b = (\text{BLMB})_0 \quad \text{" \quad "}$$

$$x_t = (\text{MB}) \quad \text{at time } t.$$



FIGURE (4-12). The Effect of  $Ce^{4+}$  Concentration on the Rate of Production of MB from BLMB, in 0.5 M  $H_2SO_4$ .

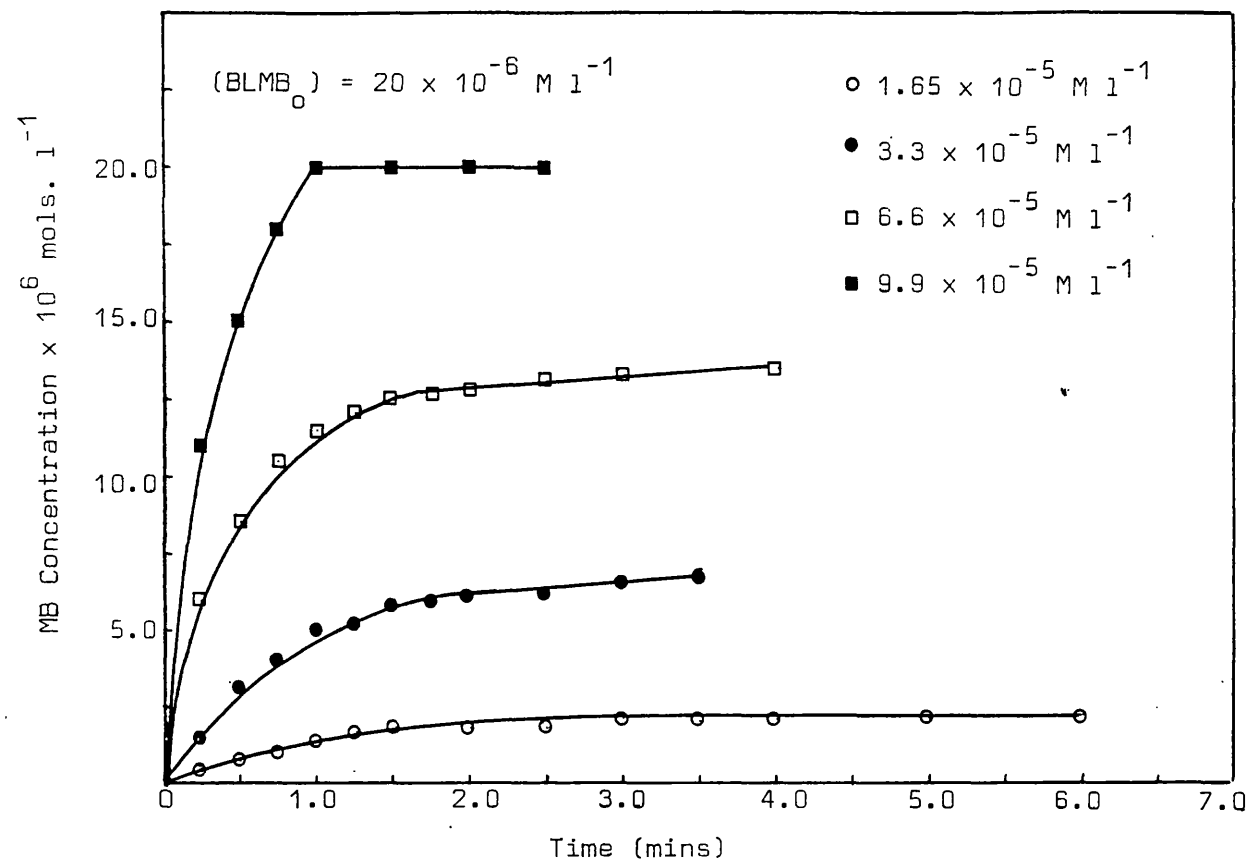
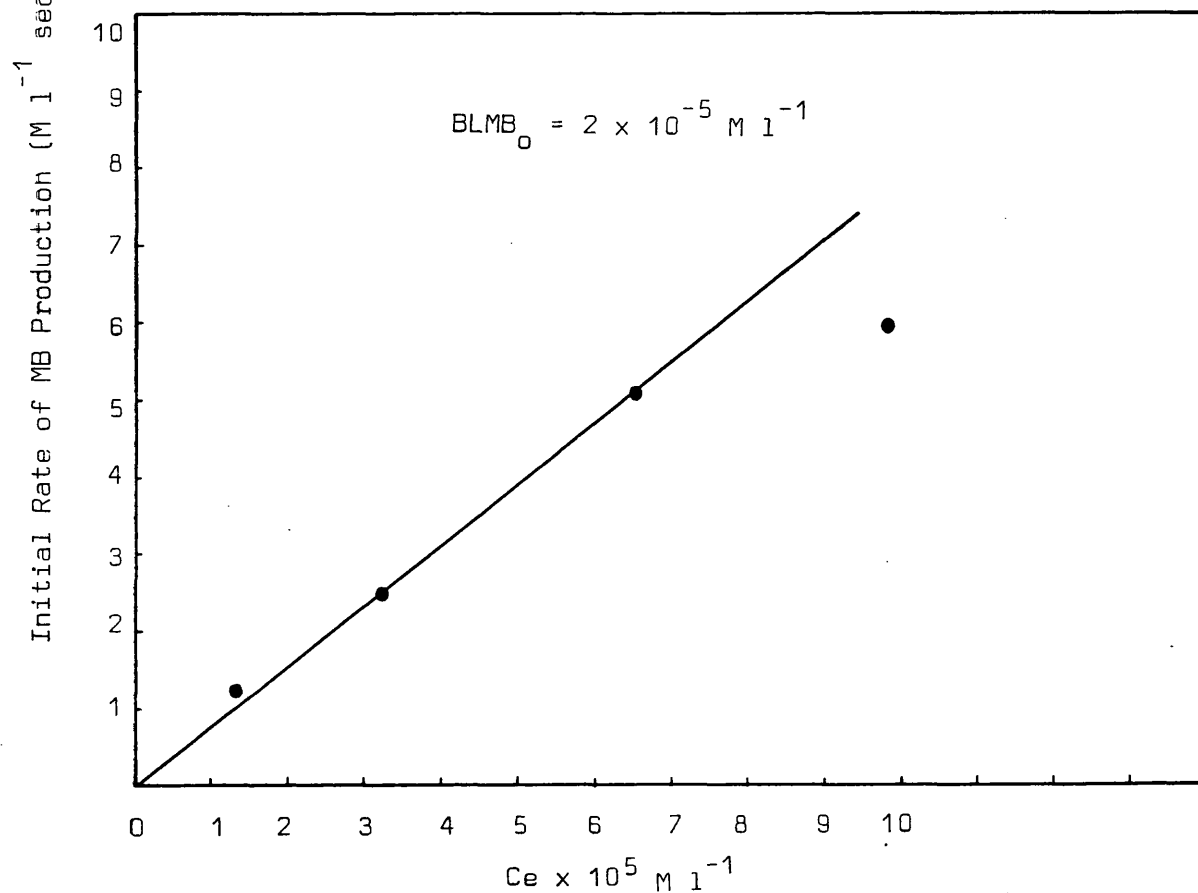


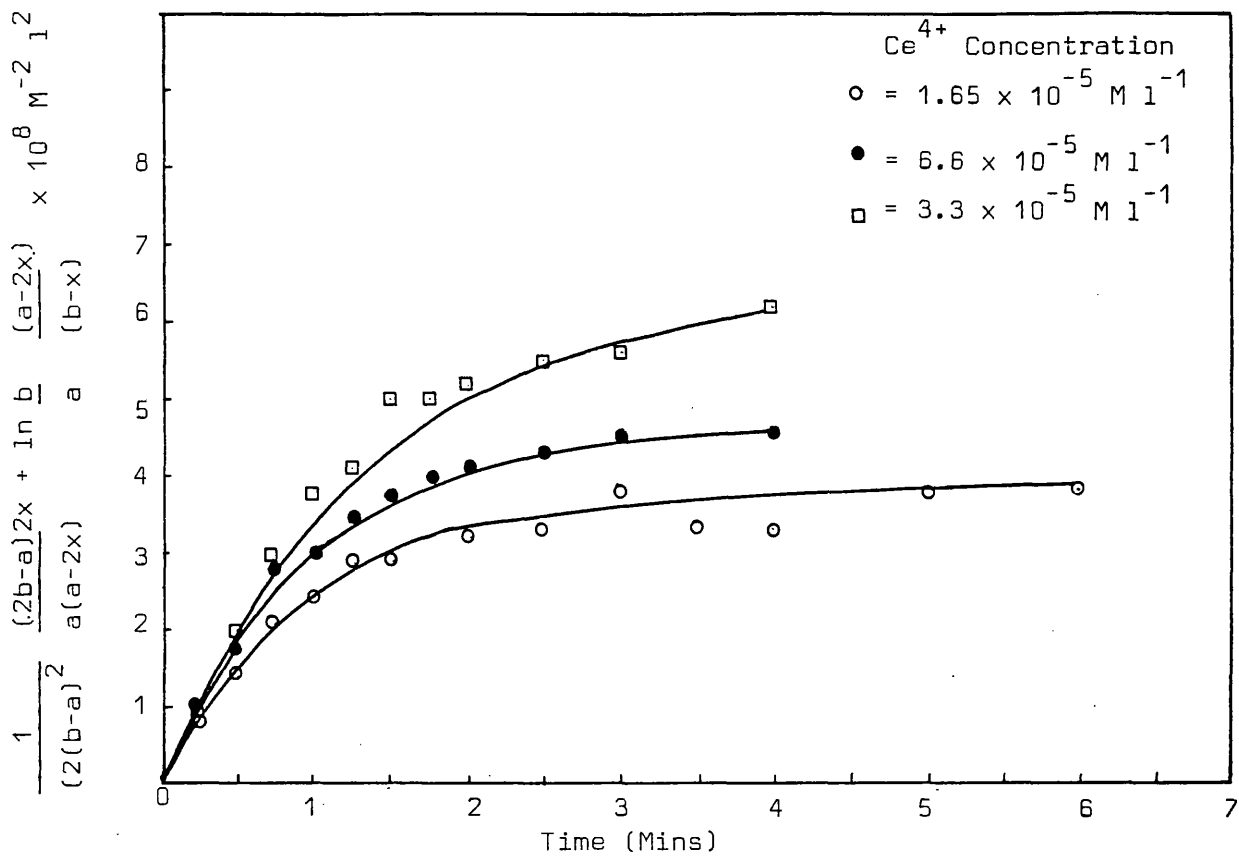
FIGURE (4-13). Initial Rate of Reaction of MB from BLMB in the Presence of  $Ce^{4+}$ , and 0.5 M  $H_2SO_4$



It can be seen from Figure (4-14) that the reaction only obeys 3rd order kinetics initially, 1 minute, after this the reaction deviates from a straight line, the rate constant for the initial period is  $6.25 \times 10^8 \text{ M}^{-2} \text{ l}^2 \text{ sec}^{-1}$ , at  $25^\circ\text{C}$ . This indicates the reaction is proceeding in a more complex manner after the initial period of reaction. The initial reaction product was methylene blue,  $\lambda \text{ max} = 668\text{nm}$ . If the solution was exposed to the atmosphere for one hour the position of the  $\lambda \text{ max}$  changed to  $550\text{nm}$ , a hypsochromic shift of  $118\text{nm}$ . This indicated further oxidation of methylene blue, causing demethylation, and this would result in the reaction rate being reduced. If the solution was allowed to stand for several days it was bleached.

It was expected that the reaction would be 2nd order with respect to  $(\text{NH}_4)_2(\text{Ce}(\text{NO}_3)_6)$ , as ceric ammonium nitrate is known to be a single electron acceptor, and is used as such to initiate polymerizations.

FIGURE (4-14). A 3rd Order Plot of the Production of MB from BLMB  
in the Presence of  $Ce^{4+}$  and 0.5 M  $H_2SO_4$



4.3.6. Radial Thin Layer Chromatography of Methylene Blue  
and Related Thiazine Dyes

Tables (4-3 to 4-7) show the Rf values and absorbance maxima of methylene blue, thionine, azure A, azure B and azure C, when separated using radial thin layer chromatography. The Rf values quoted were the mean of at least six separate samples, with a standard deviation of  $R_f \pm 0.01$ . The absorbance maxima were also the mean of at least six separate samples with a standard deviation of  $\pm 2.0\text{nm}$ .

The separated bands were identified, where possible, by their Rf value and absorbance maximum. Spots were removed from the TLC plate as described on page 83 Chapter 3, and the absorbance maxima were measured in aqueous solution. The identity of the spot was then assigned, by comparison with standards and the literature values, shown in Table (4-8).

When separated a sample of Azure A showed no major band, Table (4-5), all seven coloured components being of equal intensity and size. Azure A was identified by elimination of the other components, which were of known Rf and absorbance maximum. The absorbance maximum of band No.3, Rf 0.43, Table (4-5) has a similar wavelength maximum, 640nm, to the literature values (620-638nm) of Azure A, Table (4-8). Large discrepancies occur in the literature values for Azure A, presumably because the materials used differ in purity. The other thiazine dyes had a major component which was readily identifiable using the absorbance maximum. These were compared with literature values Table (4-8). The component in Azure A, B and C,  $R_f = 0.48$ , was tentitively identified as sym-dimethylthionine,  $\lambda_{\text{max}} = 630\text{nm}$ , Tables (4-5 to 4-7).

Table (4-3) Radial TLC of Methylene Blue at 20°CAbsorbent : Sil Gel GF<sub>254</sub> (Merck).Running Solvent : butan-1-ol/NH<sub>4</sub>Cl 2% aq/formic acid 1% aq. (12:5:2)

Running Time 6hrs

Spot No	Colour	Size	Mean Rf $\pm$ 0.01	Comments	Experimental $\lambda$ max (nm)
1	Blue	l	.29	MB	665
2	Blue	m	.36	Azure B	649

Table (4-4) Radial TLC of Thionine at 20°CAbsorbent : Sil Gel GF<sub>254</sub> (Merck).Running Solvent : butan-1-ol / NH<sub>4</sub>Cl 2% aq/Formic acid 1% aq (12:5:2)

Running Time 6hrs

Spot No	Colour	Size	Mean Rf $\pm$ 0.01	Comments	Experimental $\lambda$ max (nm)
1	Red	s	.49		
2	Red	l	.63	Thionine	605
3	Yellow/ Green	s	.76		
4	Green	s	.83		
5	Red	s	.89		
6	Yellow	s	.94		
7	Yellow/ Green	s	.98		

Table (4-5) Radial TLC of Azure A at 20°CAbsorbent : Sil Gel GF<sub>254</sub> (Merck)Running Solvent : butan-1-ol/NH<sub>4</sub>Cl 2% aq/Formic Acid 1% aq (12:5:2)

Running Time 6hrs

Band No	Colour	Size l,m,s.	Mean Rf	Comments	Experimental $\lambda$ max (nm)
1	Blue	m	0.29	MB	665
2	Blue	m	0.36	Azure B	649
3	Blue	m	0.43	Azure A	640
4	Blue	m	0.48		631
5	Blue	m	0.56	Azure C	616
6	Red/ Blue	m	0.62	Thionine	604
7	Red/ Blue	m	0.68	Thionine	605
8	Colourless u/v absorb.	s	0.84		

All Rf values refer to the mean of at least 7 different samples

Table (4-6) Radial TLC of Azure B at 20°CAbsorbent : Sil Gel GF<sub>254</sub> (Merck).Running Solvent : butan-1-ol/NH<sub>4</sub>Cl 2% aq/Formic Acid 1% aq (12:5:2)

Running Time 6hrs

Spot No	Colour	Size	Mean Rf	Comments	Experimental $\lambda$ max (nm)
1	Blue	m	.29	MB	665
2	Blue	l	.37	Azure B	648
3	Blue	m	.48	?	630
4	Blue	s	.56	Azure C	618
5	Red	s	.60	Thionine	605

Table (4-7) Radial TLC of Azure C at 20°CAbsorbent : Sil Gel GF<sub>254</sub> (Merck)Running Solvent : butan-1-ol/NH<sub>4</sub>Cl 2% aq/Formic Acid 1% aq (12:5:2)

Running Time 6hrs

Spot No	Colour	Size	Mean Rf	Comments	Experimental $\lambda$ max (nm)
1	Blue	m	.29	MB	665
2	Blue	m	.35	Azure B	648
3	Blue	m	.43	Azure A	640
4	Blue	m	.48	?	630
5	Blue	l	.56	Azure C	617
6	Red	m	.59	Thionine	604

Table (4-8) Literature Values for the Absorbance Maxima of Thiazine Dyes

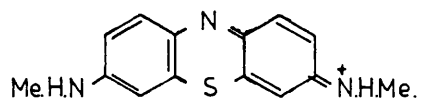
No. Subst methyl group.						
Compound	MB	Azure B	Azure A	Sym dimethyl thionine	Azure C	Thionine
Reference						
a	656	640	624	617		605
b	665	652	620		616	599
c	668		638			603
d	667.5	651.7	638	620.1	611.4	602.5
a	Schaefer F.C. and Zimmerman, W.D. (1968)			Solvent ETOH.		
b	Wotherspoon N. and Oster G. (1957)			H <sub>2</sub> O		
c	Kehrmann F. et al., (1906)			H <sub>2</sub> O		
d	Formanek, J., (1908)			H <sub>2</sub> O		

Table (4-9) Experimental Values for Absorbance Maxima and  
Rf of Thiazine Dyes

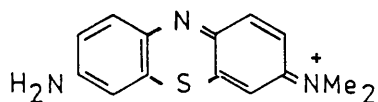
Common Name	MB	Azure B	Azure A	Sym methyl thionine	Azure C	Thionine
No of Substitd. methyl group	4	3	2	2	1	0
H <sub>2</sub> O λ Max (nm)	665	649	640	630	618	605
Rf. solvent: Marshall, P.N., and Lewis, S.M., (1974)a	.29	.36	.43	.48	.56	.61



## Sym-dimethylthionine



This was based on the Rf of the component, relative to Azure A. Sym-dimethylene has the same number of methyl groups as Azure A.



Azure A

But the positive charge on Azure A will be localized on the terminal nitrogen atom adjacent to the methyl groups, whereas on sym-dimethylthionine the positive charge will be shared between the two terminal nitrogen atoms. The positive charge on Azure A will therefore be stabilized by the strongly electron donating methyl groups to a greater extent than sym-dimethylthionine. It is therefore likely that sym-dimethylthionine will travel faster in this solvent than Azure A. The suspect sym-dimethylthionine had a greater Rf than Azure A, 0.48 c.f. 0.43 for Azure A, and a  $\lambda$  max = 630nm. The  $\lambda$  max being midway between the literature values for sym-dimethylthionine and Azure A, Table (4-9). It is possible that the band represented two unresolved species.

All the thiazine dyes, with the exception of MB, were highly contaminated with other thiazine dyes.

4.3.7. A Diffuse Reflectance Study of Methylene Blue  
Adsorbed upon Silica Gel

The spectrum of methylene blue adsorbed upon silica gel is shown in Figure (4-15). It will be seen that the position of maximum absorbance ( $\lambda_{max}$ ) changes with the amount of methylene blue applied. The position of the  $\lambda_{max}$  of MB, as a function of concentration is shown in Figure (4-16). It has been mentioned previously, page 204, that other workers have reported similar changes taking place in solution, Holst, G., (1938); Rabinowitch, E., and Epstein, L.F., (1941); Lewis, G.N. et al., (1943); Michaelis, L., and Granick S., (1945); Vickerstaff, T., and Lemin, D.R., (1946) and Schubert, M., and Levine, A., (1955). The spectral changes were attributed to the formation of dimers. Also it has been shown by Bergmann, K., and O'Konski, C.T., (1963), that a monomer-dimer equilibrium exists when MB is adsorbed upon Na-montmorillonite, and it is this equilibrium which caused spectral shifts at different coverages. It was therefore concluded that the spectral changes observed when differing amounts of MB were adsorbed onto silica gel were caused by dimer formation.

The monomer absorbs at 660nm, and the dimer at 612nm. Difficulties are thus introduced when measuring the concentration of MB present. It would be difficult to measure the two composite wavelengths and summate them due to spectral overlap. Figure (4-17) shows the absorbance at the  $\lambda_{max}$  for different concentrations of MB, and the absorbance at 660nm, and 612nm. It will be seen that the absorbance at the  $\lambda_{max}$  most closely coincides with the dimer absorbance, 612nm, at higher concentrations, and most closely coincides with the monomer absorbance at lower concentrations.

FIGURE .(4—15). Diffuse Reflectance Spectra of MB on Silica Gel

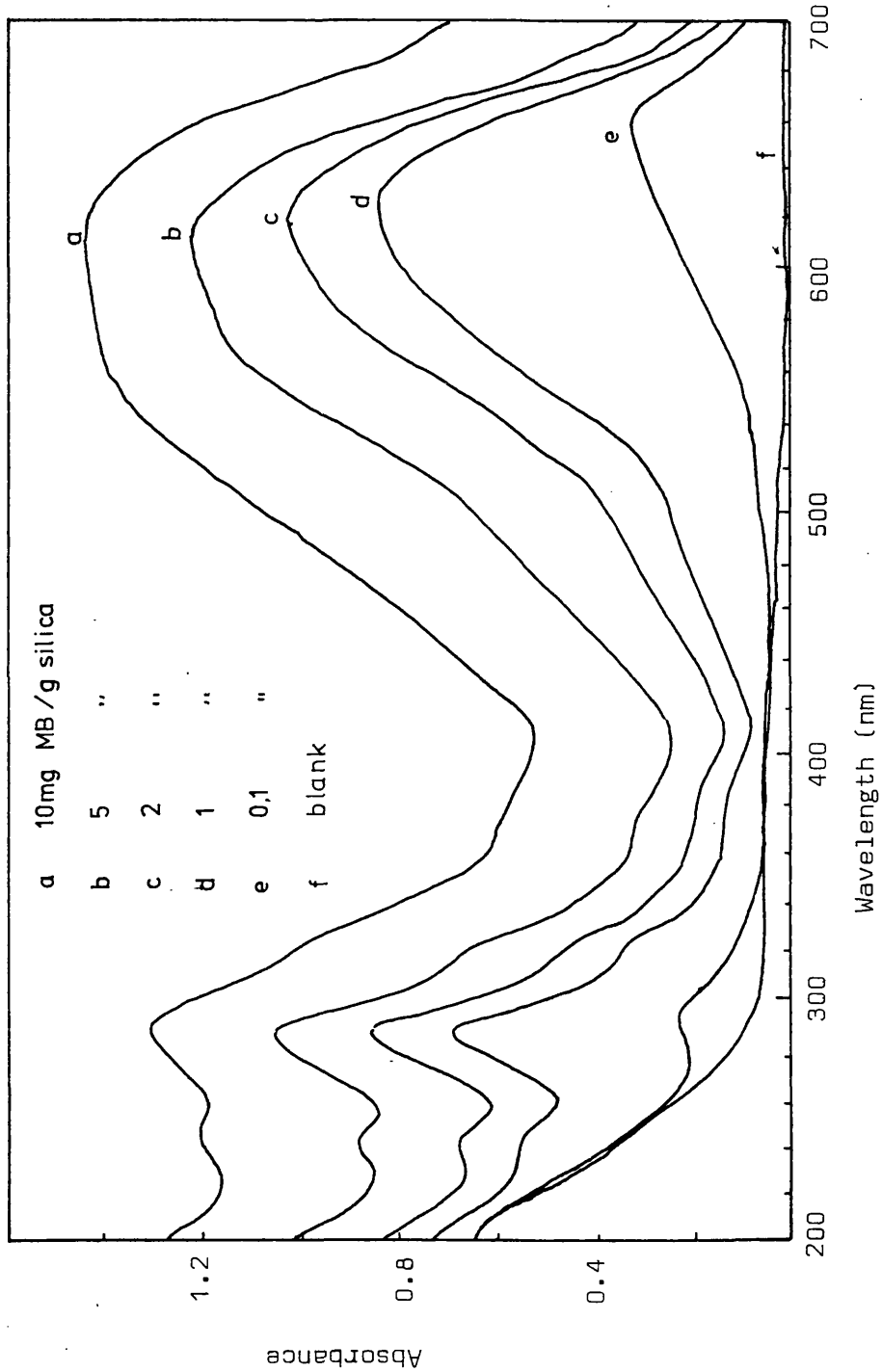


FIGURE. (4-16). Position of the Absorbance Maximum of Methylene Blue at a Function of the Concentration of Methylene Blue on Silica.

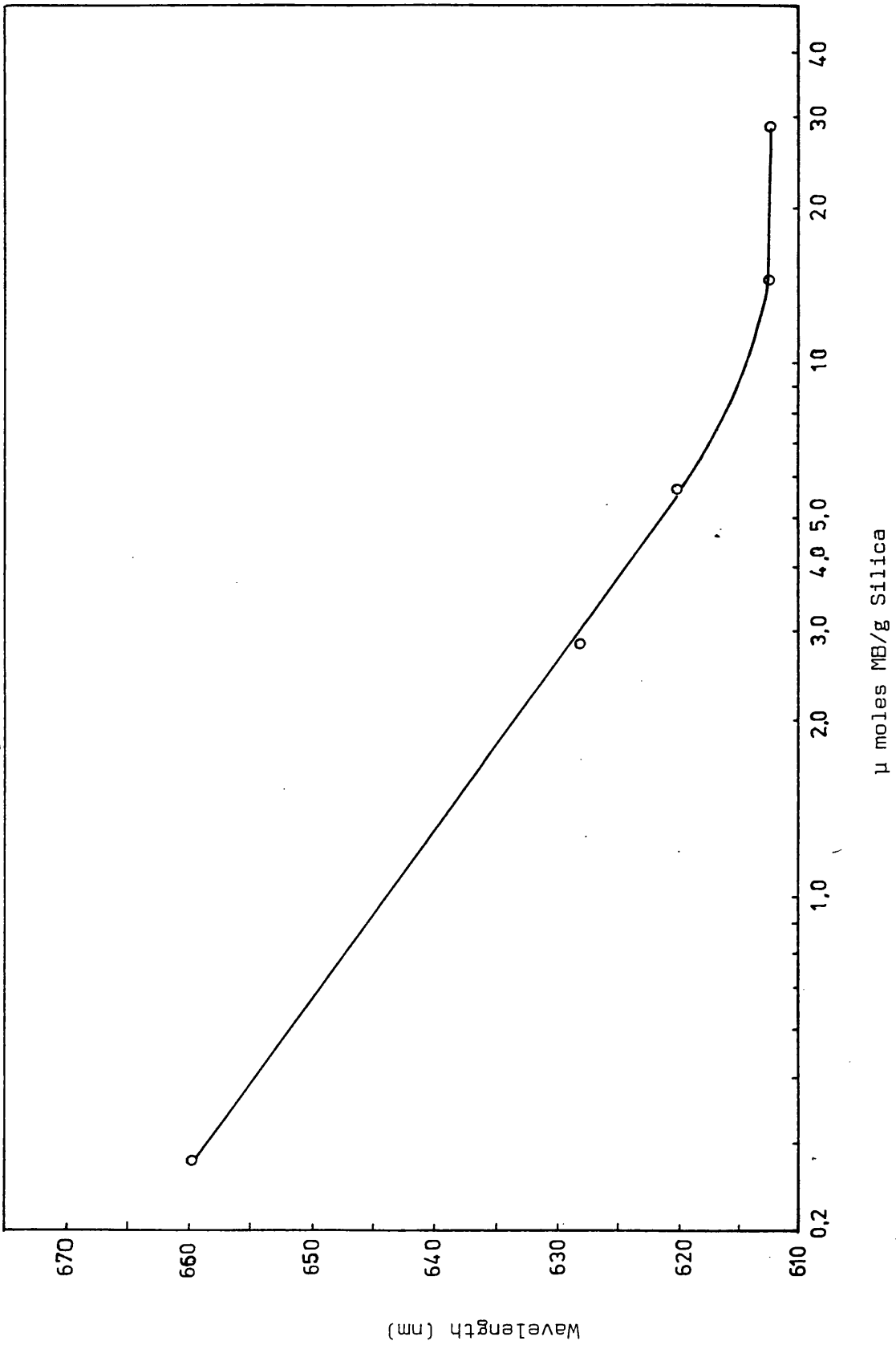
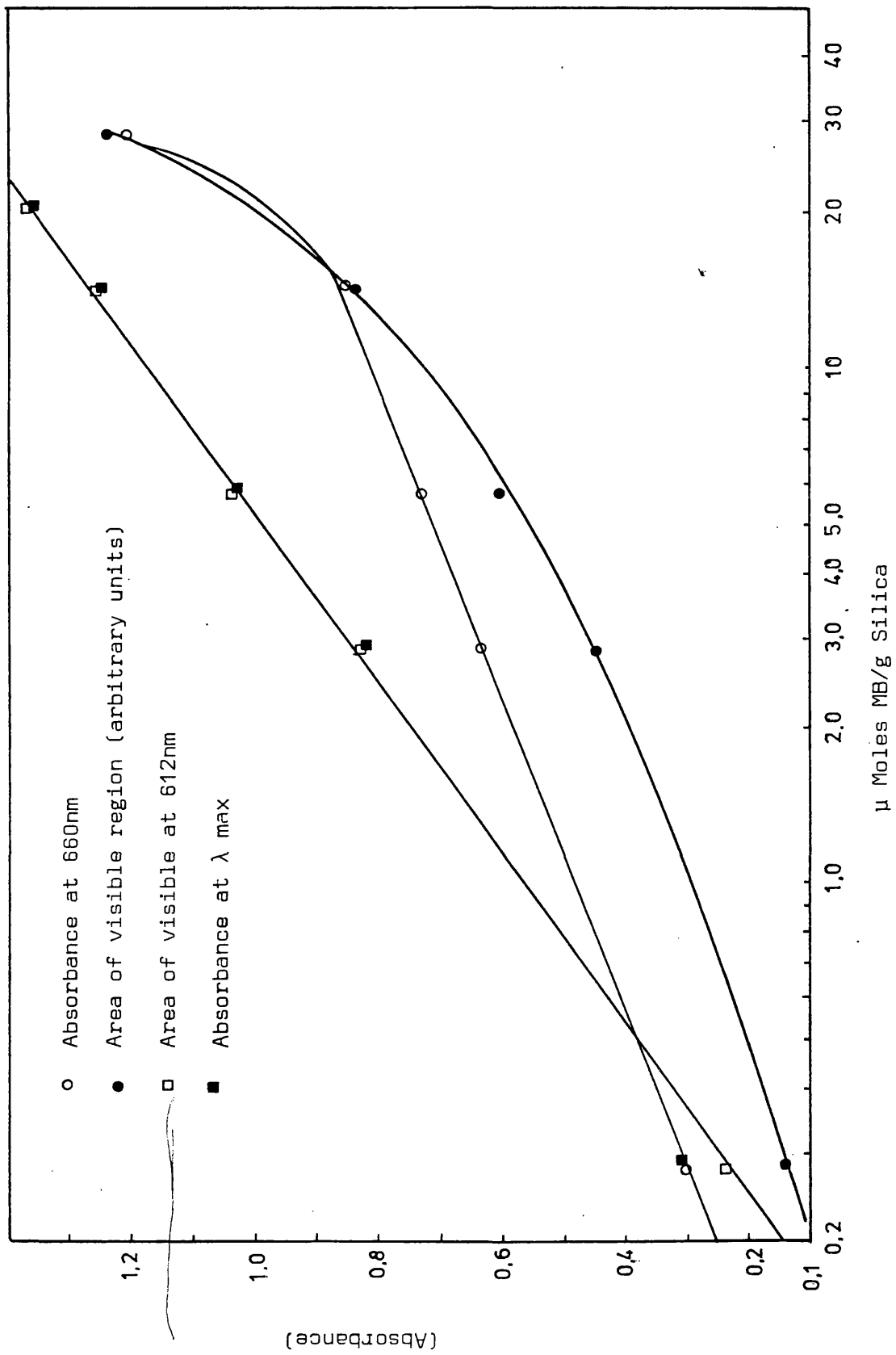


FIGURE (4-17). The Absorbance of MB on Silica Gel



This is explained by:-

From page 208

$$E = E_m + (1 - \alpha)E_d/2$$

If  $\alpha = \frac{CM}{C}$  and  $\alpha \rightarrow 1.0$

Then  $E = E_m$

Also if  $\alpha \rightarrow 0$

Then  $E = E_d$

The extrapolated spectrum of pure dimer has been calculated by Bergmann, K., and O'Konski, C.T., (1963). The dimer in aqueous solution has a  $\lambda$  max of 605nm, and  $E_m^{H_2O} = 13.2 \times 10^4$ .

Calculation of the relative concentrations of monomer to dimer present although possible would be tedious. Also the measurements would be limited by the accuracy of diffuse reflectance,  $\approx 2\%$  error. The area under the spectrum provides a reliable measure of both species, Figure (4-17). This will also measure the presence of other species, particularly decomposition products. This cannot of course be an accurate method due to the differences in the molar extinction coefficients of the species.

The spectrum of methylene blue adsorbed onto silica gel (2.8  $\mu$  moles/g) as a function of time, with and without

irradiation can be seen in Figure (4-18) and Figure (4-19).

The non-irradiated sample remained unchanged, throughout the 13 days of the experiment; within the error of the measurements. But the irradiated sample shows a marked decrease in the absorbance throughout the period of exposure.

Figure (4-20) shows the percentage of the zero time absorbance remaining, estimated by the area method, with time, for the irradiated and non-irradiated samples of methylene blue. It will be seen that the non-irradiated sample remains at  $106 \pm 5\%$ . Errors of up to 10% can be caused by changes in humidity when transferring the sample to the spectrophotometer, and/or by replacing the quartz window over the sample. The experimental error could be reduced by using a sample holder which had a fixed quartz window, and a self contained, relative humidity control. Experimental error would then be approximately 2%. The non-irradiated sample remained at its original value within the experimental error. In contrast the irradiated sample of MB showed a marked reduction in absorbance with time.

Diffuse reflectance gives no indication as to the amount of any particular species present in a mixture, but gives a measure of the total amount of coloured species in the mixture, i.e. a total absorbance in the visible region (400-700nm). The amount of MB present with time cannot therefore be evaluated. Comparing the area measured between 400 and 700nm with the peak height measured at 660nm, the agreement is good between the two methods i.e. 1% difference for 0.28 umoles MB/g silica gel. Demonstrating that the major species present at this coverage was the monomer, and in

FIGURE (4-18). Diffuse Reflectance Spectra of MB on Silica as a Function of Time. Irradiated Sample, 0.1 mg MB/g Silica

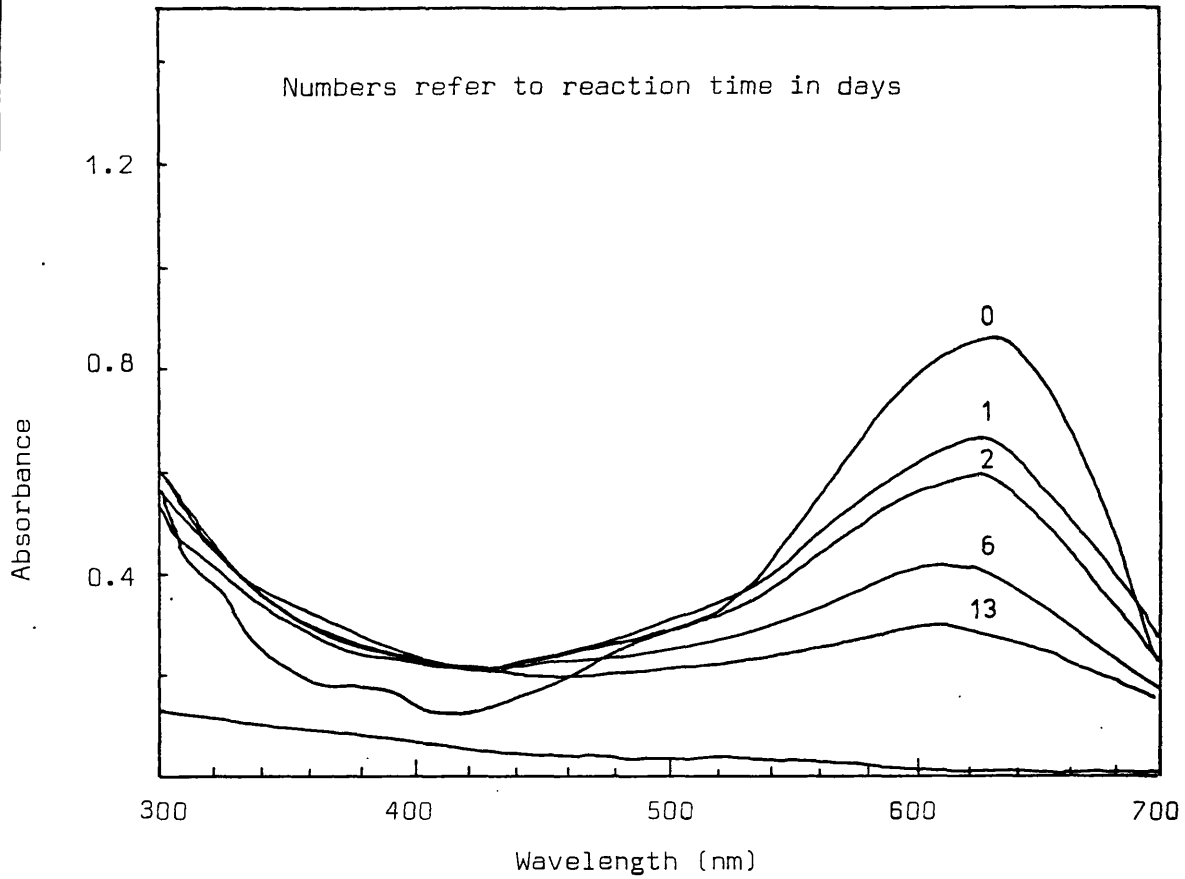


FIGURE (4-19). Diffuse Reflectance Spectra of MB on Silica Gel as a Function of Time. Non-irradiated Sample. 0.1 mg/g Silica

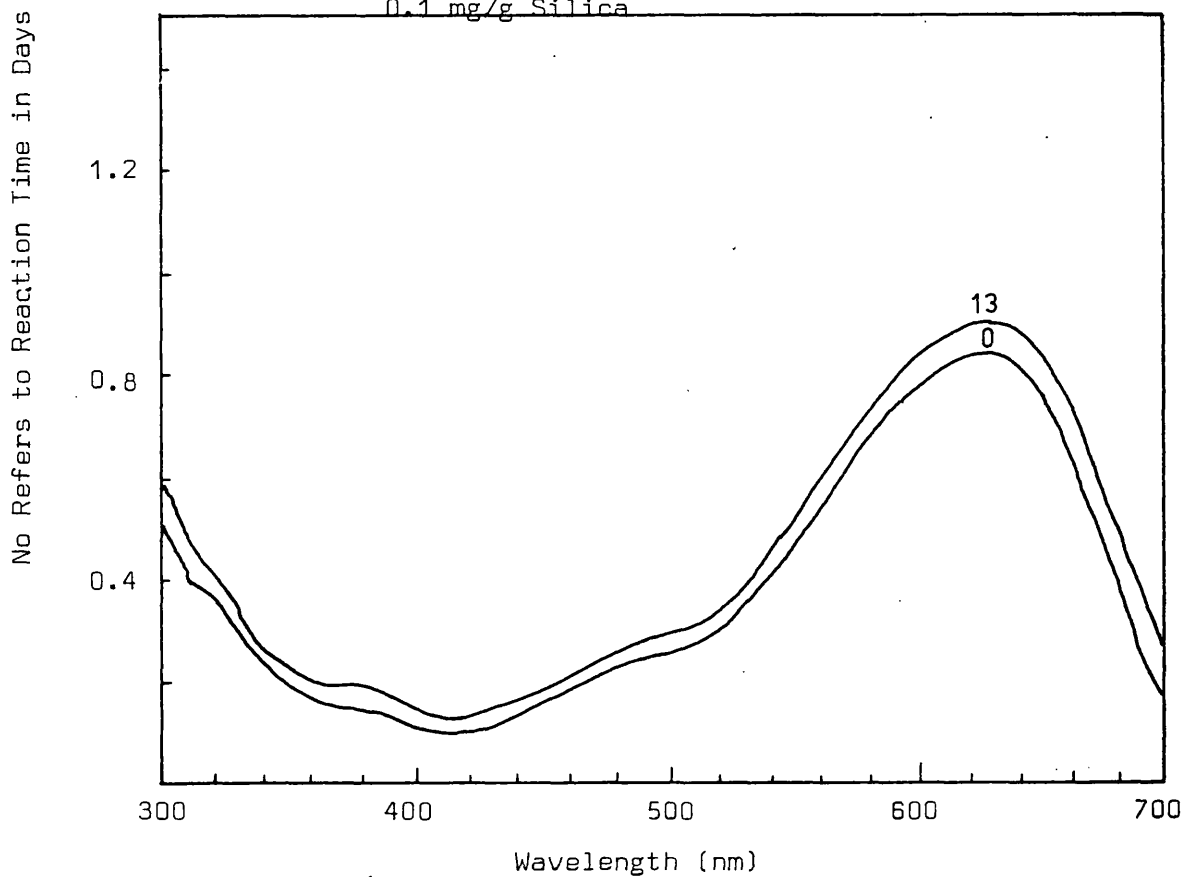




FIGURE (4-20). The Percentage of the Zero Time Absorbance of Methylene Blue on Silica Gel

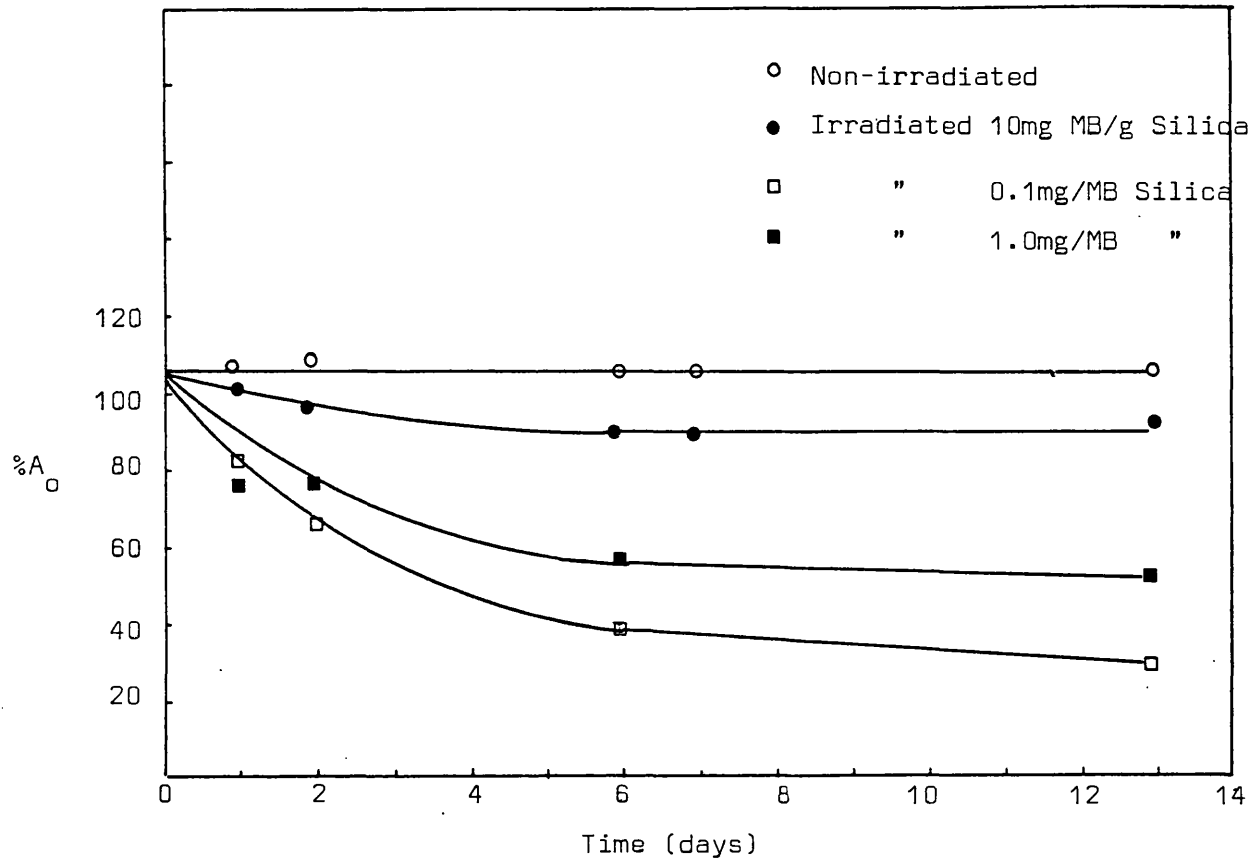
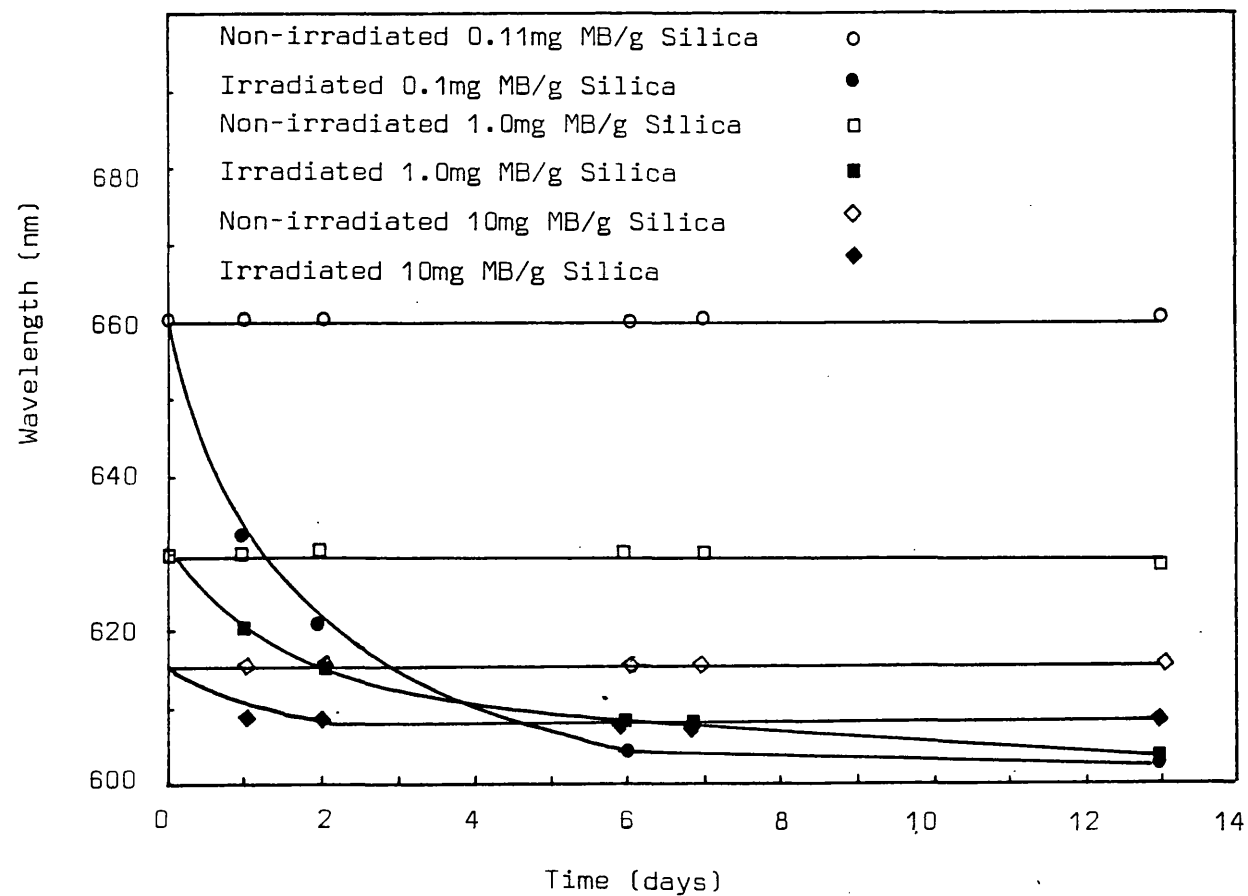


FIGURE (4-21). The Position of the  $\lambda_{max}$  of Methylene Blue on Silica as a Function of Time



this case the reduction in peak height can be ascribed to loss of MB. At other coverages the problem is more complex, since removal of either dimer or monomer from the equilibrium  $2MB \rightleftharpoons MB_2$  will result in a change of concentration of the other component, in order to maintain the equilibrium. It is apparent that the total absorbance of coloured species remaining, with time, changes with different coverages, but not in a predictable way,  $28 > 0.28 > 2.8 \mu \text{ moles g}^{-1}$ .

Figure (4-18) shows the general loss of shape of the absorbance curve, both in the ultra-violet and visible region of the spectrum. The change of shape indicates decomposition of methylene blue, but cannot specifically identify individual components. The position of the absorbance maximum, with time, at 28, 2.8 and 0.28  $\mu$  moles MB/g silica is shown in Figure (4-21). As expected, the different coverages have different absorbance maxima, at zero time, (660nm, 0.28  $\mu$  moles/g; 628nm, 2.8  $\mu$  moles/g; 612nm, 28  $\mu$  moles/g), due to dimer formation at the higher coverages. The position of the absorbance maxima of the non-irradiated samples remained constant throughout the experimental period. Whereas irradiation of the samples caused a hypsochromic shift. The largest shift was seen at the lowest coverage, 0.28  $\mu$  moles/g, (660 to 602nm). The absorbance maximum after 13 days was independent of coverage, 602 to 608nm. This suggests that one of the final products of irradiation was thionine,  $\lambda \text{ max} = 599 \text{ to } 605\text{nm}$ .

4.3.8 A Diffuse Reflectance Study of Benzoyl leuco  
Methylene Blue, Adsorbed upon Silica Gel

When BLMB was absorbed upon silica gel G, a pale blue colour was formed. Diffuse reflectance shows a peak in the visible region at 660nm, Figure (4-22). Since MB has a  $\lambda$  max at 660nm, it was concluded MB was formed initially. The amount produced varied with the amount of BLMB applied to the silica, Table (4-10).

Table (4-10) The Percentage of MB Initially Formed from BLMB  
Upon Silica

BLMB $\mu$ moles/g Silica	$\mu$ moles MB (660nm)	% MB (peak height at 660nm)
28	0.36	1.25
14	0.34	2.49
5.6	0.28	5.0
2.8	0.22	7.9
0.28	0.11	39.3

It will be seen that the total amount of MB initially produced tends to a limiting value of 0.36  $\mu$  moles MB/g silica. This suggests that there are a limited number of sites which will react instantaneously with BLMB to form MB. If the MB were simply an impurity the percentage would remain constant for all coverages.

FIGURE (4-22). The Diffuse Reflectance Spectra of MB Produced from BLMB on Silica Gel. Non-irradiated Sample 10mg MB/g Silica

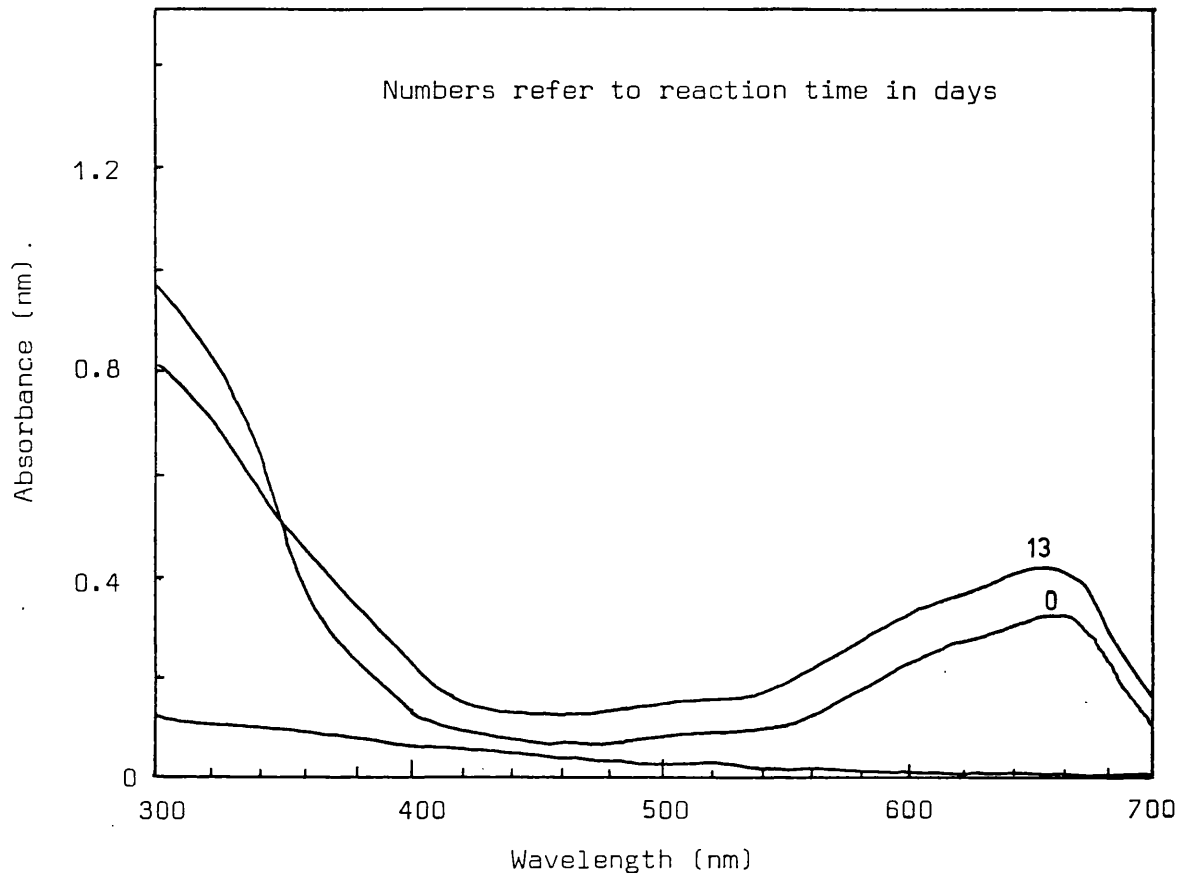
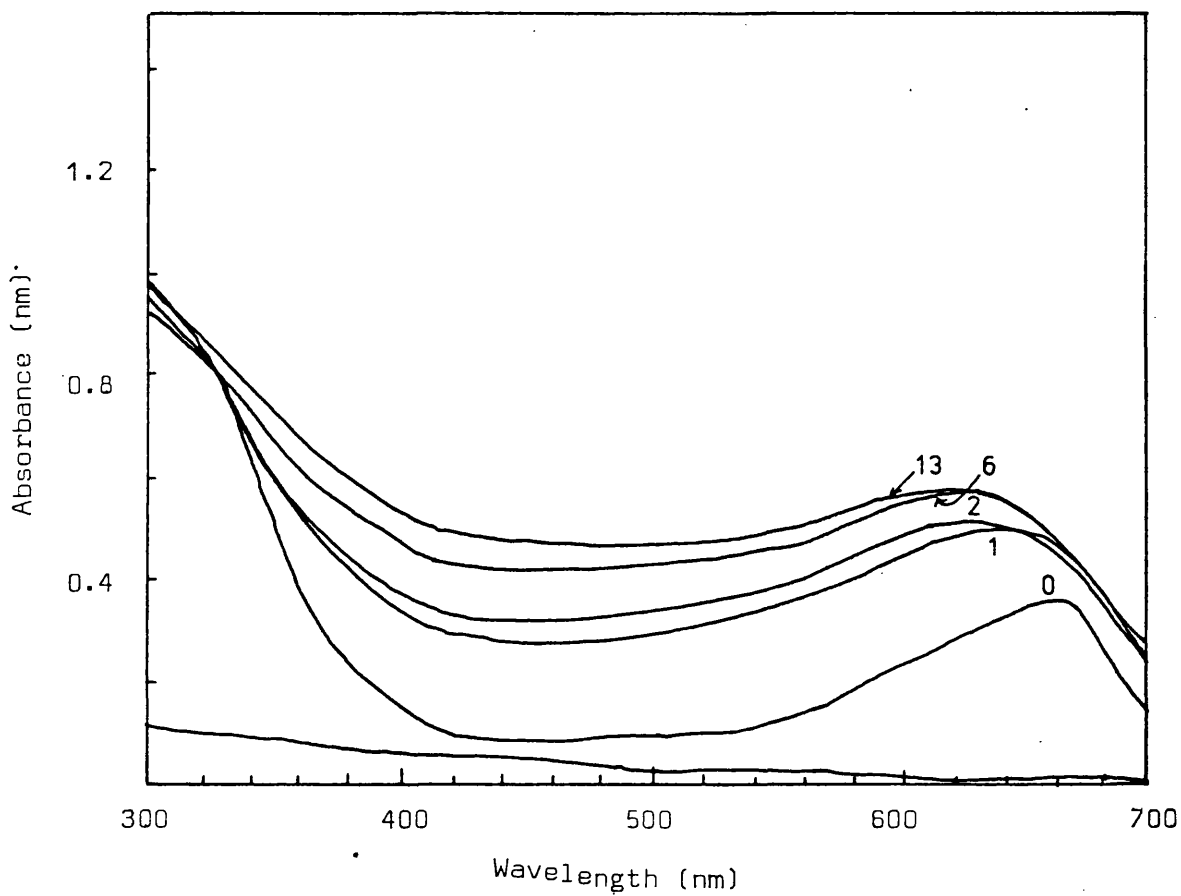


FIGURE (4-23). The Diffuse Reflectance Spectra of MB Produced from BLMB on Silica Gel. Irradiated Sample 10mg MB/g Silica.



The MB produced from BLMB must be subject to the same reactions as MB directly applied. The area underneath the absorbance curve of the MB produced was measured and the percentage of the possible total MB was calculated, Table (4-11)

Table (4-11) The Percentage of Methylene Blue Produced from BLMB Applied to Silica Gel

(BLMB) $\mu$ moles/g Silica	$\mu$ moles MB Produced	% MB Produced
28	0.64	2.3
2.8	0.21	7.5

These values agree closely with Table (4-10), especially for the values at 2.8  $\mu$  moles/g, where the agreement was within 4%. Area values were not used for 0.28  $\mu$  moles/g silica. The area measurements deviated further from the peak height measurements, as more MB was produced.

The reaction of BLMB on silica gel, measured by the absorbance produced, as a function of time is shown in Figure (4-24). The non-irradiated samples did not increase in absorbance after the initial period, i.e. 2.3 and 7.5% for 28 and 2.8  $\mu$  moles BLMB/g silica respectively. Irradiation caused a significant increase in the total absorbance produced see Figure (4-23) and (4-24) at 28  $\mu$  moles/g the absorbance initially increased but then plateaued. If the

results are plotted as  $\log_e$  percent BLMB vs. time, first order kinetics are observed, with a rate constant at  $40^\circ\text{C}$  of  $1.4 \times 10^{-7} \text{ sec}^{-1}$ , see Figure (4-25). The rate constant measured was approximately 1/10 of the rate constant in acidic solution ( $0.5\text{M H}_2\text{SO}_4$ ), as measured by Gensler W.J., et al., (1966). This would give a half life for the reaction of 57 days.

At a coverage of  $2.8 \mu$  moles/g silica the reaction proceeds differently. After a rapid initial increase in absorbance, the absorbance then falls at a constant rate so that 20% of the total possible absorbance was produced after 2 days, but by 13 days only 17% remained. It is a well known phenomenon that fading is dependent upon the total quantity of material present, and that larger quantities of dye applied tend to resist photochemical degradation to a greater extent than do smaller quantities, Egerton, G.S., and Morgan, A.G. (1970). This may be related to the surface area available to each molecule, the lower the coverage the greater the surface area per molecule, and hence more reactive sites are available to each molecule.

There was also a general increase in the absorbance at wavelengths lower than 660nm. MB produced on silica gel, from the BLMB, requires light, and the MB so produced is concurrently degraded, (demethylated), Figure (4-26), causing an increase in the absorbance at wavelengths below 660nm.

This supports the findings of other workers, who have shown by other methods that MB was produced from BLMB on silica gel via a light induced free radical mechanism, Potts, H.A., et al (1972).

FIGURE (4—24). The Percentage of Possible Total Absorbance of MB Produced from BLMB on Silica Gel.

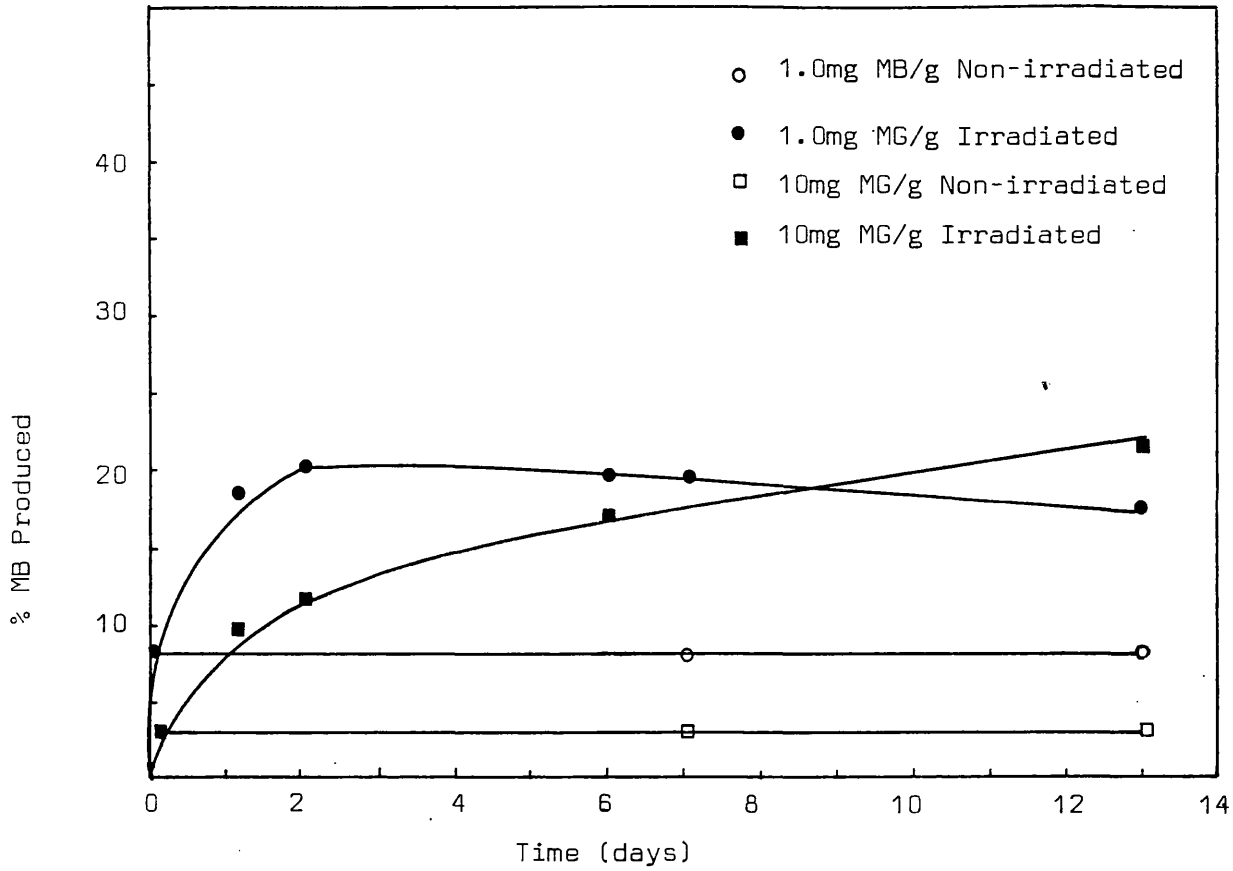


FIGURE (4—25). First Order Production of MB from BLMB on Silica Gel

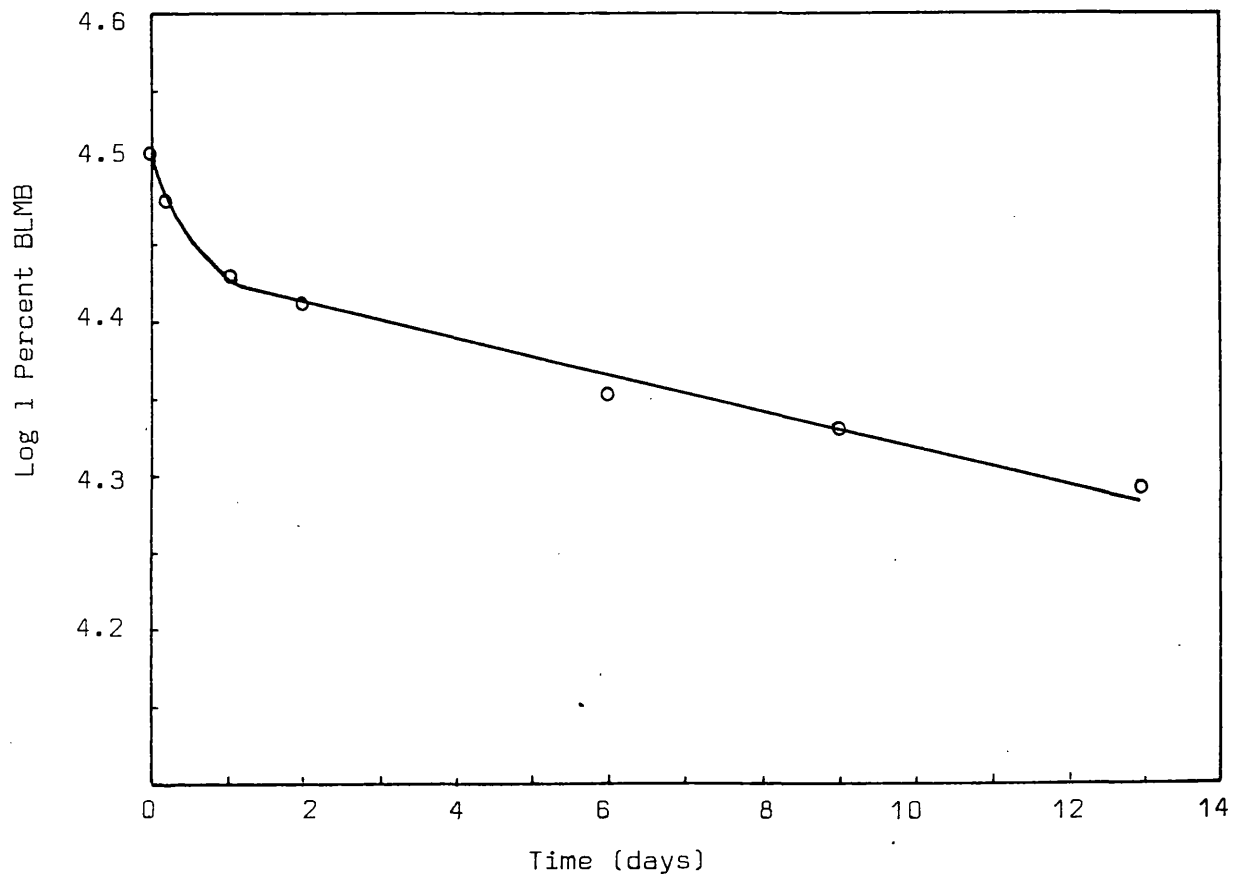
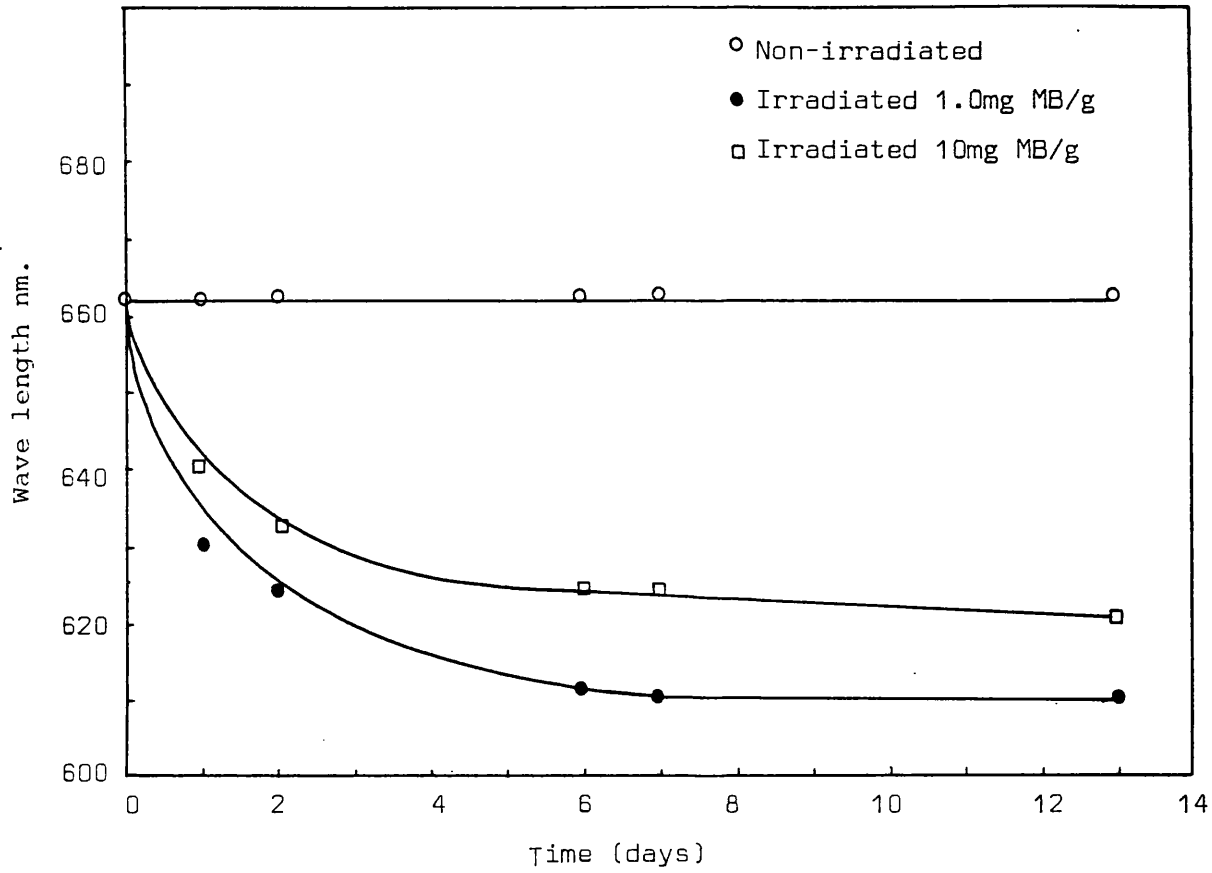
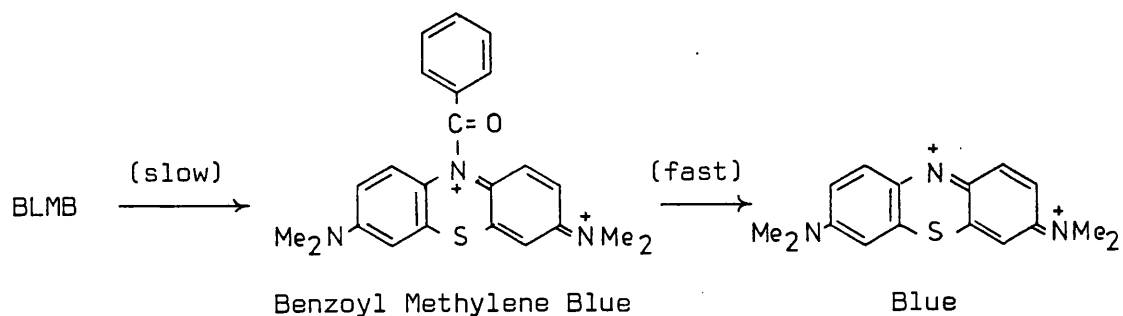


FIGURE (4-26). The position of the  $\lambda_{\max}$  of MB produced from BLMB on Silica.





The reaction would be as follows:-



Where the production of the coloured intermediate benzoyl methylene blue would be the rate determining step in the reaction.

The tendency of methylene blue and benzoyl leuco methylene blue to readily demethylate on silica gel in the presence of light causes the concurrent production of Azure B, Azure A, Azure C and Thionine. Since all the species are present on the surface at the same time there is absorbance throughout the visible spectrum. The colour produced is therefore black.

4.3.9. The Isolation and Identification of the Reaction  
Products of MB and BLMB on Silica Gel

Silica gel was chosen as the reaction medium and, also used as a medium to separate the products of the reaction, because the demethylation products of MB, could be readily desorbed from silica gel, unlike clay mineral systems where they remain firmly adsorbed. Also silica gel has been used throughout the study as a model system, due to its commercial purity and availability.

Table (4-12) shows the TLC separation of the products formed from methylene blue on silica gel with constant irradiation for 30 days at 40<sup>o</sup>C and 0% relative humidity (stored over P<sub>2</sub>O<sub>5</sub>). It will be seen that the major products formed are Azure A, B, C and Thionine. Their identities were confirmed by comparison of the R<sub>f</sub> with a standard sample see page 228, and also comparing the wavelength maxima with literature values. The products identified were highly coloured and in sufficient quantity to be analysed.

Table (4-12) RTLC Separation of Products Formed From the  
Irradiation of Methylene Blue, at 40<sup>o</sup>C, on Silica Gel

Band NO	Colour	Size (l,m,s)	Mean R <sub>f</sub>	Comments	Observed λ max (aq)
1	Blue	l	0.29	MB	665
2	Blue	m	0.36	Azure B	648
3	Blue	m	0.43	Azure A	640
4	Blue	m	0.48	Sym di methyl Thionine	631
5	Blue	s	0.56	Azure C	616
6	Red/blue	s	0.63	Thionine	604
7	Red/blue	s	0.68	Thionine	605
8	Orange	vs	0.84	-	-

Table (4-13) RTLC Separation of Products Formed From the Irradiation of Benzoyl leuco Methylene Blue on Silica, at 40°C

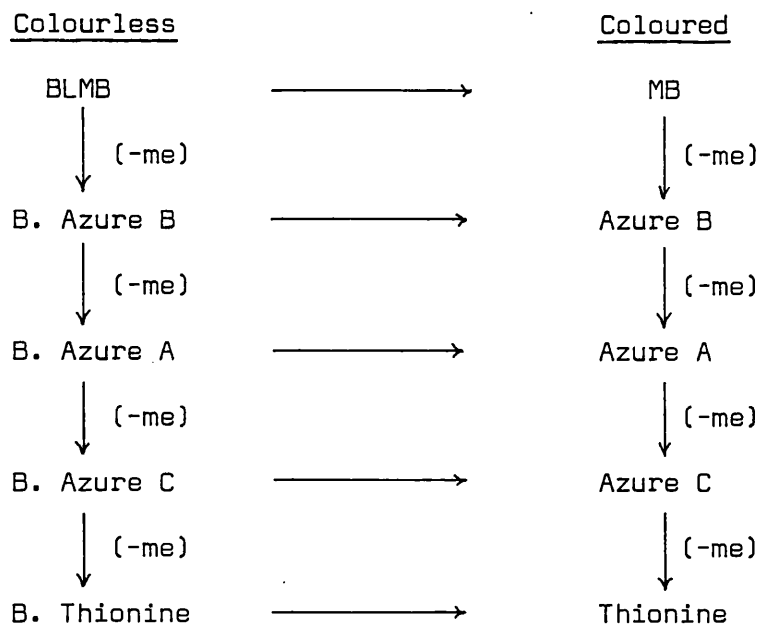
Adsorbent, Solvent and Running conditions as Table (4-12)

Band No	Colour	Size (l,m,s)	Mean Rf	Comments	Observed $\lambda$ max (aq)
1	Blue	m	0.29	MB	665
2	Blue	m	0.36	Azure B	648
3	Blue	s	0.43	Azure A	640
4	Blue	s	0.48		631
5	Blue	s	0.56	Azure C	616
6	Red/blue	vs	0.63	Thionine	604
7	Red/blue	vs	0.68	Thionine	604
8	Orange	vs	0.84	-	-
9	Colourless u/v absorbing	l	0.98	BLMB	-

Other components were separated, but were in insufficient quantity to be identified. Generally these components were not highly coloured and tended to be brown or yellow. The products of the reaction of BLMB on silica gel, are shown in Table (4-13). The BLMB was stored with constant illumination at  $40 \pm 0.5^\circ\text{C}$ , over  $\text{P}_2\text{O}_5$ , for 30 days. It will be seen that the products of the reaction are the same as the products of methylene blue, under the the same conditions; Azure B,A, C and Thionine. These products could be formed either by demethylation of BLMB directly or by the formation of methylene blue, followed by demethylation. Scheme (4-1) shows the possible routes for the formation of the

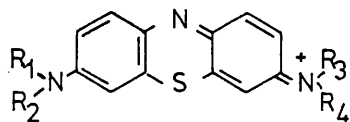
products, Azure A, B, C and thionine from BLMB

Scheme (4-1) Routes for the Demethylation of BLMB



Tables (4-12 and 4-13) indicate, the quantity of the demethylated products decreases with the number of methyl groups removed, i.e. Azure B > Azure A > Azure C > Thionine.

This would indicate that the methyl groups are removed in a sequential manner (i.e.)



MB	Azure B	Azure A	Azure C	Thionine
R <sub>1</sub> = Me	H	H	H	H
R <sub>2</sub> Me	Me	H	H	H
R <sub>3</sub> Me	Me	Me	H	H
R <sub>4</sub> Me	Me	Me	Me	H

4.3.10 The Rate of Demethylation of Methylene Blue  
Absorbed upon Silica Gel

Accurate quantitative estimates of Azure A,B,C and Sym-dimethyl thionine were difficult as reliable values for the extinction coefficients were not available. The purification of large quantities (> 300mg) of commercial Azure A,B, and C was attempted using radial preparative layer chromatography (RPLC). The preparative layer separation proved to be very unsatisfactory as the material travelled along the surface of the layer rather than through the entire thickness. The concentration of dye to silica gel was therefore very high and this probably caused the poor separation.

The extinction coefficients of Azure A, Azure B and Azure C are based on values found experimentally, from recrystallized commercial material. The results show that the extinction coefficients are of the correct order, i.e. they lie between that of methylene blue ( $E_m^{H_2O} = 8.06 \times 10^4$ ) and thionine ( $E_m^{H_2O} = 5.1 \times 10^4$ ) Table (4-14).

The Azure dyes possess fewer methyl groups than methylene blue and more methyl groups than thionine. The methyl groups tending to stabilize the positive charge on the molecule, hence increase the probable lifetime of the excited species.

Table (4-14) Molar Extinction Coefficients of Azure Dyes

	$E_m^{H_2O}$	max (nm)
Azure A	$6.5 \times 10^4$	640
Azure B	$7.3 \times 10^4$	648
Azure C	$5.8 \times 10^4$	618

Commercial samples of sym-dimethylthionine were not available, but the extinction coefficient should be similar to that of Azure A. The breakdown of methylene blue, as a function of time is shown in Table (4-15). It will be seen that the concentration of methylene blue falls off rapidly, and reaches a limiting concentration of 5% of the original concentration after 13 days.

Table (4-15) Percentage Degradation of Methylene Blue on Silica Gel

Time days	MB	Azure B	Azure A	Sym dimethyl thionine	Azure C	Thionine
0	100	-	-	-	-	-
1	43	23	6	6	2	2
2	25	12	8	6	3	2
6	9	8	10	8	4	2
7	5	5	6	6	6	5
13	5	5	5	5	5	5

Each species was formed, and then subsequently breaks down to form the next demethylated species, hence the reaction proceeds as an orderly demethylation.

4.3.11 The Rate of Demethylation of Benzoyl leuco Methylene Blue on Silica Gel

It was observed that the coloured products of the oxidation of BLMB, on silica gel, decomposed when irradiated with white light. The amount of the coloured species formed from BLMB as a function of time are shown in Table (4-16).

Table (4-16) Percentage Decomposition of BLMB on Silica Gel

Time (days)	MB	Azure B	Azure A	Sym dimethyl Thionine	Azure C	Thionine
0	4	1	-	-	-	-
1	5	4	1	1	1	1
2	5	5	2	2	1	1
6	4	4	4	4	2	2
7	4	4	3	3	3	2
13	4	4	4	4	4	4

All values are expressed as percentages of the total amount of BLMB. A complex picture develops and it was difficult to deduce what was the exact mechanism of the demethylation. Since all species are present it would suggest that no step was rate determining e.g. all steps are of a similar rate (the rate constants would therefore be numerically similar). Only the coloured components on the right hand side of scheme (4-1), page 194, have been determined, and not the colourless components. The colourless components could be separated using a different solvent system. It was therefore not possible to determine if BLMB was first demethylated, or the benzoyl group was initially lost.

4.3.12 The Reactions of Benzoyl-leuco Methylene Blue  
on Silica Gel in the Presence of  $\text{Co}^{3+}$  or  $\text{Ce}^{4+}$

The formation of methylene blue from BLMB in acidic solution in the presence of  $\text{Co}^{3+}$  or  $\text{Ce}^{4+}$  has been described earlier, page 212 and 220 Chapter 4. It can be seen from these studies that the ions are needed in at least stoichiometric amounts to accelerate the reaction. In the presence of equi-molar concentrations of these ions the reaction rate was accelerated by approximately  $10^3$  times. The rate of methylene blue production from BLMB, when on equimolar quantity of  $\text{Co}^{3+}$  or  $\text{Ce}^{4+}$  are present on a dry silica gel surface, are shown in Figure (4-27). It will be seen that the initial rate of production of MB was increased several times when either  $\text{Ce}^{4+}$  or  $\text{Co}^{3+}$  were present on the surface. In contrast to the normal reaction of BLMB on silica gel, MB was produced without irradiation, when either  $\text{Ce}^{4+}$  or  $\text{Co}^{3+}$  were present. Also the rate of formation of MB was faster in their presence, than on silica which was irradiated. When BLMB-silica were irradiated in the presence of  $\text{Co}^{3+}$  or  $\text{Ce}^{4+}$ , the rate of MB production was greater than in the absence of irradiation. Since there was no light requirement for the reaction of  $\text{Co}^{3+}$  or  $\text{Ce}^{4+}$  with BLMB, it would seem that there was a direct attack by  $\text{Ce}^{4+}$  or  $\text{Co}^{3+}$  on BLMB. These ions are of high oxidation potential, and it is likely that they oxidized BLMB to benzoyl methylene blue. Hence in the presence of  $\text{Co}^{3+}$  or  $\text{Ce}^{4+}$  when irradiated the rate of the reaction will be the sum of MB produced by the light induced free radical mechanism and that produced by electron transfer to  $\text{Co}^{3+}$  or  $\text{Ce}^{4+}$ .



FIGURE (4-27). The Production of MB from BLMB on Silica Gel in the Presence of  $Ce^{4+}$  or  $Co^{3+}$  (10mg BLMB/g Silica)

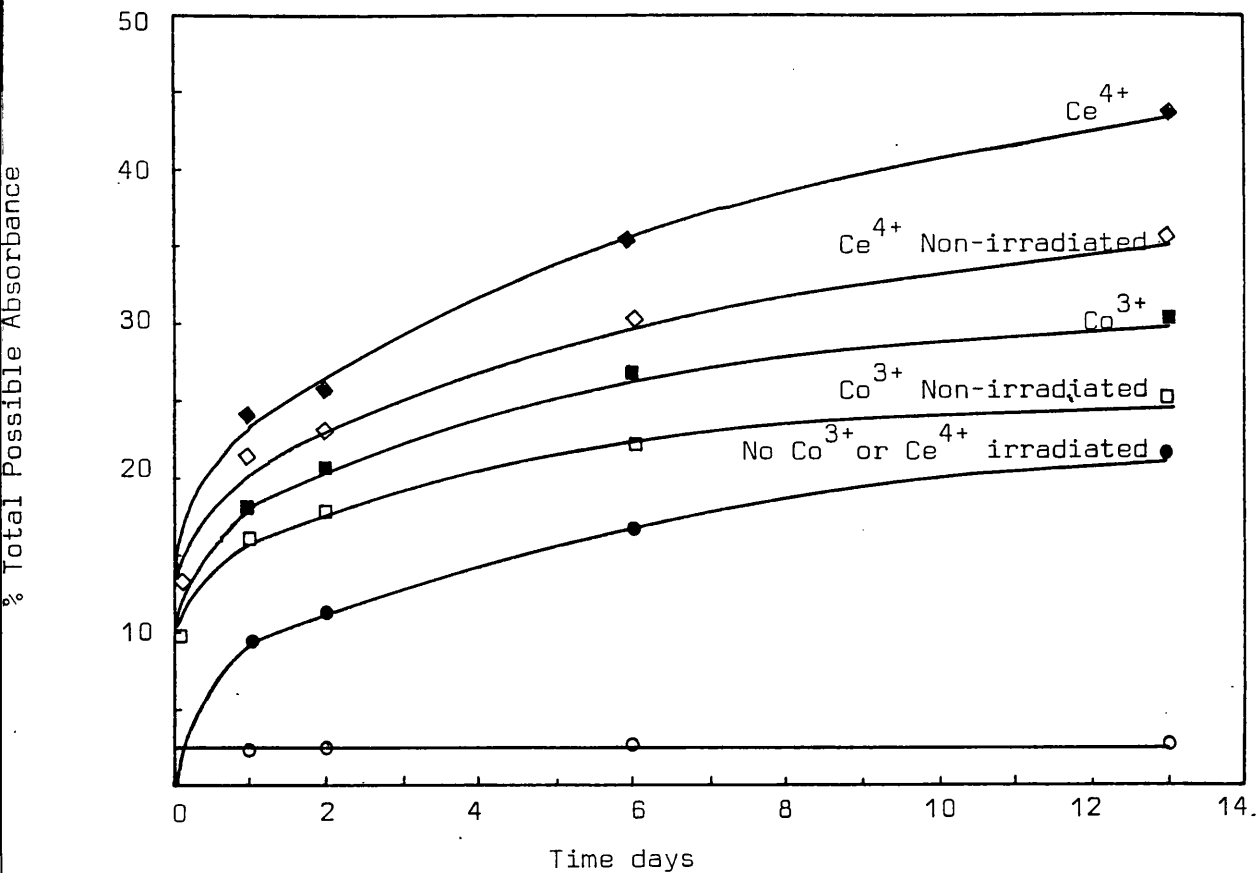
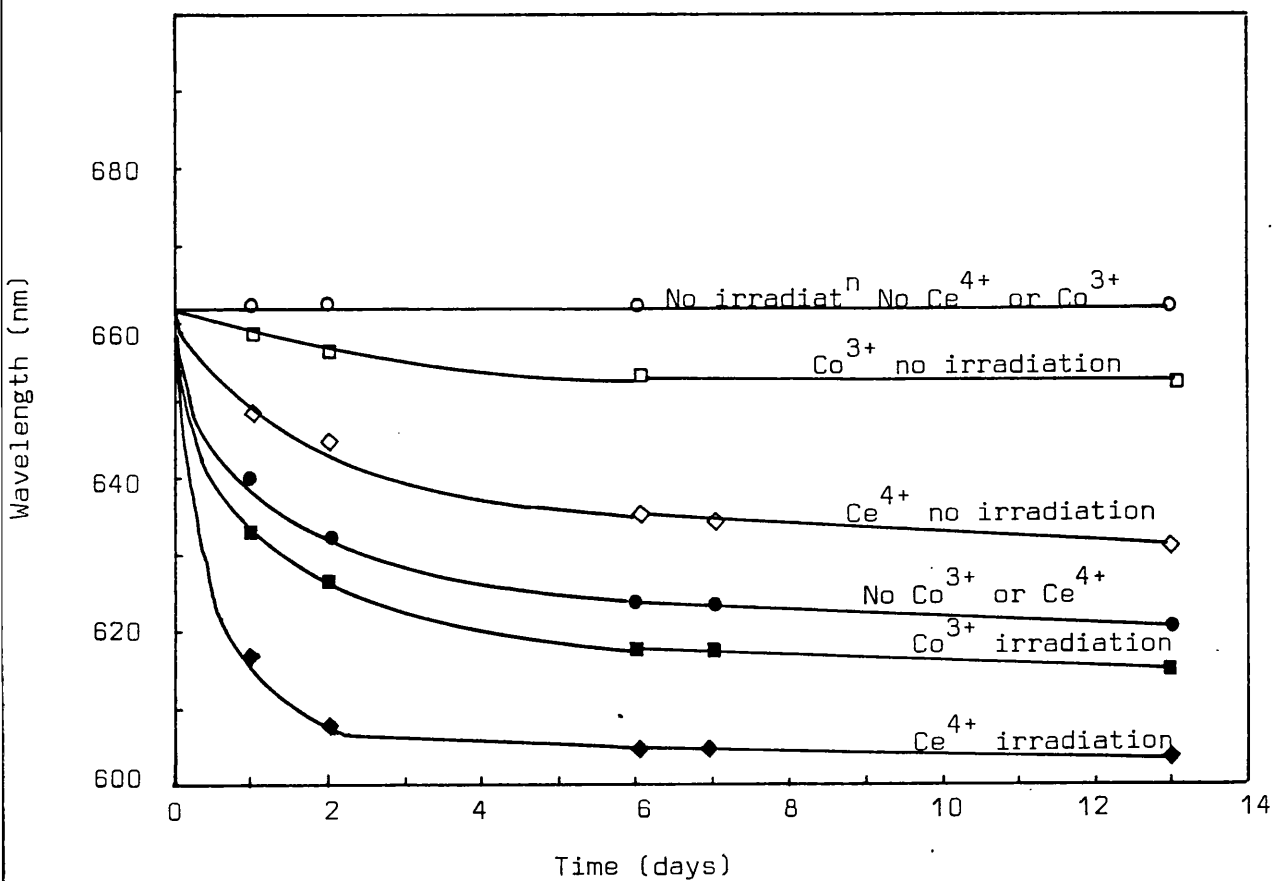
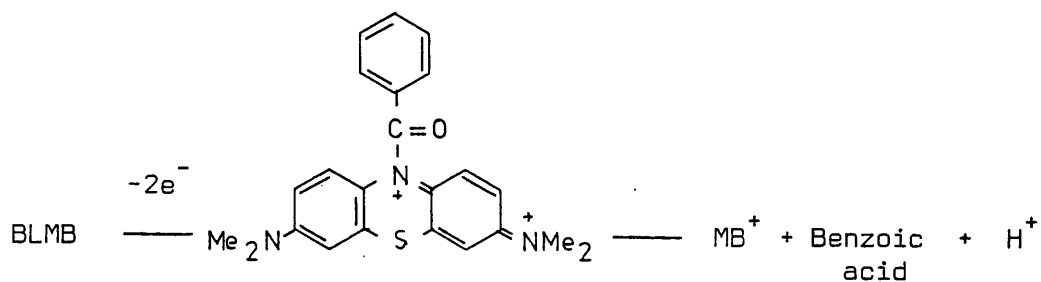


FIGURE (4-28). The Position of the max of MB Produced from BLMB in the Presence of  $Ce^{4+}$  (10mg BLMB/g Silica)





The bathochromic shift of the absorption maximum shows that the MB produced was subsequently attacked by  $\text{Ce}^{4+}$  or  $\text{Co}^{3+}$ , Figure (4-28), without the requirement for light. The  $\text{Ce}^{4+}$  therefore oxidises the MB formed, producing the demethylated derivatives of MB. The greater the excess of  $\text{Ce}^{4+}$  the more pronounced the oxidation. At an equimolar concentration a quantitative yields of MB is produced in less than a day.  $\text{Co}^{3+}$  also tends to oxidise the MB produced, but to a lesser extent than  $\text{Ce}^{4+}$ .

4.3.13      A Diffuse Reflectance Study of Methylene Blue  
Adsorbed upon Silton

The spectra of methylene blue at various concentrations, (28  $\mu$  moles to 0.28  $\mu$  moles/g Silton), adsorbed onto Silton are shown in Figure (4-29). It will be seen that the spectrum differs substantially from that on silica gel Figure (4-14). The wavelength of maximum absorbance was at 688nm compared with 660nm on silica gel, for the monomer. Also the spectrum of methylene blue on Silton did not markedly change with increasing coverage, as it did on silica gel. This suggests that the monomer was the sole species present, even at high coverages. The spectrum on Silton shows greater detail than on silica gel and in this respect more closely resembles the spectrum in solution. The position of these additional peaks were not identical to those of the solution spectrum. Additional peaks were resolved on Silton at 370, 410 and 466nm. Peaks at similar positions are resolved in ethanolic solution. The peaks were far broader on silica, and this may have obscured the detail. A change in the position of the 1st absorption band to 688nm, a +22nm bathochromic shift, indicates that the energy of the 1st excited state was lower in the bound form than in free solution. Why MB on Silton remains in the monomeric form is difficult to explain, as this cannot be due to the increased surface area of Silton. The surface area of the silica gel used was 500m<sup>2</sup>/g and the quoted surface area of Silton is at least 180m<sup>2</sup>/g, Sugahara, Y et al., (1968). Spectral changes are noticed on silica between 0.28  $\mu$  moles/g and 2.8  $\mu$  moles/g, these trends continue upto the maximum coverage of 28  $\mu$  moles/g. If it were an area effect there would be noticable spectral changes between 0.28  $\mu$  moles/g and 28  $\mu$  moles/g on Silton. These differences were not observed. Therefore the Silton-dye interactions must be of

FIGURE (4-29). The Diffuse Reflectance Spectra of Methylene Blue on Silton

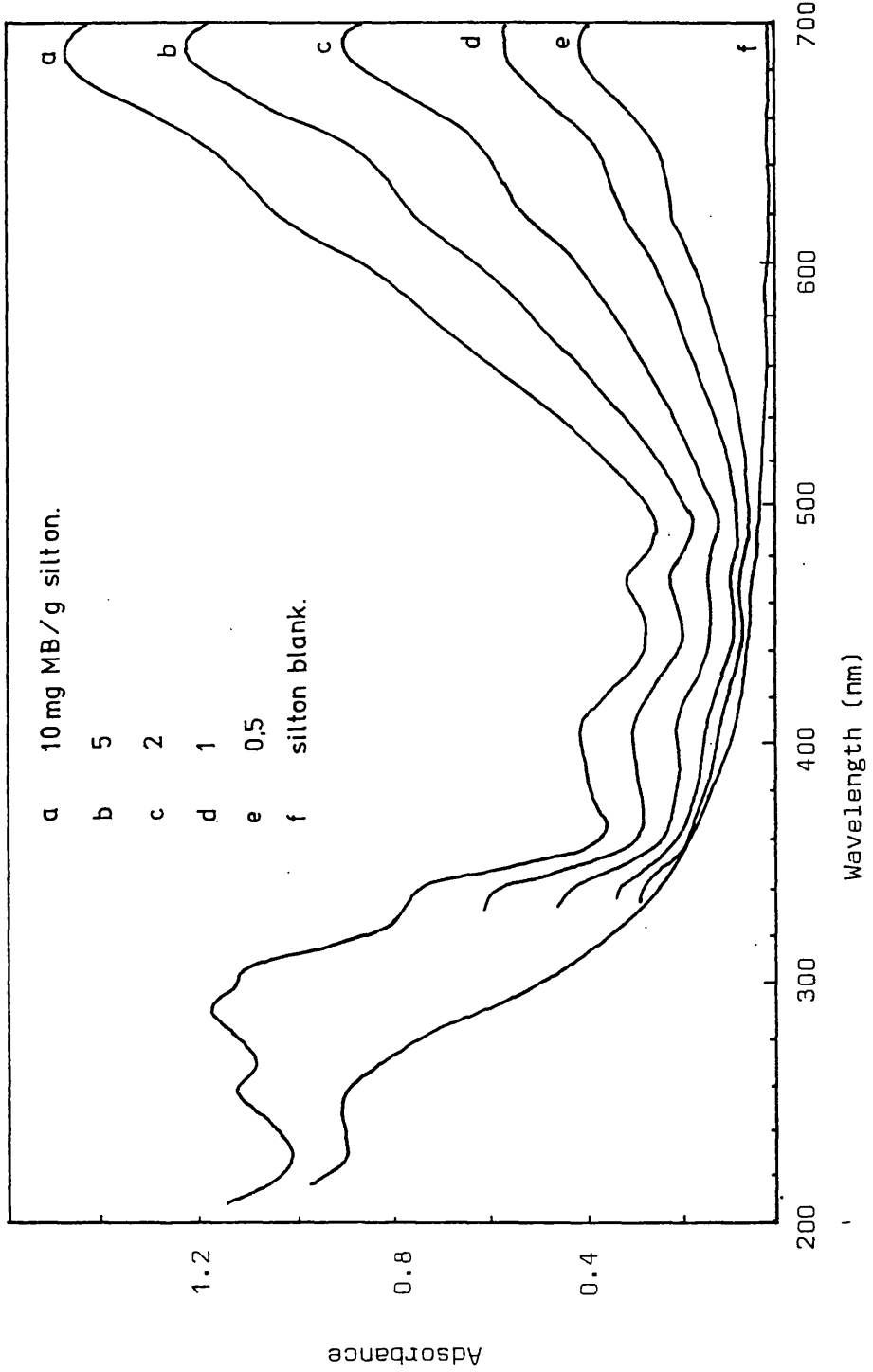


FIGURE (4-30). The Absorbance of Methylene Blue on Silton

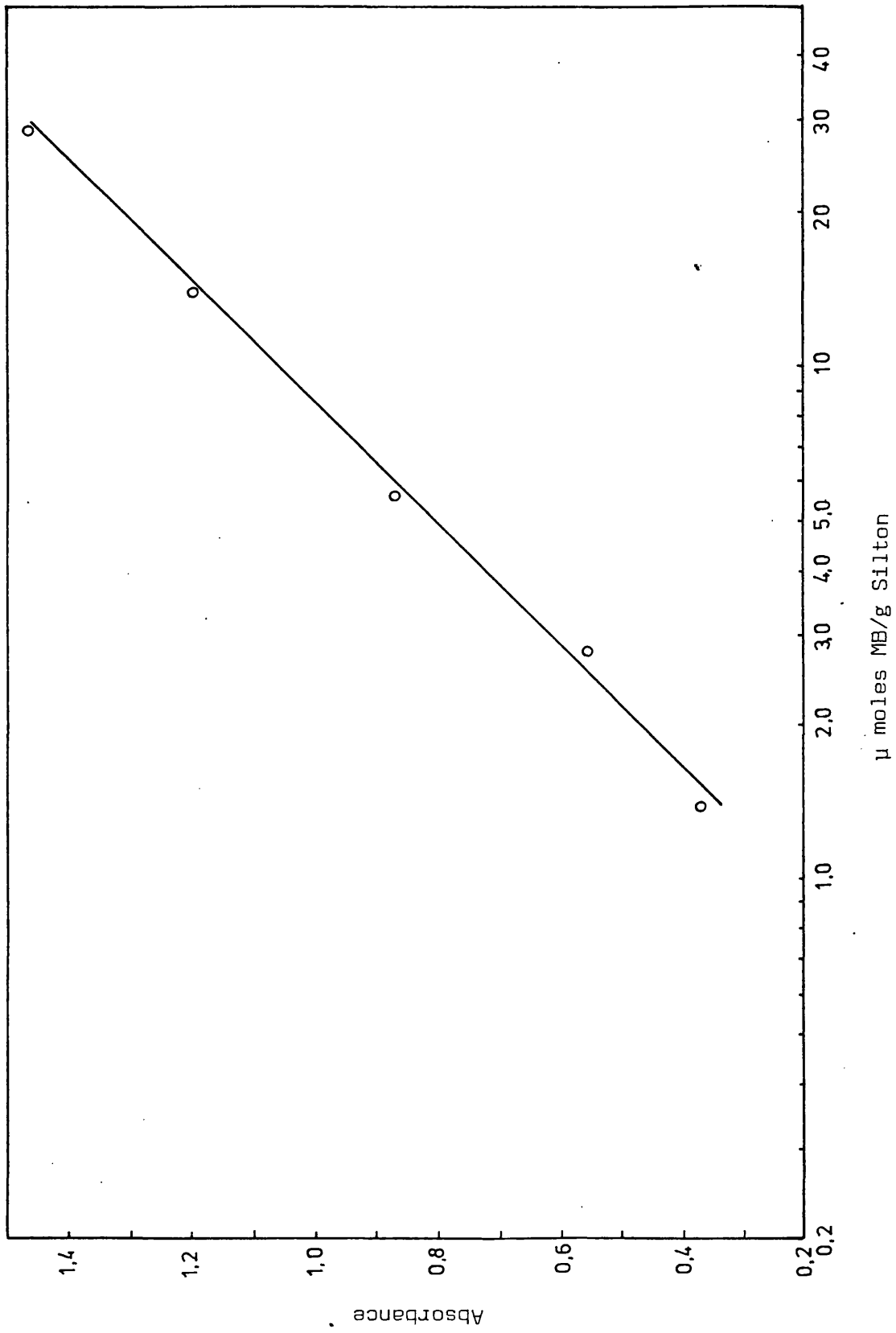


FIGURE (4-31). The Percentage of the Zero time Absorbance of MB on Silton, Non-irradiated

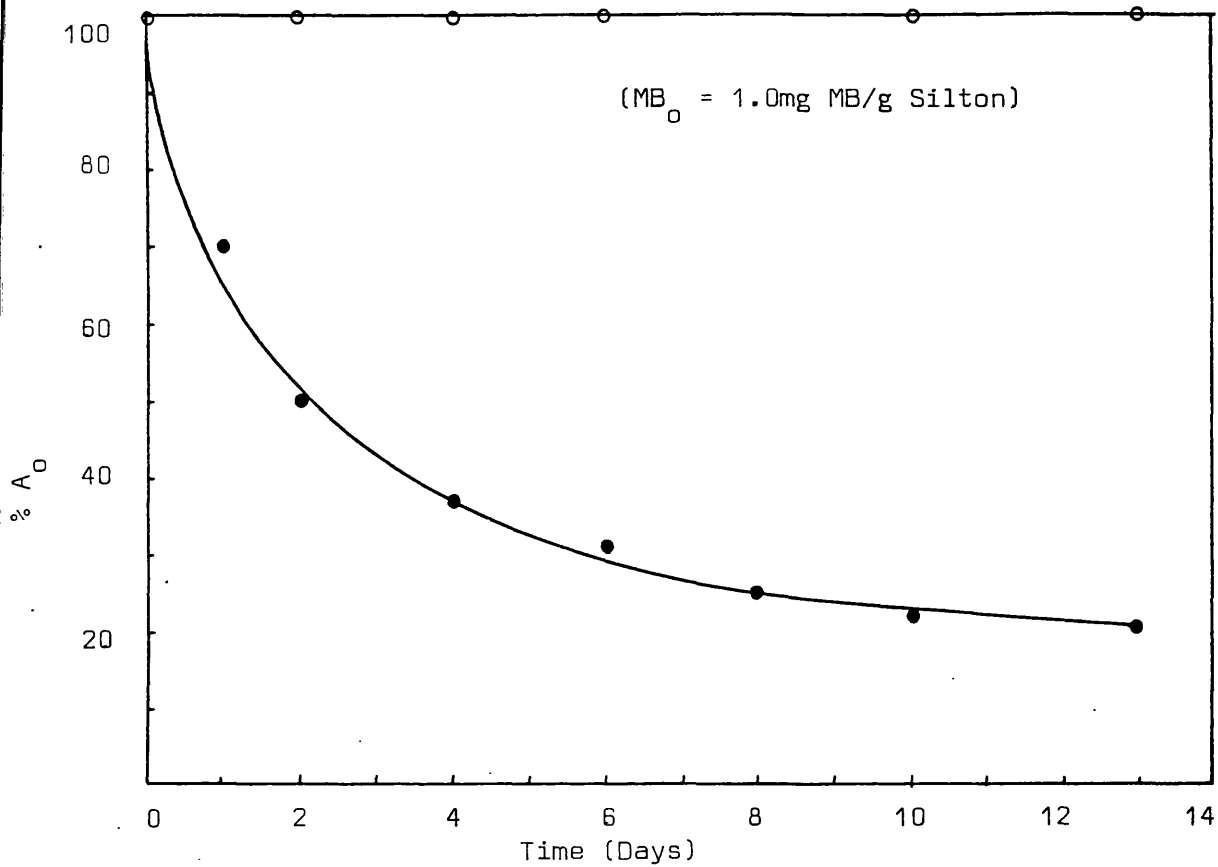
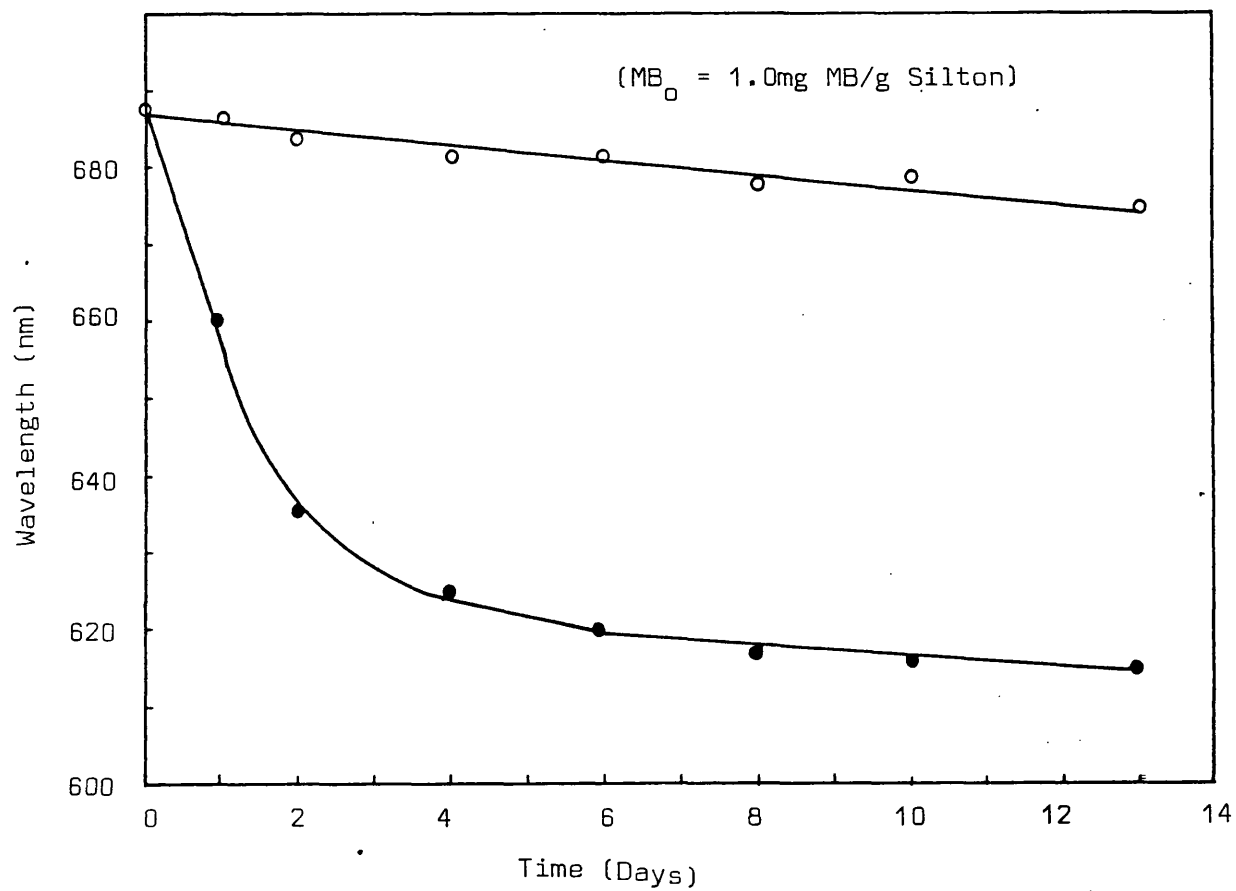


FIGURE (4-32). The Position of  $\lambda$  max of MB adsorbed on Silton



a different kind to those on silica. It has been established in this study that chromatographic solvent systems which move MB on silica cannot move MB on Silton, showing that the dye-Silton interactions are extremely strong. It is likely that dye-Silton interactions are more favourable than  $MB^+-MB^+$  interactions, which are observed on silica. It is precisely these strong dye-Silton interactions which cause large spectral perturbations. The result of having very little dimer formation can be seen in Figure (4-30), where the plot of absorbance versus amount applied is a straight line. The amount of MB remaining after irradiation is shown in Figure (4-31). It can be seen that there was approximately 20% of the original amount applied, after 13 days, irradiation, and 100% remained without irradiation, at all coverages. The positions of the  $\lambda_{max}$  as a function of time are shown in Figure (4-32). The  $\lambda_{max}$  of the irradiated sample fell rapidly after 48hrs to 635nm and then slowly to 615nm after 13 days. The  $\lambda_{max}$  of the non-irradiated sample shift towards shorter wavelengths, 688 to 675nm after 13 days. Methylene blue behaves qualitatively in a similar manner on Silton as it does on silica gel. But quantitatively there was a larger proportion of methylene blue remaining after the same period of time, approximately four times the amount. But there was still a large hypsochromic shift, indicating extensive demethylation. The non-irradiated sample also undergoes some demethylation as shown by the -13nm hypsochromic shift. This is not observed on silica.

4.3.14 A Diffuse Reflectance Study of Benzoyl Leuco Methylene  
Blue Absorbed on Silton

Irradiation of BLMB absorbed on Silton caused the production of a coloured species with an absorption maximum at 688nm. The same absorption maximum as MB adsorbed on silton. Continued irradiation caused further production of MB, and the position of the absorption maximum shifted to shorter wavelengths, indicating demethylation. The percentage of possible absorbance as a function of time is shown in Figure (4-33). Greater amounts of MB are produced on Silton, compared with that produced on silica. If  $\log_e$  per cent BLMB was plotted versus time, a straight line was produced, after an initial rapid phase, Figure (4-34). The rate constant for the reaction, at 40°C, was  $K_{40} = 4.1 \times 10^{-7} \text{ Sec}^{-1}$ . An overall increase of three times, over the reaction on silica. This gave a half life of 19.6 days. The peak height at 688nm was measured as a function of time, Figure (4-35).

This was a measure of the amount of MB present. Initially about 5% was present, this rises to 15% after 24hrs but then slowly falls and reaches a constant value of 8% after 13 days.

Hypsochromic shifts are observed Figure (4-36), indicating the general trend of demethylation, as with BLMB and MB on silica.



FIGURE (4-33). The Percentage of Possible Absorbance of MB Produced From BLMB on Silton; Measured at the  $\lambda$  max

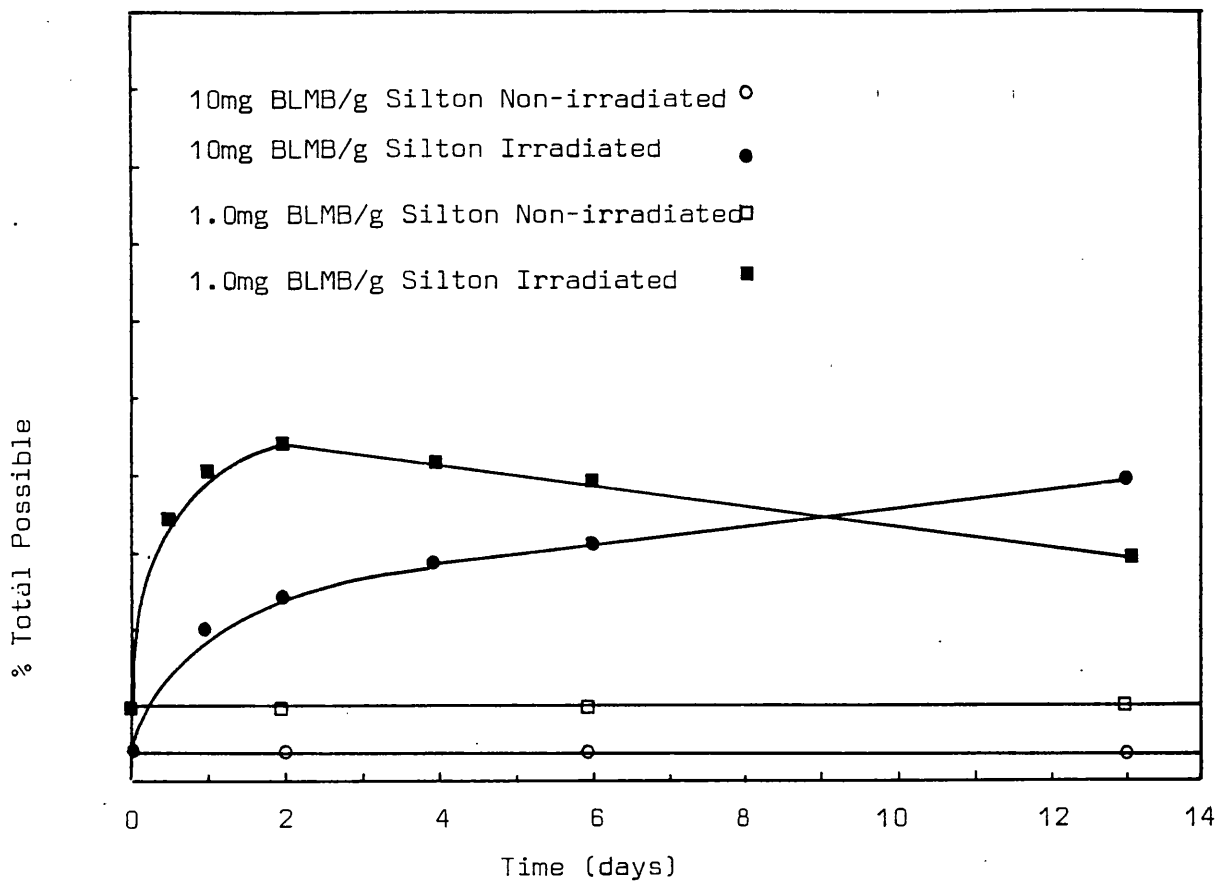


FIGURE (4-34). A First Order Plot of the Production of MB from BLMB on Silton

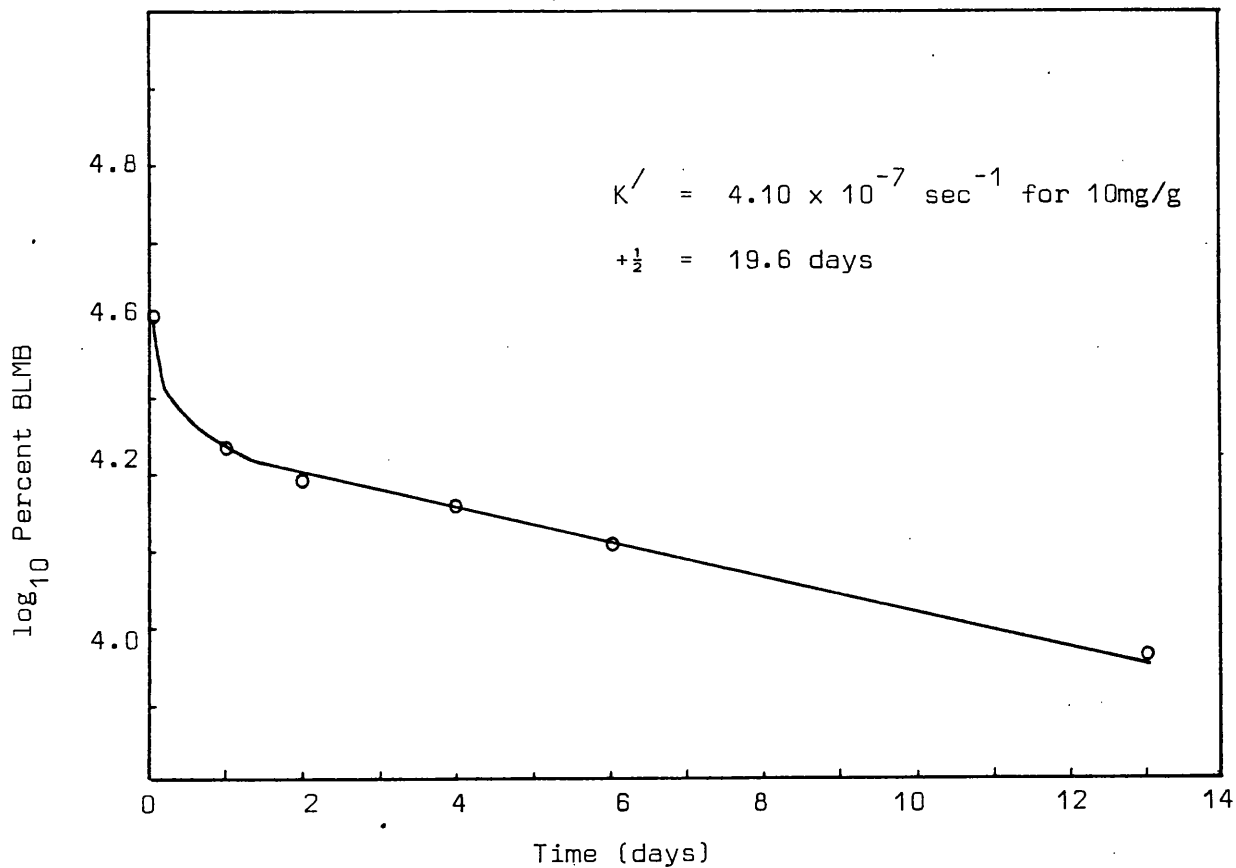


FIGURE (4-35). The Percentage of Possible Total MB Produced from BLMB on Silton, Measured at 668nm

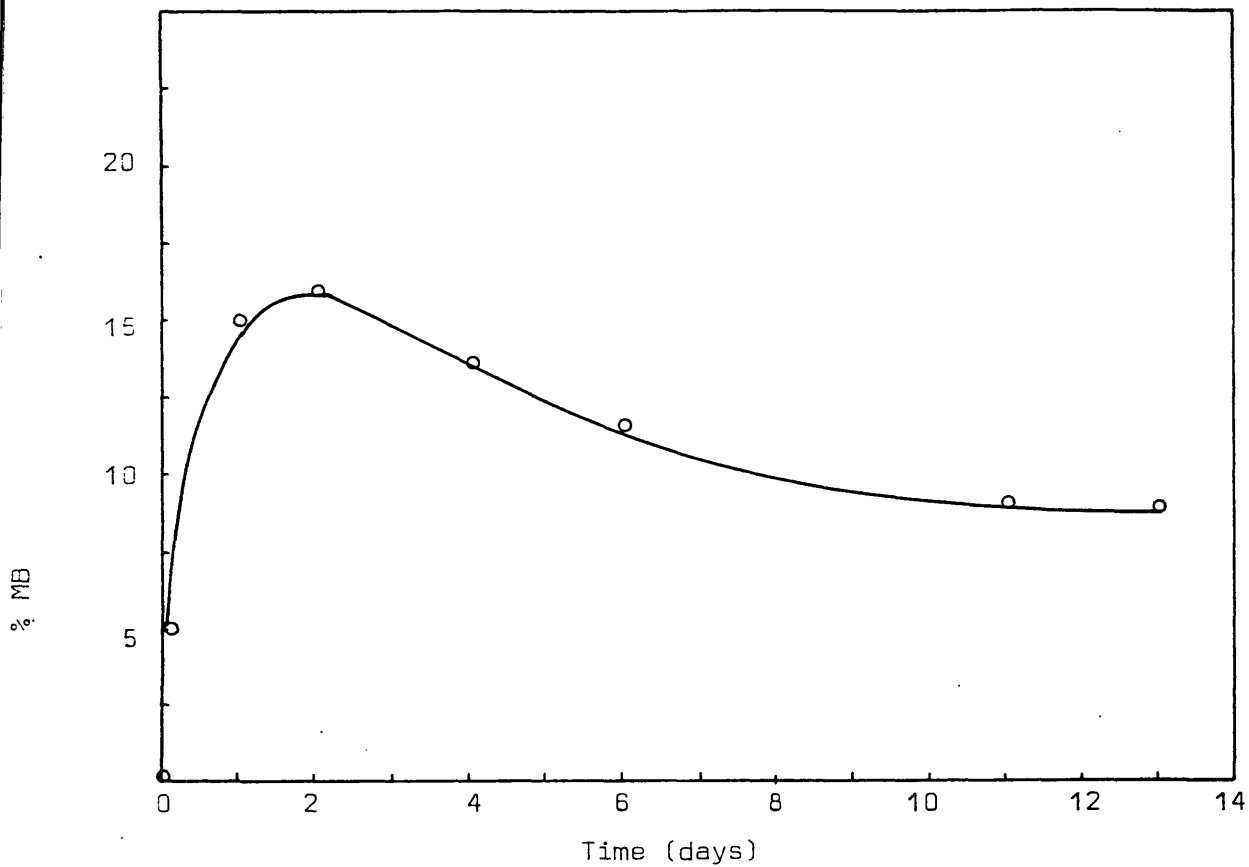
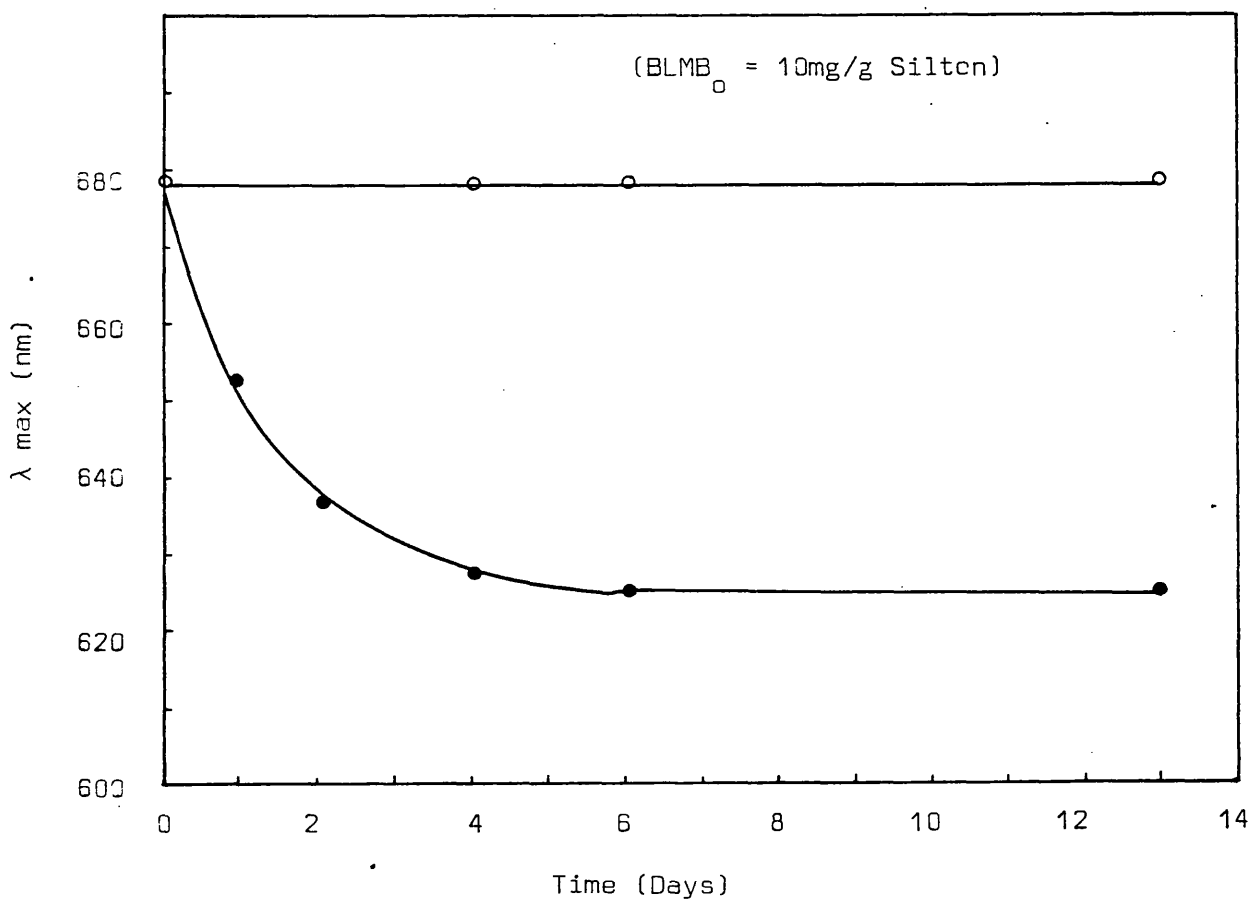


FIGURE (4-36). The Position of  $\lambda$  max of MB Produced from BLMB on Silton



4.3.15

The Reaction of BLMB on Silton in the Présence  
of  $\text{Co}^{3+}$  or  $\text{Ce}^{4+}$

The rate of production of MB from BLMB on Silton was enhanced by the presence of either  $\text{Co}^{3+}$  or  $\text{Ce}^{4+}$ , both in the initial rate of production and the final yield; Figure (4-37). As with the reactions in solution and on silica gel, the production of MB did not require light when either  $\text{Co}^{3+}$  or  $\text{Ce}^{4+}$  were present. The effect of light and  $\text{Co}^{3+}$  or  $\text{Ce}^{4+}$  were additive. The fastest rate and largest yield of colour being produced when the sample was irradiated in the presence of  $\text{Ce}^{4+}$ ; approximately 80% of the maximum colour yield, after 13 days. There was also a significant bathochromic shift of the products in the presence of  $\text{Ce}^{4+}$  or  $\text{Co}^{3+}$ , Figure (4-38).

FIGURE (4-37). The absorbance of methylene blue produced from BLMB on siltan in the presence of  $\text{Co}^{3+}$  and  $\text{Ce}^{4+}$

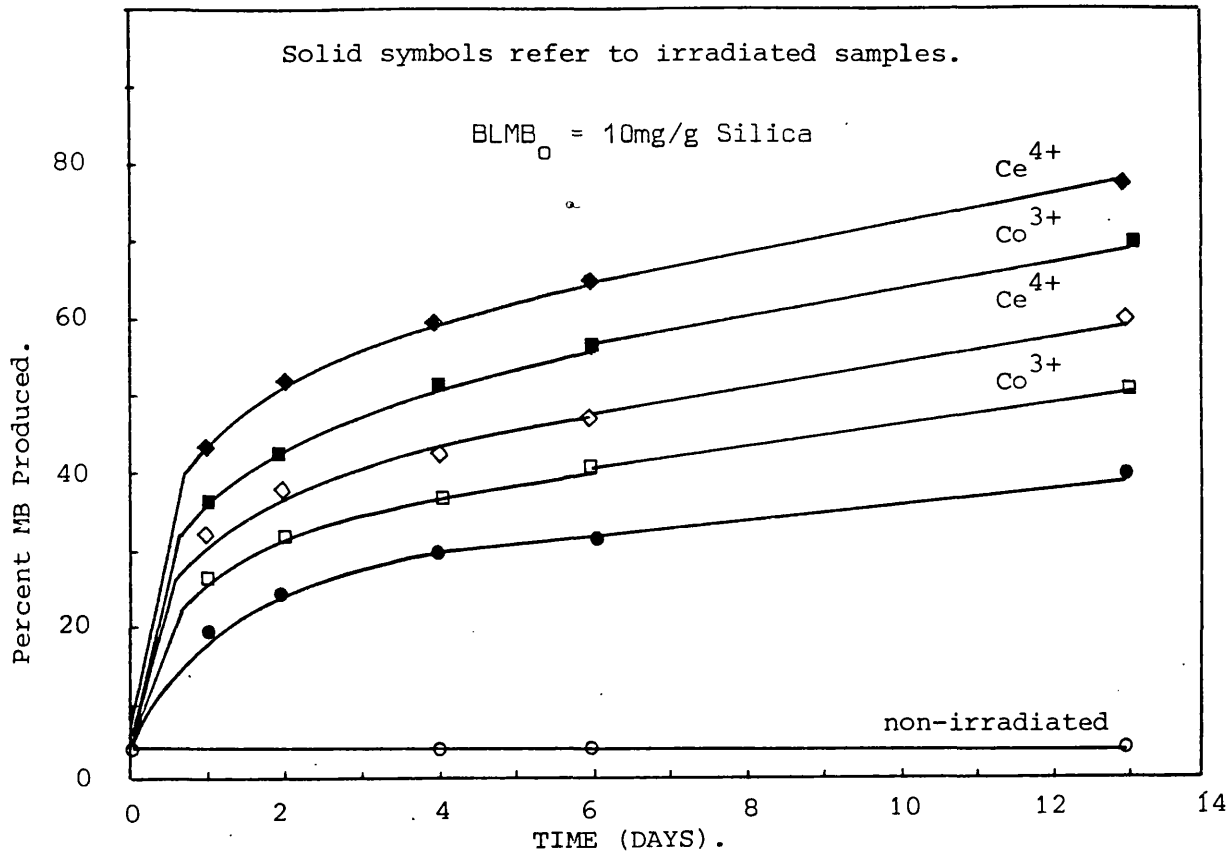
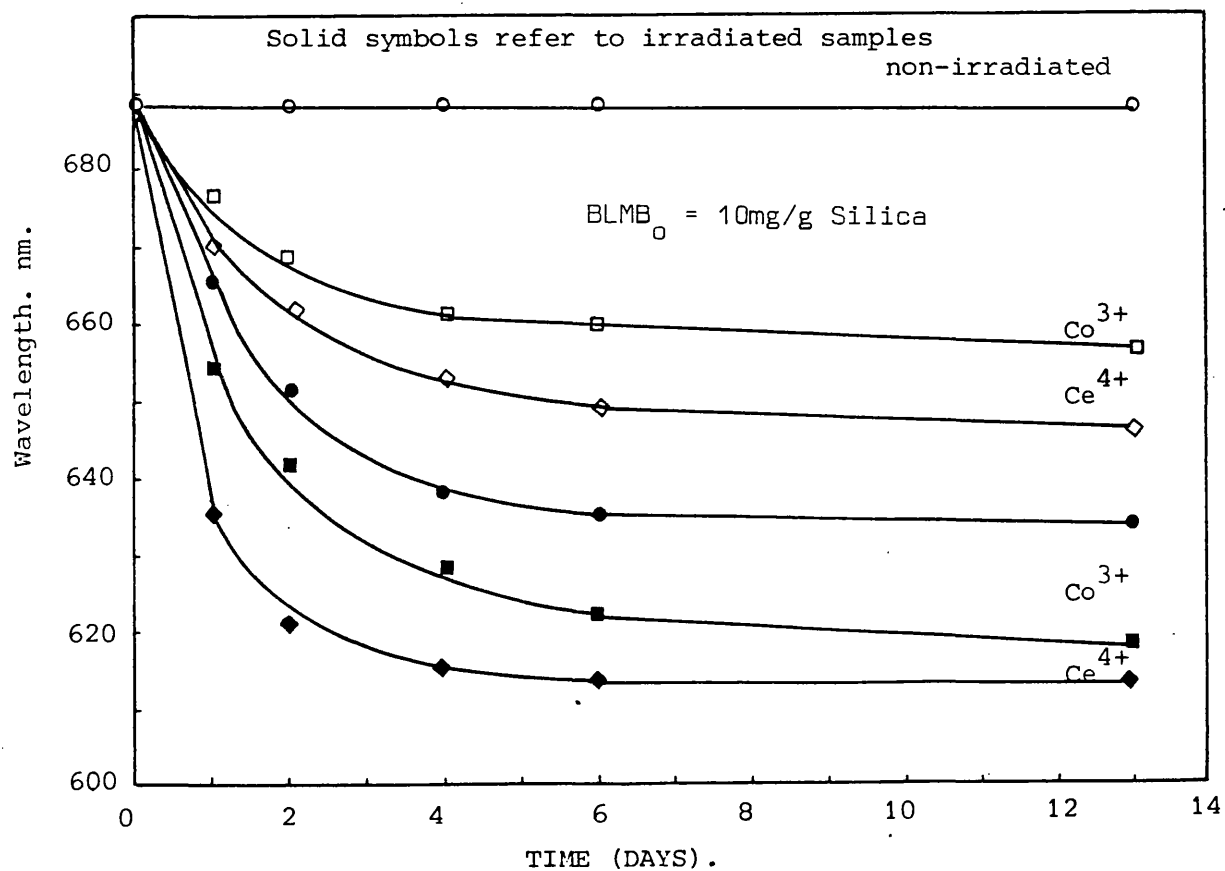


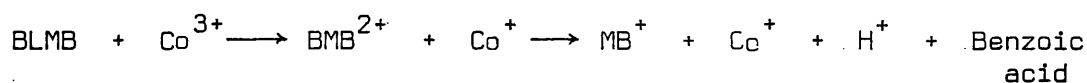
FIGURE (4-38). The absorbance maximum of Methylene blue produced from BLMB on Silton in the presence of  $\text{Co}^{3+}$  and  $\text{Ce}^{4+}$ .



## 4.4

Conclusions

The first order rate constants for the production of methylene blue from BLMB in 0.5 molar sulphuric acid at 39° and 50° were  $1.54 \times 10^{-6}$  and  $3.47 \times 10^{-6} \text{ sec}^{-1}$  respectively. If  $\text{Co}^{3+}$  is present, as sodium cobaltinitrite the reaction is greatly accelerated. Stoichiometric amounts of  $\text{Co}^{3+}$  are needed, and the reaction rate is first order with respect of the  $\text{Co}^{3+}$  concentration. The second order rate constant for the overall reaction at 25°C is  $8.95 \text{ l m}^{-1} \text{ sec}^{-1}$ . Exchange of the nitrite chelating groups for water, reduces the effectiveness of  $\text{Co}^{3+}$ , because  $(\text{Co}(\text{H}_2\text{O})_6)^{3+}$  is labile and will readily reduce to  $(\text{Co}(\text{H}_2\text{O})_6)^{2+}$  when  $\text{Co}^{3+}$  is present the reaction mechanism is by electron transfer from BLMB to  $\text{Na}_3\text{Co}(\text{NO}_2)_6$ .

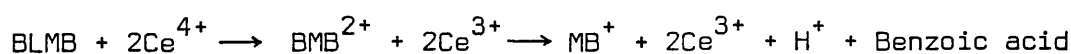


benzoyl methylene blue

(BMB)

Since the reaction is first order with respect to  $\text{Co}^{3+}$ , the two electron transfer is a concerted process. The rate of production of MB by the autooxidation of BLMB in sulphuric acid is also greatly accelerated by the presence of ceric ammonium nitrate. The overall initial reaction rate is third order, and the reaction is second order with respect to  $\text{Ce}^{4+}$  concentration. The overall initial reaction rate constant is  $k_3 = 6.25 \times 10^8 \text{ l}^2 \text{ M}^{-2} \text{ sec}^{-1}$ . Ceric ammonium nitrate is known to be a single electron acceptor.

Therefore the mechanism for the electron transfer is:



benzoyl methylene blue

( $\text{BMB}^{2+}$ )

Methylene blue adsorbed upon silica gel forms dimers on the surface. Irradiation of MB with light on silica causes demethylation, with the production of Azure A, B, C, thionine and symmetrical-dimethylthionine.

BLMB instantaneously reacts with silica gel to form a small percentage of MB, (1-2% possible total amount). Irradiation with light produces further MB. The production is first order and the first order rate constant is  $1.4 \times 10^{-7} \text{ sec}^{-1}$ , at  $40^{\circ}\text{C}$  (a half life of 57 days).

This supports the view that the reaction operates via a light induced free radical mechanism. The presence of  $\text{Co}^{3+}$  or  $\text{Ce}^{4+}$  on the surface accelerates the production of MB and the subsequent demethylation of the MB formed, on silica.

When MB is adsorbed on Silton, only the monomer is present. The rate of production of MB from BLMB on Silton is also first order,  $K_1 = 4.1 \times 10^{-7} \text{ sec}^{-1}$ , at  $40^{\circ}\text{C}$ . The presence of  $\text{Co}^{3+}$  or  $\text{Ce}^{4+}$  accelerates the production of MB and the demethylation of the MB so formed on Silton.

Azaranoff, L.V., and Bueger, M.J., (1958). McGraw-Hill.

The Powder Method in X-ray Crystallography.

Bacon, R.G.R., and Stewart, D., (1966). J. Chem. Soc. 1384-1388.

Ball, J., and Jackson, D.S., (1953). Stain Technology 28: 33-40

Barker, C.C. et al., (1959). J. Chem. Soc. 3957-3963.

Barker, C.C. et al., (1960). J. Chem. Soc. 3790-3800.

Barnes, K.K., and Mann, C.K., (1967). J. Org. Chem. 32: 1474-1479.

Beinke, T.A., and Delgaudio, J., (1968). Inorg. Chem. 7: 715-721.

Benesi, H.A., (1956). J.A.C.S. 78: 5490-5494.

Benesi, H.A., (1957). J. Phys. Chem. 61: 970-973.

Bergmann, K., and O'Konski, C.T., (1963). J. Phys. Chem. 67: 2169-2177.

Bridley, G.W., (1961). Minerals Soc. London. 51-131.

The X-ray Identification and Crystal Structures of  
Clay Minerals.

Branauer, S., Emmett, E., and Teller, E., (1938). J.A.C.S.

60: 309-319.

Caldin, E.F. (1964). Blackwell Scientific Publishers. Chapter 6, 117.

Chalkley, L. (1925). J.A.C.S. 47: 2055-2061.

Cigen, R., (1958). Acta. Chem. Scand. 12: 1456-1478.

Cigen, R., (1960). Acta Chem. Scand. 14: 979-993.

Conn, H.J., (1946). Biotech. Publications Geneva, N.Y. Biological Stains.

Cotton, F.A., and Wilkinson, G. (1972). Wiley. Interscience. 3rd Edn  
Advanced Inorganic Chemistry. 875-892.

Edelman, C.H., and Faverjee, J.C.L., (1940). Z. Krist. A102: 417-431

Egerton, G.C., and Morgan, A.G., (1970). J.S.D.C. 86: 242-249.

Eiss, M.I., and Giesecke, P. (1959) Anal. Chem 31: 1558-1560.

Formanek, J., (1908) "untersuchung und Nachweis organischer Farbstoffe  
auf spectroscopischem Wege", 2 Auflage, 1. Teil,

Berlin, 142-164.

- Frodyma, M.M., et al., (1964). J. Chromatography. 13: 61-68.
- Gensler, W.J., et al., (1966). J. Org. Chem. 31: 2324-2330.
- Giles, C.H. et al., (1960). J. Chem. Soc. 3973-3993.
- Goldacre, R.J., and Phillips, J.N., (1949). J. Chem. Soc. 1724-1731.
- Gomes de Mesquita, A.H., et al., (1965) Acta. Cryst. 18: 437-443.
- Greenland, D.J., (1965). Soil Fertilizers. 28: 415-425.
- Greenville-Williams, C. (1857). Trans. Roy. Soc. Edinburgh 21: 377-
- Griffiths, J. (1976). Academic Press. Colour and Constitution of  
Organic Molecules.
- Grim, R.E., and Kulbicki, G., (1961). Amer. Mineralogist 46:1329-1369.
- Grim, R.E., (1968) McGraw-Hill (NY) 2nd Edt. Clay Minerology.
- Hammett, L.P., and Deyrup, A.J. (1932). J.A.C.S. 54: 2721-2739.
- Hatchard, C.G., and Parker, C.A. (1961) Trans. Faraday Soc. 57: 1093-1106.
- Hauser, E.A., and Leggett, M.B., (1940) J.A.C.S. 62: 1811-1814.
- Hayon, E., et al., (1951). J. Chem. Soc. 301-311.
- Hendrick, S.B. and Alexander, J.T., (1940) J. Amer. Soc. Agron.  
32: 455-458.
- Hendricks, S.B., (1942). J. Geol. 50: 276-290.
- Henmi, T., and Wada, K., (1974). Clay Minerals. 10: 231-244.
- Henmi, T., and Wada, K., (1976). Clay Minerals. 11: 335-337.
- Henriquez, P.C., (1933). Rec. Trav. Chim. 52: 991-1000.
- Heimenz, P.C., (1977). Dekker. Inc. N.Y., Basel.  
Principles of Colloid and Surface Chemistry.
- Hofmann, U., et al., (1933). Z. Krist. 86: 340-348.
- Hofmann, U. et al., (1961). Z. Anorg. Allgem. Chem. 308: 143-154.
- Holst, G., (1935). Z. Physik-Chem A175, 99-126.
- Holst, G., (1938). Z. Physik. Chem. A182, 321-340.
- Iwamoto, K., (1935) Bull. Chem. Soc. Japan. 10: 420-425.
- Kerhmann, F., (1906). Ber. 39: 1402-1409.
- Koizumi, M., and Usui, Y., (1972) Mol Photochem. 4: 57-92.



Kortum, G., and Schottler, H., (1953). Z. Electrochem. Ber.

Bunseages. Physit. Chem. 57: 373-561.

Kortum, G., and Vogel, J., (1960). Chem Ber. 93: 706-719.

Kortum, G., (1962). Trans. Faraday. Soc. 58: 1624-1631.

Kortum G., et al., (1962). J. Phys. Chem. 66: 2439-2442.

Kortum, G., and Delkrug, D., (1962). Z. Physik. Chem. N.F. 34: 58-66.

Kortum, G., et al., (1963). Angew. Chem Internat. Edn 2: 333-404.

Kortum, G., and Delfs, H., (1964). Spectrochim. Acta 20: 405-413.

Kortum, G., (1969). Springer-Verlag. Reflectance Spectroscopy

Principles, Methods, Applications.

Kubelka, P., and Monk, F., (1931). Z. Techn. Physik 12: 593-601.

Kubelka, P., (1948). J. Opt. Soc. Amer. 38: 448-457.

Laura, R.D., (1976). Clay Minerals. 11: 331-334.

Lewis, G.N., et al., (1942). J.A.C.S. 64: 1774-1782.

Lewis, G.N. (1943). J.A.C.S. 65: 2102-2106.

Lewis, G.N. et al., (1943). J.A.C.S. 65: 1150-1154.

Lewis, G.N., and Bigeleisen, J., (1943). J.A.C.S. 65: 1144-1150.

Loach, K.W., (1971). J. Chromotography. 60: 119-126.

Lohr, W. et al., (1974). Stain Technology. 49: 359-366.

Lohr W., et al., (1975). Stain Technology. 50: 149-156.

Luck, W., and Sand, H., (1964). Angew. Chemie. Int. Edn. 3: 570-580.

MacEwan, D.M.C., (1961). Mineral. Soc. London. 143-207.

The X-ray Identification and Crystal Structure of  
Clay Minerals.

MacKenzie, R.C. and Mitchell, B.D., (1966). Clay Mineralogy.

Earth Sci. Rev. 2: 47-91.

Maedefrau, E., and Hofmann, U., (1937). Z. Krist. 98: 299-323.

Marshall, C.E., (1935). Z. Krist. 91: 433-449.

Marshall, C.E., (1949). Acad. Press. (NY) The colloid Chemistry  
of the Silicate Minerals.

- Marshall, P.N., and Lewis, S.M., (1974)a. *Stain Technology* 49: 235-240.
- Marshall, P.N., and Lewis, S.M., (1974)b. *Stain Technology*. 49: 351-358.
- Marshall, P.N., et al., (1975). *Stain Technology*. 50: 107-113.
- Marshall, P.N., and Lewis, S.M. (1975) *Stain Technology*. 59: 143-147.
- Maunier, P., (1942). *Cr. Rend. Seanc. Acad. Sci. Paris*. 215: 470-473.
- Meyer, H.W. and Treadwell, W.D., (1952). *Helv. Chem. Acta*. 35: 1444-1460.
- Michaelis, L., and Granick, S., (1945). *J.A.C.S.* 67: 1212-1219.
- Michaels, A.S., (1958). *Ind. Eng. Chem* 50: 951-958.
- Moriga, H., and Oda, R., (1964). *Kogyo. Kagaku. Zasshi*. 67: 1050-1063.
- Mortland, M.M., and Raman, K.V., (1968). *Clays. Clay Minerals*.  
16: 393-398.
- Mortland, M.M., (1970). *Advan. Agron.* 22: 75-117.
- Nemcova, I., et al., (1969). *Collection. Czechoslov. Chem. Commun.*  
34: 2880-2895.
- Norrish, K., (1954). *Discuss. Faraday. Soc.* 18: 120-134.
- Parker, C.A. (1958)a. *Nature*. 182:130
- Parker, C.A. (1958)b) *Nature* 182: 245-246.
- Parker, C.A., (1959). *J. Phys. Chem.* 63: 26-38.
- Pauling, L., (1930)a. *P.N.A.S.* 16: 123-129.
- Pauling, L., (1930)b. *P.N.A.S.* 16: 578-582.
- Potts, H.A., et al., (1972). *J. Appl. Chem. Biotech.* 22: 651-657.
- Quirk, J.P., (1960). *Nature*. 188: 253-254.
- Rabinowitch, E., and Epstein, L.F., (1941). *J.A.C.S.* 63: 69-78.
- Russell, J.D., et al., (1968). *J. Agr. Food. Chem.* 16: 21-24.
- Schaefer, F.C. and Zimmerman, W.D., (1968). *Nature* 320: 66-67.
- Schofield, R.K., (1949). *J. Soil. Sci.* 1: 1-8.
- Schubert, M., and Levine, A., (1955). *J.A.C.S.* 77: 4197-4201.
- Sequoia, E., (1971). *J. Electroanal. Chem.* 30: 506-510.
- Smith, P.A.S., and Loeppky, R.N., (1967). *J.A.C.S.* 89: 1147-1158.
- Solomon, D.H., (1968). *Clays and Clay Minerals*. 16: 31-39.

- Solomon, D.H., et al., (1968)a. J. Macromol: Sci. Chem. A5: 587-601.
- Solomon, D.H., et al., (1968)b. Clay Minerals 7: 389-397.
- Solomon, D.H., and Murray, H.H., (1972). Clays and Clay Minerals.  
20: 135-141.
- Stotz, E., et al., (1950). Stain Technology. 25: 57-68.
- Sugahara, Y. et al., (1968). Patent No. 1213835 London.  
Colour Former for Pressure Sensitive Recording Paper  
and Process for Producing Same.
- Theng, B.K.G., (1971). Clays and Clay Minerals. 19: 383-390.
- Turgeon, J.C., and Lamer, V.K., (1952). J.A.C.S. 74: 5988-5995.
- Vickerstaff, T., and Lemin, D.R., (1946). Nature 157: 373.
- Walling, C., (1950). J.A.C.S., 72: 1164-1168.
- Weil-Malherbe, H., and Weiss, S., (1948). J. Chem. Soc. 2164-2169.
- Weiss, A., (1963). Clays and Clay Minerals. 10: 191-224.
- Wotherspoon, N., and Oster G., (1957). J.A.C.S. 79: 3992-3995.
- Yoshida, Z., and Kazama, K., (1956). Kogyo Kagaku Zasshi 59: 1418-1423.
- Yoshida, Z., and Kazama, K., (1957). Kogyo Kagaku Zasshi 60: 190-194.